THE UNIVERSITY *of* EDINBURGH

Bio-Oligomers as Antibacterial Agents and Strategies for Bacterial Detection

Jagath C. Kasturiarachchi

Ph.D.

The University of Edinburgh

College of Medicine & Veterinary Medicine

2014

Declaration

This thesis represents my own work. All of the experiments described herein were performed by me.

I received technical assistance to perform flow cytometry and confocal analysis as declared in the acknowledgements. All chemical .entities were synthesised by the Department of Chemistry at University of Edinburgh.

…….

J C Kasturiarachchi

Acknowledgements

I am very grateful to Dr Kev Dhaliwal, Professor Mark Bradley and Professor Chris Haslett for their supervision and support.

I would like to thank Dr Jeff Walton and Dr Nicos Avlonitis designing and synthesis of peptoid library. I would like to thank Dr Nicos Avlonitis, Dr Marc Vendrell and Miss Alize Marangoz for their support for the synthesis of peptide probes.

I wish to thank Miss Emma Scholefield for her support during my studies including killing assay development and confocal microscopy studies.

My sincere thanks go to Dr Donald Davidson's group and Professor Adriano Rossi's group for their valuable comments and support during my PhD.

I would like to thank Mrs Shonna Johnston, Mrs Fiona Rossi and Mr Will Ramsay for their technical support performing flow cytometry and confocal microscopy studies.

My special thanks go to Edinburgh Global Research Scholarship, Medicine and Veterinary Medicine and Medical Research Council for their financial support during my PhD.

Finally, I am eternally grateful to my parents and my brothers for their encouragement and support throughout my PhD.

List of Figures

List of Tables

Abbreviations

AIDS	- Acquired Immuno Deficiency Syndrome
AMP	- Antimicrobial Peptides
APD	- Antimicrobial Peptide Database
ATCC	- American Type Culture Collection
ATP	- Adenosine Triphosphate
BAI	- Biomaterial Associated Infections
BCA assay	- Bicinchoninic Acid assay
BnCO	- Phenyl acetamide
BSA	- Bovine Serum Albumin
CAMPs	- Cationic Antimicrobial Peptides
CA-MRSA	- Community-Associated MRSA
CD	- Cluster of Differentiation
CE-SELEX	- Capillary Electrophoresis-SELEX
CL	- Cardiolipin
CM	- Cell Membrane
CPPs	- Cell Penetrating Peptides
DDS	- Drug Delivery System
DHE	- Dihydroethidium
DHFR	- Dihydro Folate Reductase
DIC	- N, N0-diisopropylcarbodiimide
DMEM	- Dulbecco's Modified Eagle Medium
DMSO	- Dimethyl Sulfoxide
DNA	- Deoxyribonucleic acid
Dox	- Doxorubicin
DsDNA	- Double Stranded DNA
Ef-G	- Elongation factor G
ESTA	- E-Selectin ThioAptamer
FAM	- Fluorescein
FDA	- Food and Drug Administration
FITC	- Fluorescein Isothiocyanate
GFP	- Green Fluorescent Protein
HBSS	- Hank's Balanced Salt Solution
HIV	- Human Immunodeficiency Virus
HPLC	- High Performance Liquid Chromatography
hRSV	- human Respiratory Syncytial Virus
HTS	- High Throughput Screening
IDMEM	- Iscoves’s Dulbecco’s Modified Eagle’s Medium
IMDM	- Iscove's Modified Dulbecco's Medium
IPTG	- Isopropyl β-D-1-thiogalactopyranoside
IT	- Intratracheal
IV	- Intravenous
KDO	- 3-deoxy-D-manno-octulosonate
LB	- Luria Bertani
LPS	- Lipopolysaccharide
MALDI-TOF	- Matrix Assisted Laser Desorption/ionization Time-of-Flight

MS - Mass Spectrometry
MBC - Minimum Bactericidal Concentration
MDR - Multidrug Resistant
MGE - Mobile Genetic Element
MHB - Mueller-Hinton Broth
MHC - Minimum Concentration that produces haemolysis
MIC - Minimum Inhibitory Concentration
MNPs - Magnetic Nanoparticles
MOA - Mode of Action
MRSA - Methicillin Resistant *Staphylococcus aureus*
mSELEX - Microfluidic SELEX
MSSA - Methicillin Sensitive *Staphylococcus aureus*
NEB - New England Biolabs
Ni-NTA - Ni Nitrilotriacetic acid
NMP - N-methylpyrrolidinone
NO - Nitric Oxide
NP - Natural Product
O.D. - Optical Density
PAO1 - *Pseudomonas aeruginosa*
PBP2A - Penicillin Binding Protein 2a
PBPs - Penicillin Binding Proteins
PBS - Phosphate Buffered Saline
PC - Phosphatidylcholine
PCR - Polymerase Chain Reaction
PEG - Polyethylene Glycol
PFU - plaque forming units
PG - Phosphatidylglycerol
Ph.D. 12 - 12 mer Amino Acid Phage Displayed Peptide Library
PI - Propidium Iodide
PSMA - Prostate Specific Membrane Antigen
QVD-OPh - quinolyl-valyl-O-methylaspartyl-[-2,6-difluorophenoxy]-methyl ketone
RNA - Ribonucleic Acid
ROS - Reactive Oxygen Species
rRNA - ribosomal RNA
RT-PCR - Reverse Transcriptase PCR
S.A.R - Structure Activity Relationships
SCCmec - *Staphylococcal* Cassette Chromosome
SDS-PAGE - Sodium Dodecyl Sulfate-Polyacrylamide Gel Electrophoresis
SELEX - Systematic Evolution of Ligands by Exponential Enrichment
SFD - *Staphylococcal* Foodborne Diseases
siRNA - Small interfering RNA
SM - Sphingomyelin
SR - Selectivity Ratio
ssDNA - Double Stranded DNA
SSTIs - Skin and Soft Tissue Infections
SYSMT - Systemic Monotherapy
TAMRA - Carboxytetramethylrhodamine

TBE	- Tris/Borate buffer
TBS	- Tris buffered saline
TEM	- Transmission Electron Microscopy
TI	- Therapeutic Index
TLR	- Toll Like Receptors
Tmb	- Thrombin
TOP	- Tosyl-Octamer Peptoid
VEGF	- Vascular Endothelial Growth Factor
VH	- Variable Heavy Chain
VL	- Variable Light Chain
VRE	- Vancomycin Resistant Enterococci
VRSA	- Vancomycin Resistant MRSA
Xgal	- 5-bromo-4-chloro-3-indolyl-β-D-galactopyranoside

Abstract

In this thesis I examined the potential of Bio-Oligomers such as peptoids, peptides and aptamers, as therapeutic and diagnostic entities.

Therapeutic Bio-Oligomers;

A series of peptoid analogs have been designed and synthesised using solid phase synthesis. These peptoids have been subjected to biological evaluation to determine structure-activity relationships that define their antimicrobial activity. In total 13 peptoids were synthesised. Out of 13 different peptoids, only one peptoid called Tosyl-Octyl-Peptoid (TOP) demonstrated significant broad-spectrum bactericidal activity. TOP kills bacteria under non-dividing and dividing conditions. The Minimum Inhibitory Concentrations (MIC) values of TOP for *S. epidermidis*, *E. coli* and *Klebsiella* were 20 μM, whereas Methicillin-resistant *Staphylococcus aureus* (MRSA) and Methicillin-sensitive *Staphylococcus aureus* (MSSA) were 40 μM. The highest MIC values were observed for *Pseudomonas aeruginosa* (PAO1) at 80 μM. The selectivity ratio (SR) or Therapeutic index (TI) was calculated, by dividing the 10% haemolysis activity (5 mM) by the median of the MIC (50 μM) yielding a TI for TOP as 100. This TI is well above previously reported peptidomimetics TI of around 20. TOP demonstrates selective bacterial killing in co-culture systems and intracellular bacterial killing activity.

Diagnostic Bio-Oligomers;

In the second part of my thesis, I investigated aptamer and peptide-based molecular probes to detect MRSA. As well as screening aptamers and peptide probes against whole MRSA, I over-expressed and purified PBP2A protein. This purified protein was used as a target for aptamer and peptide probes to detect MRSA.

Two different aptamer libraries were initially screened for utility. *In-vitro* conditions for SELEX were optimised. Biopanning with a phage derived peptides was also performed. Target sequences for both methods were identified and chemically synthesised. Evaluation of fluorescently labelled sequences with flow cytometry and confocal imaging showed no specificity for MRSA detection with either method. The Bio-Oligomers and the *in-vitro* selection methodology require further refinement to improve diagnostic utility.

Table of Contents

Chapter 1:
Introduction

Chapter 1: Introduction

In my PhD, I have focused on two thematic research areas in bacteriology; antibacterial drug development and molecular diagnostics. Therefore in the first part of my work, I have investigated the antibacterial properties of peptoid molecules for therapeutic purposes. The rest of my research work focused on efforts to develop methicillin-resistant *S. aureus* (MRSA) diagnostic molecular probes using Aptamers and Peptide derived peptides. The thesis hence encompasses the following two investigations;

(a) Study and characterisation of peptoids as a novel antimicrobial agents.
(b) Study the strategies to develop aptamer and peptide molecules to detect bacterial infection.

1.1. Antibiotics

1.1.1. Introduction to antibiotics

Antimicrobial drugs or antibiotics are biologically active molecules that act against microorganisms. Most antibiotics for use in humans are natural products, secreted by one species of microbes (bacteria or fungi) as chemical defence mechanisms to kill microbes in the neighbouring microenvironment. Semisynthetic modifications of those have produced second, third and fourth generations of antibiotics. They have different modes of action but the majority inhibit essential microbial functions such as protein synthesis, DNA replication and cell-wall synthesis. Antibiotics are the most successful form of chemotherapy developed and applied in the past century in medicine (Wright, 2010; Gualerzi, 2014).

After the introduction of antibiotics in 1940s and 1950s patients with bacteraemia had improved chance of survival and decreased mortality due to infection (Ekdahl, 1995). New classes of antimicrobial agents rapidly entered the market in the 1950s and 1960s and this led to over-confidence that infectious disease would be

eradicated. In addition to that research into discovering new broad-spectrum antimicrobial drugs with previously unexploited modes of action was discouraged by pharmaceutical companies due to the large costs of research (Beutler, 2009). This includes the discovery and development of new drugs as it is a long and increasingly expensive process until approval is obtained. Once the new compounds finally reach the market it is difficult to recover the cost invested in the development. Therefore mostly the discovery efforts are concentrated in chemical synthesis and the development of large combinatorial libraries for automated high-throughput screening (HTS), this may reduce the time and expense involved in natural product discovery (Beutler, 2009; Li and Vederas, 2009). However despite having technological advances particularly in the area of molecular biology, genomics, combinatorial chemistry HTSs have provided highly efficient tools to expedite, increase, and improve drug discovery, here has been little success in identifying new leads for the development of new classes of antibiotics approved for human use. This failure reflects the particular challenges of antibiotic discovery (Livermore, 2011).

No new classes of antibiotics were produced in the 37 years between the introduction of nalidixic acid in 1962 and linezolid in 2000 (Bax *et al*., 1998) (Figure 1.1). All of the antibacterial agents that entered the market during this period were modifications of existing molecules. Therefore more than 20 novel classes of antibiotics were produced between 1930 and 1962 and only four new classes of antibiotics were marketed. However none of these new classes were really novel: daptomycin, approved in 2000, was discovered in the early 1980s; linezolid, approved in 2000, derives from a synthetic lead discovered in the 1970s; pleuromutilins, approved in 2007, have been widely used for about 30 years in veterinary medicine; fidaxomicin, approved in 2011, was first reported in the 1970s (Endimiani *et al*., 2009; Houghton *et al*., 2010; Sutcliffe, 2011). During this window period bacteria exploited this opportunity and progressively developed resistance to all commonly used antibiotics and each year the need for new antibiotics becomes more demanding (Theuretzbacher, 2012).

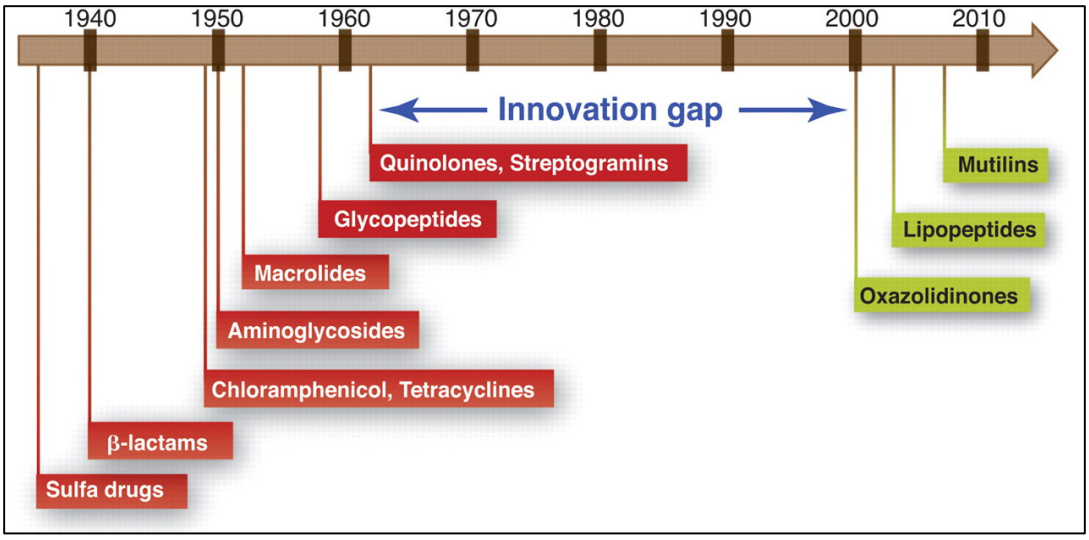

Figure 1.1: Timeline of the discovery of the most important antibiotic classes. Illustrating the innovation gap, between 1962 and 2000, no major classes of antibiotics were introduced (Fischbach and Walsh, 2009).

Now every country in the world has antibiotic-resistant bacteria. In some regions, 25% of the most common cause of community acquired pneumonia, *Streptococcus pneumoniae*, are resistant to penicillin (Thornsberry *et al*., 2002) and more than 70% of bacteria that give rise to hospital-acquired infections in the United States resist at least one of the main antimicrobial agents that are typically used to fight infection (Brinsley *et al*., 2005). Until the recent development of new antimicrobial agents, the antibiotic vancomycin was the 'antibiotic of last resort' for the treatment of multiple drug-resistant *Staphylococcus aureus*, and now the first case of fully vancomycin-resistant *S. aureus* has been reported (Sievert, 2002). The scale of the problem become much severe due to many Western countries prescribing antimicrobial drugs by community doctors at the rate of 4–5 courses per person each year and 20% of all patients who enter hospital have or acquire an infection an increased rate of nosocomial infection (Bryskier, 2000).

Approximately 50 percent of antimicrobial agents are also used in veterinary medicine and agriculture and there has been increasing concern that such practise is contributing to the emergence of antibiotic resistance. The use of antibiotics as growth promoters in animal food is particularly controversial and several antibiotics

or their close relatives are considered to be particularly important for human health such as avoparcin, which is very similar to vancomycin, have been banned from use in animal foods (Office, 1999). In Denmark in 1994, 24,000 kg of a vancomycin derivative called avoparcin was used for animal health, 1,000 times higher than the 24 kg of vancomycin used to treat human infections in the same year (Witte, 1998). When pigs treated with avoparcin were analysed for vancomycin-resistant enterococci (VRE) strains, they contained the same five gene operons that encode vancomycin resistance in enterococci isolated from nonresponsive human patients. This lead to restriction on the use of avoparcin as an additive to animal feed (Office, 1999).

1.1.2. Discovery strategies and sources of classes of antibacterial

Antibiotics have been discovered by empirical screening or phenotypic screening. The empirical screening was practised to screen chemicals that kill or inhibit growth of bacteria without prior knowledge of mechanism of action. In contrast to phenotypic screens, more specifically, whole-cell screens that detect the inhibition of a desired target or function, in a way corresponding to selecting genetic mutants by their demonstration of an expected phenotype (Wong *et al*., 2012).

The rationale behind the discovery strategies employed since the 1960s have not been very productive in bringing drugs to market. The successful era of empiric screening involved screening for inhibition of cell growth without knowing the mechanism of action coincided with the Golden Age of natural product (NP) discovery (from the 1940s to the late 1960s). Most classes of antibacterial drugs for human and animal health were indeed discovered by empirical screening of NPs. The screening used freshly fermented broths or extracts as opposed to the current methods involve rapid chemical fractionation and identification and comparison to databases of known NPs (Wong *et al*., 2012; Gualerzi, 2014). Table 1.1 shows the sources of clinically used classes of antibacterial drugs and their discovery strategies.

Table 1.1: Sources of clinically used classes of antibacterial drugs. (Gualerzi, 2014)

Drug class	**Source**	**Discovery strategy**
β-lactams	NP-Fungi, actinomycetes	Empirical; also by spheroplasting (cell wall)
Glycopeptides	NP- Actinomycetes	Empirical
Fluoroquinolones	Synthetic-Quinine analogs	Empirical
Aminoglycosides	NP-Actinomycetes	Empirical
Tetracyclines	NP-Actinomycetes	Empirical
Oxazolidinones	Synthetic-Industrial library	Empirical
Macrolides	NP-Actinomycetes	Empirical
Lincosamides	NP-Actinomycetes	Empirical
Streptogramins	NP-Actinomycetes	Empirical
Chloramphenicol	NP-Actinomycetes	Empirical
Metronidazole	Synthetic-Azomycin analogs	Empirical
Polymyxin	NP-Bacillus	Empirical
Daptomycin	NP-Actinomycetes	Empirical
Pleuromutilin	NP-Fungi	Empirical
Trimethoprim	Synthetic-Pyrimidines	Target-based for DHFR inhibition
Sulfamethoxazole	Synthetic-Azo-dyes	Empirical in limited
Rifampicin	NP-Actinomycetes	Empirical
Mupirocin	NP-Pseudomonas	Empirical
Fosfomycin	NP-Actinomycetes	Phenotypic by spheroplasting (cell wall)
Fusidic acid	NP-Fungi	Empirical
Fidaxamicin	NP-Actinomycetes	Empirical

NP, natural product.

1.1.3. Antibacterial targets

The fundamental requirement for an antibacterial target is that it is important for growth and viability of the pathogen. The vast majority of current antibiotics target similar cellular processes as their natural or synthetic predecessors. The range of these targets is limited to the components of protein synthesis, cell wall biosynthesis, DNA/ RNA metabolism and some other cellular processes. Antibiotic, such as ciprofloxacin are synthetic antibiotic structures that kill bacteria by targeting the enzyme DNA gyrase the enzyme responsible for uncoiling the intertwined circles of double-stranded bacterial DNA that arise after each round of DNA replication (Hooper and Wolfson, 1993). The RNA and protein machinery of the prokaryotic ribosomes is sufficiently distinct from the analogous eukaryotic machinery that there are many inhibitors of protein synthesis, targeting different steps in ribosome action, with selective antibacterial action. With the extensive range of genomes sequenced, it becomes possible to implement the idea in a more elaborate way, with essential targets defined much more precisely at the molecular level. This needs to be complemented by the availability of chemically diverse compound collections to screen for the target/ drug combination (Payne *et al*., 2007; Aminov, 2010).

There are five major modes of action of antibiotics involved in bacterial killing as describe below (Morar and Wright, 2010; Gualerzi, 2014) (Figure 1.2 and Table 1.2);

1 Interference with cell-wall synthesis.
2 Inhibition of protein synthesis.
3 Interference with nucleic acid synthesis.
4 Inhibition of cofactor biosynthetic pathways.
5 Membrane pore formation.

Identifying the novel drug/ target combinations in pathogens is important for future discovery of antimicrobials. For example suppression of an important virulence factors, bacterial secretion systems (Negrea *et al*., 2007), inhibition of the histidine sensor kinase, virulence gene expression in several pathogens (Rasko *et al*., 2008),

inhibiting an important enzyme involved in *Staphylococcus aureus* virulence, as a candidate drug target to control MRSA (Chia *et al*., 2008). Other potential targets for intervention in bacterial metabolism include fatty acid biosynthesis (Su and Honek, 2007), cell division (Lock and Harry, 2008), biosynthesis of tRNAs (Schimmel *et al*., 1998), quorum sensing (Njoroge and Sperandio, 2009), bacterial two-component signal transduction (Gotoh *et al*., 2010), and proton motive force (Diacon *et al*., 2009). Antibiotic resistance mechanisms themselves such as efflux pumps or β-lactamases can also be targeted to restore the efficacy of antibiotics, which is compromised by the growing resistance problem (Bush and Macielag, 2010).

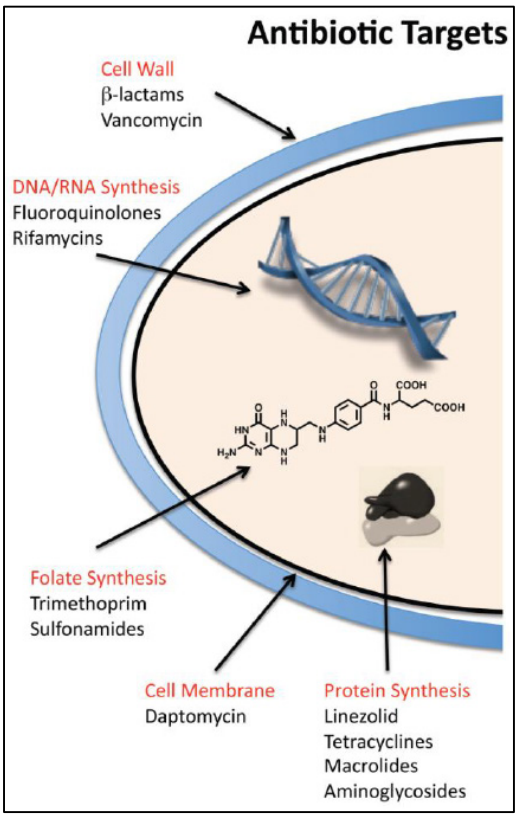

Figure 1.2: Bacterial targets of the most common antibiotics. Antibiotics target essential bacterial physiology and biochemistry, causing microbial cell death or the stop growth. There are five major antibiotic targets: the bacterial cell wall, the cell membrane, protein synthesis, DNA and RNA synthesis, and folic acid (vitamin B9) metabolism (Wright, 2010).

Table 1.2: Targets of clinically used classes of antibacterial drugs (Morar and Wright, 2010).

Drug class	**Pathway**	**Target**	**Use**
β-lactams	Cell-wall synthesis	PBPs	SYSMT
Glycopeptides	Cell-wall synthesis	Lipid II	SYSMT
Fluoroquinolones	DNA replication	DNA Gyr/Topo IV	SYSMT
Aminoglycosides	Protein synthesis	16S rRNA	SYSMT
Tetracyclines	Protein synthesis	16S rRNA	SYSMT
Oxazolidinones	Protein synthesis	23S rRNA	SYSMT
Macrolides	Protein synthesis	23S rRNA	SYSMT
Lincosamides	Protein synthesis	23S rRNA	SYSMT
Streptogramins	Protein synthesis	23S rRNA	SYSMT
Chloramphenicol	Protein synthesis	23S rRNA	SYSMT
Metronidazole		DNA	SYSMT
Polymyxin		Cell membrane	SYSMT
Daptomycin		Cell membrane	SYSMT
Pleuromutilin	Protein synthesis	23S rRNA	Topical therapy
Trimethoprim	Folate synthesis	DHFR (FolA)	Systemic in combination
Sulfamethoxazole	Folate synthesis	FolP	Systemic in combination
Rifampicin	RNA synthesis	RNA polymerase	Systemic in combination
Mupirocin	Protein synthesis	Ile tRNA synthetase	Topical therapy
Fosfomycin	Cell-wall synthesis	MurA	Systemic UTI
Fusidic acid	Protein synthesis	Ef-G	Systemic UTI
Fidaxamicin	RNA synthesis	RNA polymerase	Oral (nonabsorbed) for C. difficile

rRNA, ribosomal RNA; DHFR, dihydro folate reductase, Ef-G, elongation factor G and SYSMT-Systemic monotherapy.

1.1.4. Antibiotics and resistance

Microbial infectious diseases in human and farmed animals contribute significant morbidity and mortality throughout history. This significantly improved when penicillin and other classes of antibiotics were discovered and used to treat infectious diseases. However, almost as soon as antibacterial drugs were introduced in clinics, bacterial resistance spread resulting huge burden to the economy (Abraham and Chain, 1940; Tenover, 2006).

Molecular basis of antimicrobial resistance;

(A) Intrinsic resistance

(B) Acquired resistance

1 Mutation

2 Horizontal gene transfer

If the microorganisms become resistant above their previously predefined threshold minimum inhibitory concentration (MIC) values, then they are classified as drug resistant. Bacterial resistance is very important for medical, social, and economical viewpoint and often results in treatment failure and this implies an added cost on healthcare (Cosgrove and Carmeli, 2003). However it is fascinating and important in biology, molecular evolution of drug resistant strains and selection of fine mechanisms that allow survival under unfavourable circumstances (Gualerzi, 2014).

The evolution of drug resistant strains is common in pathogenic and non-pathogenic bacteria under the selective pressure of antibiotics. The concept of ‘‘resistome’’ was introduced to understand the evolution of resistance genes within microbial populations and the spread of these genes between species and genera (Wright, 2007). The function of the resistome genetic elements is to counteract with toxic effects of antibiotic drugs. Furthermore, the resistome also comprises the collection of genes, called proto-resistance genes, which have the potential to evolve into resistance elements against antibiotic drugs (Morar and Wright, 2010). Many resistance genes have been isolated from clinically relevant strains and non-

pathogenic organisms as well. Antibiotic-producing environmental bacteria are likely the original source reflecting the continuous evolution of antibiotic resistance strains pressure to survive in their environment (Baltz, 2008; Morar and Wright, 2010).

This hypothesis is supported by the presence of drug resistance elements in antibiotic-producing bacteria that have orthologs in clinical isolates (Benveniste and Davies, 1973; Walsh, 2000; Hubbard and Walsh, 2003; Wright, 2005). However, antibiotic-producing bacteria could not be the sole source of resistance genes. In fact, bacterial genomes contain an unexpected number of genes encoding putative resistance proteins (Draker *et al*., 2003), which could have originated through amplification and random mutation of genes but not originally involved in antibiotic resistance (Sandegren and Andersson, 2009).

Primary sequence analysis of resistance proteins revealed that the molecular mechanisms and the three-dimensional structures are homologous to known metabolic and signalling enzymes with no antibiotic-resistance activity (Morar and Wright, 2010). Therefore it is possible that resistance genes originally derived from elements having other metabolic functions similar to housekeeping genes encoding enzymes with modest and accidental resistance properties evolved into resistance enzymes as a result of selective pressure of antibiotic exposure. The fact that resistance genes are so widespread in the environment and that even resistance to synthetic antibiotics can be readily selected reveals the adaptable nature of the link between molecular evolution and resistome (D'Costa *et al*., 2011).

Bacterial resistance to antibacterial drugs manifests itself through a restricted range of molecular events (Figure 1.3). *Pseudomonas aeruginosa* is an opportunistic pathogen showing intrinsic resistance to antibiotics. In particular, some bacterial species are considered intrinsically resistant to a class of antibiotics because the drug cannot reach its cellular target or because the drug is not able to recognize its target which possesses the same function but a different structure. Intrinsic resistance is attributed to the low permeability of cellular envelopes together with the presence of chromosomally encoded multidrug efflux pumps or antibiotic-inactivating enzymes

that resemble those present in transposable elements and usually acquired by horizontal transfer. However, further intrinsic mechanisms act in synergy as many chromosomal genes that contribute to β-lactam resistance of *P. aeruginosa* were identified using a comprehensive library of transposon-tagged insertion mutants (Alvarez-Ortega *et al*., 2011).

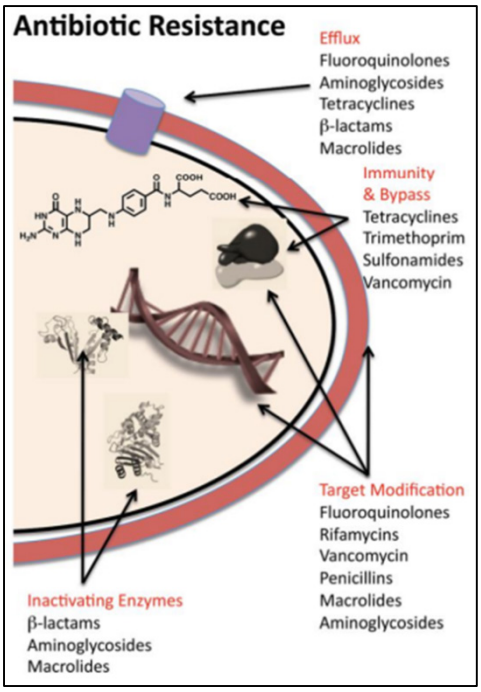

Figure 1.3: Schematic representation of major resistance strategies. Resistance to antibiotics occurs through four general mechanisms: target modification; efflux; immunity and bypass; and enzyme-catalyzed destruction (Gualerzi, 2014).

In contrast, susceptible bacteria may become resistant to a class of antibiotics through two types of genetic events:

1 Random spontaneous mutation.

2 Acquisition of the genetic information encoding resistance from other bacteria.

In susceptible bacteria that acquire resistance by spontaneous mutations resistance may be conferred by (Figure 1.4):

1 Modification or loss of the target with which the antibiotic interacts (The *mecA* gene encodes the penicillin-binding protein 2a (PBP2A) a transpeptidase membrane protein that possesses a low affinity for β-lactam antibiotics, such as methicillin and penicillin, and is responsible for β-lactam resistance in methicillin resistant *S. aureus* (MRSA) (Rice, 2012).
2 Up regulation of enzymes that inactivate the antimicrobial agent (e.g., β-lactamases that destroy the β-lactame antibiotics) or that modify the antibiotic target (e.g., ribosomal methylase in *Staphylococci* preventing erythromycin binding) (Abraham and Chain, 1940).
3 Down regulation or inactivation of the outer membrane protein channel required by the drug for cell entry (e.g., in *Escherichia coli*) (Goessens *et al*., 2013).
4 Up regulation of pumps that expel the drug from the cell (e.g., efflux of fluoroquinolones in *Staphylococcus aureus*) (Costa *et al*., 2011).

In all these cases, strains of bacteria carrying chromosomal mutations conferring resistance survive and grow under the selective pressure of antibiotic use, which instead kills the susceptible strains and promotes spreading of resistant genotypes. This kind of selection is named vertical evolution because resistance-associated genetic elements are transmitted from cell to cell through cell duplication (McManus, 1997; Tenover, 2006).

Bacteria also develop resistance through the acquisition of new genetic material from resistant organisms. This kind of selection is termed horizontal evolution and may occur in an intra- or interspecific way or even among different genera and may be facilitated via transposable elements such as transposons, which contain resistance genes (McManus, 1997). Genetic exchange mechanisms include events such as conjugation, transduction, and transformation (McManus, 1997; Tenover, 2006). During conjugation plasmid carrying resistance genes transfer to a recipient in gram negative bacterium through a mating bridge, this joins the two bacteria. In gram-positive bacteria exchange of DNA by conjugation is usually triggered by sex pheromones, which facilitate the clumping of donor and recipient cells. During

transduction, resistance genes are transferred via bacteriophage. Finally, the so-called competent bacteria may acquire and incorporate resistance genes from other bacteria that have released their DNA into the environment after cell lysis, by transformation (McManus, 1997; Tenover, 2006). Through genetic exchange mechanisms, many bacteria become resistant to multiple classes of antibacterial agents, and these are termed multidrug-resistant (MDR) bacteria.

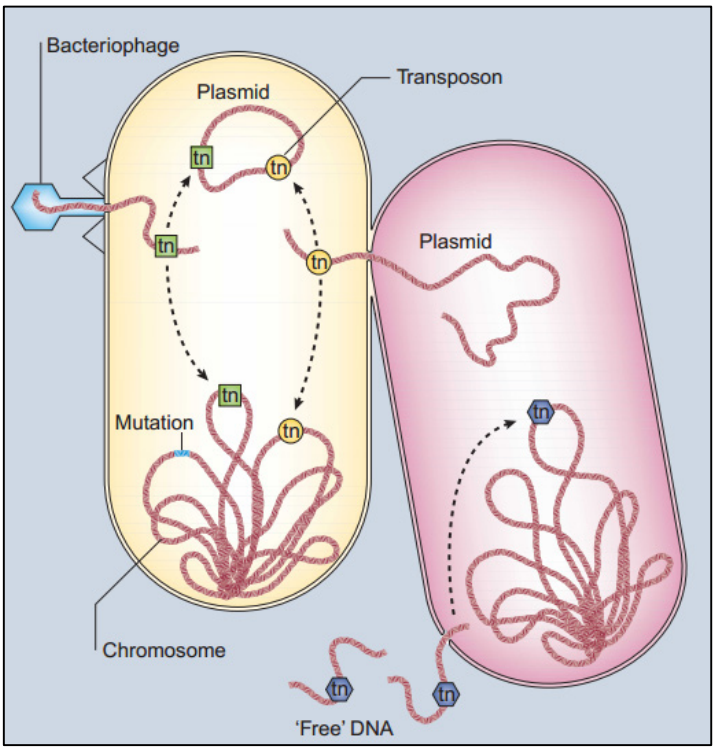

Figure 1.4: Schematic representation of the genetics and spread of drug resistance. The drug resistance is mobile and the genes for resistance traits can be transferred among bacteria of different taxonomic and ecological groups by means of mobile genetic elements such as bacteriophages, plasmids, naked DNA or transposons (Levy and Marshall, 2004).

1.2. Antimicrobial peptides

1.2.1. Their History and Evolution

Antimicrobial peptides (AMP) are heterogeneous groups of relatively small molecules usually containing less than a hundred amino acids produced by almost all living organisms. The identification of these peptides can be traced back to the discovery of lysozyme by Alexander Fleming in 1921 (Fleming, 1922). Another well-known AMP has been documented in 1939 by discovering gramicidins in prokaryotic cells. They were isolated from *Bacillus brevis*. They had activity both *in-vitro* and *in-vivo* against a wide range of Gram-positive bacteria (Dubos, 1939) were the first commercially available AMPs antibiotics (Van Epps, 2006) (Figure 1.5).

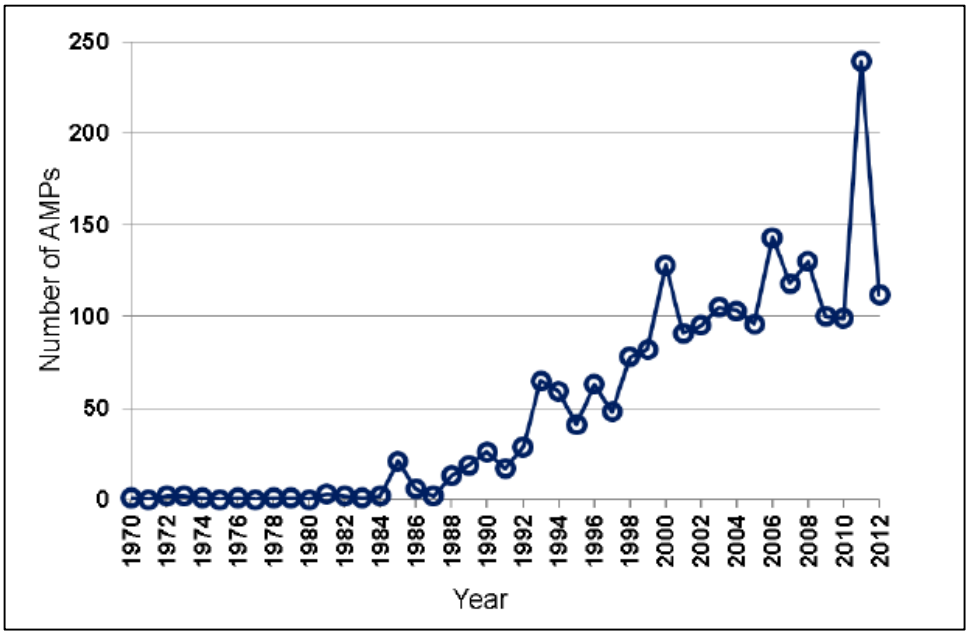

Figure 1.5: The antimicrobial peptides discoveries each year from 1970 to 2012. Data were obtained from the antimicrobial peptide database (http://aps.unmc.edu/AP) (Wang and Wang, 2004; Wang *et al*., 2009).

With the discovery of penicillin and streptomycin in 1943 during the "Golden Age of antibiotics," the interest in AMPs declined. This led to less interest in the therapeutic potential of natural host antibiotics such as lysozyme and its importance in immune defence strategies (Bentley, 2009; Zaffiri *et al*., 2012). However at the end of the

"Golden Age of antibiotics" and with the rise of multidrug-resistant microbial pathogens in the early 1960s there was a resumed interest in host defence molecules (Katz *et al*., 2006). This was prompted in the 1950s and 1960s, (Figure 1.5) by the discovery of cationic peptides and their ability to kill bacteria via oxygen-independent mechanisms in human neutrophils (Zeya and Spitznagel, 1966).

The isolation of inducible cationic antimicrobial proteins P9A and P9B in 1981 by injecting bacteria into the pupae of the silk moth, *Hyalophora cecropia*, was generally considered a landmark study the first major AMPs (Steiner *et al*., 1981; Steiner *et al*., 2009). Subsequently in 1987, another landmark study (Zasloff, 1987) isolated and characterized cationic AMPs from the African clawed frog, *Xenopus laevis*, called peptides magainin. A few years later, β-defensins and θ-defensins, which differ from α-defensins with respect to their cysteine pairings, were characterized, from bovine granulocytes (Selsted *et al*., 1993) and leukocytes of the rhesus monkey respectively (Tang *et al*., 1999). In the mid-1990s, the first anionic AMPs was discovered in *X. laevis* (Brogden *et al*., 1997) and several other such peptides were characterised in ruminants, including sheep and cattle (Brogden *et al*., 2003).

The early studies on AMPs have been extensively studied in plants, insects and other invertebrate organisms that lack an adaptive immune system (Bulet *et al*., 2004). However most of the current understanding of AMPs has been obtained from studies on those isolated from amphibian skin secretions, which is a rich source of these peptides (Nicolas and El Amri, 2009). These studies established that AMPs exist in virtually all multicellular organisms and these peptides play an important role in immunity in all organisms, including humans (Pasupuleti *et al*., 2012). AMPs have been identified at most sites of the human body normally exposed to microbes such as the skin and mucosae and are produced by a number of blood cell types, including neutrophils, eosinophils, and platelets (Malik and Batra, 2012). Studies suggest that AMPs can produce either constitutive or induced by inflammation or injury to protect the organism from infection. For example, α-defensins and dermcidin (the precursor of AMPs involved in skin defence) tend to be produced constitutively,

whereas the majority of β-defensins are inducible (Schittek *et al*., 2001; Auvynet and Rosenstein, 2009).

More than 2,000 natural AMPs have been found in eukaryotes and in bacteria (Thomas *et al*., 2010; Piotto *et al*., 2012) and the availability of databases has allowed comparison between AMPs and to postulate structure–function relationships and mechanisms of antimicrobial action. The diversity of these AMPs may have in part resulted from random substitutions involving the operation of a mutagenic error-prone DNA polymerase similar to that reported for some bacteria (Nicolas *et al*., 2003; Janion, 2008). Developing new AMPs with an ability to combat new or altered microbial pathogens would likely have an evolutionary advantage. Indeed, it has been suggested that AMPs and microbial resistance mechanisms have co-evolved. This leads to a transient host-pathogen balance that has shaped the existing range of these peptides found in nature (Peschel and Sahl, 2006). For example, plants and humans are susceptible to different pathogens and thus their defences are exposed to different selective pressures. In general plants are much more susceptible to fungi compared to other microbes, fungal pathogenicity would select for survivors with antifungal defensins. However, humans are more susceptible to bacteria than fungi and thus bacterial pathogenicity would select for survivors with antibacterial defensins (Stotz *et al*., 2009).

1.2.2. The antimicrobial peptide database

The antimicrobial peptide database (APD) also enables users to obtain the statistical parameters of peptides such as length, net charge, hydrophobic content and structure type for a single peptide or a group of candidates (Wang and Wang, 2004). The distribution of all the AMPs as a function of peptide length is given in Figure 1.6 (A). It is clear that the majority of (88%) AMPs possess 11–50 amino acids with the most variable lengths of 21–30 residues. Considering the peptide at neutral pH at 7 in solution, the net charge of an AMP involves acidic amino acids aspartic acid (D), glutamic acid (E), and basic arginine (R) and lysine (K). The charge distribution of AMPs suggests that 86% of AMPs have a net charge between 0 and +7 (maxima at

+2 and +3). The hydrophobic percentage is the ratio between the sum of the amino acids in the hydrophobic group and the total number of amino acids. A distribution of all the AMPs as a function of peptide hydrophobic percentage is given in Figure 1.6 (C). The majority of AMPs (89%) contain a hydrophobic percentage in the range of 31–70% (the maximum at 41–50%). In the APD database, the 20 standard amino acids are classified into four groups: hydrophobic (L, I, V, M, F, W, A, and C), PG (P and G), polar (S, T, N, Q, and Y), and charged (D, E, K, R, and H). To a large extent, the amino acid composition of AMPs determines peptide activity (Mishra and Wang, 2012). The APD is the first AMP database that allows users to calculate the amino acid composition profile for each peptide or a selected group of AMPs with a specific activity or property (Wang and Wang, 2004; Wang *et al*., 2009; Wang, 2013). Figure 1.6 (D) is such a profile for all the AMPs, where on average amino acids L, G, and K have the highest frequencies.

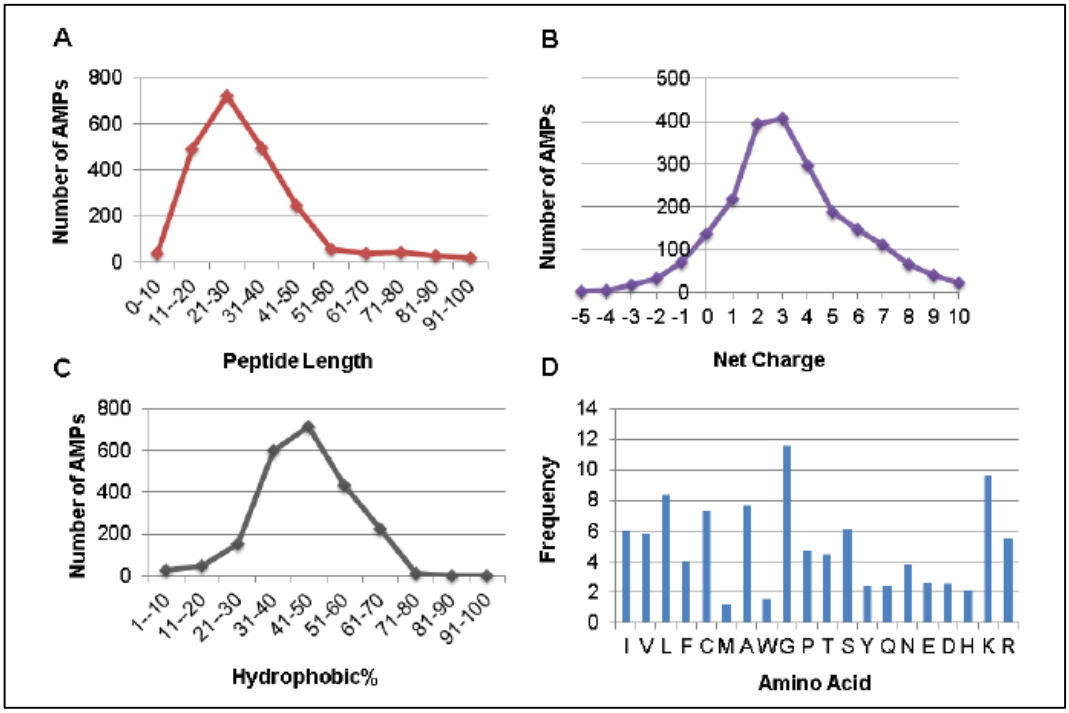

Figure 1.6: AMP characters and function distribution. The peptide length (A), the net charge (B), hydrophobic percentage (C) and the frequency of the 20 amino acids of AMPs in the APD (D). Data obtained from the APD (http://aps.unmc.edu/AP) (Wang, 2013).

1.2.3. Other biological activities of AMPs

The primary functions of AMPs are direct antimicrobial activities, but more recent studies have indicated that these peptides modulate immunity and immune-cell function under physiological conditions (Hancock *et al*., 2012) and that these activities are the primary role of these peptides in the host. The immunomodulatory properties of AMPs influence innate immunity and include (i) reduction in the levels of pro-inflammatory cytokines produced in response to microbial signature molecules; (ii) modulation of the expression of chemokines, reactive oxygen species and reactive nitrogen species (for example, nitric oxide); (iii) stimulation of angiogenesis; (iv) enhanced wound healing; (v) leukocyte activation; and (vi) macrophage and leukocyte differentiation (Figure 1.7) (Nijnik and Hancock, 2009; Afacan *et al*., 2012; Hancock *et al*., 2012).

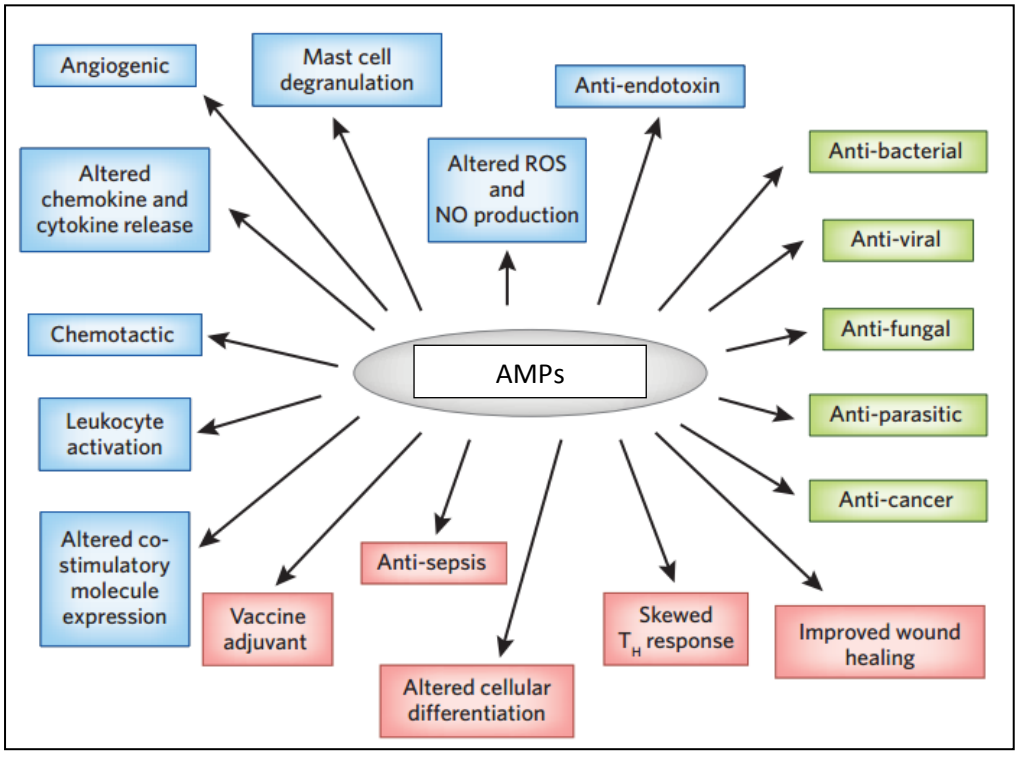

Figure 1.7: Overview of the biological activities of AMPs and Host Defence Peptides. Direct cytotoxic activities are shown in green, direct immunomodulatory properties are shown in blue and indirect immunomodulatory properties that are a consequence of direct immunomodulatory properties are shown in pink. ROS, reactive oxygen species; NO, nitric oxide (Hilchie *et al*., 2013) .

1.2.4. Cationic Antimicrobial Peptides

Cationic antimicrobial peptides (CAMPs) are important components of the innate immune systems in all living organisms including bacteria, fungi, plants and animals. These peptides are active against bacteria, fungi, viruses, and pests such as insects. They are generally between 12 and 50 amino acids, containing basic amino acids, with an overall net positive charge of +2 to +9 (Hancock and Diamond, 2000). In addition, approximately 50% of the amino acids are hydrophobic. The presence of basic and hydrophobic amino acids promotes folding of linear AMPs into amphipathic secondary structures upon contact with lipid bilayers (Hancock and Rozek, 2002). CAMPs use a variety of mechanisms to kill microbes but it is generally accepted that the interaction of these peptides with the membranes of target organisms is an important part of their mechanism of interaction. CAMPs show promise as candidates for development as novel antimicrobials (Phoenix *et al*., 2013).

CAMPs are consist of basic amino acids such as arginine and/or lysine (Wang *et al*., 2009), which gives these peptides a net positive charge, despite having positively charged moieties such as a C-terminal amide group (Brogden, 2005; Dennison *et al*., 2005). The presence of these basic residues and other charged moieties is generally accepted to be the primary driver underpinning the ability of CAMPs to target the membranes of bacteria, fungi, and other microbes. The vast majority of CAMPs also possess amphiphilic structures, revealed as a spatial segregation of hydrophobic and hydrophilic residues on their molecular surface, which allows them to partition into microbial membranes. On partitioning into membranes, CAMPs orientate such that their apolar regions interact with the membrane lipid core while their polar regions concomitantly engage in electrostatic interactions with the membrane lipid head-group region (Stromstedt *et al*., 2010; Teixeira *et al*., 2012).

CAMPs show great diversity and are classified into many subgroups depending upon the criteria chosen, including origin, size, structure, amino acid sequence, biological action, and antimicrobial mechanism (Hwang and Vogel, 1998; Wang *et al*., 2010).

There are three broad classes of CAMPs: those that adopt a (1) α-helical structure (eg. cathelicidins, magainin peptides), (2) β-sheet structure with a cysteine-stabilized architecture (e.g. defensins), and (3) extended peptides that are rich in specific residues (Nguyen *et al*., 2011). Less common are looped peptides (e.g. bactenecin) and extended structures rich in arginine, glycine, histidine, proline, and/or tryptophan (e.g. indolicidin) (Guani-Guerra *et al*., 2010; Steinstraesser *et al*., 2011). Structure-function studies suggest that certain biological properties of AMPs are dependent on specific structural characteristics. However, out of 2000 AMPs listed, approximately 3% possess more than one domain such as a α-helical and β-sheet structure while around 70% of these peptides cannot be classified or have not been structurally characterized (Wang *et al*., 2010).

The mechanisms underpinning the antimicrobial activity of human defensins is not well understood, although cationicity and hydrophobicity have been shown to be important determinants for the antibacterial activity of both human α-defensins and β-defensins. It is generally believed that the antimicrobial activity of human defensins involves compromising microbial membrane integrity which leads to collapse of the membrane's electrochemical potential and proton motive force, allowing the leakage of cellular contents and the entry of defensins into the cell to interact with cytoplasmic targets, including DNA and RNA (Ganz, 2003; Taylor *et al*., 2008; Hazlett and Wu, 2011; Lehrer and Lu, 2012).

1.2.5. Models for the Membrane Interactions of Antimicrobial Peptides

The cell membrane (CM) of cells is a complex network of lipids and proteins with a molecular organization that makes a major contribution to both maintaining the structural integrity of cells and the activities of proteins that are associated with the lipid bilayer. The lipid molecules within a lipid bilayer are dynamic and actively involved in biological functions, and scaffold for the activities of proteins and peptides (Yeagle, 2012).

The association of AMPs with CM lipid can lead directly to the inactivation of microbes via cell lysis (Nguyen *et al*., 2011; Guilhelmelli *et al*., 2013) or internalization of these peptides attack on intracellular targets (Marcos and Gandía, 2009; Nicolas, 2009). However, in order to reach and interact with microbial CMs, AMPs have to negotiate and pass through a variety of enveloping structures (Figure 1.8). These structures vary across target organisms in their physiochemical properties, permeability, and thickness, and therefore influence the susceptibility of these organisms to AMPs (Papo *et al*., 2002; Grün *et al*., 2005).

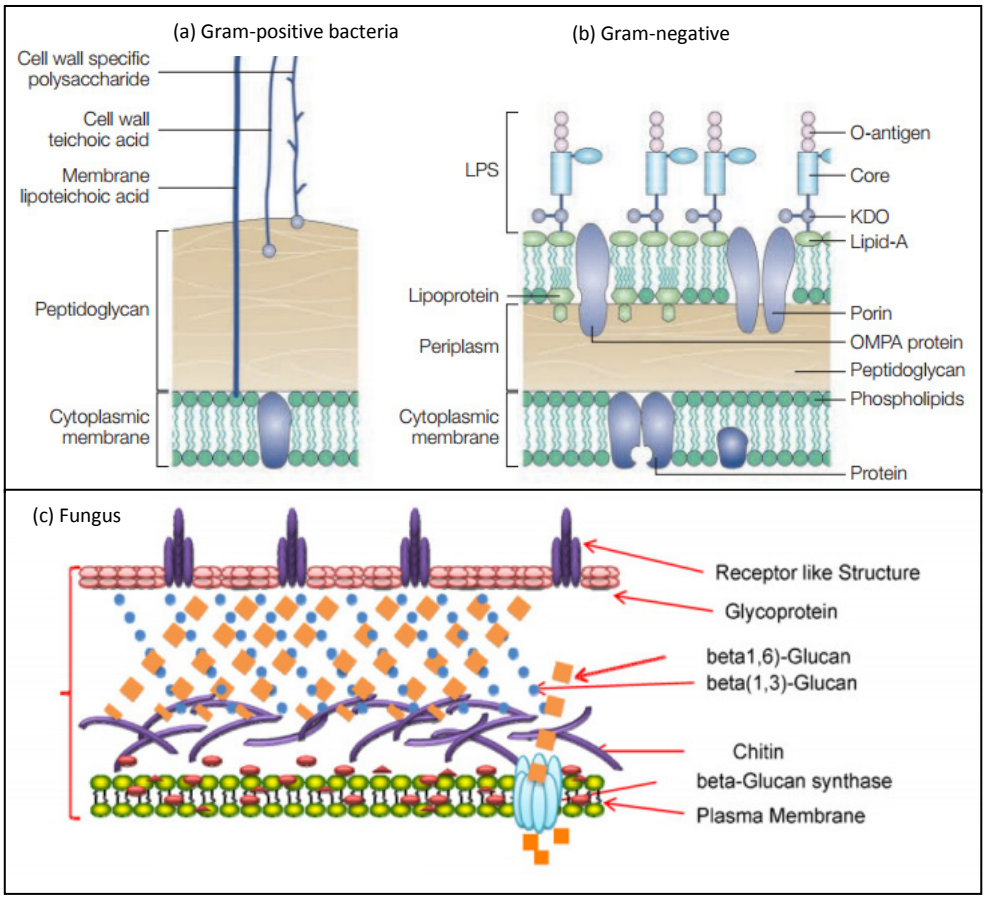

Figure 1.8: Structural features of the cell walls of Gram-positive, Gram-negative bacteria and fungus. KDO, 3-deoxy-D-manno-octulosonate; LPS, lipopolysaccharide; OMPA, outer membrane protein A Schematic representations of the cell envelopes of Gram-positive bacteria (a), Gram- negative bacteria (b), and fungi (c) (a and b adapted from (Lolis and Bucala, 2003); c adapted from (Dai *et al*., 2009).

In general, cationic AMPs (CAMPs) are by far the best characterized AMPs. These peptides passage through the microbial envelope appears to involve low-affinity, electrostatic interactions between these peptides and a range of anionic moieties that promote the migration of these peptides to the CM of the microbe (Mayers, 2009). The affinity level of CAMPs for these anionic moieties appears to be crucial as low affinity can reduce the targeting efficacy but higher affinities can bind anionic envelope components sufficiently strongly to prevent their passing through to the microbial CM and thereby inhibit their antimicrobial action. This kind of inhibitory actions have been reported for the interaction of CAMPs with a variety of anionic cell surface moieties which bind and thereby reduce the toxicity of these peptides to erythrocytes, non-cancerous cells and transformed cells (Papo and Shai, 2005; Bucki *et al*., 2008; Fadnes *et al*., 2009).

In fungi, CAMPs migrate through the cell envelope by interaction with a number of anionic components including chitin chains, (1-3)-β-glucan, and phosphomannans or related compounds (Figure 1.8) (Marcos and Gandía, 2009; De Brucker *et al*., 2011). CAMPs can pass through anionic exo-polysaccharides such as alginate (Batoni *et al*., 2011) formed by fungi and bacteria that participate in biofilms. CAMPs interact with anionic Gram-positive bacterial cell wall components such as teichoic and lipoteichoic acids while migrating via peptidoglycan layer to interact directly with the CM (Figure 1.8) (Read and Duncan, 2011). It has been shown that interaction with these anionic polymers is important for the antimicrobial activity in some CAMPs, such as defensins, which are β-sheet peptides produced by eukaryotes, indeed reducing the negative charge in those bacteria decreases their susceptibility to defensins (Peschel and Collins, 2001).

With Gram-negative bacteria, CAMPs first encounter the outer membrane, with anionic lipopolysaccharide (LPS) as the major component of its external leaflet (Figure 1.8) (Mayers, 2009). The majority of CAMPs have a high affinity for LPS, which allows these peptides to cross the outer membrane via a self-promoted uptake pathway. Essentially, these CAMPs interact with lipid A moieties of LPS, which serves as an anionic binding site, thereby competitively replacing $Mg^{2+}$and Ca^{2+} ions

that help maintain cell surface stability via the cross-linking of carboxylated and phosphorylated head-groups of lipids. Removal of these ions leads to disruption of the outer membrane, and allows the peptides to migrate across the peptidoglycan layer and accumulate in the periplasmic space before interacting with components of the CM (Laverty *et al*., 2011). A further consequence of CAMPs binding to LPS and lipoteichoic acid is the neutralization of the endotoxic activity associated with these molecules in bacterial sepsis, thereby avoiding the exalted inflammatory response induced by the antibacterial activity of other antibiotics (Brandenburg *et al*., 2011). The generally held view is that the antimicrobial action of CAMPs does not involve the use of protein and lipid membrane receptors, although such use is well established for some prokaryotic AMPs (Zhao, 2011). Recent studies have suggested that some CAMPs with non-lytic antibacterial mechanisms utilize protein receptors for membrane translocation and interaction with cytoplasmic targets (Giralt, 2014).

1.2.6. Cell membrane associated Factors That Affect the Antimicrobial Action of CAMPs

The initial association of CAMPs with the microbial CM is driven by electrostatic interactions between the net positive charged peptides and net negative charged cell membranes (Stromstedt *et al*., 2010). The CMs of bacteria are generally rich in anionic phospholipids, primarily phosphatidylglycerol (PG) and cardiolipin (CL), which are either present at low levels or absent from mammalian cells (Figure 1.9) (Lohner and Prenner, 1999). Indeed, it is the possession of this net negative charge that is believed to underpin the selectivity of CAMPs for bacterial cells over eukaryotic cells, since the latter carry a net neutral charge due to the presence of zwitterionic lipids such as PE, sphingomyelin (SM), and phosphatidylcholine (PC) (van Meer *et al*., 2008).

Nevertheless, there are considerable differences between the levels of anionic lipids found in the membranes of different bacterial species and classes as can be seen from Figure 1.9. The CMs of Gram-positive bacteria are primarily composed of lipids that are derived from PG, exemplified by that of *Staphylococcus aureus*, which contains

around 57% PG, 38% lysylated PG (LysylPG), and 5% CL, a dimer of PG (Figure 1.9). In contrast, the CMs of Gram-negative bacteria are mainlycomposed of PE, typically that of *Escherichia coli*, which contains approximately 80% PE, 6% PG, and 12% CL (Figure 1.9).

In general, anionic lipids constitute over 80% of the total lipid found in the membranes of Gram-positive bacteria, but less than 30% of the total lipid present in those of Gram-negative bacteria (Epand and Epand, 2011). It would therefore seem that varying levels of anionic lipid contribute to the differing bacterial specificities shown across CAMPs given that many of these peptides show a preference for either Gram-positive or Gram-negative bacteria (Wang *et al*., 2009).

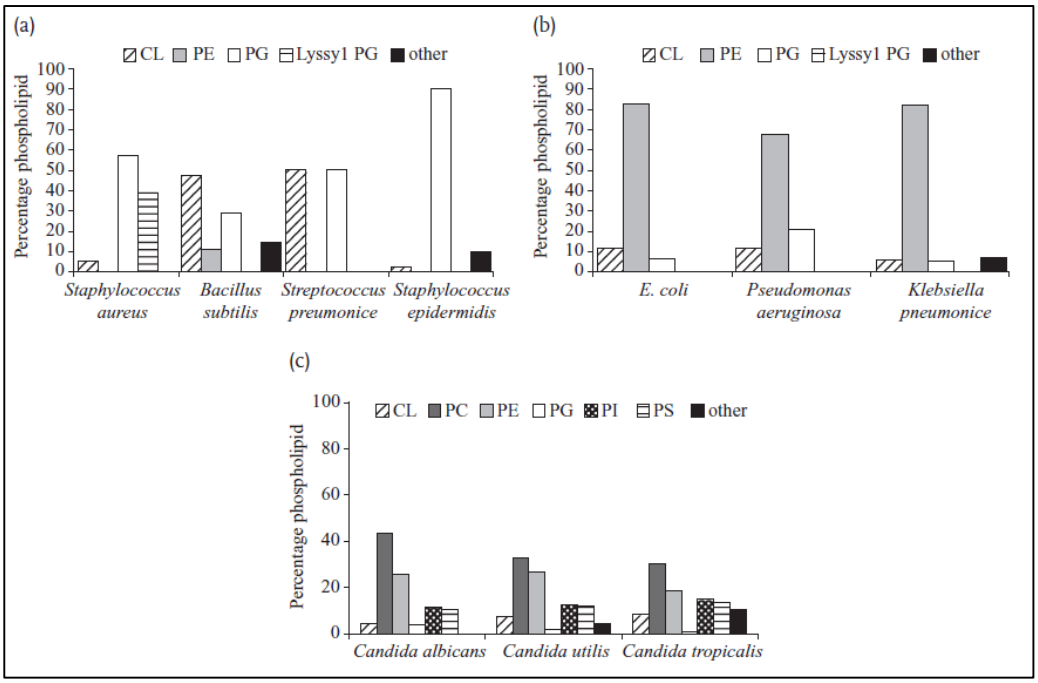

Figure 1.9: Lipid composition of phospholipids present in the cell membranes of different bacteria. Gram-positive bacteria (a), Gram-negative bacteria (b), and fungi (c). These lipids include cardiolipin (CL), phosphatidylethanolamine (PE), phosphatidylglycerol (PG), lysylated phosphatidylglycerol (Lysl PG), phosphatidylinositol (PI), and phosphatidylserine (PS) (Ratledge and Wilkinson, 1988).

Upon interaction with the microbial CM, a number of factors are able to modulate the activity of CAMPs and their ability to partition into these membranes. A major factor is the transmembrane potential, which results from differing extents and rates

of proton flux across the membrane (Fjell *et al*., 2012). Mammalian membranes maintain a weak transmembrane potential, but due in part to their high levels of anionic lipids, the CM of fungi (Harris *et al*., 2009) and bacteria (Bradshaw, 2003) maintain a relatively strong transmembrane potential. This high transmembrane potential strongly attracts CAMPs and enhances both their selectivity and toxicity for microbial cells (Wang *et al*., 2010). A similar mechanism appears to underpin the ability of CAMPs to target cancer cell membranes, which exhibit loss of lipid asymmetry, resulting in the presence of relatively high levels of anionic lipid on their outer surfaces and an accompanying high transmembrane potential (Fadeel and Xue, 2009).

In contrast to bacteria, the CM of fungal cells tend to share similar properties to mammalian membranes, having a net neutral charge due to the presence of zwitterionic lipids including PC, PE, and SM (Figure 1.8) as well as possessing a number of fungal-specific lipids (Thevissen *et al*., 2003). In comparison to bacteria, there has been far less research into the antifungal mechanisms of CAMPs, but there is evidence to show that interaction of these peptides with anionic lipid and the fungal CM leads to membrane lysis and plays a role in their antifungal mechanisms (Qi *et al*., 2010). In addition, it has been observed that CAMPs with primarily antifungal activity tend to possess a high proportion of neutral polar residues, which led to the suggestion that the peptides that interact with the fungal CM may show different structure–activity relationships to those used by CAMPs in their other antimicrobial activities (de Oca, 2013), possibly involving an ability to form complexes with fungal lipids (Lopez-Garcia *et al*., 2004). However, other CAMPs show only a weak ability to permeabilize the fungal CM and appear to inactivate fungi by other mechanisms involving multiple activities such as facilitating the efflux of ATP from the cell (Tanida *et al*., 2006). Taken with the fact that, as described above, some CAMPs utilize lipid receptors to promote their antifungal action, these peptides appear to use a diverse range of antifungal mechanisms as compared to their antibacterial mechanisms.

1.2.7. Established Models for the Membrane Interactions of AMPs

Over the last four decades, three major models have become established to study mechanisms of membrane invasion used by α-CAMPs to exert their antibacterial activity. These models are generally referred to as the barrelstave pore model, the toroidal pore model, and the carpet mechanism, and have been extensively reviewed elsewhere (Brogden, 2005; Jenssen *et al*., 2006; Huang *et al*., 2010). Here, an overview of these models is presented along with a discussion of variants that have been recently described.

1.2.8. Models of intracellular killing

Despite the fact that AMPs cause cell membrane rupture which eventually leads to the lysis of microbial cells, there is increasing speculation that these effects are not the only mechanisms of microbial killing. There is increasing evidence to indicate that antimicrobial peptides have other intracellular targets (Figure 1.10). Some antimicrobial peptide such as Bac7 fragments 1–16, 1–23 and 1–35 do not permeabilize *E. coli* but yet cause a 2–5 log reduction in the number of organisms (Gennaro and Zanetti, 2000).

Cationic peptide Pep5 activates autolysin in *Staphylococcus simulans* in the presence of lipoteichoic and teichuronic acids, which might explain the lysis of treated cells (Bierbaum and Sahl, 1987). Interestingly, in the absence of lipoteichoic acids the activity of partially purified autolysins is also stimulated directly by Pep5. The activity of host-derived secretory phospholipase for liposomes that contain anionic phospholipids or phosphatidylcholine is markedly enhanced by magainin 2, indolicidin and temporins B and L in 5 μM Ca^{2+} (Zhao and Kinnunen, 2003).

The translocation of peptides across the cytoplasmic membrane involves unique mechanisms. Buforin II, which is a linear α-helical peptide with a proline hinge penetrates and accumulates in the cytoplasm without permeabilizing the cytoplasmic membrane (Park *et al*., 2000). The mechanism by which this peptide is translocated

was revealed by fusing the proline-hinge region of buforin II with a non-cell-penetrating peptide. With amino-terminal helix of magainin 2-the hybrid peptides readily penetrated bacterial cytoplasmic membranes and accumulated in the cytoplasm, with concomitant antimicrobial activity (Park *et al*., 2000). Arginine-rich peptide groups, such as arginine-rich peptides, RNA-binding peptides, DNA-binding peptides and polyarginine and arginine-rich antimicrobial peptides, all readily and efficiently translocate across both cellular and nuclear membranes (Futaki *et al*., 2001).

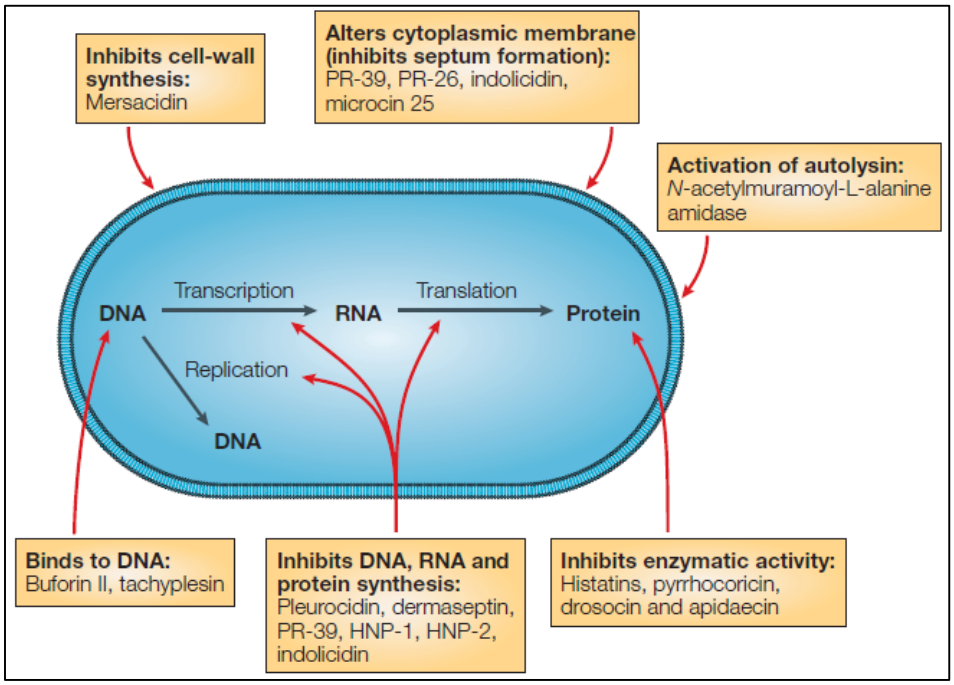

Figure 1.10: Mode of action for intracellular antimicrobial peptide activity. In this figure *Escherichia coli* is shown as the target microorganism (Brogden, 2005).

Apidaecin, a short, proline-rich antibacterial peptide, is translocated by a permease/transporter-mediated mechanism (Casteels *et al*., 1993). Once in the cytoplasm, translocated peptides can alter the cytoplasmic membrane septum formation, inhibit cell-wall synthesis, inhibit nucleic-acid synthesis, inhibit protein synthesis or inhibit enzymatic activity (Brogden, 2005). Lantibiotics are antimicrobial peptides from Gram-positive bacteria that contain the thioether amino acid lanthionine. The lantibiotic mersacidin inhibits peptidoglycan biosynthesis by interfering with membrane associated transglycosylation (Brötz *et al*., 1998). Buforin

II binds to *E. coli* DNA and RNA (Park *et al*., 1998), and tachyplesin binds in the DNA minor groove (Yonezawa *et al*., 1992). The α-helical peptides (pleurocidin and dermaseptin), proline- and arginine-rich peptides (indolicidin) and defensins block thymidine, uridine and leucine uptake in *E. coli*, showing that they inhibit DNA, RNA and protein synthesis (Lehrer *et al*., 1989; Boman *et al*., 1993; Subbalakshmi and Sitaram, 1998; Patrzykat *et al*., 2002).

At their minimal inhibitory concentrations, pleurocidin and dermaseptin both inhibit nucleic acid and protein synthesis without damaging the *E. coli* cytoplasmic membrane (Boman *et al*., 1993; Patrzykat *et al*., 2002). Indolicidin (100 μg/ ml) completely inhibits DNA and RNA synthesis in *E. coli* but does not have any effect on protein synthesis. At concentrations of 150 and 200 μg/ ml, protein synthesis is markedly inhibited (Subbalakshmi and Sitaram, 1998). Histatins bind to receptors on the fungal cell membrane, enter the cytoplasm and induce the nonlytic loss of ATP from actively respiring cells (Kavanagh and Dowd, 2004). Their action can also disrupt the cell cycle and lead to the generation of reactive oxygen species (Andreu and Rivas, 1998).

1.3. Antimicrobial peptoids

1.3.1. Introduction

AMPs have been actively studied for decades but they have not widely been used in the clinic (Hancock and Sahl, 2006). This is due in part to the vulnerability of these peptides to rapid *in-vivo* degradation and low bioavailability. AMPs have found difficulty in the transition of *in-vitro* activity into *in-vivo* efficacy (Hancock and Sahl, 2006). This is due to their sensitivity to biologically relevant conditions such as high salinity of plasma, as divalent cations may compete with such peptides for binding sites on the negatively charged bacterial surface (Deslouches *et al*., 2005). Moreover, AMPs are susceptible to degradation by serum proteases (Knappe *et al*., 2010) as well as to protein binding (Yeaman *et al*., 2002). However, peptidomimetic polymers (peptide isomers) of AMPs can play a crucial role replacing peptides due to their

susceptibility to proteolytic enzymes while retaining their beneficial features (Chongsiriwatana *et al*., 2008; Dohm *et al*., 2011).

The backbone of the peptidomimetic polypeptoid is identical to that of a polypeptide in protein, but the side chain is added to the amide nitrogen rather than the α-carbon in peptoids (Figure 1.11). This difference removes inter- and intrachain hydrogen bonding in the backbone and also eliminates the main-chain chirality (Rosales *et al*., 2010; Rosales *et al*., 2012). They lack backbone hydrogen bonding due to the absence of hydrogen bond donors and they cannot form β-sheets and due to this they do not aggregate as easily as peptides (Dohm *et al*., 2011). Peptoids can be considered essentially peptide isomers, but the seemingly simple shifting of the side chains to the amide nitrogen significantly changes the properties of the isomer peptoid relative to the peptide. The most biologically relevant consequence of this shift is protease resistance, which arguably increases their therapeutic potential (Dohm *et al*., 2011).

Polypeptoids or poly-*N*-substituted glycines are known as peptidomimetic polymers. They offer many advantageous properties for studies in biochemistry, molecular biophysics, diagnostics, and medicine (Dohm *et al*., 2011; Zuckermann, 2011). Peptoids are synthesised using solid phase synthesis, a stepwise polymerization method is applied to grow polymer chain and it is anchored to a solid support while coupling reagents are iteratively passed over the matrix and adding one monomer at a time to afford a polymer with an exact monomer sequence and near absolute monodispersity (Figure 1.12). The submonomer polymerisations are simple chemical building blocks that can be used to assemble a monomer in the course of stepwise polymer formation in which the functional side chain is incorporated. This approach towards oligo- and polypeptoids has been pioneered by Bartlett and co-workers and later modified and refined in the groups of Zuckermann, Kirshenbaum, Barron, and Messersmith in late-1980s (Simon *et al*., 1992; Armand *et al*., 1997; Park *et al*., 2011).

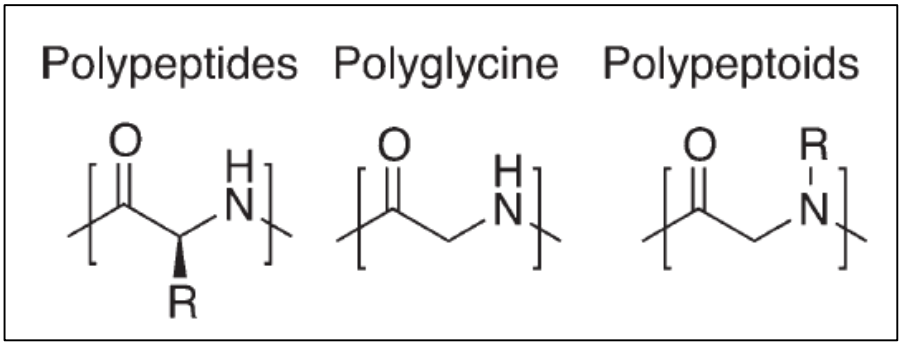

Figure 1.11: Schematic representation of polypeptoids (Luxenhofer *et al.*, 2013).

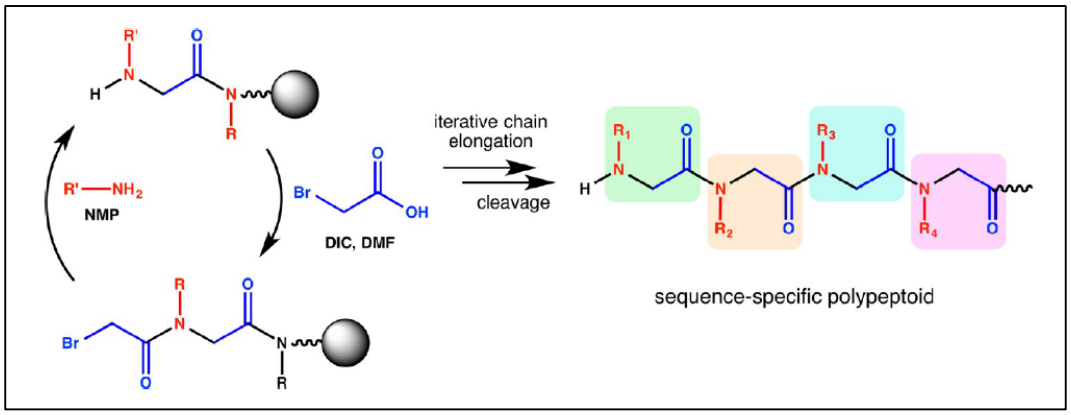

Figure 1.12: Schematic representation of Solid-phase submonomer method. This allows the rapid synthesis of sequence-specific peptoids from cheap and readily available starting materials (amines and haloacetic acid submonomers), using a repeating two-step monomer addition cycle of acylation. Each two-step cycle is performed at or near room temperature and takes <1 h and can be performed manually or by automated synthesizers. DIC = N,N0-diisopropylcarbodiimide, NMP =N-methylpyrrolidinone (Sun and Zuckermann, 2013).

The microwave-assisted solid-phase synthesis of polypeptoids can reduce the reaction time dramatically (from ~1 hour to just a few minutes per monomer addition) with high purity and yields of products as good as or even better than those achieved using standard methods (Fara *et al.*, 2006; Messeguer *et al.*, 2008). Additionally, the two-step submonomer cycle involves only the simple pipetting of stable reagent solutions at room temperature. Therefore, the entire procedure can be accomplished either manually or automatically and can be readily adapted to most commercial peptide synthesizers (Bradley *et al.*, 1997; Tran *et al.*, 2011).

Peptoids are also called poly-*N*-substituted glycine monomers. These monomers can be variable depending on the amino acid side-chain attached to the N atom. From a synthetic point of view, polypeptoids are a class of highly designable polymers. They are particularly well suited for AMP mimicry because they are easily synthesized on solid phase (by using conventional peptide synthesis equipment) with access to diverse sequences at relatively low cost (Zuckermann *et al*., 1992; Chongsiriwatana *et al*., 2008). From a synthetic point of view, polypeptoids are a class of highly designable polymers. Any chemical functionality available as a primary amine can be incorporated via a submonomer synthetic method and therefore these peptoids are highly and finely tunable (Zuckermann *et al*., 1992). This method also gives precise control over the exact placement and choice of monomers with exceptionally fine degree of control over potential functional properties (Zuckermann *et al*., 1992; Rosales *et al*., 2010).

1.3.2. Peptoids and their potential use

In 1994, Zuckermann and co-workers discovered several potent peptoid trimmer ligands for G-protein coupled receptors (Zuckermann *et al*., 1994) and the urokinase receptor (Ross *et al*., 2008). They used large synthetic peptoid libraries of chemically diverse short oligomers and screened them for biological activities. This was one of the first demonstrations that a diverse combinatorial library of synthetic compounds could provide high-affinity ligands for pharmaceutically relevant receptors (Gibbons *et al*., 1996). This discovery inspired many groups in both biopharmaceutical industry and academic laboratories to investigate potential therapeutics from peptoid libraries (Garcia-Martinez *et al*., 2002; Mora *et al*., 2005). Many specific biologically active peptoid oligomers have been described. For example, a library of cationic and hydrophobic peptoids yielded novel compounds with antimicrobial activity. These peptoids are a promising class of antimicrobial therapeutics, as they exhibit broad-spectrum antibacterial activity and low mammalian cytotoxicity (Chongsiriwatana *et al*., 2008).

Using combinatorial peptoid microarrays, the Kodadek lab developed a general method to identify diagnostically useful antibodies without the need for antigen identification. They demonstrated the discovery of potentially useful diagnostic biomarkers in humans via identification of candidate IgG biomarkers for Alzheimer's disease (Reddy *et al*., 2011). In addition to linear protein ligands, several cyclic peptoid ligands have also been explored. Peptoid fluorophore conjugates have also been prepared as reporters for intracellular delivery (Kwon and Kodadek, 2008; Dhaliwal *et al*., 2011) or for folding into secondary structures (Birtalan *et al*., 2011; Fuller *et al*., 2011). These examples demonstrate that peptoid libraries are a powerful, inexpensive, and convenient source of diverse ligands for a variety of biomedical applications. Peptoids could be improved if we could understand their pharmacokinetics parameters such as; (1) bioavailability, (2) excretion mechanisms, (3) are peptoids and (4) toxicity such as hepatotoxicity. However, very little has been published in this area, and such studies are critical for the development of peptoids as potential pharmaceuticals (Dohm *et al*., 2011).

Peptoid polymers exhibit excellent biocompatibility and potent biological activities similar to polypeptides (Fowler and Blackwell, 2009; Lee *et al*., 2010). For example, they can fold into protein-mimetic secondary and tertiary structures (Lee *et al*., 2008) serve as an effective siRNA transfection reagent (Utku *et al*., 2006), diagnostic agents (Reddy *et al*., 2011), lung surfactant mimetics (Brown *et al*., 2008), antimicrobial agents (Chongsiriwatana *et al*., 2008) and other therapeutics (Zuckermann and Kodadek, 2009) and can be incorporated site-specifically into polypeptide sequences (Lee and Zuckermann, 2011) and exhibit stability to proteolysis (Miller *et al*., 1995).

1.3.3. Antimicrobial peptoids

Non-natural mimics of AMPs are needed to provide better structural stability and bioavailability as therapeutic candidates to treat bacterial infection (Bessalle *et al*., 1990; Arnt and Tew, 2002; Sanborn *et al*., 2002). The *in-vivo* structural stability of peptoids affords them a great potential for development as effective antimicrobial

agents (Patch and Barron, 2003; Chongsiriwatana *et al*., 2008). Recently, Fowler and Blackwell (2009) reviewed the structure activity relationships of antimicrobial peptoids or "ampetoids" that were developed by Barron and co-workers in 2003. Peptoids have been developed to mimic the AMP, with an emphasis on N-terminal alkylation, cyclization, and reduction in hydrophobicity with the aim of improving activity while substantially reducing mammalian cytotoxicity. Strategies to incorporate a single peptoid residue into a peptide, creating a peptide-peptoid hybrid with improved therapeutic potential, are also presented. Finally, the *in-vivo* biocompatibility and efficacy of antimicrobial peptoids to treat bacterial infections have been discussed (Chongsiriwatana *et al*., 2008).

Previous studies have shown that antimicrobial peptoids are both structural and functional mimics of AMPs (Patch and Barron, 2003). Ampetoids are mimics of the magainins, a class of AMPs that are relatively short, cationic, and α-helical, and have similar antimicrobial properties (Patch and Barron, 2003). A study in 2008 determined that the selectivity of peptoids towards bacteria (*E. coli* ATCC 35218 and *B. subtilis* ATCC 6633) over mammalian cells (lung epithelial A549 cell line) was enhanced by net cationicity and moderate hydrophobicity, whereas haemolytic activity (red blood cell lysis) increased with high hydrophobicity and amphipathicity (Chongsiriwatana *et al*., 2008). In order for peptoids to be successful therapeutics, they must preferentially interact with bacteria over mammalian cells; when this criterion is met, peptoids are referred to as "selective". Considering the net cationicity, hydrophobicity, and amphipathicity, subsequent design and testing of several families of ampetoids in order to fully understand the effects of sequence length, hydrophobicity, helicity, and charge-to-length ratio on the activity and selectivity of ampetoids (Dohm *et al*., 2011). Notably, the reduction of hydrophobicity by removing hydrophobic residues made peptoids less haemolytic while retaining the antimicrobial activity (Dohm *et al*., 2011).

Multi-drug resistant (MDR) microorganisms have been used to study the true antibacterial potential of the peptoids derived from pexiganan. Further studies based on the peptoids' antimicrobial activities were scrutinised using computational model

prediction, their structures and sequences characters. The activities of the peptoids when predicted by the model were consistent with their corresponding activities witnessed *in-vitro* in cell-based assays, escalating the potential for computational studies to aid in the designing and testing of peptoids for this and other therapeutic applications (Dohm *et al*., 2011).

An earlier study in the Shai lab showed that the presence of an alkyl tail is believed to enhance peptoid penetration into and transport through the bacterial membrane. Interestingly similar behaviour was observed for alkylated peptides (Shai, 2002). This is due to the formation of micellization or other form of association based on hydrophobic chain-chain interactions that could explain their increased antimicrobial activity relative to the unalkylated variant. The N-terminal alkylation study also demonstrated that peptoid cytotoxicity toward red blood cells did not increase, whereas alkyl tail made peptoid were more toxic. Therefore, it is difficult to say if N-terminal peptoid alkylation would improve the therapeutic potential of peptoids; nevertheless, it is a promising technique to increase the therapeutic applicability of certain peptoids as drug candidates against certain bacterial strains (Dohm *et al*., 2011).

Another strategy put forth to reduce haemolysis of red blood cells by peptoids was to design cyclized peptoids. Studies revealed that cyclic linear peptoids have improved antimicrobial properties and selectivity. Since cyclization tends to reduce conformational flexibility by constraining the residues, it is believed that structural rigidity would increase the ability of peptoids to permeabilize the bacterial membrane (Unciti-Broceta *et al*., 2009). Successfully synthesized selective α-cyclic peptoids were created with better antibacterial and antifungal activity than linear peptoids. However, despite cyclization, the improvement in antibacterial activity was not comparable to the activity of previously reported linear peptoid-based mimics of magainin (Patch and Barron, 2003; Chongsiriwatana *et al*., 2008; Dohm *et al*., 2011).

1.3.4. Peptoid-Peptide Hybrid Mimics

Adding a peptoid residues or segments can improve the proteolytic stability of peptides, increase the antimicrobial activity and also reduce the cytotoxicity of AMPs. Engineering of a single amino acid in a peptide by a peptoid residue can introduce beneficial improvements to peptide. Shin and co-workers demonstrated that substituting Trp_{19} in the bee venom AMP melittin with "*N*Trp," a Trp-based peptoid residue, significantly reduced the mammalian cytotoxicity of the melittin analogue while still retaining its antibacterial and antifungal properties (Zhu *et al*., 2006; Dohm *et al*., 2011). In another study, the substitution of all Pro residues in Trp/Pro-rich AMPs such as indolicidin, tritrpticin-amide, and a symmetric tritrpticin analogue (all Arg's substituted with Lys's) with *N*Lys residues afforded more activity against Gram-negative and Gram-positive bacteria (MIC ~ 0.5 – 8 μM) and less haemolysis (minimum concentration that produces haemolysis (MHC) > 200 μM) (Zhu *et al*., 2007).

Further studies replaced a single Arginine or Leucine residue with *N*Arg and *N*Leu, respectively, in apidacin Ib, an AMP found in insects. Replacing cationic amino acids with cationic peptoid residues increased the proteolytic stability and reduced haemolysis, but with reduced antimicrobial activity (Gobbo *et al*., 2009). Introducing a single oligo-*N*-methoxyethyl-glycine (*N*meg) peptoid residue along with a spacer at the *N*-terminus of a peptide-based human respiratory syncytial virus (hRSV) fusion inhibitor, C_{20} peptide improved proteolytic stability and solubility, while retaining the peptide binding affinity (Park *et al*., 2011). These studies emphasize that incorporating a single peptoid residue or replacing positively charged amino acids by structurally similar peptoid residues improve the bioavailability and structural stability of peptides, thus increasing their attraction as therapeutic candidates.

1.3.5. Lysine-peptoid hybrids

A novel class of antibacterial compounds called lysine-peptoid hybrids were studied to identify antibacterial activity. The study revealed several lysine-containing analogues which displayed antibacterial activity against *S. aureus* and *E. coli*; MIC values for the most active ranging from <2–8 μM and 4–20 μM, respectively (Ryge and Hansen, 2005). The best candidates have an activity profile that is fully comparable with previous literature reports on naturally occurring antibacterial peptides like buforin II, cecropin P1, magainin II and nisin (Giacometti *et al*., 1999), antibacterial peptoids (Goodson *et al*., 1999) and peptide–peptoid hybrids (Shankaramma *et al*., 2003). Furthermore, they identified two analogues which showed a high selectivity toward *S. aureus* but not *E. coli*, and four analogues which were very active, but did not show any selectivity toward either of the bacterial strains tested (Ryge and Hansen, 2005).

Secondly, the haemolytic activity of the analogues correlated well with the number of lysine residues present in the hybrids and that haemolytic activity reduced very significantly, while retaining antibacterial activity (Ryge and Hansen, 2005). All of the analogues containing four or more lysine residues, showed a very low haemolytic activity and good antibacterial activity. They conclude that the lysine-peptoid hybrids are promising lead structures for developing new antibacterial agents.

In another study on lysine-peptoid hybrid, LP5 exerts a dual mode of action (MOA). At 1 × MIC the lysine-peptoid hybrid traverses the cytoplasmic membrane of *S. aureus* without causing lethal damage and binds the chromosomal DNA, inhibits topo IV and DNA gyrase and thereby the replication machinery by blocking the accessibility to DNA. The inhibitory effect on DNA replication induces the SOS response leading to inhibition of growth. At higher concentrations of 5 × MIC and above, LP5 also targets the cell membrane leading to leakage of intracellular compounds like ATP, resulting in cell death. These results add new information about the MOA of a new synthetic peptide, and advance our knowledge of these compounds as potential antimicrobial therapeutics (Gottschalk *et al*., 2013).

1.3.6. Lysine-like polypeptoids

Based on the well-known cell penetrating HIV Tat protein, (Unciti-Broceta *et al*., 2009) have designed low toxicity lysine-like cell-penetrating peptoid for cell labelling. Based on the comparative uptake studies on compounds measured via flow cytometry and confocal microscopy they concluded that the 9-mer repeating units of lysine-like peptoid have greater penetration into mammalian cells.

The work presented by (Unciti-Broceta *et al*., 2009) was based on the lysine monomeric peptoids and proved to be a quite remarkable carrier for all the cell lines, showing good mammalian cell membrane penetrability. However bacterial membrane damage or bacterial killing was not studied with these novel peptoids and their derivatives. Therefore my studies have been focussed to understand the structure-activity relationships on bacterial killing and mammalian cell toxicity on those derivatives.

The core structure of the whole peptoid library was a 9-mer lysine-like peptoid unit (Figure 1.13) and the peptoid derivatives made by; (i) changing the length of the carbon side chain (Figure 1.14); and (ii) N-terminus modifications (Figure 1.15). The three different side chain lengths were introduced to a 9-mer consisted of butyl (four-carbon), hexyl (six-carbon) and octyl (eight-carbon) monomers. Further structural changes have been made to the N-terminus end of the polymer encompassing different chemical groups conjugated to the N-terminus end such as H-non modified, BnCO-Phenyl acetamide, Tosyl-Toluene sulfonamide, Suc-Succinic amide, Ac-Acetamide and Fmoc-9-Fluorenemethanol (Figure 1.15 and Table 1.3). A number of different bio assays have been developed and carried out to study the structure-activity relationship on these peptoids on bacterial killing and potential mechanisms.

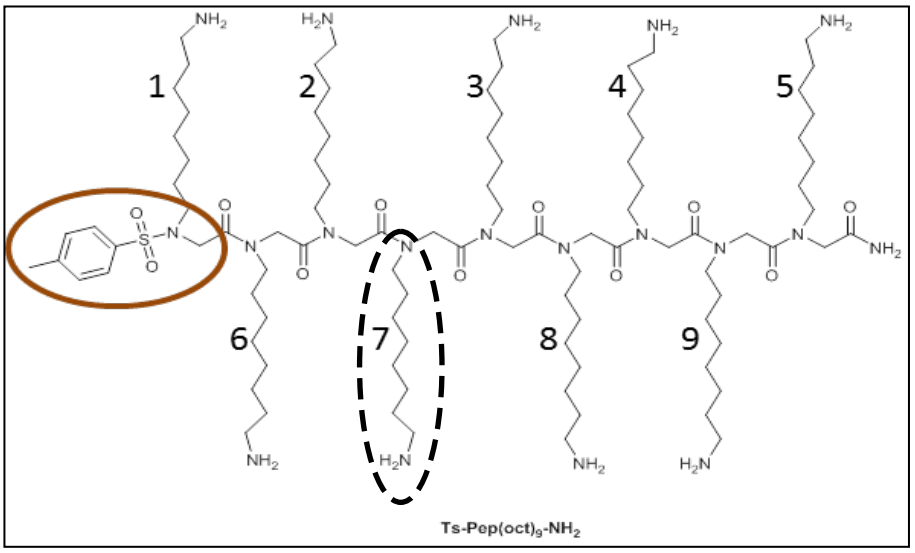

Figure 1.13: The core structure of 9-mer peptoid. All peptoids have nine repeats of a monomer unit and each monomer unit either has butyl, hexyl or octyl carbon chain length (highlighted in dotted line). Modifications were made on N-terminus (highlighted in continuous line). This figure shows the Tosyl-Octamer peptoid (TOP) (Unciti-Broceta *et al*., 2009).

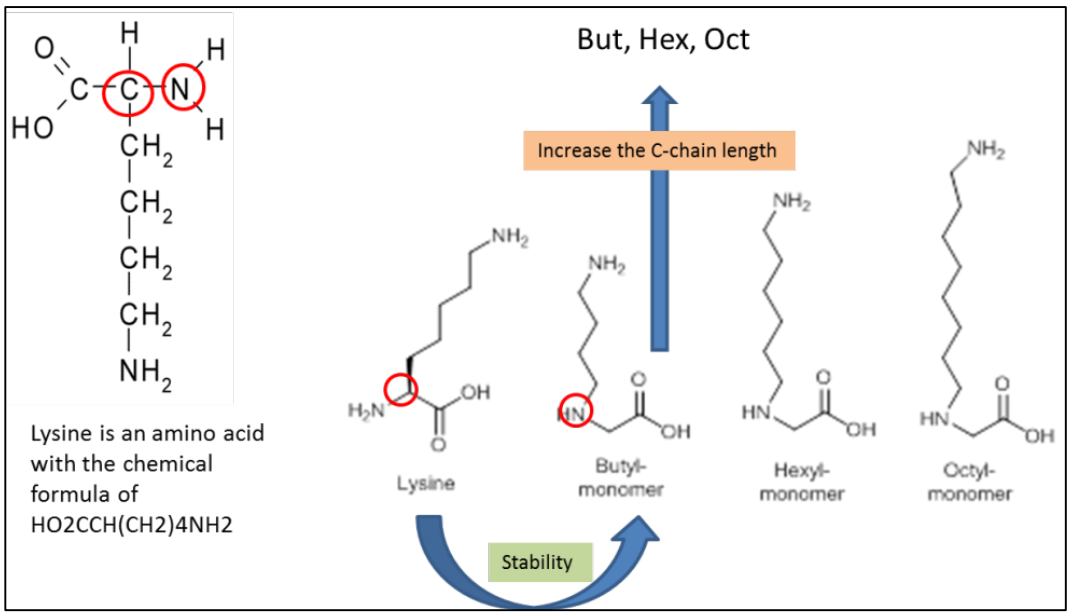

Figure 1.14: The chemical formula of lysine amino acid and peptide to peptoid modification. Substituting the carbon side chain from α-carbon to nitrogen increases the stability of the peptoids compared to peptides. Increasing the length of the side chain facilitates mammalian cell membrane permeability (Unciti-Broceta *et al*., 2009).

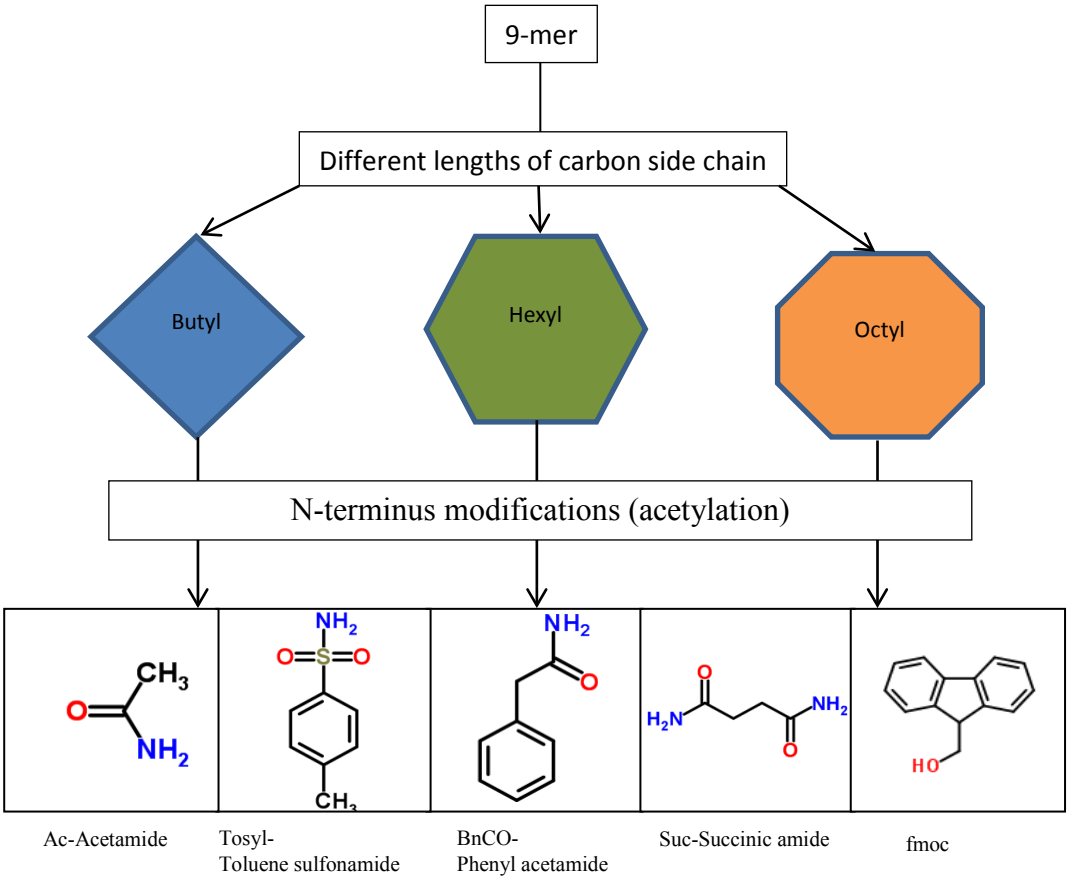

Figure 1.15: Schematic diagram of the development and design of the peptoid library. Butyl, hexyl and octyl are defined the length of the carbon side chain. Each peptoids also has different N-terminus modifications of the 9-mer such as H-non modified, BnCO-Phenyl acetamide, Tosyl-Toluene sulfonamide, Suc- Succinic amide, Ac- Acetamide and Fmoc-9-Fluorenemethanol, amounting to 13 9-mer peptoids polymers to study.

Table 1.3: Summary table of the peptoid library. Three main groups as butyl-monomers (four-carbon), hexyl-monomers (six-carbon) and octyl-monomers (eight-carbon) represent the three different lengths of carbon side chain and each category also has different N-terminus modifications such as H-non modified, BnCO-Phenyl acetamide, Tosyl-Toluene sulfonamide, Suc- Succinic amide, Ac- Acetamide and Fmoc-9-Fluorenemethanol.

Peptoid structure	Names of peptoids
H-Pep(but)$_9$-NH2	H-butyl
BnCO-Pep(but)$_9$-NH2	BnCO-butyl
Ts-Pep(but)$_9$-NH2	Tosyl-butyl
Suc-Pep(but)$_9$-NH2	Suc-butyl
Ac-Pep(but)$_9$-NH2	Ac-butyl
H-Pep(hex)$_9$-NH2	H-hexyl
Ts-Pep(hex)$_9$-NH2	Tosyl-hexyl
Fmoc-Pep(hex)$_9$-NH2	Fmoc-hexyl
H-Pep(oct)$_9$-NH2	H-octyl
BnCO-Pep(oct)$_9$-NH2	BnCO-octyl
Ts-Pep(oct)$_9$-NH2	Tosyl-octyl
Suc-Pep(oct)$_9$-NH2	Suc-octyl
Ac-Pep(oct)$_9$-NH2	Ac-octyl

1.4. Optical strategies for bacterial detection

Bacterial imaging is an emerging technology that has an important role in health and environmental applications (Bleeker-Rovers *et al*., 2004). Imaging bacterial pathogens to address quantity, growth kinetics, interactions and real-time monitoring within the host environment has the potential to provide important information for the choice of antibacterial drugs and to develop novel antimicrobial therapies (Coombes and Robey, 2010; Andreu *et al*., 2011; Bobard *et al*., 2011).

Optical imaging of bacteria has recently gained significant attention due to its relative low cost, near-patient testing capability and potential sensitivity. Recent approaches include detecting bacteria using fluorescent tagged cationic probes that preferentially bind the anionic phospholipids found on the bacterial cell membrane rather than the relatively neutral eukaryotic cell surface. These compounds are predominantly based around synthetic Zinc (II)-dipicolylamine probes which bind to both gram-negative and gram-positive bacteria both *in-vitro* and in murine models of infection (Leevy *et al*., 2006; White *et al*., 2010). The specific detection of Gram positive bacterial infections has been reported achieving optical imaging using (optically labelled vancomycin) vanco-800CW *in-vivo* in a mouse myositis model. These authors have also tested vanco-800CW in a human post-mortem biomaterial-associated infections (BAI) implant model, with the intent of developing a novel bedside tool for detecting soft tissue infections and BAI. They showed that the vanco-800CW as a very promising clinical optical imaging agent for the detection of Gram-positive bacterial infections (van Oosten *et al*., 2013).

Previous studies have not successfully developed MRSA specific imaging probes. Therefore my research was focused on developing MRSA specific probes using both aptamer and peptide labelling approaches.

1.4.1. Introduction to *Staphylococcus aureus*

Staphylococcus (from the Greek; grape-berry) were first described and classified in 1882 by the Scottish surgeon Sir Alexander Ogston (Wilson, 1987). *S. aureus* is a member of the *Staphylococcaceae* family and this organism appears as gram-positive cocci in clusters. *S. aureus* is distinguished from other staphylococcal species on the basis of the gold pigmentation of colonies and positive results of coagulase, mannitol fermentation and approximately 1 μm in diameter (Crossley and Archer, 1997). The golden pigmentation of *S. aureus* colonies is caused by the presence of carotenoids and has been reported to be a virulence factor protecting the pathogen against oxidants produced by the immune system (Liu *et al*., 2005). More than 130 years later, *S. aureus* remains a versatile and dangerous pathogen in humans. Treatment of these infections has become more difficult because of the emergence of multidrug-resistant strains (Blot *et al*., 1998). The staphylococcal genome consists of a circular chromosome approximately 2800 base pairs in size including prophages, plasmids, and transposons. Genes governing virulence and resistance to antibiotics are found on the chromosome, as well as the extra chromosomal elements (Novick, 1990). These genes are transferred between staphylococcal strains, species, or other gram-positive bacterial species through the extra chromosomal elements (Schaberg and Zervos, 1986).

1.4.2. Importance of *S. aureus* infections

S. aureus is a commonly isolated human microorganism that is able to colonise the anterior nares and other skin regions of healthy individuals. It has been estimated that 50% of adults are either persistent or intermittent *S. aureus* carriers (Wertheim *et al*., 2005). *S. aureus* is one of the main causes of hospital- and community-acquired infections which can result in serious consequences. This microorganism has become a versatile pathogen causing a broad spectrum of infections due to a large arsenal of virulence factors. *S. aureus* is an important cause of skin and soft tissue infections (SSTIs), endovascular infections, pneumonia, septic arthritis, endocarditis, osteomyelitis, foreign-body infections, and sepsis (Lowy, 1998). *S. aureus* ranks first

or second among bacterial pathogens causing bloodstream infections according to different studies (Biedenbach *et al*., 2004; Wisplinghoff *et al*., 2004), and is the leading cause of nosocomial pneumonia (Hoban *et al*., 2003). In addition, *S. aureus* causes infections of surgical wounds and prosthetic implants (Pantosti and Venditti, 2009).

In addition to the infections listed above, *S. aureus* is often responsible for toxin-mediated diseases, such as toxic shock syndrome, scalded skin syndrome and *Staphylococcal* foodborne diseases (SFD). Hospitalized patients are particularly exposed to *S. aureus* infections due to their compromised immune system and frequent catheter insertions and injections (Lindsay and Holden, 2004). This pathogen is the leading cause of bloodstream, lower respiratory tract and skin/soft tissues infections in all regions surveyed (Diekema *et al*., 2001). The importance of this human pathogen, apart from its ability to cause life-threatening infections, is its remarkable potential to develop antimicrobial resistance. The mortality rate from severe MRSA infections is about 20% and it has been estimated that MRSA infections are the leading cause of death by a single infectious agent in the US, exceeding deaths caused by HIV/AIDS (Klevens *et al*., 2007). Furthermore, MRSA as opposed to MSSA infection is associated with significantly higher costs, due to prolonged stay in the hospital, and mortality (Hanberger *et al*., 2011).

1.4.3. The emergence of MRSA

S. aureus resistance to penicillin emerged in the 1940s (Barber and Rozwadowska-Dowzenko, 1948). Penicillin resistance is due to the acquisition of genes producing penicillinase, a β-lactamase enzyme which was found even before the introduction of penicillin into clinical use (Abraham *et al*., 1940). This enzyme cleaves the β-lactam ring of β-lactam antibiotics such as penicillin and its derivatives. Indeed in the 1950s, penicillin-resistant strains of *S. aureus* were pandemic in hospitals and the community. Nowadays, most *S. aureus* isolates are resistant to penicillin.

The semisynthetic antibiotic, methicillin was introduced to overcome penicillin-resistant *S. aureus*. Methicillin is a semisynthetic antibiotic derived from penicillin resistant to β-lactamase inactivation. Methicillin was introduced by Beecham in 1959. However one year later, methicillin-resistant *S. aureus* (MRSA) was detected in the United Kingdom (Jevons *et al*., 1963). Unlike resistance to penicillin, the mechanism underlying methicillin resistance protects the bacteria from the entire class of β-lactam antibiotics including penicillins, cephalosporins, and carbapenems.

MRSA is defined by the presence of a large mobile genetic element called the staphylococcal cassette chromosome, (SCCmec). It carries the *mecA* gene that codes for an alternative penicillin binding protein, PBP2A, with low binding affinity to all β-lactams (Ito *et al*., 2012). MRSA strains were first described in hospital settings, after the introduction of β-lactamase-resistant penicillins into medical practice, and they continue to be a serious problem in health care due to their ability to acquire multidrug resistance determinants. Although outbreaks of diseases in a hospital may also be caused by methicillin sensitive *S. aureus* (MSSA) (Kurlenda *et al*., 2010), MRSA infections are especially easily spread throughout a hospital and, without implementation of a special surveillance program with control procedures, the risk of an epidemic in hospitals is high (Kurlenda *et al*., 2010).

Today, many developed countries report that methicillin resistant strains account for at least 25 – 50% of infectious *S. aureus* isolates in hospitals (Diekema *et al*., 2001). In contrast, some countries such as The Netherlands and the Scandinavian countries historically have low MRSA infection rates (often < 1 %), most likely owing to rigid search-and-destroy surveillance policies, as well as restraint in antibiotic prescription. In fact, a recent Japanese study indicates that high antibiotic consumption rates led to increased MRSA burden over time (Nakamura *et al*., 2012). Initially MRSA infections were limited to hospitalized patients, the most recent epidemic MRSA wave, beginning in the mid to late 1990s, was characterized by the emergence of community-associated MRSA (CA-MRSA) with the capacity to infect otherwise healthy individuals.

1.4.4. Genetics of methicillin resistance in *S. aureus*

The staphylococcal cassette chromosome *mecA* (SCCmec) is responsible for methicillin resistance in staphylococci and this is due to the acquisition of a mobile genetic element (MGE) (Katayama *et al*., 2000). The DNA fragment SCCmec ranges from 21 to 67 kb in size, depending on the SCCmec type (Hiramatsu *et al*., 2001). The number of SCCmec types is constantly increasing with the discovery of new elements and there are currently 11. All SCCmec types include the *mecA* gene, which codes for the low-affinity penicillin binding protein PBP2A (Hartman and Tomasz, 1981) and is responsible for methicillin resistance in MRSA. Resistance is due to the fact that β-lactam antibiotics cannot inhibit PBP2A, in contrast to other *S. aureus* PBPs. SCCmec elements vary in composition and they may contain additional antibiotic resistance genes (Queck *et al*., 2009).

MRSA also have acquired resistance to other antibiotics, such as erythromycin, clindamycin, ciprofloxacin, tetracycline, etc. (Shorr, 2007). It is alarming that multi-drug-resistant strains of *S. aureus* are often only susceptible to vancomycin, an antibiotic with considerably lower efficiency to β-lactams. Furthermore, rare cases of highly vancomycin-resistant MRSA strains (VRSA) have been reported. Fortunately, these did not spread substantially, possibly owing to increased fitness cost associated with high-level resistance to vancomycin. The majority of CA-MRSA strains have not acquired resistance to additional antibiotics, with the exception of limited outbreaks of multi-drug-resistant CA-MRSA (Diep *et al*., 2008).

1.4.5. The *mecA* Gene

The *mecA* gene originally identified in methicillin-resistant *S. aureus* (MRSA) (Beck *et al*., 1986; Matsuhashi *et al*., 1986) encodes a PBP of 668 amino acid residues which is responsible for beta-lactam resistance (Utsui and Yokota, 1985). The *mecA* gene is carried by SCCmec and has been identified in various staphylococcal species, such as *S. aureus, Staphylococcus epidermidis, Staphylococcus haemolyticus, Staphylococcus saprophyticus, and Staphylococcus fleurettii* (Tsubakishita *et al*.,

2010). The *mecA* genes present in these species have 98% sequence identity with the *mecA* carried by the first fully sequenced prototype MRSA strain N315 (Kuroda *et al*., 2001). The first divergent *mecA* gene homologues were identified on the chromosomes of *Staphylococcus sciuri subsp. sciuri, S. sciuri subsp. rodentius, and S. sciuri subsp. carnaticum.* These homologues are very similar to each other and have approximately 80% nucleotide sequence identity to *mecA* of N315 (Wu *et al*., 1996; Wu *et al*., 1998; Couto *et al*., 2003). A second group of *mecA* gene homologues identified in *Staphylococcus vitulinus* have about 90% nucleotide identity to *mecA* of N315 (Schnellmann *et al*., 2006).

1.4.6. Regulation of *mecA* gene expression

The expression of the *mecA* gene is regulated in analogous manner to that of the β-lactamase gene, blaZ. Similar to blaZ, *mecA* is divergently transcribed from its two regulatory genes organized in an operon, *mecI* and *mecR1*. Homodimeric methicillin repressor, *MecI*, constitutively represses expression of *mecA* as well as transcription of the *mecI-mecRI* operon by binding to two palindromes contained within the promoter-operator region (Safo *et al*., 2006). Derepression occurs through cleavage of *MecI* upon activation of the metalloprotease domain of the *mecRI* sensor-transducer by a β-lactam antibiotic.

MecRI is a membrane protein that has an extracellular penicillin-binding domain that, when bound by β-lactams, undergoes a conformational change inducing autocleavage of the intracellular protease domain. The active *MecRI* cleaves *MecI* which leads to derepression of *mecA* as well as the *mecI-mecRI* operon (Mallorquí-Fernández *et al*., 2004). In addition to regulation of *mecA* expression by its cognate *MecI* and *MecRI* regulators, it can also be regulated by structurally and functionally similar β-lactamase regulators, *BlaI* and *BlaRI*. Due to their structural and functional similarity, *MecI* and *BlaI* are able to bind as homodimers to the promoter-operator region of *mecA* (Gregory *et al*., 1997). The *MecI* or *BlaI*-mediated repression is only relieved by induction through homologous and not heterologous sensor-transducers, demonstrating the repressor specificity of induction. Induction of *mecA* expression

by the *MecRI-MecI* system is slower than the induction by *BlaRI-BlaI* and never leads to maximal *mecA* transcription (Potempa *et al*., 1991).

1.4.7. The PBP2A protein

PBP2A (Figure 1.16) belongs to the group of high molecular mass (78 kDa) family of PBPs and consists of a transpeptidase domain and a non-penicillin binding domain of unknown function (Goffin & Ghuysen, 1998). PBP2A is known to possess low affinity for β-lactams that allows MRSA strains to grow in antibiotic concentrations that inactivate all native PBPs (Gaisford and Reynolds, 1989). PBP2A is a poorly active enzyme, compared to other native PBPs that synthesize highly cross-linked peptidoglycan (de Jonge and Tomasz, 1993). Even when the transpeptidase activity of all native PBPs is inhibited by the presence of methicillin, PBP2A has been shown to rely on the transglycosylase, β-lactam-insensitive, domain of the native PBP2 to confer resistance (Pinho *et al*., 2001).

The serine in the active site of the transpeptidase domain in PBP2A (Figure 1.16) is responsible for nucleophilic attack on both the β-lactam ring and the D-alanyl-D-alanine substrate and is located in an extended narrow groove. The groove mediates non-covalent interactions with the β-lactam that place the β-lactam in an unfavorable position for interaction with the serine in the active site. As a result, the acylation between the β-lactam and the active site does not occur. PBP2A successfully balances the crucial transpeptidase activity with a decreased affinity toward β-lactam antibiotics. Therefore PBP2A is able to synthesize the cell wall at otherwise lethal concentrations of β-lactams (Pinho *et al*., 2001; Lim & Strynadka, 2002; Chambers, 2003).

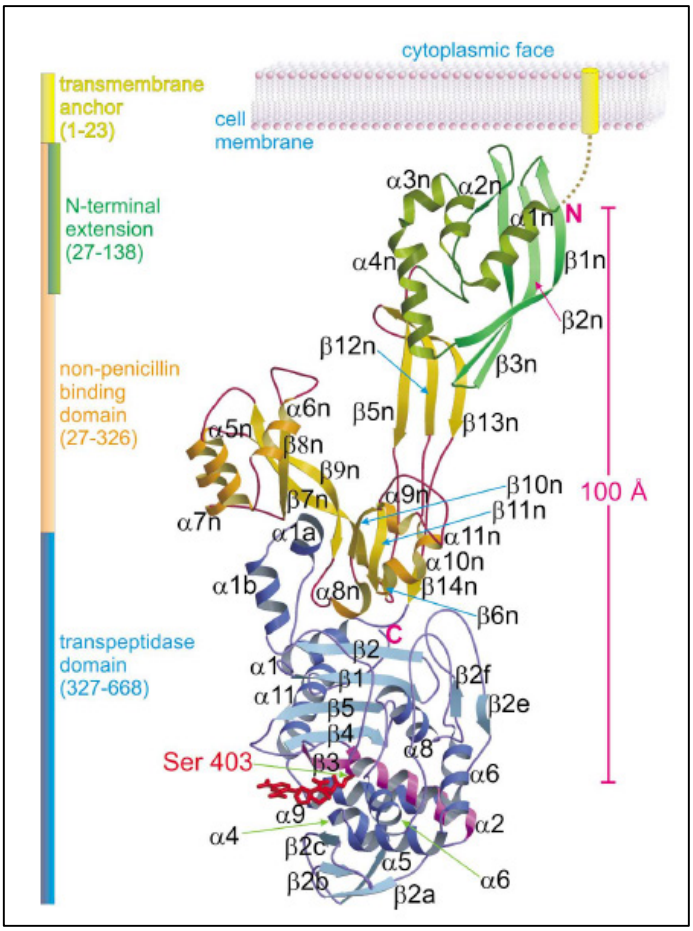

Figure 1.16: The structure of PBP2A. The bi-lobed N-terminal non-penicillin binding domain is orange, with the N-terminal lobe coloured green. The transpeptidase domain is blue, with the position of the active site indicated by the red. The N- and C- termini are labelled N and C, respectively (Lim and Strynadka, 2002).

1.4.8. Research objective to over-express the PBP2A protein

Expression of PBP2A is the basis for the broad clinical resistance to the β-lactam antibiotics by MRSA. Hence, I aimed to clone, overexpress and purify PBP2A to generate sufficient protein to develop molecular probes targeting PBP2A. In the field of molecular imaging, detecting PBP2A protein associated with MRSA could be an important molecular target to develop novel molecular imaging agents to identify MRSA amongst other bacterial strains and within the multicellular organism.

1.5. Aptamer molecular probe development

1.5.1. Introduction-Aptamer technology

Aptamers are short, single-stranded oligonucleotides (DNA or RNA) discovered in the early 1990s and have found diverse applications in biotechnology (Gold *et al*. 1995; Nimjee *et al*. 2005). Aptamers are isolated through a process called systematic evolution of ligands by exponential enrichment (SELEX) (Ellington and Szostak, 1990; Tuerk and Gold, 1990) in which a starting library of oligonucleotides are screened for sequences that can bind specifically and with high affinity to a target of choice. The process itself is very versatile and the choice of targets to obtain aptamers can vary from small molecules (nucleotides, vitamins, amino acids, carbohydrates, dyes, antibiotics) (Fickert *et al*., 2006; Lorenz and Schroeder, 2006), peptides and proteins (Nimjee *et al*. 2005) to whole cells (Ye *et al*., 2012). Depending upon the requirements of the target, strategies for aptamer selections are adjusted and can vary widely. Aptamers are also described as chemical versions of antibodies and can inhibit their targets through specific and strong interactions that are superior to those of biologics and small molecule therapeutics. They also avoid the toxicity and immunogenicity concerns of these traditional agents due to their nucleic acid compositions (Nimjee *et al*., 2005).

1.5.2. The SELEX process

SELEX starts with a single stranded nucleic acid library of either RNA or DNA. The library contains aptamers which have a variable or randomised region in the middle flanked by two constant regions called primer binding regions (Ellington and Szostak, 1990; Tuerk and Gold, 1990). This randomised region can range from a few nucleotides to hundreds of nucleotides and can be continuous or found in blocks. Importantly, enough nucleotide sequence randomisation in the library needs to occur to generate various conformations from which aptamer diversity originates. The diversity of the aptamer library increases with the larger randomised region of the aptamer. For example a library with 40 randomised nucleotides could yield

approximately 10^{14} unique aptamer sequences (considering four nucleotides in 40 randomised positions) for screening (Gold *et al*. 1995).

SELEX begins with a randomised aptamer library incubated with a target molecule (purified protein target or cells). A number of partitioning strategies exist, including centrifugation, nitrocellulose binding, column chromatography, or immune precipitation. The aptamer molecules that bind to the target molecule are then eluted and amplified by PCR for DNA aptamer selection (Bayrac *et al*. 2011), or RT-PCR for RNA aptamer selection (Adler *et al*. 2008). This generates an enriched pool with increased binding affinity for the target from the first round to the following SELEX rounds. The process of incubation, partitioning, elution, and amplification comprises one round of SELEX (Fitzwater and Polisky, 1996) (Figure 1.17). This process is then repeated under increasingly stringent conditions to isolate specific aptamers (Adler *et al*. 2008) that bind with the highest affinity for the target. Conditions can be created for promoting greater binding to the target by increasing the aptamer to target molecule ratio, increasing salt concentrations, or decreasing the overall amount of target molecule used. The number of rounds required to drive a selection to completion depends on both the target and how much stringency is increased in each round and selection can be completed in 8–18 rounds (Fitzwater and Polisky, 1996). The counter-SELEX method was introduced to increase the efficiency of aptamer selection by traditional SELEX (Figure 1.17) (Jenison *et al*., 1994). Compared to traditional SELEX, counter-SELEX has a pre-clearing step using closely related structural analogs of the target to effectively discard non-specific aptamer. This allows improvement in aptamer selection and can also be applied to other modified SELEX methods.

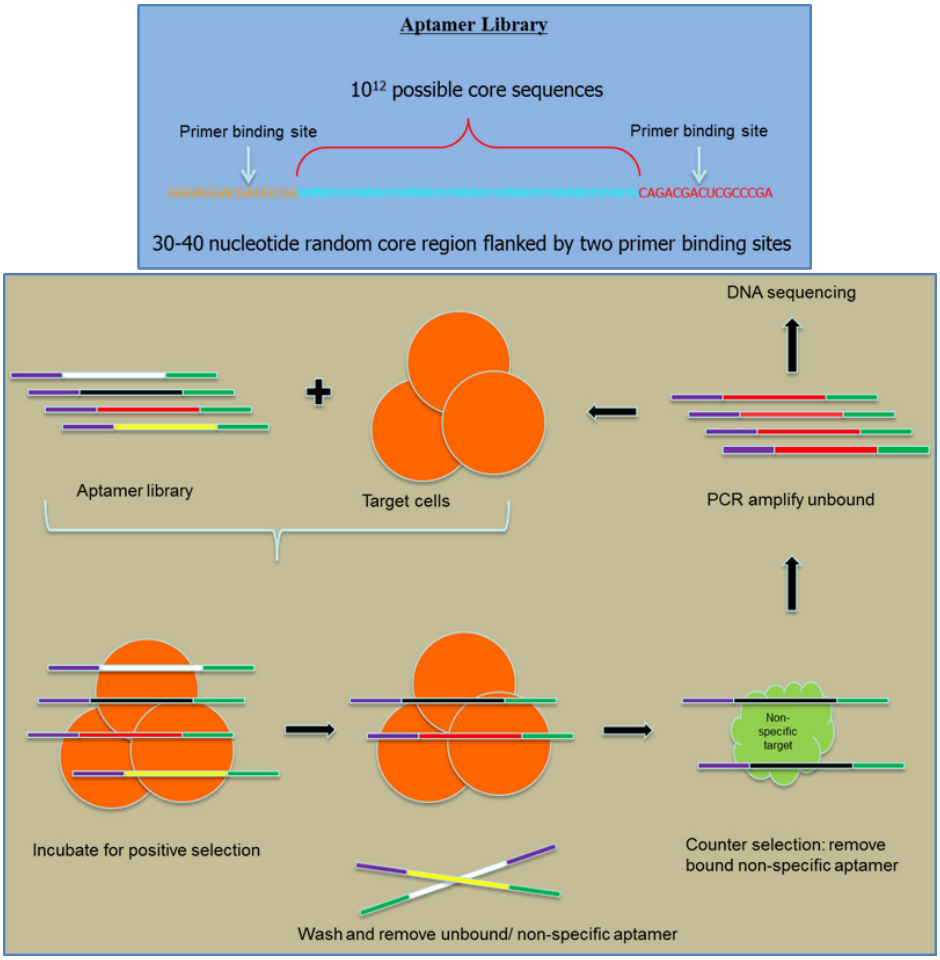

Figure 1.17: Aptamer library and a simplified schematic of systematic evolution of ligands by exponential enrichment (SELEX): The starting oligonucleotide library (RNA or DNA) is incubated with the target of interest in the binding-reaction. The bound oligonucleotide-target complexes are partitioned from the unbound oligonucleotides. Then the unbound oligonucleotides are discarded and the bound oligonucleotides are eluted from the target and amplified. The amplified oligonucleotide ''pool'' is incubated with the target protein in the next-round of SELEX. This process is repeated with the counter selection step which can reduce non-specific binding and increase specificity.

1.5.2.1. Cell-SELEX

SELEX can target more than one individual molecule by applying cell-SELEX strategies. This utilises living cells as the SELEX target (Figure 1.17). Although traditional SELEX is typically carried out using purified target molecules, whole live cells are also employed as selection targets. Not only normal/abnormal mammalian cells such as virus-infected and cancer cells but also live pathogenic organisms such as bacteria and viruses have been utilised as cell-SELEX targets (Tang *et al*., 2009; Hamula *et al*., 2011). The aptamers generated are functional with an original conformation that binds the target molecule on live cells. Compared to aptamers selected using a purified target, a cell-SELEX-derived aptamer may have more control to be used directly for clinical applications.

A screened aptamer resulting from cell-SELEX using abnormal cells can be used to detect disease or cancer cells. Furthermore, biomarkers can be developed that identify the aptamer target for a specific abnormality (Blank *et al*., 2001). Aptamers can be selected for host cell proteins if their expression levels are up-regulated upon viral infection. Lastly, stable cell lines can be generated that express viral protein as a cell-SELEX target and the aptamer obtained can be used to detect virus infected cells (Chen *et al*., 2007). Novel biomarkers can be discovered using the cell-SELEX technique because the target molecules of the may be previously unrecognised as cell-specific surface molecules. Thus, cell-SELEX can be applied for de-novo discovery of novel biomarkers for a desired cell by identifying the aptamer binding partner. The cell-SELEX concept can be extended for *in-vivo* selection, which was first demonstrated using a hepatic tumour xenograft mouse model (Mi *et al*., 2010). Oligonucleotides were injected intravenously, liver tumours were harvested, and the injected RNA molecules were extracted and amplified. A tissue-specific aptamer can be more easily screened through this *in-vivo* selection process. Therefore a screened aptamer may be a useful for targeting specific tissues *in-vivo*.

1.5.2.2. Capillary Electrophoresis-SELEX

The SELEX process has disadvantages in that it is time consuming to repeat the rounds of enriching molecular biology methods have been introduced to SELEX to overcome these disadvantages. Capillary electrophoresis-SELEX (CE-SELEX) was designed for selecting aptamers to reduce repeating rounds with low dissociation constants (Mosing *et al*., 2005). In this method, the nucleic acids that bind the target migrate with different mobilities than those of unbound sequences and allow them to be collected as separate fractions. Although traditional SELEX requires 6-12 rounds, CE-SELEX significantly reduces the number of rounds and increases binding affinity (Schneider *et al*., 1995). CE-SELEX decreases the time, effort and cost to screen a higher affinity aptamer compared to those of traditional SELEX. Based on CE technology a non-SELEX method that selects an aptamer without amplification was demonstrated (Berezovski *et al*., 2006). This procedure can be automated using a single commercially available capillary electrophoresis instrument.

1.5.2.3. One step MonoLEX

The MonoLEX approach combines a single affinity chromatography step with subsequent physical segmentation of the affinity resin and one single final exponential amplification step of the bound aptamers (Nitsche *et al*., 2007). Using the Biomek 2000, an automatic SELEX device (Cox *et al*., 1998). They demonstrated that 10 rounds of selection against eight targets in parallel can be performed in 4-5 days.

1.5.2.4. Microfluidic SELEX

Microfluidic SELEX (mSELEX) was designed that combines traditional SELEX with a microfluidic system. Protein immobilisation is the most important aspect of mSELEX. In previous studies a mSELEX prototype device was developed and biotinylated lysozymes were immobilized to silica microline previously coated with streptavidin (Hybarger *et al*., 2006). It is possible to use magnetic bead-based

SELEX process with microfluidics technology and a continuous-flow magnetic activated chip based separation device was developed (Lou *et al*., 2009). Using this mSELEX method, an enriched aptamer pool was obtained that tightly bound to the light chain of recombinant Botulinum neurotoxin type A after a single round of selection with a 33 nM Kd value. Recently, a novel formulation of sol-gel protein microarray material was developed, which produced physical properties suitable for protein immobilization, protein-protein interactions, and immunoassays (Kim *et al*., 2006). Based on sol-gel, the authors developed a microfluidic device and method for binding nucleic acids to immobilized proteins and efficiently eluted and recovered the intact nucleic acids (Park *et al*., 2009). The mSELEX system has enhanced selection efficiency and reduces time and effort compared to those of traditional SELEX.

1.5.3. Aptamer modifications to increase stability

RNA and DNA oligonucleotides are naturally unstable molecules and are rapidly degraded in biological fluids due the presence of endogenous nucleases. Therefore, nucleotide modification strategies are often utilised to increase resistance. In the case of RNA aptamers, modified bases are typically introduced in the starting library for selection to have increased nuclease resistance from the outset. A common modification is to alter the functional group on the 2' ribose position of pyrimidines, including 2'-fluoro, 2'-amino, and 2'-O-methoxy substituted nucleotides (Keefe and Cload, 2008). These modifications can easily be incorporated during *in-vitro* transcription using a mutant form of T7 RNA polymerase (Chelliserrykattil and Ellington, 2004). After selection, internal modifications can be made to the aptamer; however these may influence structure and functionality of the aptamer. Therefore, most chemical modifications for enhancing the nuclease stability of the aptamers are incorporated at the beginning of selection.

Other modifications yielding aptamers with higher stability include the use of L-nucleotides and locked nucleic acids. Aptamers created with L-nucleotides are known as spiegelmers, from the German word for mirror (Sooter and Ellington,

2002; Klussmann, 2006). L-nucleotides are the mirror image or enantiomers of the naturally occurring D-nucleotides. However, being the L-nucleic acid, they are not the substrate for DNA or RNA polymerases. Thus, they are not substrates for enzymatic polymerisation and cannot be directly used to make aptamers using the standard SELEX process. Aptamers composed of natural D-oligonucleotides can be selected against mirror image targets (such as L-amino acid peptides, rather than natural D-amino acid peptides). Once the aptamers are isolated, they can be chemically synthesised as L-oligonucleotides (Spiegelmers), and will bind to the natural D-amino acid peptide targets. Because Spiegelmers are composed of unnatural monomers, they are not good substrates for nucleases and have been shown to be stable over 60 hours in biological fluids. So far, there are 2 such aptamers in clinical trials (Kulkarni *et al*., 2007; Kulkarni *et al*., 2009; Sayyed *et al*., 2009).

Aptamers are low molecular weight; therefore they are rapidly cleared by the renal system. This can be reduced through the addition of polyethylene glycol (PEG) or cholesterol to the aptamer. These kinds of modifications are made post-selection. They increase the overall molecular weight of the aptamers without disrupting their structure and the therapeutic functions. This can increase the half-life of an aptamer from <10 min to >12 h depending on the specific aptamer modifications (Becker *et al*., 2005). An aptamer with a longer half-life can be administered less frequently and potentially outside the hospital setting. Aside from traditional intravenous administration, recent work has suggested that aptamers can also be administered subcutaneously, which can increase the half-life up to 6 days (Vavalle *et al*., 2012).

1.5.4. Aptamer characteristics

Aptamers have several characteristics that make them useful as potential therapeutic molecules and set them apart from small molecules and antibodies. Aptamers are relatively small (8–15 kDa) compared to antibodies (50–100 kDa), while still demonstrating high specificity and affinity for their target, with equilibrium dissociation constants in the low nanomolar to high picomolar range (Nimjee *et al*. 2005). This specificity and affinity stem from the fact that aptamers fold into unique

three-dimensional structures and form specific contacts between functional groups on both nucleic acid and protein targets (Long *et al*., 2008). Since an aptamer covers a functional portion of the target protein, they tend to act as antagonists by blocking their interactions with either protein partners or their substrates that results in the inhibition of their enzymatic activity (Long *et al*. 2008). This loss in enzymatic activity of protein targets by the action of aptamers is reversible in most cases. This is important therapeutically because once aptamer activity is reversed; the target protein is able to function immediately (Becker *et al*., 2005).

Another advantage of aptamers, over antibodies, is their stability during long-term storage; they can be refolded into their functional structure after multiple freeze-thaw cycles. A major benefit of aptamers is that they can be generated, in small or large scale *in-vitro,* by either solid-phase chemical synthesis or by *in-vitro* transcription, both of which are much faster than the *in-vivo* generation of antibodies (Becker *et al*., 2005).

Furthermore, unlike antibodies, aptamers have not been shown to produce an immune response in animal and clinical studies and are well tolerated in the body and this allows for repeated administration (White *et al*., 2000). The synthetic oligonucleotides, containing modified nucleotides, possibly do not provoke the adaptive immune response and generally do not produce antibodies. In 2009, Yu *et al*. demonstrated that the oligonucleotides containing 2'-modified nucleotides (2'-O-methylribonucleotides, 5-methyl-dC or 2'-O-methyl-5-methyl-C) inhibit the toll-like receptors (TLR7 and TLR9) activity. Some of these 2'-modified nucleotides like, 2'-O-methylribonucleotides are regularly used to synthesise aptamer. It is possible that aptamers containing modified nucleotides inhibit TLRs and do not provoke the innate immune system. This might be the other possible reason for their non-immunogenic nature. In clinical trials, the only known immune responses to aptamer administration were thought to be caused by antibody generation to the PEG (Aravind *et al*., 2012) group appended to the aptamer to increase overall molecular weight.

Another important characteristic for aptamers as therapeutic molecules is the ability to rapidly and effectively reverse an aptamer with either a sequence-specific antidote or a universal antidote that reverses aptamer activity independent of sequence (Oney *et al*., 2009). This is a characteristic not found in small molecule inhibitors or antibodies, and lends itself well to application in the clinic, as well as a tool for studying a target of interest. Since the development of the SELEX process in 1990, this process has been used to create designer ligands, or aptamers, to essentially any target. This has opened up the possibility of using aptamers not just for basic sciences, but also for diagnostics, therapeutics, imaging, and biosensing. Notably, aptamers have already made the transition from the bench to the clinic. For example nuclease-resistant RNA aptamer against vascular endothelial growth factor modified with PEG (pegaptinib or Macugen, Eyetech Pharmaceuticals) is now in clinical use for the wet form of age-related macular degeneration (Ng *et al*., 2006). For the list of aptamers that are currently in clinical trial please refer (see table 1.4). The number of publications with aptamer applications is rapidly increasing. There are a variety of applications of aptamers as both therapeutic molecules and as sensing molecules (diagnostics).

Table 1.4: Aptamers undergoing clinical trials (Kong and Byun, 2013).

Name	Target	Condition	Phase
Pegaptanib sodium (Macugen)	VEGF	Age-Related Macular Degeneration	Approved
EYE001	VEGF	Macular Degeneration / Choroidal Neovascularization	Phase 2/3
E10030	PDGF	Age-Related Macular Degeneration	Phase 2
Pegaptanib sodium (Macugen)	VEGF	Diabetic Macular Edema	Phase 2
AS1411	Nucleolin	Acute myeloid leukemia	Phase 2
ARC1779	A1 domain of von Willebrand Factor	von Willebrand Disease / Purpura / Thrombotic Thrombocytopenic	Phase 2
REG1 (RB006 and RB007)	Coagulation factor IXa	Coronary Artery Disease	Phase 2
NOX-E36	CCL2	Chronic Inflammatory Diseases / Type 2 Diabetes Mellitus / Systemic Lupus Erythematous	Phase 1
NOX-A12	CXCL12	Autologous or Hematopoietic Stem Cell Transplantation	Phase 1
ARC19499	tissue factor pathway inhibitor (TFPI)	Hemophilia	Phase 1
ARC1905	Complement Component 5 (C5)	Age-Related Macular Degeneration	Phase 1
EYE001	VEGF	von Hippel-Lindau Disease	Phase 1

1.5.5. Applications of aptamer

1.5.5.1. Therapeutics

Aptamers can be modified to create different functions and can be specifically tailored for many potential applications in biotechnology and molecular medicine. Aptamers can bind to their cognate protein and also efficiently inhibit the function of target as an antagonist. Many aptamer therapeutic studies have been conducted to treat certain diseases by inhibiting therapeutic target activity and decreasing the partner binding property (Siller-Matula *et al*., 2012; Vater *et al*., 2013) (Figure 1.18). The first FDA approved Macugen aptamer drug for age-related macular degeneration, is a typical antagonistic aptamer (Zhou and Wang, 2006). Macugen (pegaptanib) is a 28-base RNA oligonucleotide with two branched 20 kDa PEG moieties (Ruckman *et al*., 1998). It selectively binds to the vascular endothelial growth factor (VEGF)165 isoform when introduced intravitreally. Thus, the intracellular signal cascade is inhibited by the pegaptanib-VEGF165 complex, which cannot bind to the VEGF receptor. Thus, pegaptanib has the potential to inhibit growth of blood vessels and vascular leakage by inhibiting the intracellular signal cascade induced by the pegaptanib-VEGF165 complex. Diverse therapeutics based on antagonistic functions of aptamers are undergoing clinical trials (Table 1.4). They inhibit the signalling cascade by decreasing activity of the target protein or altering binding with the physiological binding partner.

Aptamers may also function as agonists in certain biochemical reactions, e.g. agonistic use of an aptamer with 4-1BB, which is a major co-stimulatory receptor (McNamara *et al*., 2008). 4-1BB increased expansion and survival of activated T cells. Dimerization of the anti-4-1BB aptamer treated with the CD3 antibody not only increased T-cell activation and interferon-γ in-vitro but also tumour regression *in-vivo*. Moreover, Dollins *et al*. designed an aptamer-based agonist by dimerising the OX4 RNA aptamer, which targets one of the tumour necrosis factor receptor families (Dollins *et al*., 2008). Two 2′-fluoropyrimidine-modified RNA aptamers were selected that bind to CD28 (CD28Apt2 and CD28Apt7) (Pastor *et al*., 2013).

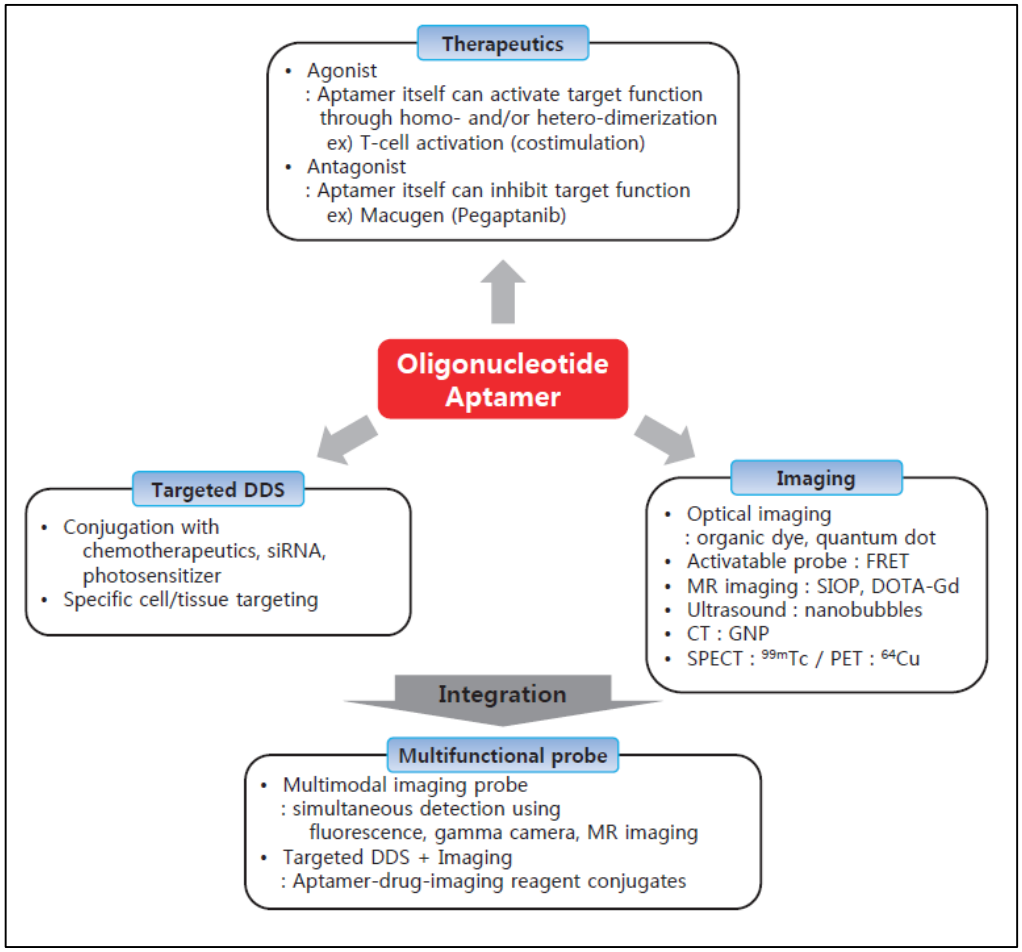

Figure 1.18: Applications of aptamer. Aptamer can be used as therapeutics, targeted drug delivery system (DDS) and imaging. These three parts can be put together using aptamers and conjugation in multifunctional probes (Kong and Byun, 2013).

This study suggested that an agonistic dimerised anti-CD28 aptamer increases co-stimulatory efficacy and reduces therapeutic dose and toxicity compared to conventional agonistic anti-CD28 antibodies. Similar research on aptamers for use as co-stimulatory agonistic molecules is being conducted (Suntharalingam *et al*., 2006; Romer *et al*., 2011). Moreover, not only homo-dimerisation of an aptamer for agonistic use but also hetero-dimerization of two individual aptamers that recognize different targets for dual purposes, specific targeting and stimulating, have been reported (Gilboa *et al*., 2013). Two individual aptamers were hetero-dimerized including a 4-1BB binding aptamer to stimulate the immune response and a prostate-specific membrane antigen (PSMA) binding aptamer for prostate cancer targeting.

This bi-specific aptamer was developed to revert prostate tumours through the host immune response. A bi-specific aptamer is more effective and synergizes with vaccination strategies and exhibits a superior therapeutic index compared with non-targeted co-stimulation with 4-1BB antibodies or 4-1BB aptamers. Agonistic/antagonistic aptamers offer significant advantages over antibodies in terms of synthesis, cost, and immunogenicity as well as conjugation chemistry.

1.5.5.2. Target drug delivery

Aptamers exhibit many desirable properties for targeted drug delivery such as ease of selection and synthesis, high binding affinity and specificity, low immunogenicity, and versatile synthetic accessibility. The therapeutic agents that have been delivered using aptamers as the targeting ligands can be categorized into three major classes; drugs, toxins, and small interfering RNAs (siRNAs) (Figure 1.18) (Zhang *et al*., 2011).

Doxorubicin (Dox) used in chemotherapy for haematological malignancies, carcinomas, and soft tissue sarcomas can intercalate within the double-stranded CG sequences of DNA and RNA. Based on the intercalation property of Dox to the aptamer, targeted Dox delivery for targeting cancer and Dox mediated cancer therapy has been actively studied (Ling *et al*., 2012; Liu *et al*., 2012; Meng *et al*., 2012; Subramanian *et al*., 2012). A Dox intercalated aptamer that binds to prostate-specific membrane antigen (PSMA), which is abundantly expressed on the cell surface of a human prostatic adenocarcinoma (LNCaP) metastatic lesion has been studied. PSMA expressing LNCaP-specific cell death was observed by treatment with Dox-intercalated PSMA-specifi c 2′-fluoropyrimidine aptamer, but not in PSMA-negative PC3 cells (Bagalkot *et al*., 2006). Covalent conjugation of aptamer harboring the drug is relatively stable such that drug release during transport is prevented before the drug localizes at its cellular target. Drugs can be chemically modified to form stable ester, amide, and disulfide bonds that serve to conjugate the drug to the aptamer. Other chemotherapy drugs such as daunorubicin, thalidomide, and dactinoimycin can also intercalate to double-stranded oligonucleotides. They are

expected to show a good therapeutic effect in specific cancers, and their application in various aptamers is actively sought.

Liposomes, small lipid bilayer structures, can be adopted as an excellent drug delivery carrier for aptamers. Aptamer-tagged liposomes have been synthesised to contain the anticancer drug paclitaxel and a fluorescent dye (Nile Red) for tumour-specific drug delivery and imaging (Aravind *et al*., 2012). In another study, Cy3-labeled, carboxylated, thiolated oligonucleotide aptamer (thioaptamer) against E-selectin (ESTA, E-Selectin ThioAptamer) was designed. This modified ESTA was coupled to an amino PEGylated stealth liposome to make the vasculature targeting ESTA-conjugated liposome (Mann *et al*., 2011), which achieved tumour vasculature-specific drug delivery. Moreover, a photosensitizer-aptamer conjugate was developed for cancer specific delivery to be used in photodynamic cancer therapy (Yang *et al*., 2011; Han *et al*., 2013).

Aptamers can be used to deliver siRNA to specific cells and the receptor-mediated endocytosis mechanism is involved in cellular uptake. In general, non-covalent conjugation through a connector and covalent linkage through formation of an aptamer-siRNA chimera are two major strategies for aptamer and siRNA conjugation. In 2006, two biotinylated anti-PSMA aptamers were linked to two biotinylated anti-lamin A/C siRNAs using streptavidin as the connector (Chu *et al*., 2006). As a result, PSMA-positive prostate cancer cell-specific siRNA was internalised and siRNA-specific gene expression was inhibited *in-vitro*. However, the siRNA release mechanism has not been demonstrated *in-vivo*.

1.5.5.3. Aptamer based imaging

Another application of aptamers is diagnosis via *in-vivo and in-vitro* imaging, using an aptamer that is conjugated to a fluorophore, quantum dots, or other material such as gadolinium, which is useful for magnetic resonance imaging (MRI) (Figure 1.18). Optical imaging is a cost-effective imaging method that typically uses fluorescent or bioluminescent molecules. Aptamer based optical imaging can be divided into direct

targeting and activatable probes (Hong *et al*., 2011). Direct conjugation with an aptamer and a fluorescent molecule is widely studied (Shi *et al*., 2010; Cui *et al*., 2011; Talbot *et al*., 2011; Zhang *et al*., 2012; Song *et al*., 2013; Zhang *et al*., 2013). It is the simplest way to image via a visualised aptamer by fluorescence. Aptamers probes activated following conformational changes are particularly useful. They are designed such that fluorescence will "turn-on" when the aptamer binds to its target. Typically, a fluorescently labelled substrate is designed to be maximally quenched by a quencher in close proximity due to FRET (McIntyre and Matrisian, 2003; Tsien, 2005). For example, Zhang *et al*., designed a bifunctional fluorescent oligonucleotide probe for the detection of adenosine triphosphate (ATP) and thrombin (Tmb). The molecular beacon contains two hairpin loops that serve as the sensing elements, and a fluorophore at one end and a quencher at the opposite end, as the reporter (Li *et al*., 2013). This "Turn-on" fluorescence mechanism by quenching is widely used in aptamer-based biosensors. Compared to a conventional "always-on" probe, the activatable probe could substantially minimise the background signal originating from non-target tissues, thereby giving significantly enhanced image contrast (Hong *et al*., 2011). Not only optical imaging, but super paramagnetic iron oxide nanoparticle-aptamer conjugate have been used in MRI imaging (Yigit *et al*., 2007). Aptamers can also be applied for targeted ultrasound imaging using covalent conjugation of nanobubbles. These aptamer-conjugated nanobubbles can be harnessed to release a certain amount of drugs upon targeted ultrasound-trigger (Wang *et al*., 2011).

1.5.6. *Staphylococcus aureus* aptamer

Staphylococcus aureus specific ssDNA aptamer panels are developed by a whole bacterium-based SELEX procedure. After several rounds of selection with *S. aureus* as the target and *Streptococcus pneumoniae and S. epidermidis* as counter targets, a panel of aptamers to detect *S. aureus* was developed using cell-based SELEX by (Cao *et al*., 2009). They demonstrated that the simultaneous probing of several targets by a set of specific aptamers proved to be more efficient than probing by an individual aptamer in detection of *S. aureus*. Unlike single target SELEX which

generates an enriched pool of aptamers to the single target, the complex SELEX ends up with an enriched pool of aptamers to various targets on the cells (Wang *et al*., 2003; Shangguan *et al*., 2007).

In another study, a novel and sensitive fluorescence bioassay for the simultaneous detection of *S. typhimurium and S. aureus* was developed. This technique used aptamer-conjugated magnetic nanoparticles for both recognition and concentration elements and using nanoparticles as highly sensitive dual-colour labels (Duan *et al*., 2012). The luminescent signal was effectively amplified with the help of both magnetic separation and concentration. This method demonstrates the first use of aptamer-conjugated magnetic nanoparticles as the capture and concentration element and the use of up-conversion nanoparticles as the fluorescence element for the simultaneous detection of two types of pathogenic bacteria. According to published literature, several studies have focused on developing *S. aureus* specific aptamers *in-vitro*. However MRSA specific aptamer molecules have not been developed yet and currently we do not have reliable and sensitive technique to detect MRSA *in-vivo* over other *Staphylococcus* species. Hence my thesis focused on initiating the development of aptamer based molecular probes to detect MRSA.

1.6. Peptidic-based molecular probe development

1.6.1. Background and Principles of Phage-Displayed Peptide Library

Bacteriophage (phage), are single-stranded DNA viruses that infect various bacteria, including *E. coli*. Phage display technology first introduced in 1985 by George Smith, has had great applications in biology. Unique and other structural and genetic characteristics of the filamentous phage make phage display an extremely powerful tool for bioengineering. The technique can be used for screening ligands, developing new drugs, designing vaccines, evolving molecules, diagnosing diseases, drawing genetic maps, delivering targeted drugs or biosensing (Brigati *et al*., 2004; Liu *et al*., 2009; Mao *et al*., 2009). Numerous proteins and peptides with high specificity and affinity have been isolated from phage display libraries using affinity selection

(biopanning) and have been widely used in different fields (Takakusagi *et al*., 2010; Ueberberg and Schneider, 2010).

Encoded proteins are expressed on the phage surface as a fusion product with one of the phage coat proteins (Figure 1.19), this is achieved by the introduction of defined exogenous protein sequences into a location in the genome of the phage capsid proteins. By applying this technology, phage display libraries containing up to 1010 different proteins have been easily developed (Ueberberg and Schneider, 2010).

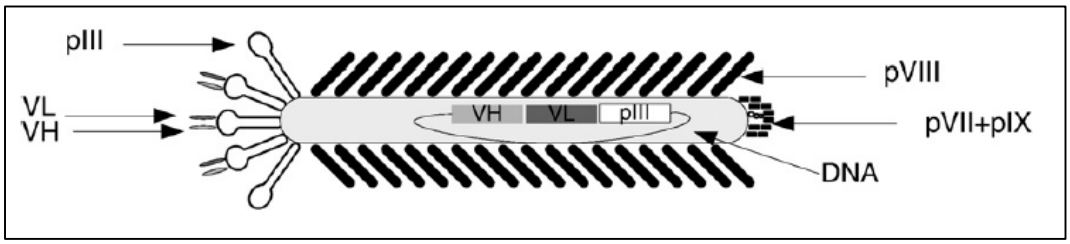

Figure 1.19: Schematic structure of a phage displaying multiple copies of a single-chain antibody (VH = variable heavy chain, VL = variable light chain). The information for the single chain antibody was introduced in a location of the genome for the phage coat protein pIII, and thus the antibodies are displayed fused to the pIII coat protein on the phage surface. An alternative startegy would be to express the single-chain antibodies with the other coat proteins of the phage pVIII or pVII+pIX (adapted from Ueberberg and Schneider, 2010).

Therefore Phage displayed peptide libraries are a heterogeneous mixture of such phage clones, each carrying a different foreign DNA and therefore displaying a different peptide on its surface (Smith and Petrenko, 1997). The foreign peptides to be displayed by phage are fused into phage coat proteins through random foreign DNA insertion into the phage genome, particularly in the N-terminus of pIII coat protein between the vector-insert and insert-vector junctions. Consequently, coat protein and foreign peptide become a hybrid fusion protein that is exposed to the exterior environment. pIII, a minor coat protein, is located at one tip of the phage with five copies. Hence, theoretically, foreign peptides fused with pIII protein are displayed in five copies as well. In addition to pIII, pVIII major coat protein and pVI minor coat protein have been used to fuse with the foreign peptides. Nonetheless, pIII display system is much more common because it allows different foreign DNA

insertion sites (N-terminus of pIII, middle of pIII or replaces N-terminal domain or C terminal via leucine zipper) while pVI only allows fusion of foreign peptide at C-terminal and pVIII at N terminal. According to Smith and Petrenko (1997), numerous pVIII displayed peptides, comprise a substantial fraction of the phage's mass and might dramatically alter the physical and biological properties of the phage.

Selection of the antibacterial peptide begins through affinity biopanning using phage-displayed peptide library. The target can react with the phage-displayed peptides in solution, followed by the affinity capture of phage-target complexes. After the first round of selection, only peptides with strong binding affinity to bacteria are captured while unbound phages are washed away. The captured phages are then eluted and amplified to generate more copies of each selected individual phage in order to secure ever-fitter subsets of peptides in further rounds of selection. At the end of the selection, the selected phages should be low in yield but high in stringency, with the specific and tight binding phage-displayed peptides (Zhang *et al*., 2012). Individual phage is subsequently isolated, followed by the DNA sequencing for the inserted DNA region that encodes the displayed peptide. Based on the DNA sequences, peptide sequences can be deduced.

1.6.2. Phage Display 12 Peptide Library

Phage display 12 amino acid peptide library consists of linear peptides with 12 amino acid residues. Phage display is not applicable to larger polypeptides in which the fusions might lead to detrimental effects on the function of coat protein (Christensen *et al*., 2001). According to New England BioLabs, each phage has short linker sequence (Gly-Gly-Gly-Ser) that connects the peptide to pIII coat protein. The phage displays 12 amino acids on the pIII minor coat protein with five copies per phage. It fulfils the minimum requirement of antibacterial peptide of 12-50 amino acids. Therefore, it is believed to have good binding efficacy to the target bacterial membrane. Ph.D 12 from New England Biolabs is supplied with large population of phage clone, approximately 10^9 phage clones each with unique displayed peptide and 10^{11} phage particles in total.

1.6.3. Applications of Phage Display Technology in bacterial detection

Short-synthetic peptides have been gaining importance as probes for microbial detection. Previous studies successfully identified at least one family of peptide ligands that binds spores of every *Bacillus* species examined (Turnbough, 2003) and to detect species specific peptide ligands for the detection of *Bacillus anthracis* spores (Williams *et al*., 2003). The microbial cell surface as a whole, displays unique molecular compositions made of lipids, carbohydrates and proteins that may alter the mechanism by which a peptide might interact with an epitope or receptor, thereby providing unique binding sites for peptide interaction (Yarbrough *et al*., 2010; Yarbrough *et al*., 2011). Phage-displayed peptides have been successfully used to identify *Salmonella typhimurium* (Olsen *et al*., 2003; Sorokulova *et al*., 2005; Olsen *et al*., 2006; Meyer *et al*., 2012), demonstrate *E. coli* using streptavidin conjugated quantum-dots (Edgar *et al*., 2006), and highlight the use of lytic phage for specific capture and detection of *S. aureus* (Balasubramanian *et al*., 2007) and *Bacillus anthracis* (Sainath Rao *et al*., 2010).

Bishop-Hurley *et al*., (2005) described the utility of using live whole bacterial cells as a target for the isolation of antimicrobial phage displayed peptides. They targeted receptor(s) on *Haemophilus influenza* and described that peptides binding to bacterial surface structures isolated by phage display may prove of value in developing new antibiotics. In another study a subtractive phage-display protocol to select for peptides binding affinity to the cell surface of poultry isolate of *Campylobacter jejuni* was used with the aim of finding peptides that could be used to control this microorganism in chickens. In total, 11 unique clones were found to inhibit the growth of *C. jejuni* by up to 99.9% *in-vitro*, and one clone was bactericidal *in-vitro*. The phage peptides were highly specific (Bishop-Hurley *et al*., 2010). They completely inhibited the growth of two of the four poultry isolates of *C. jejuni* tested with no activity detected towards other Gram-negative and Gram-positive bacteria.
Rao *et al*., (2013) studied an improved subtractive phage display approach to identify short peptides that can bind specifically to the cell surface of *S. aureus*. They envisioned that a synthetic peptide representing the consensus sequence of several of

these individual peptides that bound to the cell surface of *S. aureus* in combination with quantum dot nanocrystals can serve as a novel probe for the detection of *S. aureus*.

Kaur *et al*., (2012) have investigated the effects of protein synthesis inhibiting antibiotics on the plaque size and morphology of staphylococcal phages and suggest developing MRSA-virulent phages as therapeutics. However this technology has not been addressed to develop MRSA specific peptides to detect MRSA. Therefore my studies were focused to develop phage derived peptide to detect MRSA. Two approaches have been used, 1) MRSA specific and 2) PBP2A specific peptide development.

1.7. Hypothesis and Aims

Hypothesis 1:

- Lysine monomeric peptoids are a novel class of antibiotic with antimicrobial activity on bacteria, low mammalian cell toxicity and immunomodulatory properties.

Aims:

- Study the structure-activity relationships on bacterial killing using clinically important gram positive and gram negative bacteria.
- Study the mammalian cell toxicity on those derivatives using standard cell toxicity assays.
- Study the effect of those peptoids on inflammatory response using human neutrophil.

Hypothesis 2:

- Aptamer and peptide molecular probes are novel diagnostic tools to detect MRSA infection.

Aims:

- Purify PBP2A protein to develop aptamer and peptide probes targeting the protein.
- Conduct experiments to enrich aptamer using SELEX procedure against whole MRSA bacteria and the purified PBP2A protein.
- Conduct phage panning experiments against whole MRSA bacteria and the purified PBP2A protein.
- Sequence the enriched aptamer and phage to synthesise aptamer and peptide molecular probes.
- Study the binding ability on these probes against panel of clinically relevant bacterial species including MRSA.

Chapter 2:
Materials and Methods

Chapter 2: Materials and Methods

2.1. Materials

2.1.1. Chemicals used in this study

All chemicals were obtained from Sigma unless otherwise noted.

1kb DNA ladder (NEB)
4-12% Bis-Tris polyacrylamide gels NuPAGE-Novex (Invitrogen)
Agar
Ampicillin
Annexin V-647(Invitrogen)
Benzonase
BSA (NEB)
Dextran T-500 (Amersham Pharmacia Biotech, Buckingham, UK)
Diff-Quick (Gamidor, Didcot, UK)
Dihydroethidium (DHE) (Invitrogen)
DMEM media (Gibco)
DNase-free water
Ethanol
Fetal bovine serum (FBS)
GelRed (Cambridge Bioscience)
HBSS (PAA, Pasching, Austria)
IMDM media
Imidazole
IPTG
Iscove's modified Dulbecco's medium (PAA, Pasching, Austria)
Loading dye (Promega)
Luria Bertani (LB)
Lysostaphin
Lysozyme
MTS reagent (Promega)
Mueller-Hinton broth (MHB)
NaCl
NaH_2PO_4
$NaPO_4$
NcoI (CCATGG) and XhoI (CTCGAG) restriction enzymes NcoI (NEB)
Ni-NTA (Qiagen)
PBS
PCR master mix (Promega)
Penicillin-Streptomycin
Percoll (Amersham Pharmacia Biotech),
Propidium iodide (PI) (Invitrogen)
Qiagen Plasmid Midi Kit (Qiagen)
QVD-OPh

Roscovitine
SDS-PAGE protein gel (Invitrogen)
SOB media
Sodium citrate solution (Phoenix Pharma Ltd., Gloucester, UK)
Sytox-Orange dye (Invitrogen)
T4 DNA ligase (NEB)
Triton X-100

2.1.2. The bacterial strains used in this study

1. Methicillin Resistant *Staphylococcus aureus* (MRSA-ATCC252),
2. Methicillin Sensitive *Staphylococcus aureus* (MSSA-ATCC 25923),
3. *Escherichia coli* (ATCC 25922)
4. *Pseudomonas aeruginosa* (PAO1)
5. *Staphylococcus epidermidis*-clinical strain
6. *Klebsiella pneumonia* (ATCC BAA1706)
7. *Burkholderia cepacia* (ATCC25416)
8. *Staphylococcus aureus* RN6390-plasmid pSB2030 (PxylA::gfp-luxABCDE)
9. *E. coli* BL21(DE3) (Sigma; cat# B2935)

2.2. Methods

2.2.1. Microbiology

2.2.1.1. Bacterial growth inhibition assay in MHB

The bacterial growth inhibition assays were carried out to assess the efficacy of peptoids against bacterial growth. This assay was carried out to screen the whole peptoid library initially at 200 µM peptoid (all 13 different peptoids) concentration and then TOP with the panel of bacteria at 100 µM concentration. The assay has been carried out in 96 well plates with peptoid in 100 µl of Mueller-Hinton broth (MHB). In test wells, 50 µl of bacterial inoculum ($2x10^6$ cfu/ ml) in MHB was added to 50 µl of peptoid solution in MHB. Positive controls contained 50 µl of inoculum and 50 µl of MHB without peptoid. The bacterial growth was measured by measuring the O.D. at 600 nm over 16 hrs of incubation at 37ºC. The O.D. was

measured every 15 minutes using a spectrophotometer. The growth inhibition was determined as the concentration of peptoid that completely inhibited bacterial growth after incubation. The values reported were reproducible between three independent experimental replicates, each consisting of three parallel trials (Qazi *et al*., 2004; Chongsiriwatana *et al*., 2008).

2.2.1.2. MIC and MBC determination

MICs were using 96-well microtiter plate. In test wells, 50 µl of bacterial inoculum ($2x10^6$ cfu/ ml) MHB was added to 50 µl of peptoid solution in MHB (prepared 100, 80, 60, 40, 20, 0 µM serial dilutions). Positive controls contained 50 µl of inoculum and 50 µl of MHB without peptoid. The MIC was defined as the lowest concentration of peptoid that completely inhibited bacterial growth after incubation at 37°C for 16 hrs. MIC values reported were reproducible between three independent experimental replicates, each consisting of three parallel trials.

MBC was determined by calculating the absolute bacterial counts at the following day by enumerating an aliquot from the culture on LB agar plates. At the end of the 16 hrs of incubation for MIC, took 10 µl of the samples and did the serial dilutions in LB broth, plated a 10 µl onto LB agar plates (three replicates). The viable bacteria were enumerated on the next day after incubating plates at 37^{o}C.

2.2.1.3. Killing kinetics non-growth phase bacterial killing-PBS killing assays

This assay has been carried out to determine the bactericidal effect of peptoids on non-dividing, latent or slow-growing bacteria (Coates *et al*., 2002; Ooi *et al*., 2010). In this assay used 500 µl PBS instead of MHB and carried out in 1.5 ml eppendorf tubes. Bacteria were grown overnight in Luria Bertani (LB) broth at 37^{o}C in an orbital shaker at 200 rpm, subcultured the next day for 3-4 hours and washed three times with PBS before the assay. Then 250 µl of bacterial inoculum ($2x10^6$ cfu/ ml) in PBS was added to 250 µl of peptoid solution (serial dilutions) in PBS. Incubated

for 5 hrs and each hour took 10 µl of the samples and did the serial dilutions in LB broth, plated 10 µl onto LB agar plates (three replicates). The viable bacteria were enumerated on the next day after incubating plates at 37^{o}C.

2.2.1.4. Transmission electron microscopy (TEM) analysis

To visualise the ultra-structural damage caused by TOP, MRSA and PAO1 were incubated in 100 µM of TOP for 1 hour and the samples processed as below. For TEM, samples were fixed in 3% glutaraldehyde in 0.1M Sodium Cacodylate buffer, pH 7.3, for 2 hours then washed in three 10 minute changes of 0.1M Sodium Cacodylate. Specimens were then post-fixed in 1% Osmium Tetroxide in 0.1M sodium cacodylate for 45 minutes, then washed in three 10 minute changes of 0.1M Sodium Cacodylate buffer. These samples were then dehydrated in 50%, 70%, 90% and 100% normal grade acetones for 10 minutes each, then for a further two 10-minute changes in analar acetone. Samples were then embedded in Araldite resin. Sections, 1µm thick were cut on a Reichert OMU4 ultramicrotome (Leica Microsystems (UK) Ltd, Milton Keynes), stained with Toluidine Blue and viewed in a light microscope to select suitable areas for investigation. Ultrathin sections, 60nm thick were cut from selected areas, stained in Uranyl Acetate and Lead Citrate then viewed in a Phillips CM120 Transmission electron microscope (FEI UK Ltd, Cambridge, England). Images were taken on a Gatan Orius CCD camera (Gatan UK, Oxon, England).

2.2.1.5. Flow cytometry analysis of (Reactive Oxygen Species) ROS

MRSA was treated with different peptoids (TOP, THP-Tosyl-hexyl and HHP-H-hexyl) at 100 µM in a 96 well plate for 1 hour. Aliquots of bacterial cells were washed twice and stained with dihydroethidium (DHE). Cells were immediately used for flow cytometry analysis on a BD FACS Calibur (BD Biosciences, San Jose, CA). For each sample, 10,000 events were acquired, and analysis was done by gating intact cells using log phase controls. Epifluorescence microscopic images were taken at to show TOP induces ROS production in MRSA.

2.2.1.6. Phage Display library screening-General Experimental Design

A 12-mer phage-display peptide library was panned against whole MRSA and PBP2A purified protein. A total of three rounds of solution bio-panning was carried out separately on bacteria and purified protein. Then 120 randomly selected phage clones from the third round of bio-panning were sequenced individually and deduced into peptide sequences. Bioinformatics analysis predicted the conserved sequences of peptides and two lead peptides were selected for synthesis. Bacterial binding assays were carried out to assess the specificity of the synthesised peptides against MRSA.

2.2.1.7. Bacterial culture and reagents

All bacterial strains used in this study were maintained and sub-cultured periodically on nutrient agar plates and stored at 4-8^{o}C until tested. Stock cultures of all bacteria were stored in microbank beads (Pro-Lab Microbank) at -70^{o}C. In all experiments, log-phase cultures of bacteria grown in Miller's Luria–Bertani (LB) broth were centrifuged at 13,000 g, washed with PBS, pH 7.4 and serial ten-fold dilutions were prepared with PBS (Mediatech Inc., Herndon, VA). Bacterial titers were estimated by optical density and confirmed by plating and counting on nutrient agar plates after overnight incubation at 37^{o}C.

2.2.1.8. Study of aptamer as a therapeutic agent for bacterial infection

The assay was carried out in 96 well plates with aptamers at 1µM concentration in 100 µl of Mueller-Hinton broth (MHB). In test wells, 50 µl of bacterial inoculum ($2x10^6$ cfu/ ml) in MHB was added to 50 µl of aptamer solution in MHB. Controls contained 50 µl of inoculum and 50 µl of MHB without aptamer. Bacterial growth was measured by recording the optical density (O.D.) at 600 nm over 16 hrs of incubation at 35^{o}C. The O.D. was measured every 15 minutes using a spectrophotometer. Growth inhibition was determined as the concentration of

aptamer that completely inhibited bacterial growth after incubation. Experiments were conducted in triplicate on three separate occasions (Qazi *et al*., 2004; Chongsiriwatana *et al*., 2008).

2.2.1.9. Bacterial biding assay

A panel of bacteria were grown overnight and washed three times with PBS Then bacteria at 10^8 cfu/ ml and 10 µM FAM labelled peptide probes were co-incubated in 1ml PBS for 30 minutes at 37ºC on rotator shaker. Unbound peptides were washed off and bound peptides analysed using flow cytometry and confocal microscopy.

2.2.1.10. Evaluation of MRSA and PBP2A-aptamer probe binding *in-vitro* bacterial binding assay

A panel of bacteria were grown overnight and washed three times with PBS. A concentration of 10^8 cfu/ ml bacteria and the FITC labelled aptamer probes at 100 nM were co-incubated in 1ml PBS for 30 minutes at 37ºC on rotatory shaker. Excess unbound aptamer was washed off and analysed using flow cytometry and confocal microscopy.

2.2.1.11. Bacteria Suspension Preparation and PBP2A coated Ni-beads preparation

A single colony of bacteria (MRSA, MSSA and PAO1) was added to 5 ml of LB medium and incubated overnight at 37ºC with 250 rpm agitation. The following day, the suspensions were sub-cultured for 3-4 hrs, and then centrifuged at 13,000 g at 4ºC for 1 minute. The supernatant was discarded and the bacterial pellet washed with 1 ml of PBS. Upon washing, the bacteria were resuspended with 1 ml PBS and kept at 4ºC. Serial dilution of the bacteria was performed. One hundred microlitres of the serially diluted bacteria was plated on MacConkey agar to determine the bacterial titer. Then 10^9 cfu bacteria were used for biopanning and counter selection carried out in 2 ml low-bind eppendorf tubes.

A 300 µl of Ni-NTA agarose beads (washed three times with 1 ml PBS) were incubated with 100 µg/ ml of PBP2A at room temperature for 1 hour on a rotary shaker and unbound proteins washed off. These protein coated beads were then used as target substrates for the phage panning experiments in 2 ml eppendorf tubes. $2x10^9$ clones of the 12-mer phage-displayed peptide library were used for biopanning.

2.2.1.12. Phage Biopanning

Counter selection was performed against bacteria (MSSA or PAO1) (10^9 cfu/ ml) resuspended in 1 ml of phage library ($2x10^9$) in 2 ml eppendorf tube. The bacteria-phage mixture was incubated at room temperature with gentle agitation on a rotary shaker. After an hour, the bacteria-phage mixture was centrifuged at 13,000 g for 1 minute. The supernatant was passed through a 0.22 µm filter to remove all bacteria and removed the unbound phage into a fresh eppendorf tube. The unbound supernatant was collected for biopanning against MRSA bacteria and PBP2A protein. A separate counter selection was carried out with BSA coated Ni-beads and the supernatant used for biopanning against PBP2A protein.

PBS (with Ca^{+2} and Mg^{+2}) with 1% BSA was used for biopanning solution throughout the experiments. Biopanning was carried out against MRSA with and without counter selection. After incubation at room temperature for 1 hour, the MRSA-phage were collected by centrifugation and washed 10 times with PBS to remove any unbound phages. To increase the stringency, 1 % Tween 20 was added during the second and third biopanning. PBP2A coated Ni-beads were also biopanned with and without counter selected phage libraries. PBP2A coated Ni-beads described above (300 µl) resuspended in 1 ml of phage library ($2x10^9$) in 2 ml eppendorf tube for PBP2A protein biopanning and treated as same as above during the incubation and washing steps.

After a final washing with PBS, 1 ml of elution buffer (0.2 M glycine-HCl, pH 2.2) was added to resuspend the pellet (MRSA-phage or PBP2A-phage). The tube was

incubated at room temperature on a rotary shaker for 10 minutes. Then 150 µl of neutralization buffer (1 M Tris-HCl, pH 9.1) was added immediately to the tube. 10 µl of the phage elute was titered and the remaining phage were amplified to enrich the phage clones for subsequent rounds of biopanning.

2.2.1.13. Phage Amplification and phage precipitation

A loop of single colony of *E. coli* ER2738 was added into 5 ml of LB medium supplemented with tetracycline (20 mg/ ml) and incubated overnight at 37ºC. The next day, 200 µl of the overnight culture was added into 20 ml of fresh LB medium in 250 ml conical flask and incubated for 30 minutes in a shaking incubator until the O.D. reached 0.05 at 600nm. The remaining phage elute was added into *E. coli* for propagation at 37ºC, 200 rpm. After 5 hours incubation, the culture was transferred into a 50 ml polypropylene tube and centrifuged at 14,000 g, 4ºC for 10 minutes. The supernatant was transferred into a fresh tube and centrifuged, then 80% of the upper supernatant (16 ml) was transferred into a fresh tube that was filled with 1/6 volume of 20% (v/v) PEG/ 2.5 M NaCl (3 ml). The mixture was mixed well and incubated overnight at 4ºC to precipitate the phages. The next day, the mixture was centrifuged at 12,000 g, 4ºC for 15 minutes. The supernatant was discarded and the tube was centrifuged again to completely remove the residual supernatant. The precipitated pellet was resuspended with 1 ml of TBS and transferred to a fresh microcentrifuge tube. The suspended phage was centrifuged for 5 minutes at 14,000 g at 4ºC to pellet residual cells. Supernatant containing amplified phage was transferred (80%) to a fresh tube and the phage has precipitated adding 1/6 of the volume (200 µl) of 20% PEG/ 2.5M NaCl. The tube was incubated on ice for one hour, followed by centrifugation at 14,000 g at 4ºC for 10 minutes. The supernatant was discarded and the tube was centrifuged. After removing the residual supernatant, the pellet was resuspended with 200 µl of TBS and centrifuged to remove any cells. Supernatant was transferred to new tube and 200 µl of sterile glycerol and stored at -20ºC. This is the amplified elute. The pre-amplified elute and the amplified elute were titered to determine the input titer for the subsequent rounds of biopanning.

2.2.1.14. Phage titering (quantification of phage number)

The phage stocks were titered by diluting so that the multiplicity of infection (MOI) was < 1 prior to infection therefore each plaque contains one phage DNA sequence. A loop of single colony of *E. coli* ER2738 was added into 5 ml of LB medium supplemented with tetracycline (20 mg/ ml) in a 50 ml centrifuge tube and incubated for 5 hours in shaking incubator until the O.D. at 600 nm of the bacteria reached 0.5. Pre-amplified phage was serially diluted to 10^{-4} while amplified phage was diluted to 10^{-10}. Ten microlitres of the diluted phage from the last three dilutions (10^{-2}, 10^{-3} and 10^{-4}) from the pre-amplified phage eluate and 10^{-8}, 10^{-9} and 10^{-10} from the amplified phage eluate, were added to 200 µl of *E. coli* ER2738 (O.D.~0.5). After 5 minutes of infection in room temperature, the phage-infected *E. coli* ER2738 was transferred to 5 ml of melted top agar (7 g/ L agar) at 45ºC and briefly mixed well before pouring onto LB agar supplemented with IPTG/ Xgal (1.25 g IPTG and 1 g Xgal in 25 ml dimethylformamide-DMF). The plate was incubated overnight at 37ºC. The number of blue plaques was counted and recorded as plaque forming unit (PFU)/ ml on the next day.

2.2.1.15. Individual Phage Clones Stock Preparation

Twenty colonies from each biopanning were selected at the third round and amplified individually. Small scale amplification was carried out to make individual phage clone stocks. Overnight *E. coli* ER 2738 was diluted 1:100 in LB medium. One millilitre of the diluted culture was aliquoted into a microcentrifuge tube. A single, well-separated blue plaque from pre-amplified phage titer plate was picked using sterilized cut blue tips by stabbing on the agar then slowly aspirated the agar over the plaque. The culture together with plaque was incubated at 37ºC, 200 rpm for 5 hours. The culture was centrifuged at 14,000 g for 30 seconds. The supernatant was transferred into new microcentrifuge tube and centrifuged. The upper 600 µl of the supernatant was then mixed with 600 µl of 50% glycerol in another new tube. Individual phage clone stocks were kept at -20ºC.

2.2.2. Cell biology

2.2.2.1. Haemolytic activity and Therapeutic index for TOP

Whole blood were isolated from healthy blood donor, using sodium citrate solution (Phoenix Pharma Ltd., Gloucester, UK) as an anticoagulant and resuspended to 20 vol% in PBS (pH 7.4). In a 96-well microtiter plate, 100 µl of erythrocyte suspension was added to 100 µl of peptoid solution in PBS (prepared by 1:2 serial dilutions) or 100 µl of PBS in the case of negative controls. One-hundred percent haemolysis wells contained 100 µl of blood cell suspension with 100µl of 0.2 vol% Triton X-100. The plate was incubated for 1 h at 37°C, and then each well was diluted with 150 µl of PBS. The plate was then centrifuged at 1,200 g for 15 min, 100 µl of the supernatant from each well was transferred to a fresh microtiter plate, and absorbance at 350 nm was measured. Percentage of haemolysis was determined as $(A-A_0)/(A_{total}-A_0)x100$, where A is the absorbance of the test well, A_0 the absorbance of the negative controls, and A_{total} the absorbance of 100% haemolysis wells, all at 350 nm (Chongsiriwatana *et al*., 2008).

The selectivity ratio (SR) or Therapeutic index (TI) was calculated, where TOP concentration has 10% haemolysis activity (5 mM) divided by the median of the MIC value (50 µM). The calculated TI for TOP was 100 which is higher than previously discovered peptidomimetic (TI were around 20) (Chongsiriwatana *et al*., 2008).

2.2.2.2. Bacteria and lung epithelial cell (A549) co-culture assay

This co-culture assay was carried out to demonstrate the peptoids selective killing of bacteria over mammalian lung epithelial cells (A549). A549 cells were seeded at 10^4 cells /well in 96-well microtiter plate and cultured in IMDM media with Penicillin-Streptomycin (100 U/ ml). After 24 hrs was changed the IMDM media to no antibiotics (Penicillin-Streptomycin). The cells were cultured for further 24 hrs without antibiotics. At the end of the total 48 hrs of incubation, was removed the

media and added 100 µl of bacteria ($1x10^6$ cfu/ ml) in IMDM (no antibiotics). The plates were then centrifuged at 2500 rpm for 30 minutes to adhere the bacteria on to the A549 cells and the supernatant was replaced by fresh IMDM (no antibiotics). The cells and bacterial co-cultures were incubated with and without peptoid in IMDM (no antibiotics) for 8 hrs at 37°C.

At the end of the 8 hrs incubation, bacterial growth was measured by calculating the absolute bacterial counts and measuring the gfp fluorescence (RN6390). The A549 cell death was measured by staining the cells with Sytox-Orange dye (Invitrogen, final concentration 5 µM) which only labelled the nucleus of the cells with compromised cell membranes. Lysed cell-free supernatants were cultured overnight to confirm bacterial colony counts at the end of the assay.

2.2.2.3. Confocal microscope live image of A549 cells with peptoids

The cell permeability of the TOP was evaluated and visualised using confocal microscopy live image analysis. A549 cells were seeded at 10^8 cells/ coverslip (Fisher Scientific; Cat No: 0730.016) which were ethanol (70%) washed, dried and placed on the bottom of a 6 well microtiter plate (Corning Costar). A549 cells were grown to 80% confluence in DMEM media with Penicillin-Streptomycin (100 U/ ml) and 5% FBS for 24 hrs at 37°C with 5% CO_2. Then A549 cells were incubated with TOP-TAMRA for 30 minutes and the excess peptoid washed off and imaged at 565/ 580 nm.

2.2.2.4. Intracellular bacterial killing assay

For internalization assays, *S. aureus* (RN6390) were internalized into A549 cells and the assay performed and quantified as previously described (Qazi *et al*., 2004). Monolayers of A549 epithelial cells grown to confluence (80%) were co-incubated with 100 µl of (10^7 cfu/ ml) gfp *S. aureus* for 1 hour after 30 minutes of centrifugation (2500 rpm, for 30 minutes) to enhance bacterial epithelial interaction and subsequent internalization. The wells were then washed (3x in PBS) and

incubated for 1 hour (37ºC, 5% CO_2). Non-internalized bacteria were removed by subsequent treatment with lysostaphin (10 μg/ml, Sigma) in HEPES buffered DMEM (Gibco) for 20 min at 37°C. Plates were washed and co-cultures were then incubated in phenol red-free DMEM (37ºC 5%CO_2) along with TOP (50 μM) or control. Luminescence and gfp fluorescence were measured on a Biotek plate reader every 15 minutes for 20 hours.

2.2.2.5. Prophylactic treatment of TOP

This assay was performed to elucidate the utility of the pre-treatment of TOP to prevent bacterial colonisation in lung epithelial cells. A549 cells were pre-treated with TOP (50 μM and 100 μM) for 1 hour and washed excess prior to internalisation of RN6390-gfp-lux *S. aureus* the intracellular bacterial growth was measured by gfp fluorescence. Extracellular bacteria were removed by using lysostaphin (10 μg/ ml) as before and the growth monitored by measuring the gfp fluorescence at 48 hrs.

2.2.2.6. Isolation of human blood neutrophils

Fresh human venous blood was collected from volunteers, according to University of Edinburgh (Scotland) Research Ethics Committee approval #1702/ 95/4/72 or UBC Clinical Research Ethics Board protocol C02-0091, using sodium citrate solution (Phoenix Pharma Ltd., Gloucester, UK) as an anticoagulant. For neutrophil isolation, blood was centrifuged at 300 g for 20 min at room temperature, platelet-rich plasma was removed, and cells were suspended gently in 1% Dextran T-500 (Amersham Pharmacia Biotech, Buckingham, UK) in 0.9% saline and sedimented for 30 min at room temperature. The leukocyte rich upper layer was then fractionated by using three-step discontinuous, isotonic Percoll gradients as described previously (Dransfield *et al*., 1994). Briefly, cells were centrifuged at 300 g for 6 min, resuspended in 55% isotonic Percoll (Amersham Pharmacia Biotech), layered on top of 68% and 81% isotonic Percoll layers, and centrifuged at 700 g for 20 min at room temperature. Neutrophils were collected, washed in phosphate-buffered saline (PBS) without calcium or magnesium, and resuspended in Iscoves's Dulbecco's modified

Eagle's medium (IDMEM; Invitrogen, Paisley, UK, or Burlington, Ontario, Canada) with 10% (v/v) heat-inactivated Fetal bovine serum (FBS).

2.2.2.7. Neutrophil apoptosis

Figure 2.1 shows the microscopic images of normal and apoptotic neutrophils. The apoptotic neutrophils containing condensed nuclei compared to the fragmented nuclei in normal neutrophils. Freshly isolated human blood neutrophils were incubated at 37°C, 5 % CO_2, for 6 h and 20 h, at $5x10^6$ cells/ ml in Iscove's modified Dulbecco's medium (PAA, Pasching, Austria) with 10% (v/v) heat-inactivated FBS, flat bottom 96-well culture plates (total volume 150 µl) in the presence of TOP (50 µM and 100 µM), Roscovitine from Sigma, Dorset, UK (apoptosis inducer- positive control) and the control.

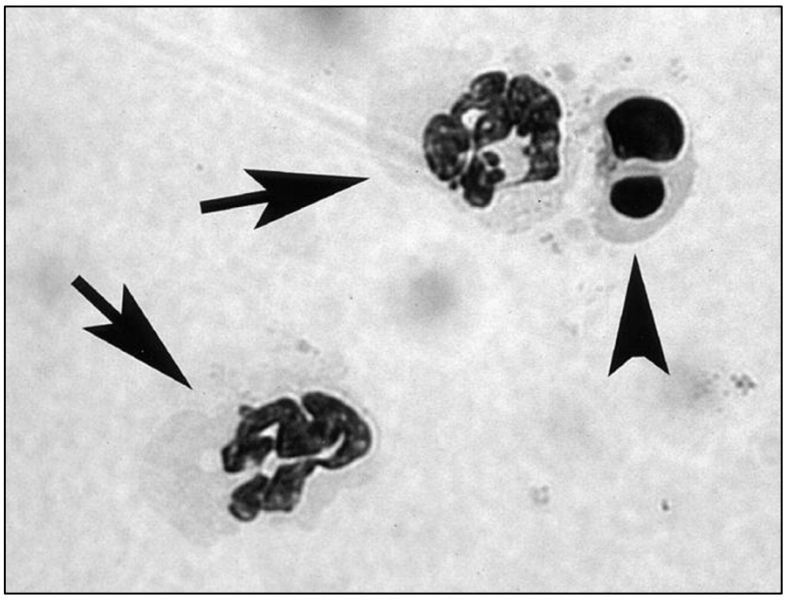

Figure 2.1: Representative microscopic images of normal and apoptotic neutrophils. Arrows indicate normal neutrophils and arrowhead indicates an apoptotic neutrophil containing condensed and fragmented nuclei (original magnification, ×1,000, May-Giemsa stain) (Hamasaki *et al*., 1998).

Apoptosis cells were analysed by flow cytometry with Annexin V-647 and counterstained with propidium iodide (PI) for necrotic cells. For the analysis, 50ul of cells were added to 250 µl of AnnexinV-647 (Invitrogen) (1:500 dilutions in HBSS with 2.5 mM Ca^{2+}) and after 10 min of incubation at 4°C, 1 µl of PI (1 mg/ ml) was added to each sample before immediate analysis on a FACScan flow cytometer (BD, Oxford, UK). Neutrophil apoptosis was confirmed by cyto-centrifugation of 80 µl of sample at 300 rpm for 3 min. Samples were then fixed with methanol and stained with Diff-Quick (Gamidor, Didcot, UK) before morphological analysis under the microscope.

2.2.2.8. Study the interaction of TOP with known modulators of neutrophil apoptosis

To investigate whether TOP can interact with and modulate the effects of known modifiers of neutrophil apoptosis pathways, cells were incubated with TOP in the presence or absence of QVD-OPh (Sigma, Dorset, UK) a potent pan-caspase inhibitor that protects cells from capsase-dependent apoptosis. The rest of the conditions are similar to section 2.2.2.7.

This investigates whether the TOP induces the apoptosis induced cell death (secondary necrosis) or primary necrosis (cell injury). These assays have been carried out for 6 and 20 hours and the neutrophils labelled with Annexin V-647 and PI to evaluate the pattern of cell death.

2.2.2.9. TOP-cytotoxicity activity on A549 cells

MTS Assays; the CellTiter 96® AQ_{ueous} One Solution Cell Proliferation Assay (Promega - Cat No: G5421) is a colorimetric method for determining the number of viable cells in proliferation or cytotoxicity assays. A549 carcinoma-derived lung epithelial cells (CCL-185; American Type Culture Collection) were cultured in DMEM. A peptoid solution plate (100 µl per well) was prepared by serial dilution of aqueous peptoid stocks in media. Peptoid solutions were transferred to a 96-well

plate of a day-old cell monolayers containing 100 µl per well media with ~5,000 cells per well. MTS reagent (Promega) 40 µl per well was added to each well, and the plate was incubated at 37°C for 3h, after which absorbance at 490 nm was read. Percentage of inhibition = $[1-(A- A_{testblank})/(A_{control}- A_{blank})] \times 100$, where A is the absorbance of the test well and $A_{control}$ the average absorbance of wells with cells exposed to media and MTS(no peptoid).A test blank (media, MTS, and peptoid) and A_{blank} (media and MTS) were background absorbance measured in the absence of cells (Chongsiriwatana *et al*., 2008).

2.2.2.10. Aptamer cytotoxicity studies on 3T3 cells

To evaluate the potential cytotoxicity of the aptamers, the CellTiter-Glo® Luminescent Cell Viability Assay was carried out to determine the number of viable cells in culture based on quantitation of the ATP present, which signals the presence of metabolically active cells (Promega - Cat No: G7570). Mouse embryonic fibroblast cells (3T3) were cultured in a 96-well plate, with ~5,000 cells per well in DMEM. Aptamers (50 µM) were mixed with cell culture media and transferred (100 µl) to one day old cell monolayers. For the positive control, 50 µM of H_2O_2 in DMEM was added. Cells were incubated for 24 hrs at 37^{o}C with a humidified atmosphere of 5 % CO_2. After 24hrs incubation, the plate was equilibrated at room temperature for 30 minutes. A 100 µl of CellTiter-Glo® Reagent was added to each well and the plate placed on an orbital shaker to induce cell lysis and allowed to incubate at room temperature for 10 minutes to stabilise the luminescent signal. The plate was then centrifuged at 1000 g to remove cell debris and supernatant transferred (150 µl) to a black 96-well plate and luminescence recorded.

2.2.3. Molecular biology

2.2.3.1. Lysine peptoid library synthesis

The core structure of the whole peptoid library was based on 9-mer lysine-like peptoid unit (Figure: 1.13) and the peptoid derivatives have been made by; (i)

changing the length of the carbon side chain (Figure: 1.14); and (ii) N-terminus modifications (Figure: 1.15). The three different side chain lengths introduced to a 9-mer consisted of butyl (four-carbon), hexyl (six-carbon) and octyl (eight-carbon) monomers. Further structural changes have been made to the N- terminus end of the polymer encompassing different chemical groups conjugated to the N-terminus end such as H-non modified, BnCO-Phenyl acetamide, Tosyl-Toluene sulfonamide, Suc-Succinic amide, Ac-Acetamide and Fmoc-9-Fluorenemethanol (Figure: 1.15 and Table: 1.3). A number of different bio assays have been developed and carried out to study the structure-activity relationship on these peptoids on bacterial killing and potential mechanisms.

All the peptoids were made in the department of chemistry university of Edinburgh in Mark Bradley's group. All chemicals, solvents and biological materials were purchased from Sigma–Aldrich or Fischer. Peptoids were synthesised using solid phase synthesis, a stepwise polymerization method is applied to grow polymer chain and it is anchored to a solid support while coupling reagents are iteratively passed over the matrix and adding one monomer at a time to afford a polymer with an exact monomer sequence and near absolute monodispersity (Chongsiriwatana *et al*., 2008; Unciti-Broceta *et al*., 2009). Peptoids were HPLC purified and purity was determined using MALDI-TOF MS analysis.

2.2.3.2. Bioinformatics data mining for *mecA* gene

Bioinformatics data tools have been used to obtain information about the *mecA* gene. The 'Comprehensive Microbial Resource' was the main resource (http://cmr.jcvi.org/tigr-scripts/CMR/CmrHomePage.cgi). The genome search has been carried out using *Staphylococcus aureus* as the input. The General Information for *S. aureus* subsp. aureus MRSA252 was obtained. The Annotation Search Report for *mecA* was obtained using Gene Symbol as *mecA* for the search. The Primary Annotation Display and Primary Annotation Sequences for the *mecA* gene and the PBP2A protein were obtained browsing the locus SAR0039. This DNA sequence has been used for the primer designing to amplify the *mecA* gene in MRSA.

2.2.3.3. *mecA* gene specific primers designing

mecA gene specific primers were designed to avoid a N-terminal membrane-spanning segment which is the non-soluble fraction of the protein. The designed primers only amplify the soluble fraction of PBP2A protein (amino acid residues 24 to 668aa). C-terminal His-tagged protein was designed to over express incorporating NcoI (CCATGG) and XhoI (CTCGAG) restriction enzymes (Table 2.1).

Table 2.1: Oligonucleotide primers used for cloning of *mecA* gene in this study

Name	Sequence 5'-3'
Forward primer-Jck12DC	ATAATA**CCATGG**CTTCAAAAGATAAAGAAATTAATAATAC
Reverse primer-Jck12BC	ATAATA**CTCGAG**TTCATCTATATCGTATTTTTTATTACC

2.2.3.4. PCR amplification of *mecA* gene and agarose gel electrophoresis

Set up for 100 µl PCR amplification volumes as shown in below:

PCR master mix (Promega cat # :M7502)	50 µl
Jck12DC	1 µl
Jck12BC	1 µl
Chromosomal DNA	1 µl (10 ng)
DNase-free water	47 µl

Initial denaturation at 95°C for 2 min then:

95°C for 30s

60°C for 30s

72°C for 2min

PCR was run for a total of 30 cycles and then 72°C for 2 min for the final extension.

A 1% agarose gel was prepared and loaded as shown below. To visualise the DNA bands on the gel, GelRed (Cambridge Bioscience Cat#:41003) was added (5 µl/ 50 ml) into the agarose gel preparation.

	Positive (µl)	Control (µl)	Ladder (µl)
Loading dye (Promega -Cat#:G1881)	1	1	1
PCR products	5		
PCR negative control (only primers)		5	
1kb DNA ladder (NEB-Lot #: 0971104)			1
H_2O			4

2.2.3.5. Restriction enzyme digestion and ligation

For the restriction enzyme digestion the following volumes were added as shown below:

Two enzymes, Ncol (NEB-Lot#: 0021106) and Xhol (NEB-Lot#: 0581101) were used for the restriction enzyme digestion of the vector pET21d(+) and PCR amplified *mecA* insert. Each restriction enzyme digestion was carried out separately and gel purified prior to the digested fragments being included in the second restriction enzyme digestion.

	Volume (µl)
DNA 10 µg	50
BSA	5
Buffer	5
Enzyme each (Ncol & Xhol)	3

Ligation of the insert and the vector was done using T4 DNA ligase (NEB-Lot#: 0991102). The insert (*mecA*) and the vector pET21d(+) were mixed in a 3 to 1 ratio and incubated at 16ºC for overnight with the 1 µl of T4 DNA ligase and 2 µl of ligase buffer in a total volume of 20 µl. The ligated products were precipated with ethanol and run on a 1% agarose gel to visualise the ligated products.

2.2.3.6. Transformation of cloned plasmid into *E. coli* BL21 cells

PBP2A protein was over-expressed in *E. coli* BL21(DE3) (Sigma; cat# B2935) expression strain. *E. coli* BL21 cells were thawed on wet ice and 10 ng of cloned DNA vector added and gently mixed. BL21 cells and plasmid vector were incubated on wet ice for 30 minutes. Cells were heat shocked by incubating tubes at 37ºC in a water bath for 45 seconds and returned to ice for 2 minutes. The mixture was added to warm (37ºC) SOB media (450 µl) and incubated for 1hour at 37ºC at 225 rpm. The cells were spread over LB agar plates containing ampicillin (50 µg/ ml) and incubated overnight at 37ºC to grow the transformed colonies.

2.2.3.7. Colony PCR

Colony PCR was carried out on ten selected transformed colonies. These colonies were grown in 500 µl of LB for 5hrs with ampicillin (50 µg/ ml) at 37ºC and washed three times in PBS. The cells were resuspended in 30 µl of water prior to extracting DNA by heating the cells up to 100ºC for 5 min. The cell debris was spun down and supernatant containing DNA transferred to a fresh tube. 5 µl of this DNA product was used to run a PCR using *mecA* specific primers as detailed above. 5 µl of PCR products were run on 1% agarose gel to confirm the *mecA* gene amplification.

2.2.3.8. Plasmid Midi preparation

Plasmid extraction was carried with a Qiagen Plasmid Midi Kit (Qiagen Car# 12143) following instructions from the manufacturer. Four positive colonies from colony PCR were selected for plasmid preparation. Colonies were grown in 100 ml of LB broth with ampicillin (50 µg /ml) at 37ºC overnight at 250 rpm. The overnight cultures were centrifuged at 5500 rpm for 10 min at 4ºC and supernatants discarded. The pellet was washed in 25 ml of PBS and pelleted at 5500 rpm for 10 min at 4ºC and resuspended in 4 ml of lysis buffer P1, in which RNase A was added. 4 ml of Buffer P2 was added and the mixture gently inverted 4-6 times.

Four millilitres of Buffer P3 was then added and mixed immediately by inverting 4-6 times and incubated on ice for 15 minutes to precipitate genomic DNA, protein and cell debris. To separate the plasmid DNA, the mixture was spun down at 9500 rpm for 30 minutes at 4ºC. While spinning the QIAGEN-tips 100 was equilibrated by applying 4 ml of Buffer QBT and allowed to empty by gravity flow, 10 minutes before adding the sample.

The QIAGEN-tips 100 were washed three times with 10 ml Buffer QC before eluting the plasmid DNA with 5 ml of Buffer QF into a new falcon tubes. The plasmid DNA was precipitated by adding 3.5 ml of Isopropanol and spun down at 9500 rpm for 30 min at 4ºC before decanting the supernatant. The DNA pellet was washed with 2 ml of 70% ethanol (at room temperature) and spun down at 9500 rpm for 30 min at 4ºC. The DNA pellet was air dried overnight at room temperature and the plasmid DNA dissolved in 200 µl of water before storing at -20ºC. The size of the plasmid DNA was determined by running a 1% agarose gel.

2.2.3.9. Sequencing of cloned plasmids and ClustalW analysis

Purified plasmids (5 µl) were sent for Sanger sequencing with 1µl of sequencing primers (3.2 pmol/ µl) premixed to a volume of 6 µl per sample. Plasmids were sequenced from both ends using T7-Promoter and T7-Reverse primers as shown below.

JCK138-T7-Promoter	TAATACGACTCACTATAGGG
JCK138-T7-Reverse	TAGTTATTGCTCAGCGGTGG

Received data were visualised using FinchTV DNA analysing software and sequences were analysed using ClustalW2 analyser to confirm alignment with the *mecA* gene sequence.

2.2.3.10. Over-expression of the PBP2A protein

Colony PCR data and sequencing data confirmed the accurate molecular cloning of the gene *mecA* into pET21d(+) vector. Two positive colonies (JCK138-34 and 35) were selected for the over expression of the protein PBP2A in *E. coli* BL21. The transformants were cultured in LB (5 ml) broth containing ampicillin (50 µg/ ml) at 250 rpm at 37^{o}C overnight. The following morning 5 ml of the overnight culture was added into 500 ml (1:100) of LB broth containing ampicillin (50 µg/ ml) in a 1L flask and grown for 5 hrs at 37^{o}C at 250 rpm before over expression. Expression of the His-tagged PBP2A protein was induced by adding 0.5 mM of IPTG and the cultures were then incubated at 22^{o}C at 250 rpm for an additional 24 hrs. Cells were harvested by centrifugation at 5,000 g for 20 min at 4^{o}C and the pellet washed twice with phosphate buffer (0.1 M $NaPO_4$, 0.5 M NaCl and pH 7.2) before freezing for purification.

2.2.3.11. PBP2A protein purification Cell lysis and generation of cleared lysates

The frozen bacterial cells were placed at room temperature and allowed to thaw for 15 minutes. Thawed cells were resuspended in 10 ml of buffer NPI-10 (50 mM NaH_2PO_4, 300 mM NaCl and 10 mM Imidazole pH 8) and added to 1 ml lysozyme solution (10 mg/ ml). To the resuspended cells, 3 units of Benzonase were added for every ml of the original cell culture volume. The cells were mixed by pipetting up and down and incubated for 30 min at room temperature. The crude lysate was transferred into 50 ml falcon tubes and centrifuged for 30 min at 15,000 g at 4^{o}C. The insoluble fraction was pelleted at the bottom and the supernatants containing soluble His-tagged protein were transferred into a new fresh tube.

2.2.3.12. Protein purification under native conditions using gravity flow

Ni-NTA superflow columns (1.5 ml) were drained by removing the seals at the outlet of the columns before opening the screw cap allowing them to drain by gravity flow on QIArack (cat# 19015). The column was equilibrated by adding 10 ml Buffer NPI-10 into column and allowed to drain through completely by gravity flow. The cleared lysate was added into the equilibrated columns and allowed to drain by gravity flow. The column was washed twice by adding 10 ml Buffer NPI-20 (50 mM NaH_2PO_4, 300 mM NaCl and 20 mM Imidazole pH 8) into the column. His-tagged protein PBP2A was eluted by adding 3 ml Buffer NPI-250 (50 mM NaH_2PO_4, 300 mM NaCl and 250 mM Imidazole pH 8) into a new tube. The buffer was replaced by PBS using 50,000 MW protein elution columns. The purity of the protein was evaluated by running SDS-PAGE protein gel and visualised by coomassie blue.

2.2.3.13. SDS-PAGE protein gel

Purified protein PBP2A was run on pre-cast 4-12% Bis-Tris polyacrylamide gels NuPAGE-Novex from Life technologies (Cat# NP0321BOX, Invitrogen) to visualise the protein purity and to determine the size of the protein. Protein sample was prepared by adding 20 µl of purified PBP2A protein, 5 µl of sample buffer (NuPAGE® LDS Sample Buffer Cat# NP0007, Invitrogen) and 2 µl of reducing agent (NuPAGE® Sample Reducing Agent Cat# NP0009, Invitrogen) before heating at 60ºC for 5 min. Protein size was determined by running 8 µl of SeeBlue® Plus2 Pre-Stained Standard (Cat# LC5925, Invitrogen).

2.2.3.14. BCA protein quantification assay

The Thermo Scientific™ Pierce™ BCA Protein Assay is a detergent-compatible formulation based on bicinchoninic acid (BCA) for the colorimetric detection and quantitation of total protein. This method combines the well-known reduction of Cu^{+2} to Cu^{+1} by protein in an alkaline medium (the biuret reaction) with the highly

sensitive and selective colorimetric detection of the cuprous cation (Cu^{+1}) using a unique reagent containing bicinchoninic acid. The purple-colored reaction product of this assay is formed by the chelation of two molecules of BCA with one cuprous ion.

A set of protein standards were prepared diluting the contents of one Albumin Standard (BSA) ampule into several clean vials, using the same diluent as the sample(s) for three replications of each diluted standard. The final concentrations of the standards were made to 2000, 1500, 1000, 750, 500, 250, 125, 25 (µg/ml) and the blank (no BSA). Working Reagent (WR) was prepared by mixing 50 parts of BCA Reagent A with 1 part of BCA Reagent B (50:1, Reagent A: B).

Microplate procedure was adopted according to the manufacturer's instructions as below. Pipette 25 µl of each standard or unknown sample replicate into a microplate well. Added 200 µl of the WR to each well and mix plate thoroughly on a plate shaker for 30 seconds. Covered the plate and incubated at 37°C for 30 minutes. Cooled the plate to room temperature and measured the absorbance at 562 nm on a plate reader. A standard curve was plotted by the average Blank-corrected 562 nm measurement for each BSA standard vs. its concentration in µg/ ml. Used the standard curve to determine the protein concentration of each unknown sample of PBP2A.

2.2.3.15. Penicillin binding protein (PBP2A) Latex Agglutination test

This test is a rapid latex agglutination assay, detecting PBP2A protein in isolates of *Staphylococcus*. The Oxoid PBP2A Latex Test (Cat# DR0900) was used to detect the PBP2A protein.

MRSA and MSSA strains were grown in LB agar plates overnight at 37ºC. Bacterial colonies were grown separately in 500 µl of LB for 5hrs at 37ºC at 250 rpm. The cells were harvested by centrifugation at 13,000 rpm for 1 minute and washed three times with PBS. The cells were resuspended in 4 drops of Extraction Reagent 1 in a

micro-centrifuge tube. The sample was boiled for three minutes and cooled down to room temperature before adding one drop of Extraction Reagent 2 into the tube and mixed well. The sample was spun at 13,000 rpm for 5 minutes and the supernatant used for the latex agglutination test.

The Latex reagents were mixed by inversion several times, and one drop of Test Latex or Control Latex added to each labelled test circle of the test paper according to the manufacture instructions. Test samples of 50 µl of supernatant of MRSA, MSSA or PBP2A purified protein were added on the test circle and the control circle. Using mixing stick mixed the latex and samples in each circle thoroughly. Sample cards were rocked gently up to three minutes and agglutination observed under normal lighting conditions.

2.2.3.16. Designing of Aptamer libraries

Primers, PCR conditions and library were designed and adapted according to Sefah *et al*., (2010). PCR plays a major part of aptamer selection and therefore it was important to select primers and libraries to have high PCR amplification efficiency. The 'sense' strand of the primer was functionalised at the 5′ end with an amino group (NH_2). The importance of the NH_2 group was to increase the resistance against nuclease degradation. The 'antisense' strand was functionalised at the 5′ end with biotin. The presence of biotin helps to separate the sense and antisense strands after PCR by streptavidin-biotin interaction, followed by alkaline denaturation. The length of the randomised region determines the diversity of the library. It is only necessary to label the initial library with NH_2. All oligonucleotide sequences were purified by high-performance liquid chromatography (HPLC) in 1µM scale. The primers and library sets are shown below in the Table 2.2. Fluorescein isothiocyanate (FITC) labelled forward primers were used to monitor the progress of selection by flow cytometry.

Table 2.2: Eight aptamer libraries used in this study.

G and M libraries different due to the variable primer binding sites as mentioned in the table.

Variable region	Library G Primer binding sites 5′ CTACACGACGCTCTTCCGATCT (-NNN-) AGATCGGAAGAGCGGTTCAGCA 3'	Library M Primer binding sites 5′ ATACCAGCTTATTCAATT (-NNN-) AGATAGTAAGTGCAATCT 3'
-(30N)-	G1 (74bp)	M1 (66bp)
-(40N)-	G2 (84bp)	M2 (76bp)
-(NNGGNNNNNNGGNNNNNNGGNNNNNNGGNN)-	G3 (74bp)	M3 (66bp)
-(NNNGGGNNNNGGGNNNNGGGNNNNGGGNNN)-	G4 (74bp)	M4 (66bp)

Primer sequences:

Jck11GA- Forward-AminoMod 5’CTACACGACGCTCTTCCGATCT3’
Jck11GB- Reverse-biotin 5’ TGCTGAACCGCTCTTCCGATCT 3’
Jck11GA- Forward-FAMMod 5’CTACACGACGCTCTTCCGATCT3’
Jck10MA- Forward-AminoMod 5’ ATACCAGCTTATTCAATT 3’
Jck10MB- Reverse-biotin 5’ AGATTGCACTTACTATCT 3’

2.2.3.17. PCR amplification of aptamer libraries

To assess the correct PCR conditions, several PCR protocols were carried out and the optimum conditions were determined. Ten PCR cycles were applied to primer set Jck11 above, using the following amplification conditions: hot start at 95°C for 2 minutes, denaturation at 95°C for 30s, annealing at 60°C for 30s and elongation at 72°C for 30s, followed by final extension for 4 min at 72°C. For the primer set Jck10, annealing temperature at 55°C was used and the rest of the conditions were the same as Jck11. Agarose gels were run to visualise the correct size of the PCR products.

2.2.3.18. Agarose gel electrophoresis

A 4% agarose gel was prepared with Tris-borate-EDTA (TBE) buffer (Promega-Cat No: V4251) and GelRed (Cambridge Bioscience-Cat No: BT41003) (1:10,000) added to visualize the ssDNA. After making the gel, 5 µl of DNA sample was loaded with gel loading dye (1:6) and electrophoresis performed at 100 V for 40 min in TBE buffer. The bands were observed under UV light and images of the gels captured.

2.2.3.19. Study of different buffers on the efficiency of SELEX protocol

After optimising the PCR conditions to amplify the aptamer libraries, optimisation of selection buffers were studied. G and M libraries were utilised in this experiment and selection was carried out with (MRSA) and without bacteria (control). Four different buffers were evaluated;

- PBS (with Ca^{+2} and Mg^{+2})
- Buffer B (Tris–HCl-25 mM, KCl-50 mM, NaCl-200 mM, EDTA-0.2 mM, Glycerol-5% (v/v), DTT-0.5 mM)
- Iscove's Modified Dulbecco's Media (IMDM)
- Dulbecco's Modified Eagle Medium (DMEM)

A 1 µl of the library (100 µM) was used in 1 ml of buffers and incubated for 30 minutes at 37ºC on a rotary shaker. Followed by three washes, the elution step was performed at 95ºC for 10 minutes in 500 µl of water. Elutes were subjected to PCR amplification and 5 µl of the PCR products were applied and run on agarose gel as above (2.2.3.18.).

2.2.3.20. Preparation of ssDNA from PCR products

A 200 µl of Streptavidin Sepharose beads (GE Healthcare Life Sciences-Cat No: 17-5113-01) were washed with 1 ml of water (molecular biology grade) and mixed with 1 ml of PCR products in a 1.5 ml eppendorf tube and incubated for 5 minutes at room temperature on a rotary shaker and washed three times with water. Single-stranded aptamers (non-biotinylated strand) were separated from the immobilised complementary strand with a 5 minute incubation of 50 µl of fresh 200 mM NaOH. Supernatant was taken after centrifugation at 13,000 g for 1 minute (ssDNA aptamer). The supernatant was diluted into 1 ml of PBS-T, containing 10 µl of 200 mM monobasic phosphate buffer to adjust the pH to 7.5. Finally, the material was heated to 95°C for 10 minutes then immediately placed at 4°C until the next round of SELEX.

2.2.3.21. Experimental design and SELEX procedure

The SELEX procedure was carried out independently against MRSA (ATCC252), MSSA (ATCC 25923), PAO1-*Pseudomonas aeruginosa*, *Kebsiella pneumonia* (ATCC BAA1706) *E. coli* (ATCC 25922) and alveolar epithelial cell line (A549) for five rounds without counter selection. These aimed to generate aptamers against individual bacteria and eukaryotic cells but were not specific due to lack of counter selection. These ssDNA aptamers were sequenced using an Ion Torrent sequencing method. Non-specific aptamers were attempted to be eliminated at the sequence level (where the sequenced data was carefully analysed and common sequences shared with the other bacteria eliminated).

For the purified PBP2A protein, 15 SELEX rounds were carried out before Ion Torrent sequencing with counter selection against BSA and FBS. No counter selection against whole bacteria was performed. The initial ssDNA library pool was prepared by adding 50 µl of 100 µM (5 nmol) DNA library (10^{15} different sequences) to 500 µl of SELEX buffer, mixed and heated at 95 °C for 5 min. The resulting mixture was snap-cooled on ice and kept on ice until ready to use later the same day.

Bacteria were grown in LB media overnight and washed with PBS three times before the incubation with ssDNA aptamer library (prepared above). For the purified protein (PBP2A) SELEX, the protein (0.1 mg/ ml) was coated on Ni-NTA Agarose beads (Qiagen-Cat No: 30210) (300 µl beads washed 3 times with PBS) for 1 hour at room temperature in water and excess protein washed off with PBS.

Bacteria and PBP2A coated Ni-NTA beads were incubated separately with the ssDNA library pool in 1 ml of PBS, the binding buffer using low binding eppendorf tubes to minimise the non-specific binding to the tube. The aptamer library and the target molecules (bacteria and PBP2A) were incubated for 30 minutes at 37ºC on a rotary shaker. After incubation, unbound aptamer was removed by washing three times and centrifuging the content at 13,000 g for 1 min at 4 °C and discarding supernatants.

For the first round of selection, elution of the bound sequences was conducted by adding 500 µl of DNase-free water to the cell pellet. Bacteria were resuspended and transfered into a 1.5 ml microfuge tube. Only in the first round was DNA eluted in purified water. As the entire eluted pool was amplified by PCR, DNase-free water was used for the elution of the bound DNA sequences during the first round of selection. If the DNA was eluted in PBS, high salt concentration affects the efficiency of PCR. The pellet mixture was heated at 95°C for 10 min, centrifuged at 13,100 g for 5 min and supernatant containing eluted DNA collected.

In subsequent rounds, DNA was eluted in binding buffer.
PCR conditions for the first amplification are shown below:

Reagents	Reaction mixture (µl)
PCR master mix (Promega-Cat No:M7502)	500
Primer mixture	50 (0.5 µM final)
DNA selected pool (template)	450

For primer set Jck11, amplification conditions used: hot start at 95°C for 2 minutes, denaturation at 95°C for 30s, annealing at 60°C for 30s and elongation at 72°C for 30s, followed by final extension for 4 min at 72°C. For the primer set Jck10: exactly same as primer set JcK11 except annealing temperature at 55°C.

2.2.3.22. Ion Torrent sequencing and data analysis

Seven DNA samples were transferred to The Institute of Genetics and Molecular Medicine, Western General Hospital, Edinburgh, UK for sequencing. The sequenced data was analysed using TextWrangler, text editor software which generated two probable aptamer probes called PBP2A specific and MRSA specific. The hairpin structures of MRSA and PBP2A aptamer probes were determined using the website at Integrated DNA Technologies (IDT), the OligoAnalyzer 3.1. To evaluate the binding efficacy of the aptamer probes, they have been re-synthesised with 5' FITC modification by SIGMA-ALDRICH, UK.

2.2.3.23. Evaluation of PBP2A-aptamer probe binding *in-vitro*; Ni-NTA beads assay

Ni-NTA agarose beads (washed three times with PBS, 300 µl) were incubated with 100 µg/ ml of PBP2A, BSA, FBS and trypsin separately at room temperature for 1 hour on a rotary shaker unbound proteins washed. These protein coated beads were used as target substrates for the FITC labelled PBP2A-aptamer probe to evaluate the efficacy of binding by using plate reader, confocal microscopy and fibre-based confocal microendoscopy (FCM-Cellvizio) after incubation for 30 minutes at 37^{o}C. Before analysis the beads were washed three times with PBS to remove excess aptamer probes. For the plate reader analysis, 100 µl of labelled beads were loaded into 96 well plates (three wells) and fluorescence measured at 488/520 nm. The beads were also visualised with live confocal microscopy (Zeiss LSM510meta) and also FCM-Cellvizio).

2.2.3.24. DNA Extraction and Sequencing

One millilitre of diluted overnight *E. coli* ER2738 was incubated with 100 µl of individual phage clone stock at 37ºC, 200 rpm for 4-5 hours. After centrifuging the culture at 14, 000 g for one minute at 4 ºC, 800 µl of the supernatant was then mixed with 200 µl of 20% (v/v) PEG/ 2.5 M NaCl. After one hour standing on ice, the mixture was centrifuged at 14,000 g for 10 minutes at 4ºC. Pellet was resuspended with 100 µl of iodide buffer by gently tapping the tube. Then 250 µl of absolute ethanol was added and mixed. The suspension was incubated at room temperature for 20 minutes. Later the suspension was centrifuged and washed with 0.5 ml of cold 70% ethanol. The supernatant was removed completely while the pellet was vacuum dried at 37ºC for 30 minutes and resuspended with 30 µl of TE buffer.

The DNA was then analysed in 1% agarose gel electrophoresis at 100 V for 1 hour in 1 X TBE buffer. The gel was stained with added GelRed and the DNA was viewed under UV light. Dense and uniform band was considered as purified DNA and compared with 0 .5 µg of purified single-stranded M13mp18 DNA (NEB #N4040). DNA was sequenced using 96 gIII sequencing primer 5´- HOCCC TCA TAG TTA GCG TAA CG-3´ by The Gene Pool, University of Edinburgh.

2.2.3.25. Sequence Analysis

The resulting DNA sequences were translated into an amino acid sequences using FinchTV software tool and the corresponding 12-mer peptide sequences were analysed by ClustalW online tool. The analysis data resulted in four groups (with and without counter selection against MRSA and PBP2A). The conserved region “ATGGGATTTTGCTAAACAACTTTCAACAGTTTCGGCCGA” of the phage genome was identified using ClustalW. The oligonucleotide that encodes the displayed peptide was located after the conserved region. The oligonucleotide was then translated into peptide sequence using FinchTV DNA translate tool.

2.2.3.26. Peptide synthesis

The sequence analysis and ClustalW data analysis elucidated high frequency hits for MRSA specific and PBP2A specific peptides. Therefore these FAM labelled peptides were synthesised alongside with control peptides (low frequency) to assess the efficacy of binding.

2.2.4. Bio-distribution and bio-availability of aptamer in mouse model

Naïve aptamer library was amplified using 5'-Cy5.5 conjugated forward primers and 5'-biotinylated reverse primers (see section 2.2.3.17.). The PCR products were purified and ssDNA obtained using Streptavidin Sepharose beads (see section 2.2.3.20.). 5'-Cy5.5 conjugated ssDNA aptamer (125 µg/ mice) were delivered into mice via intratracheal (IT) or intravenous (IV) routes. The distribution of 5'-Cy5.5 conjugated aptamer were monitored at 20 minutes and 72 hours using IVIS Pre-clinical *In-Vivo* Imaging Systems PerkinElmer (at 640/720 nm filters, 5 second exposure times and high binning). Mice were continuously anaesthetised (metomidate/ ketamine) during imaging. Animals were sacrificed after 72 hrs and organs imaged separately. PCR was performed on supernatant of homogenised organs (Homogenise bags from Fisher Scientific; BAJ-820-010N) samples and visualised on 4% agarose gel.

2.2.5. Licenses

All animal experimentation was performed with U.K. Home Office authorization and after local ethical review.

2.2.6. Statistics

All statistical analysis was performed on GraphPad Prism (version 5). The results are represented as the mean±s.e.m. Data sets were compared using a two-tailed unpaired Student's t-test. Statistical significance was set at $P < 0.05$.

Chapter 3:
Lysine like Peptoids as Antibacterial Agents

Chapter 3: Lysine like Peptoids as Antibacterial Agents

3.1. Abstract

A collection of peptoid analogs have been designed and synthesised by collaborators in the University of Edinburgh, Department of Chemistry (Dr Jeff Walton & Professor Mark Bradley) using solid phase synthesis. These peptoids have been subjected to biological evaluation to determine structure-activity relationships that define their antimicrobial activity. Each peptoid consists of 9 repeating N-substituted glycine monomers (9-mer). The monomer units were synthesised possessing three different lengths of alkyl chains; butyl-monomers (four-carbon), hexyl-monomers (six-carbon) and octyl-monomers (eight-carbon). Hence a family of 9-mers were synthesised with 4, 6 or 8 carbons in the side chain. To further increase diversity, the analogues were synthesised in varying capping groups at the N-terminus. These were either capped with an amide (-CONH-), sulphonamide (-SO_2NH-) or left uncapped. In total 13 peptoids were synthesised. Out of 13 different peptoids, only one peptoid called Tosyl-Octyl-Peptoid (TOP) demonstrated significant broad-spectrum bactericidal activity. TOP kills bacteria under non-dividing and dividing conditions. The Minimum Inhibitory Concentrations (MIC) values of TOP for *S. epidermidis*, *E. coli* and *Klebsiella* were 20 μM, whereas Methicillin-resistant *Staphylococcus aureus* (MRSA) and Methicillin-sensitive *Staphylococcus aureus* (MSSA) were 40 μM. The highest MIC values were observed for *Pseudomonas aeruginosa* (PAO1) at 80 μM. The selectivity ratio (SR) or Therapeutic index (TI) was calculated, by dividing the 10% haemolysis activity (5 mM) by the median of the MIC (50 μM) yielding a TI for TOP as 100. This TI is well above previously reported peptidomimetics TI of around 20. TOP demonstrates selective bacterial killing in co-culture systems and intracellular bacterial killing activity.

3.2. Introduction

Decades of widespread and indiscriminate usage of antibiotics in the healthcare sector has led to emergence of multidrug resistant bacteria such as vancomycin-resistant *Enterococci* (Arias and Murray, 2012) and methicillin-resistant *Staphylococcus aureus* (MRSA) (Theuretzbacher, 2011); (Gould *et al*., 2012; Phoenix *et al*., 2013). Hardly any new antibiotics have been introduced within the last decade and most novel antibacterial drugs are designed through modification of existing scaffolds (Jabes, 2011; Livermore, 2011; Tomasini *et al*., 2013). Hence there is clearly an urgent need for new antibiotics with novel mechanisms of antimicrobial action.

Antimicrobial peptides (AMPs) are a heterogeneous group of relatively small molecules containing less than 100 amino acids that are evolutionarily ancient molecules produced by nearly all living organisms. They are an essential part of the innate immune response (Zasloff, 2002). In addition to their antimicrobial function, AMPs are involved in variety of other roles such as modulation of the innate and adaptive immune systems via their ability to function as chemotactic agents (Easton et al., 2009; Nijnik and Hancock, 2009; Zasloff, 2002). AMPs and bacteria have co-evolved, hence few examples of resistance development have occurred in nature (Woolhouse *et al*., 2002).

A major obstacle in the further development of AMPs is difficulty in the transition of *in-vitro* activity into *in-vivo* efficacy (Hancock and Sahl, 2006). This is due to their sensitivity to biologically relevant conditions such as high salinity of plasma and divalent cations. Divalent cations compete with AMPs for binding sites on negatively charged bacterial surfaces (Deslouches *et al*., 2005). Moreover, AMPs are susceptible to degradation by serum proteases (Knappe *et al*., 2010) as well as to protein binding and subsequent inactivation (Yeaman *et al*., 2002).

In contrast to AMPs, Peptoids represent a class of peptidomimetic that are not found in nature. Peptoids have been generated to mimic the biological functions of naturally occurring cationic host defense peptides. They differ from peptides as the side chains are attached to the nitrogen atom instead of the α-carbon (Figure 1.13 and Figure 1.14) (Chongsiriwatana *et al*., 2008; Park *et al*., 2013). Due to this, peptoids are highly resistant to proteolysis. Peptoids have a wide range of potential biomedical applications such as cell target drug delivery, cell labelling and as antimicrobial agents (Park *et al*., 2013).Peptoids have recently been developed as antimicrobial agents (Park *et al*., 2013). In particular, similar to AMPs, peptoids have been generated to have both hydrophilic and hydrophobic properties. Recent structure/function investigations of these ampetoids (antimicrobial peptoid oligomers) suggested a requirement for net cationic charge and moderate hydrophobicity for effective antimicrobial activity, with high hydrophobicity and strongly amphipathic structures inducing haemolysis (Chongsiriwatana *et al*., 2008).

The development of peptoids was based on the HIV-tat cell penetrating peptide, a basic peptide derived from human immunodeficiency virus (HIV)-1. The Tat protein (positions 48-60) translocates through cell membranes and accumulates in the nucleus, the properties of which have been utilized for the delivery of exogenous proteins into cells (Futaki *et al*., 2001). The sequence of the optimal region is RKKRRQRRR, comprising basic amino acids containing 6 arginine and 2 lysine residues within a linear sequence of 9 amino acids (Ruben *et al*., 1989). Hence, arginine and/ or lysine-rich cell penetrating peptides (CPPs) cargo have been extensively studied as intracellular delivery agents (Futaki *et al*., 2001; Mo *et al*., 2012). Previous published data (Dhaliwal *et al*., 2011; Unciti-Broceta *et al*., 2009) based on the lysine monomeric peptoids demonstrated remarkable non-toxic mammalian cell membrane penetrability. However bacterial membrane damage or bacterial killing was not studied with these peptoids or derivatives. Therefore this chapter focussed on the structure-activity relationships that may determine bacterial killing and mammalian cell toxicity with derivatives of the original peptoid (Figure 1.15 and Table 1.3).

In contrast to the requirements previously suggested for optimal antimicrobial activity (Chongsiriwatana *et al*., 2008), our peptoids are highly hydrophilic achiral cationic molecule with no amphipathicity. These properties were specifically designed to confer antimicrobial killing and efficient entry into eukaryotic cells without incurring host toxicity. The previous studies suggested that 9-mer lysine-like peptoids facilitated efficient and rapid mammalian cell membrane penetration and entry with minimal toxicity (Unciti-Broceta *et al*., 2009). The core structure of the synthesised peptoid library was a 9-mer lysine-like peptidomimetic (Figure 1.13). Derivatives were made by;

(i) Changing the length of the carbon side chain (Figure 1.14), three different side chain lengths consisted of butyl (four-carbon), hexyl (six-carbon) and octyl (eight-carbon) monomers.

(ii) N-terminus modifications (Figure 1.15). Different chemical groups have been conjugated to the N-terminus end such as H-non modified, BnCO-Phenyl acetamide, Tosyl-Toluene sulfonamide, Suc-Succinic amide, Ac-Acetamide and Fmoc-9-Fluorenemethanol (Figure 1.15 and Table 1.3).

A number of different bio assays have been developed and carried out to study the structure-activity relationship on these peptoids on bacterial killing and their potential mechanisms.

3.3. Initial screening of peptoids – Bacterial growth inhibition

Bacterial growth inhibition assays were conducted to rapidly screen peptoids for antimicrobial activity against methicillin-resistant *Staphylococcus aureus* (MRSA), methicillin-sensitive *Staphylococcus aureus* (MSSA), *E. coli* and *Pseudomonas aeruginosa* (PAO1) (Figure 3.1 and Figure 3.2). The assays were conducted in 96 well plates with 200 μM of peptoid in 100 μl of Mueller-Hinton broth (MHB) over 16 hrs. The growth of bacteria was assessed by measuring the Optical Density (O.D.) at 600 nm. Summary results are shown in the table 3.1. The data demonstrate that the

Tosyl-octamer peptoid (TOP) shows significant growth inhibition of MRSA, MSSA, PAO1 and *E.coli*. Also there is some growth inhibition with H-octamer and BnCO-octamer. This antibiotic activity screen indicated that the tosyl group and octamer carbon side chain are important structural determinants of antibacterial activity of the synthesised library.

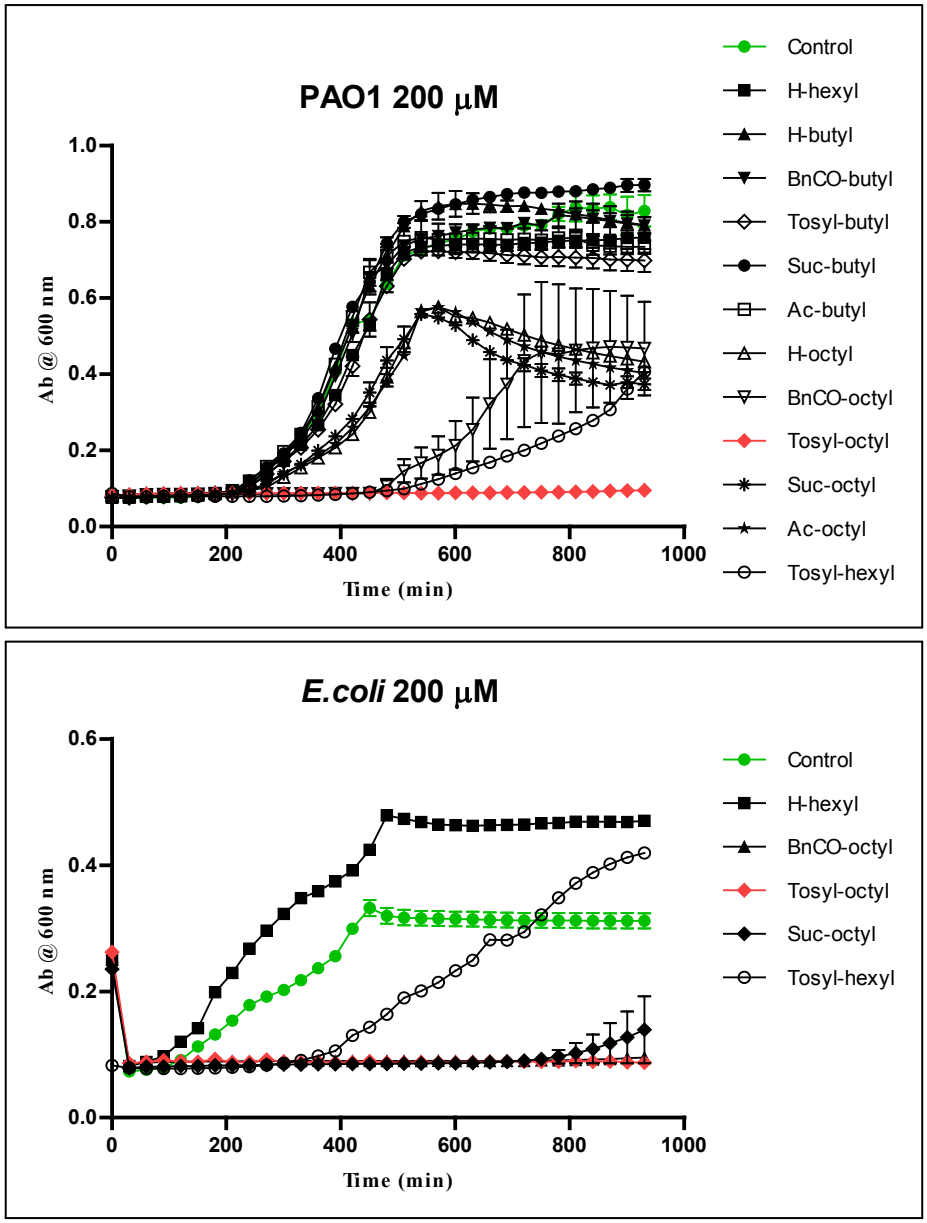

Figure 3.1: TOP is the most antibacterial peptoid against Gram-negative bacteria. *E. coli* and PAO1 (10^6 cfu/ml) were incubated in MHB at 37°C for 16 hrs with library peptoids (200 μM) in 96 well plates to assess the growth inhibition. Only Tosyl-Octyl peptoid (TOP) demonstrated bacterial growth inhibition at 16 hrs (Figures represent representative data of n=3).

Interestingly, the tosyl capping group in butyl and hexamer carbon chain peptoids confers no bacterial killing indicating that the importance of the octamer length of the carbon chain for bacterial killing. Based on this initial screen, the Tosyl-Octamer-Peptoid (TOP) was selected as the lead compound to carry out for further analysis.

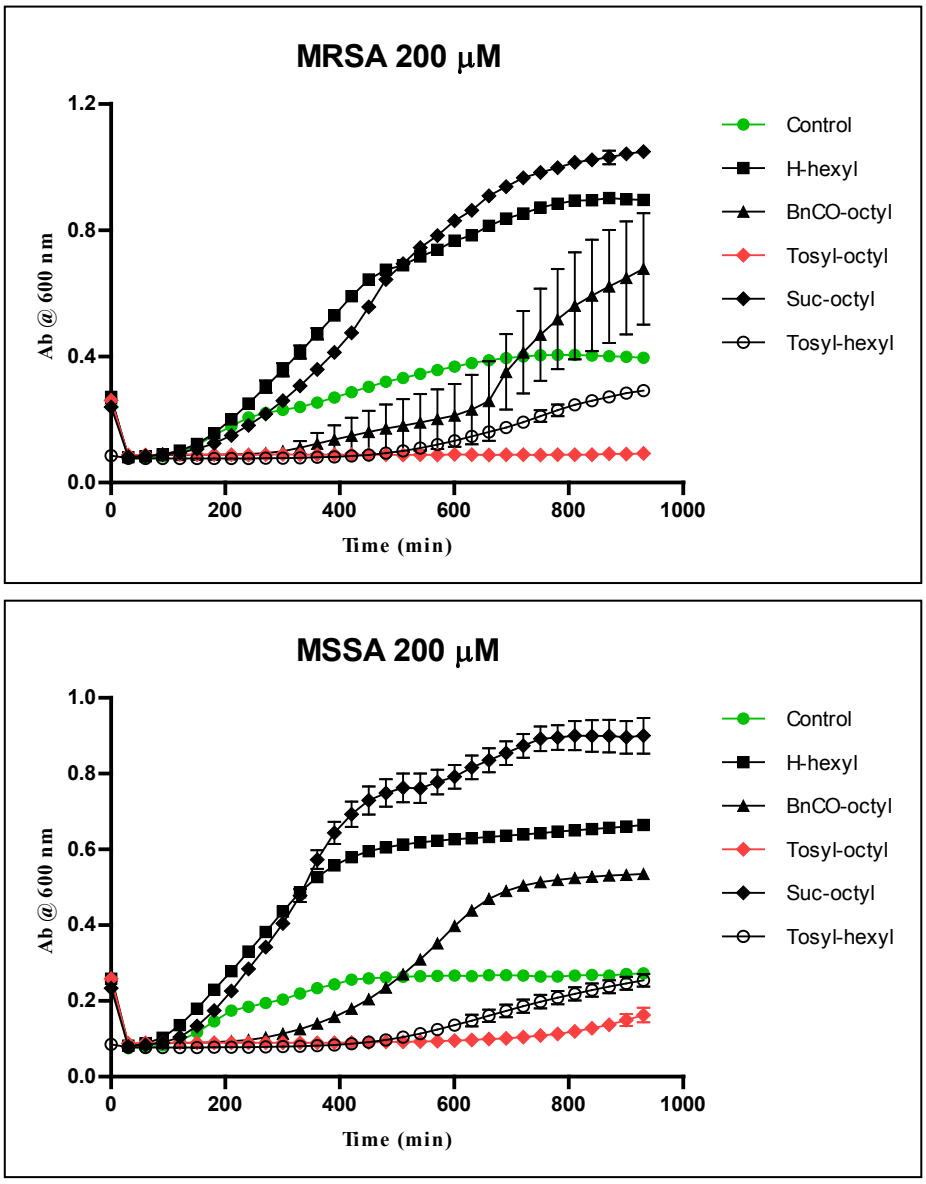

Figure 3.2: TOP is the most antibacterial peptoid against Gram-positive bacteria. MRSA and MSSA (10^6 cfu/ml) were incubated in MHB at 37°C for 16 hrs with library peptoids (200 μM) in 96 well plates to assess the growth inhibition. Only Tosyl-Octyl peptoid (TOP) demonstrated bacterial growth inhibition at 16 hrs (Figures represent representative data of n=3).

Table 3.1: The summary results of growth inhibition assay on bacterial killing.

Names of peptoids	Antimicrobial activity
H-butyl	No
BnCO-butyl	No
Tosyl-butyl	No
Suc-butyl	No
Ac-butyl	No
H-hexyl	No
Tosyl-hexyl	No
Fmoc-hexyl	No
H-octyl	Some
BnCO-octyl	Some
Tosyl-octyl (TOP)	Yes*
Suc-octyl	No
Ac-octyl	No

Yes*- No bacterial growth observed after 16 hrs of incubation at 37ºC.

Some- Observed some bacterial growth after 16 hrs of incubation at 37ºC.

No- Observed bacterial growth the same as the control.

3.3.1. Killing kinetics non-growth phase bacterial killing-PBS killing assays

Latent or slow-growing bacteria frequently exhibit tolerance to antibiotics that are active against rapidly dividing bacteria. This contributes to the prolonged treatment periods required for persistent infections and leads to emergence of multidrug resistant bacteria (Coates *et al*., 2002; Ooi *et al*., 2010). Hence a PBS killing assay has been performed to study the bactericidal effect of TOP on non-dividing bacteria (Figure 3.3).

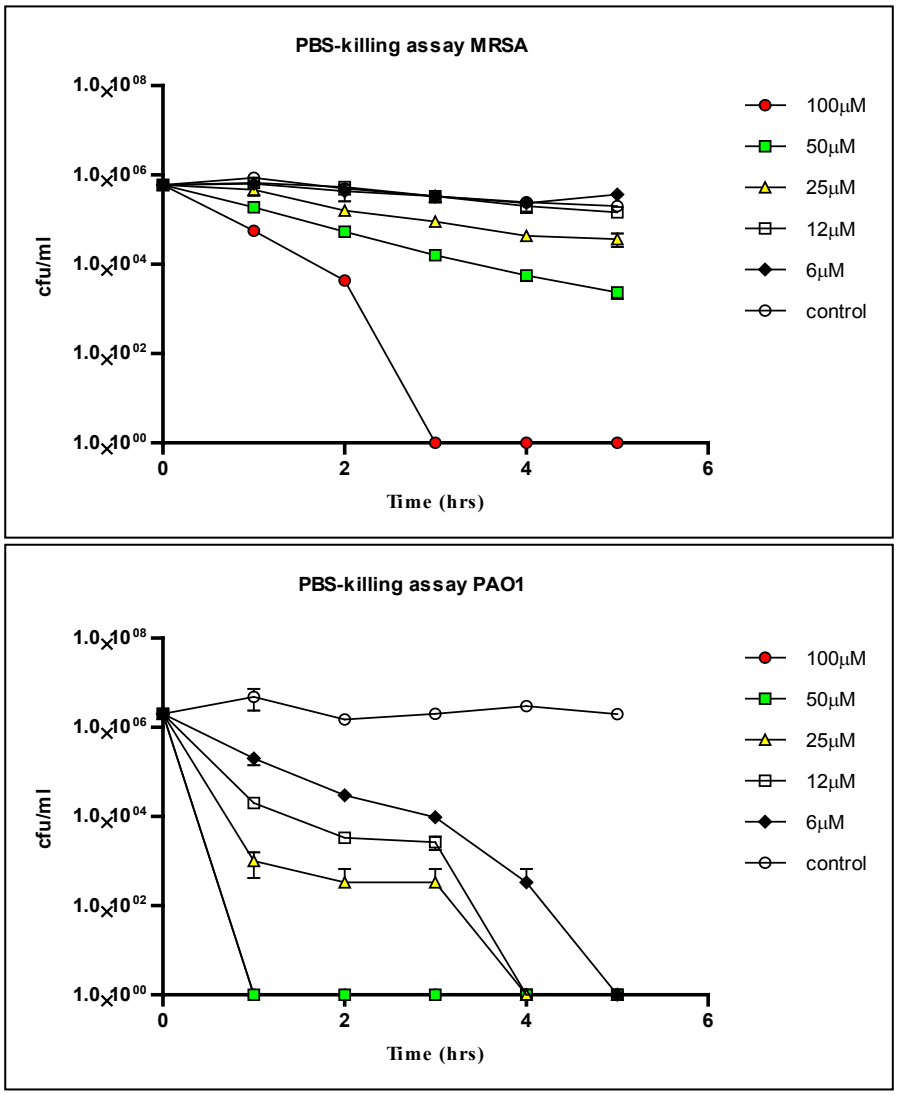

Figure 3.3: PBS killing assay data demonstrates that TOP kills non-dividing gram-positive and gram-negative bacteria. Bacteria (10^6 cfu/ ml) were incubated in PBS (1.5 ml eppendorf tubes) with TOP and the viability of the bacteria were assessed by plating 10 µl of the samples on LB plates after serial dilutions. The viable bacteria were enumerated on the next day after incubating plates at 37°C. Figures represent mean values ± SEM for n=3).

3.3.2. Killing kinetics on dividing bacteria-growth inhibition assay

At present, most clinically used antibiotics target one of the classical metabolic pathways of DNA, RNA, protein or cell wall syntheses (Poole, 2012; Sass and Brotz-Oesterhelt, 2013). Therefore antibacterial drug candidates are normally identified by screening libraries of natural, recombinant or chemically synthesized compounds against actively dividing bacteria targeting metabolic pathways (Sass and Brotz-Oesterhelt, 2013). Extending the screening assays that were performed (Figure 3.4), and the antibacterial activities of TOP against clinically relevant bacterial strains were performed to evaluate TOP's spectrum of activity.

Eight clinically important bacterial strains including gram-positive and gram-negative bacteria were incubated with and without TOP to study the effect of the peptoid on bacterial growth for 16 hrs. The results are shown in the figure 3.4. The TOP demonstrated bactericidal activity against most gram-positive and negative bacterial strains except in *Burkholderia cepacia* (*B. cepacia*) at 100 μM.

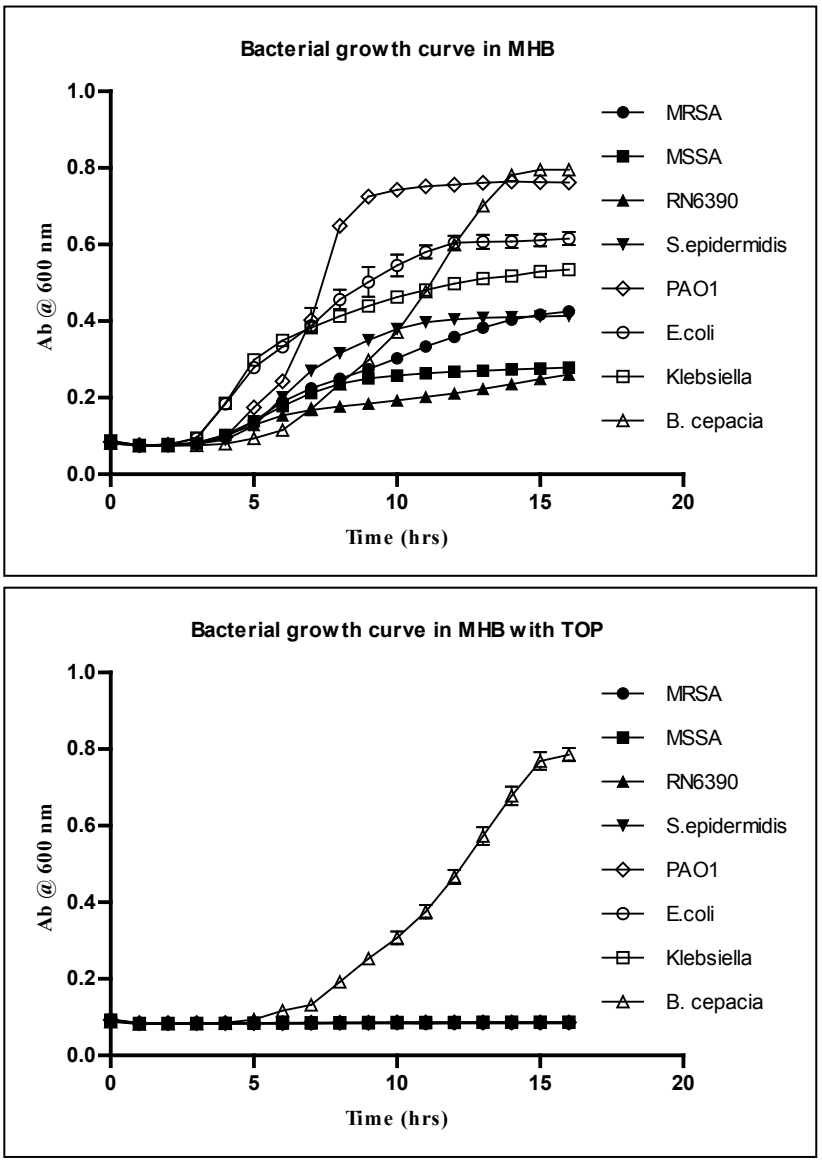

Figure 3.4: TOP shows bactericidal effect on dividing bacteria in MHB. Clinically relevant bacteria (10^6 cfu/ml) were incubated with and without TOP in MHB in 96 well plates for 16 hrs at 37°C and the growth measured by serial recording of O.D. at 600 nm. The bottom graph shows the effect of TOP at 100 µM on bacterial growth where the top graph shows the growth curves without TOP. Aside from *B.cepacia,* the remaining seven bacterial strains show complete growth inhibition to TOP at 100 µM concentration (data represent mean values ± SEM for n=3).

3.4. Minimum inhibitory concentration (MIC) and Minimum Bactericidal Concentration (MBC) determination for TOP

Following the initial screening at 100 μM (Figure 3.4), further assays were performed to determine MIC values for TOP. MIC is a laboratory test to determine the minimum concentration of an antibiotic that inhibits visible bacterial growth in MHB (Coates *et al*., 2002; Pompilio *et al*., 2011). Gram-positive and negative bacteria were grown in MHB with and without peptoid and the lowest concentration of TOP that completely inhibited the bacterial growth after incubation at 37^{o}C for 16 hrs were determined. The growth curves were generated by measuring the O.D. at 600 nm for 16 hrs (Figure 3.5 and Figure 3.6).

Minimum Bactericidal Concentration (MBC) was calculated at the end of the 16 hrs of incubation in MHB to determine the TOP concentration resulting in 0% bacterial survival (Coates *et al*., 2002). This was determined by calculating the absolute bacterial counts the following day by enumerating an aliquot from the culture on LB agar plates (Table 3.2).

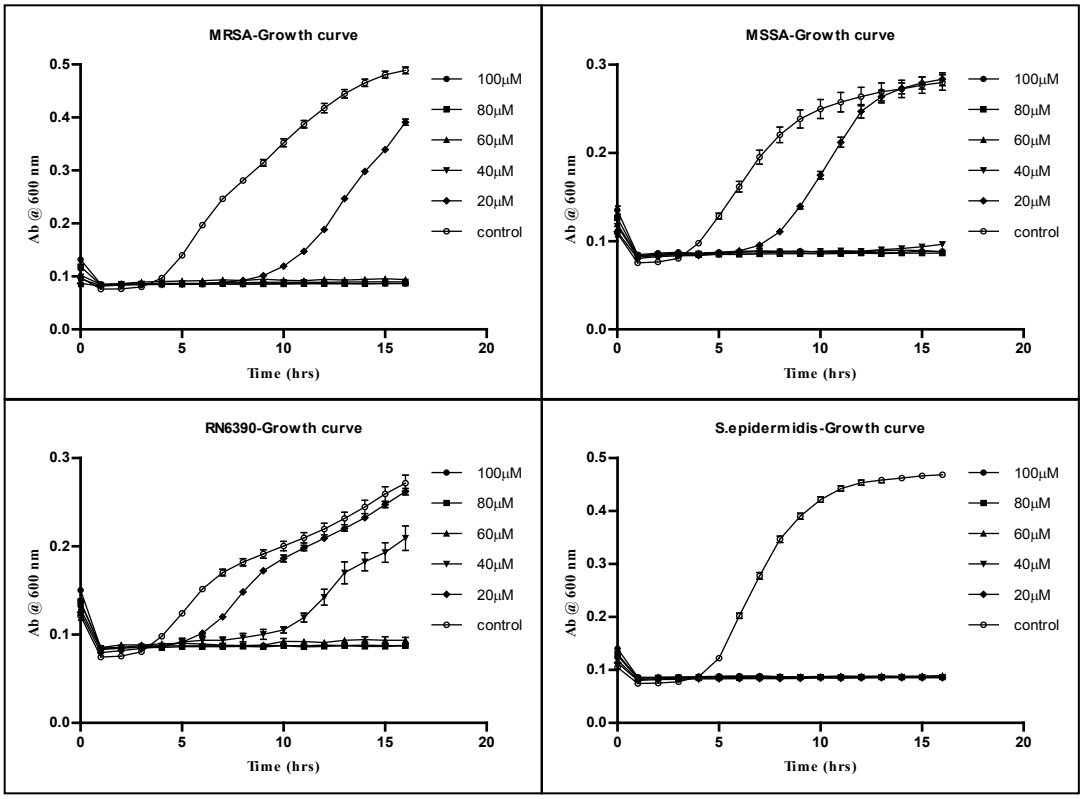

Figure 3.5: MIC for TOP against gram-positive bacteria. Serial dilutions of TOP were incubated with 10^6 cfu/ml bacteria in MHB and O.D. measured at 600 nm over 16 hrs at 37°C. Different bacterial strains showed different levels of growth inhibition. *S. epidermidis* showed higher susceptibility with growth inhibition at 20 µM and MRSA and MSSA showed growth inhibition at 40 µM whereas RN6390 showed growth inhibition at 60 µM (n=3; mean and SEM).

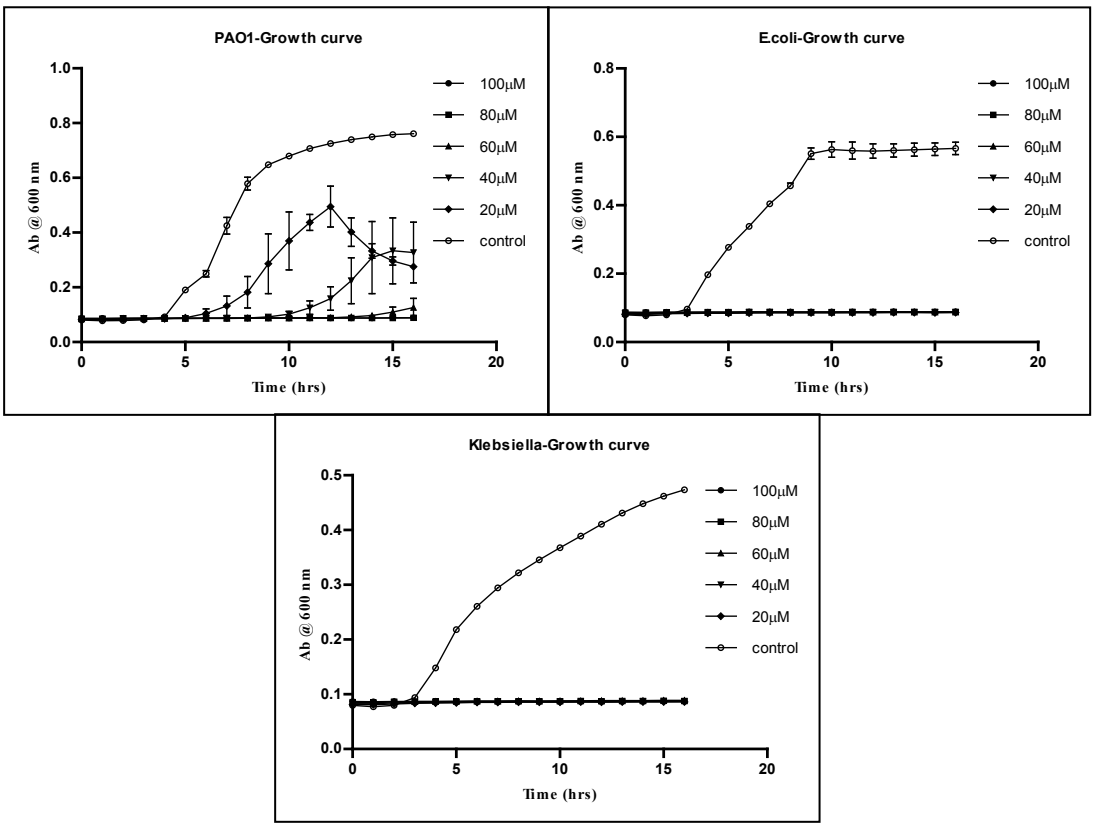

Figure 3.6: MIC for TOP against gram-negative bacteria. Serial dilutions of TOP were incubated with 10^6 cfu/ml bacteria in MHB and O.D. measured at 600 nm over 16 hrs at 37°C. *E. coli* and *Klebsiella* show growth inhibition at 20 µM, whereas PAO1 showed growth inhibition at 80 µM (n=3; mean and SEM).

Table 3.2: The summary table shows the MIC and MBC values for TOP

Bacteria	MIC (µM) (n=3)	MBC (µM) (n=3)
MRSA	40	60
MSSA	40	80
S.epidermidis	20	20
RN6390-gfp-lux	60	100
PAO1	80	100
E.coli	20	60
Klebsiella	20	40

3.5. Haemolytic activity and Therapeutic index for TOP

Haemolytic activity is conventionally used to assess eukaryotic membrane toxicity of antibacterial as red blood cells are extremely fragile (Ilker *et al*., 2004; Yang *et al*., 2000). Cationic AMPs are thought to attach to negatively charged bacterial membranes and then 'pore form' in bacterial membranes through hydrophobic interactions. Unlike bacteria, mammalian cell membranes are charge neutral, therefore AMPs have reduced electrostatic attraction to mammalian cell membranes. However, the hydrophobic nature of many of the AMPs still results in eukaryotic cell membrane toxicity. These characteristics of AMPs result in a selectivity ratio or therapeutic index defined as (Ilker *et al*., 2004) the ratio of the AMP concentration resulting in 10% haemolytic activity (Haemolytic Dose 10%-HD_{10}) over the MIC of AMP (Al-Ahmad *et al*., 2013; Brogden, 2005). Hence, the haemolytic activity of TOP was determined (Figure 3.7).

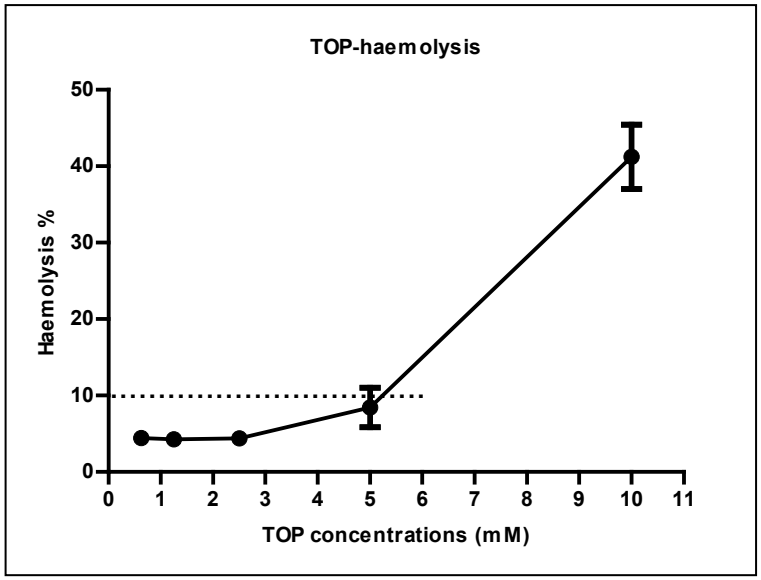

Figure 3.7: TOP haemolysis activity. TOP induces haemolysis in a dose dependent manner and it demonstrates less than 10% haemolytic activity at 5 mM level (n=3). Human red blood cells were incubated with different concentrations of TOP for 1 hour at 37ºC and haemolysis determined by measuring the release of haemoglobin by spectrophotometric quantification. The percentage of haemolysis was calculated considering 100% haemolysis induced by incubating red blood cells with 0.2% tween.

The selectivity ratio (SR) or Therapeutic index (TI) was calculated using 10% haemolysis activity (5 mM) (Figure 3.7) divided by the median of the MIC value (50 µM) (Table 3.2). The calculated TI for TOP was 100 (HD_{10}-5000/MIC-50) which is well above previously discovered peptidomimetics (Table 3.3) (TI's were around 20) (Chongsiriwatana *et al*., 2008).

3.6. Bacteria and lung epithelial cell co-culture assay to determine selectivity of TOP

A co-culture assay was developed and conducted to demonstrate TOP selective killing of bacteria over mammalian lung epithelial cells. The rationale of the assay was to model *in-vitro* bacteria-epithelial cell viability in the continued presence of TOP. Bacteria and A549 cells were incubated with TOP (50 µM) for 8 hrs in 96 well plates and bacterial growth and lung epithelial cell damage evaluated at 8 hrs (Figure 3.8).

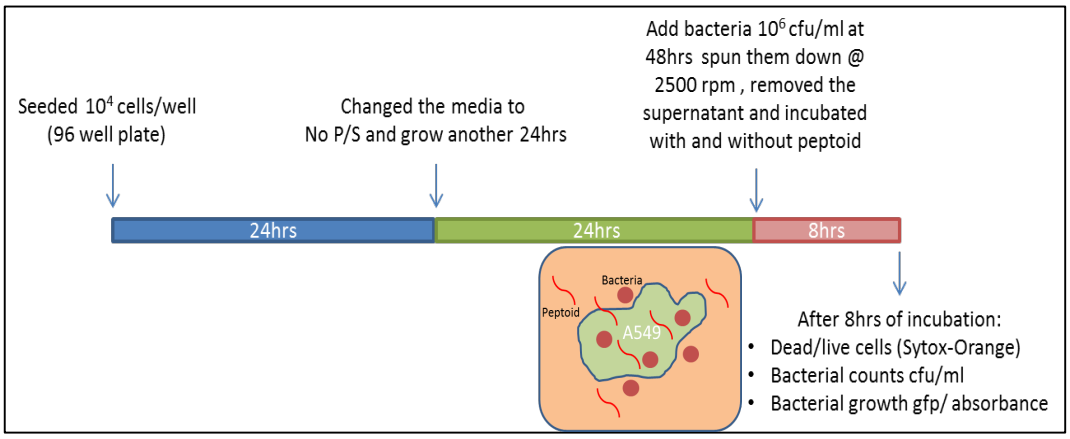

Figure 3.8: Schematic diagram shows the bacteria and A549 co-culture assay.

At the end of the 8 hrs incubation, absolute bacterial numbers were determined by plating aliquots of supernatant and enumerating cfu/ml the following day alongside measuring the gfp fluorescence (RN6390). A549 cell viability was determined by staining the cells with Sytox-Orange dye (nuclear labelling dye that only labels in presence of permeable cell membranes) (Figure 3.9 and Figure 3.10).

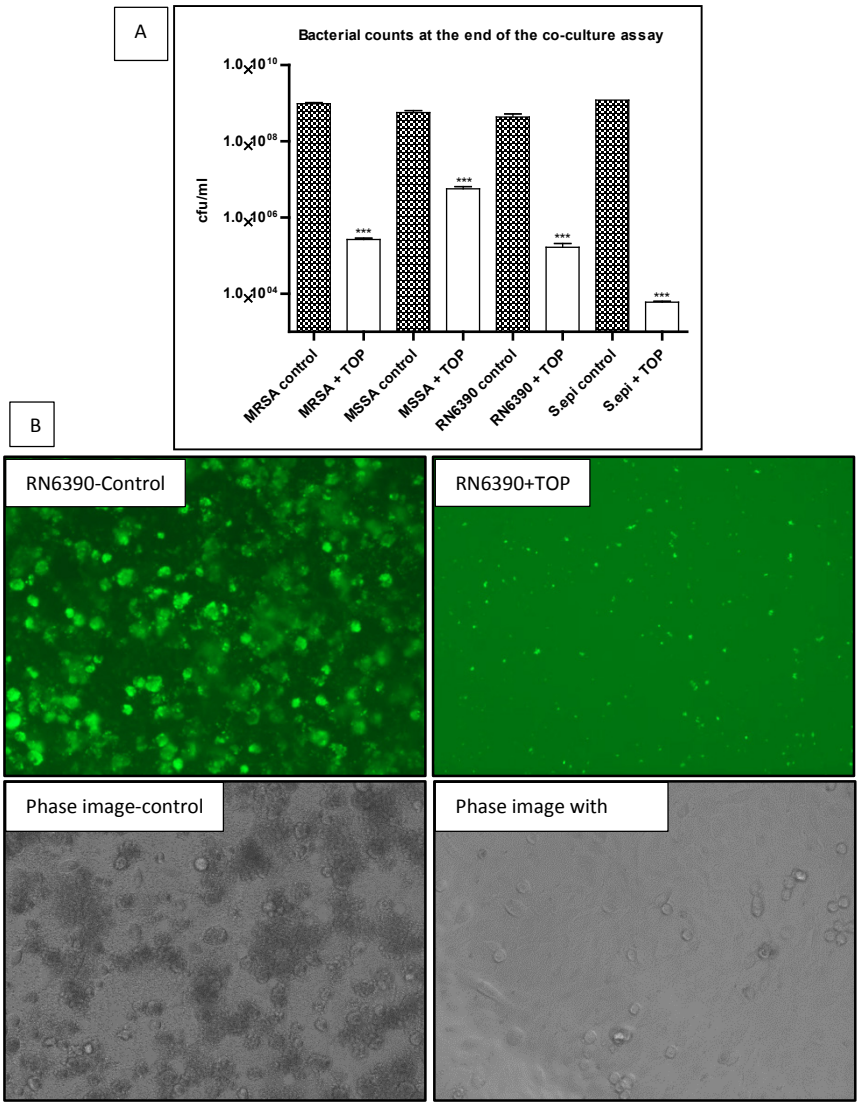

Figure 3.9: TOP inhibits bacterial growth in co-culture assay. (A) The top graph shows the absolute bacterial counts with and without TOP (50 µM) after 8 hrs incubation. Figures represent mean values ± SEM of n=3. (B) The representative images of epifluorescence microscopic images show the RN6390-gfp-lux bacterial growth with and without TOP. The control image shows the A549 cells with RN6390-gfp-lux bacteria (left panel) vs TOP treated cells (right panel) where the bacterial growth has been inhibited, clearly shown by reduced gfp fluorescence (magnification x60).

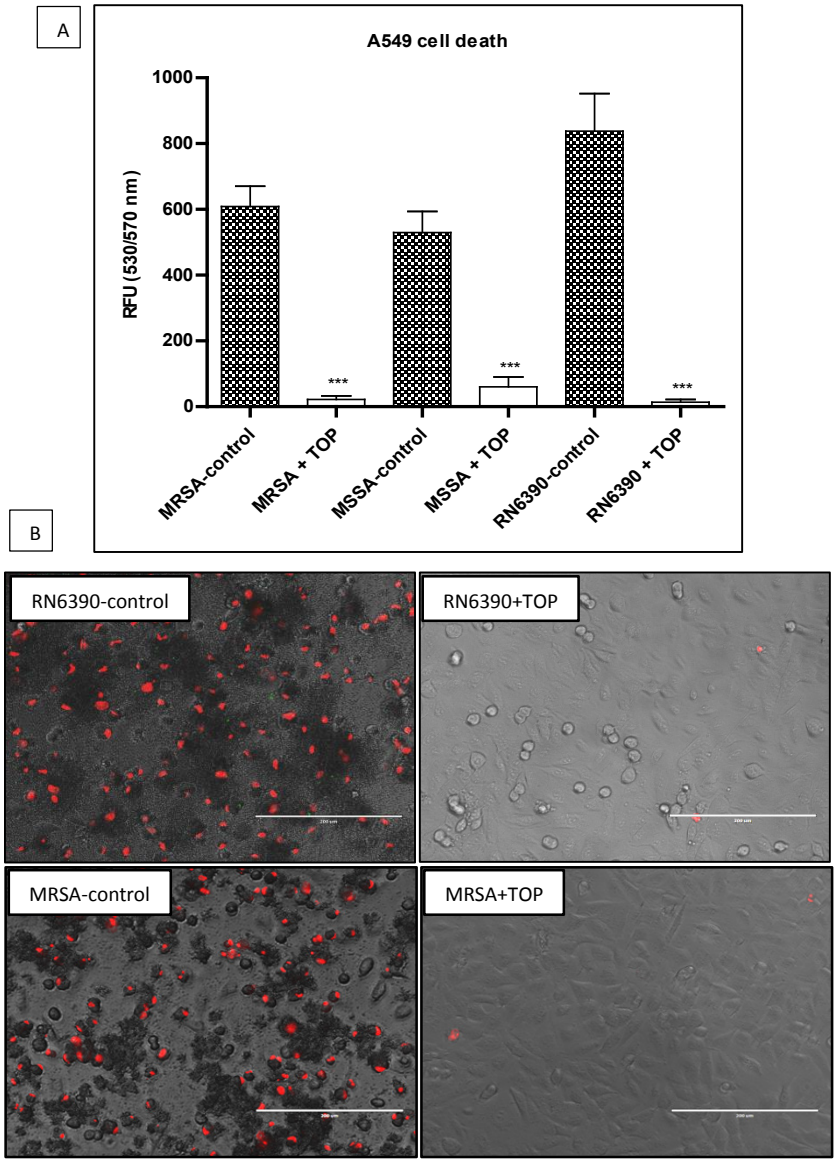

Figure 3.10: A549 epithelial cells are protected by TOP in co-culture assay. (A) The top graph shows Sytox-Orange reads (dead cells), GFP-green bacteria. Figures represent mean values ± SEM of n=3. *In-vitro* TOP protects A549 epithelial cells from bacterial induced death. (B) The representative images of epifluorescence show RN6390-gfp-lux bacteria and MRSA with and without TOP. The TOP treated A549 epithelial cells are protected from bacterial invasion and cell damage/ death (magnification x60).

3.7. TOP rapidly enters lung epithelial cells-A549

Previous studies demonstrated that 9-mer lysine-like peptoids rapidly cross mammalian cell membranes (Unciti-Broceta *et al*., 2009). To determine if the TOP could rapidly translocate through mammalian cell membranes, a fluorescent analogue of TOP was synthesised (TAMRA-TOP) to visualise TOP localisation with confocal microscopy. Figure 3.11(a) shows live confocal image of A549 cells with internalised TOP-TAMRA and quantification of the TOP-TAMRA uptake in figure 3.11(b).

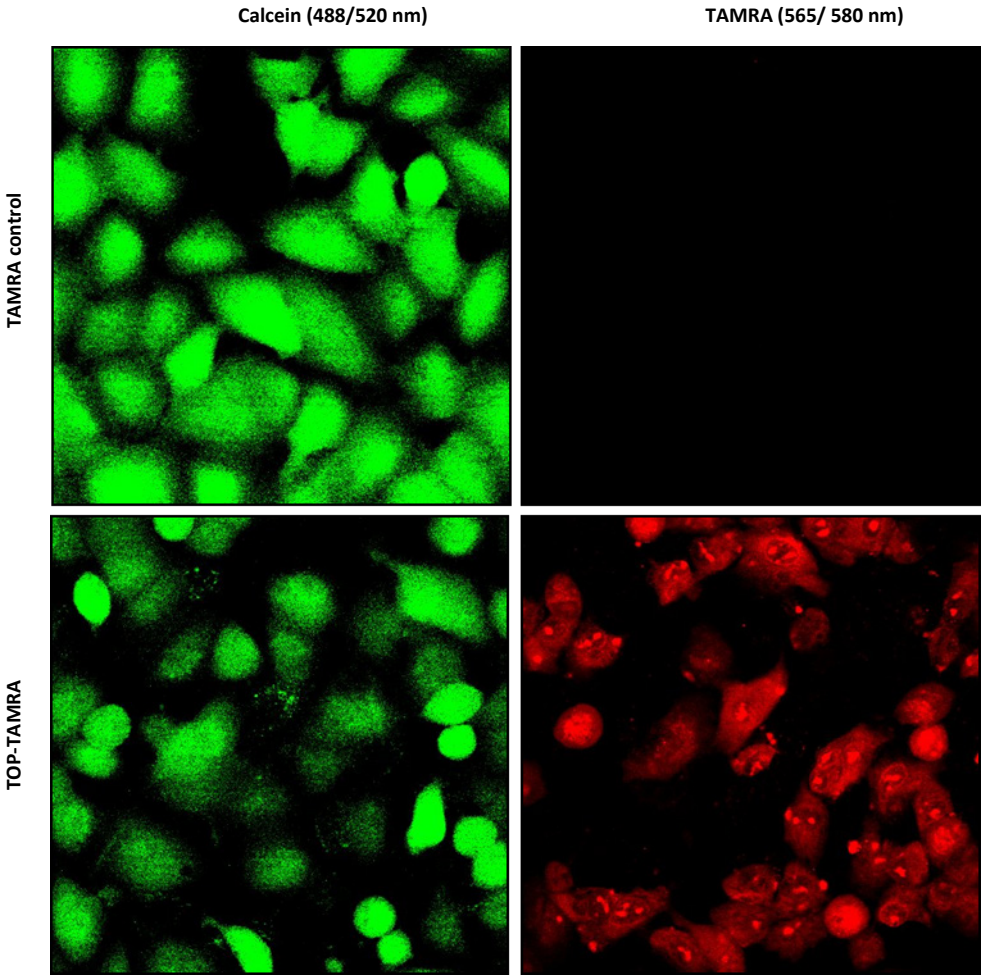

Figure 3.11(a): Confocal microscope live image of A549 cells after incubation with TAMRA-control and TOP-TAMRA for 10 minutes at 100 µM. The cell-permeant dye Calcein (488/520 nm) used as counter stain A549 cells. Internalised TOP-TAMRA localised in the cytoplasm (magnification x100).

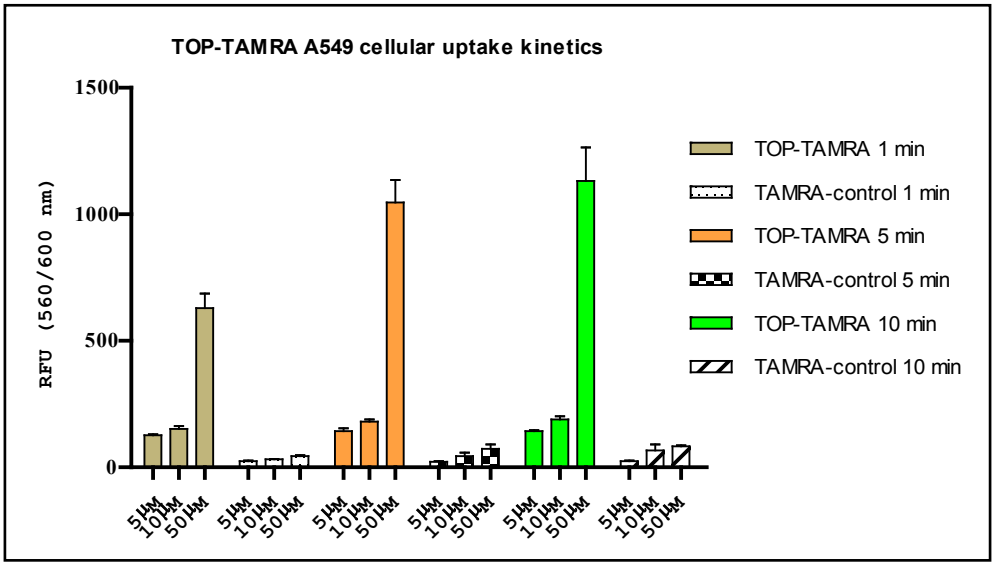

Figure 3.11(b): Kinetics of TOP-TAMRA A549 cellular uptake. A549 cells were incubated at 37°C with 5, 10, 50 µM concentrations of TOP-TAMRA for 1, 5 and 10 minutes. Washed cells were imaged and red the fluorescence intensity at 560/600 nm.

3.8. TOP kills intracellular bacteria

The intracellular 'niche' is a potential environment for antibiotic evasion (Qazi *et al*., 2004) and bacterial persistence. In order to kill intracellular bacteria, antibiotics need to be capable of penetrating the eukaryotic cell membrane and accumulating intracellular to a sufficiently high concentration to be effective against intracellular bacteria (Qazi *et al*., 2004). To study the intracellular antimicrobial activity of TOP, *S. aureus* (RN6390) expressing a gfp-luxABCDE reporter operon under the control of a growth-dependent promoter was used. The dual luminescence and fluorescence reporters in the bacteria were used to track bacterial replication within the intracellular niche in A549 cells in a 96-well microplate format (Figures 3.12 and 3.13).

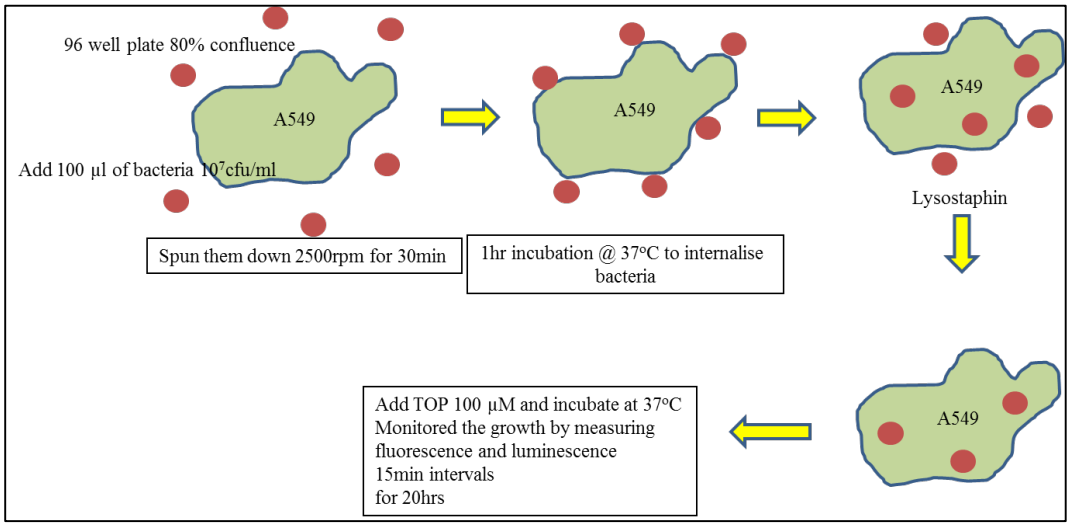

Figure 3.12: Schematic diagram of the internalisation assay and assessment of intracellular activity of TOP. A549 cells were grown to 80% confluence prior to addition of RN6390 (approximately 10^6 cfu), centrifugation and incubation for 1 hour to permit internalisation. Following this, lysostaphin 10 µg/ ml was added to the well to kill non-internalised bacteria. The adhered A549 cells were extensively washed prior to addition of TOP and microplate reader recording of fluorescence and luminescence over 20 hrs at 37°C with readings every 15 mins.

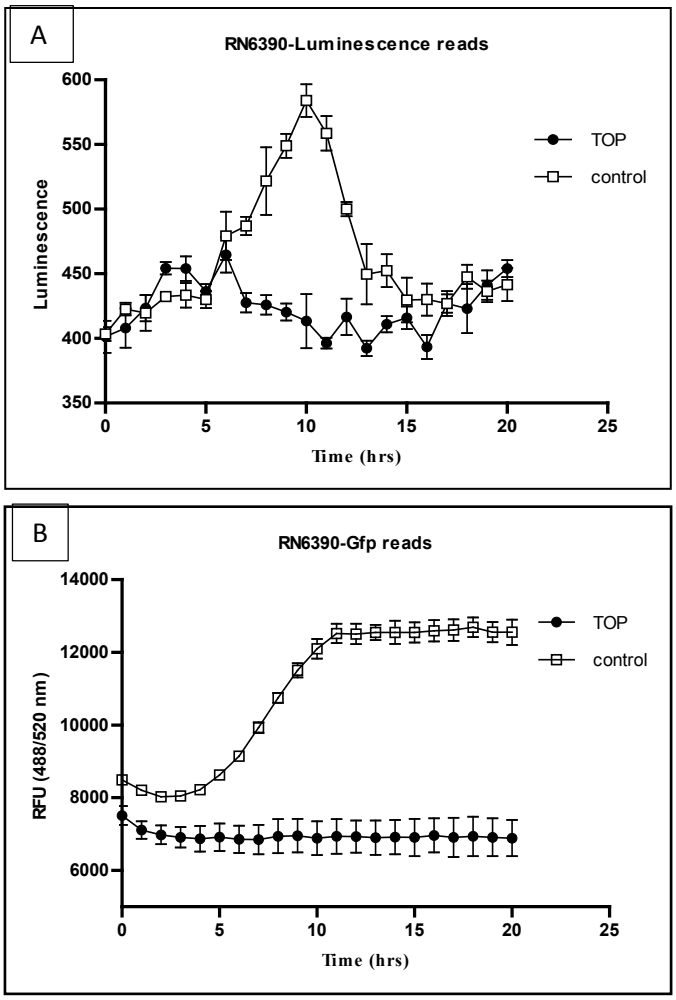

Figure 3.13: TOP demonstrates intracellular bacterial killing. TOP treated A549 cells (with intracellular bacteria) show significantly reduced luminescence (A) and gfp (B) indicating that TOP possesses intracellular bacterial killing ability (n=3; mean and SEM).

3.9. Prophylactic TOP treatment of A549 cells reduces internalised bacterial growth

The respiratory airway epithelium is continually exposed to bacteria. Prophylactic treatment of A549 cells with TOP was tested to confirm if subsequent bacterial growth within the intracellular niche was reduced. Following similar methods to those represented in Figure 3.12, the treated A549 cells with TOP prior to exposure to bacteria. Prophylaxis treatment of antibiotics has been recommended by American Heart Association during for high risk patients such as immune compromised patient

(Capitano *et al*., 2001). This assay was performed to explain the utility of the pre-treatment of TOP to prevent bacterial colonisation in lung epithelial cells. A549 cells were pre-treated with TOP and washed excess prior to internalisation of RN6390-gfp-lux *S. aureus* the intracellular bacterial growth was measured by gfp fluorescence (Figure 3.14).

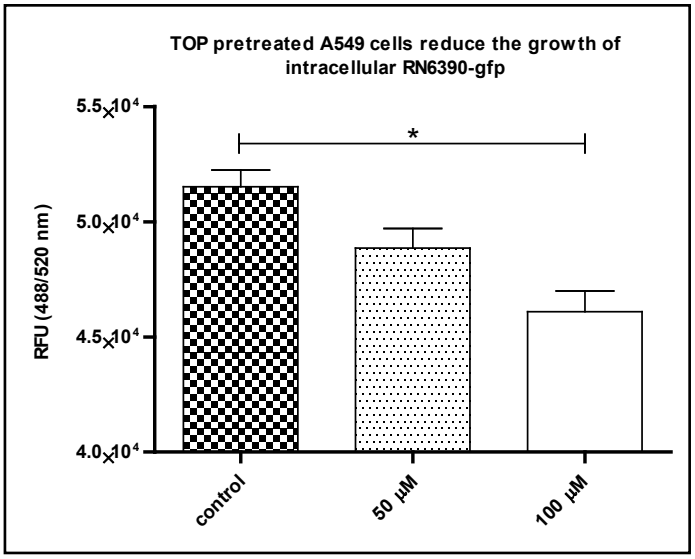

Figure 3.14: TOP pre-treated A549 cells reduced intracellular RN6390-gfp-lux. A549 cells were pre-treated with 100 µM and 50 µM of TOP and washed before the internalisation of RN6390-gfp-lux. The growth of bacteria was monitored by measuring gfp fluorescence over 48 hrs. Intracellular bacterial growth was reduced in TOP pre-treated A549 cells in a dose dependent manner (Panels represent mean values ± SEM for n = 5).

3.10. TOP disrupts bacterial membrane

AMPs disrupt bacterial membranes (Haney and Hancock, 2013) but it is not clear whether membrane disruption is the primary mechanism of killing that TOP uses to kill bacteria (Figures 3.1, 3.2). To visualise ultra-structural damage, TOP treated bacteria were subjected to Transmission electron microscopy (TEM) analysis. TEM clearly showed bacterial membrane disruption of (A) Gram positive and (B) Gram negative bacteria (Figure 3.15).

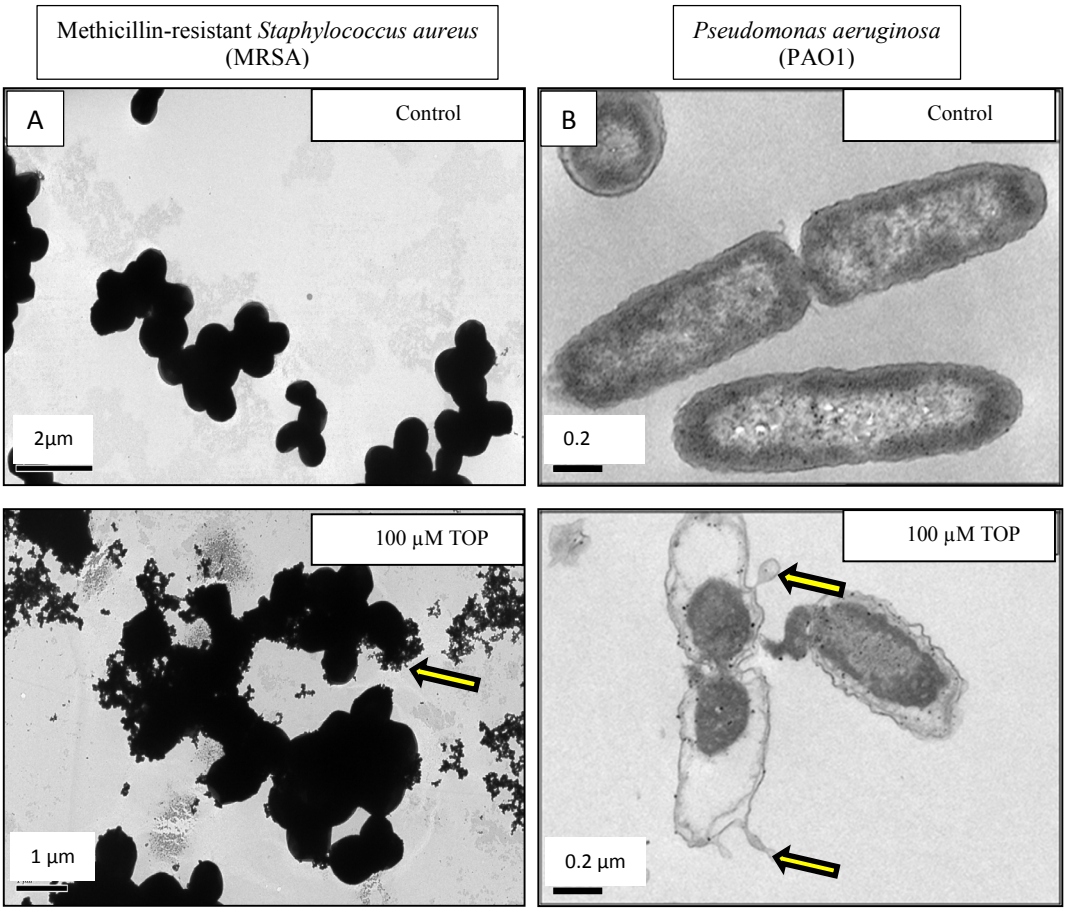

Figure 3.15: TEM images demonstrate bacterial cell membrane disruption. Bacterial membranes have ruptured with disruption and extrusion of bacterial contents (yellow arrows). Bacteria were incubated with 100 µM of TOP for one hour at 37°C in PBS prior to fixation for TEM analysis.

3.11. TOP may induce reactive oxygen species production in bacteria

Reactive oxygen species (ROS) production is a mechanism for antibiotic bactericidal activity leading to DNA, protein and lipid damage (Vilchèze *et al*., 2013). Hence, the induction of ROS in bacteria after TOP addition was evaluated. MRSA was treated with different peptoids (TOP, THP-Tosyl-hexyl and HHP-H-hexyl) in a 96 well plate for 1 hour followed by addition of Dihydroethidium (DHE) to measure ROS production (Figure 3.16).

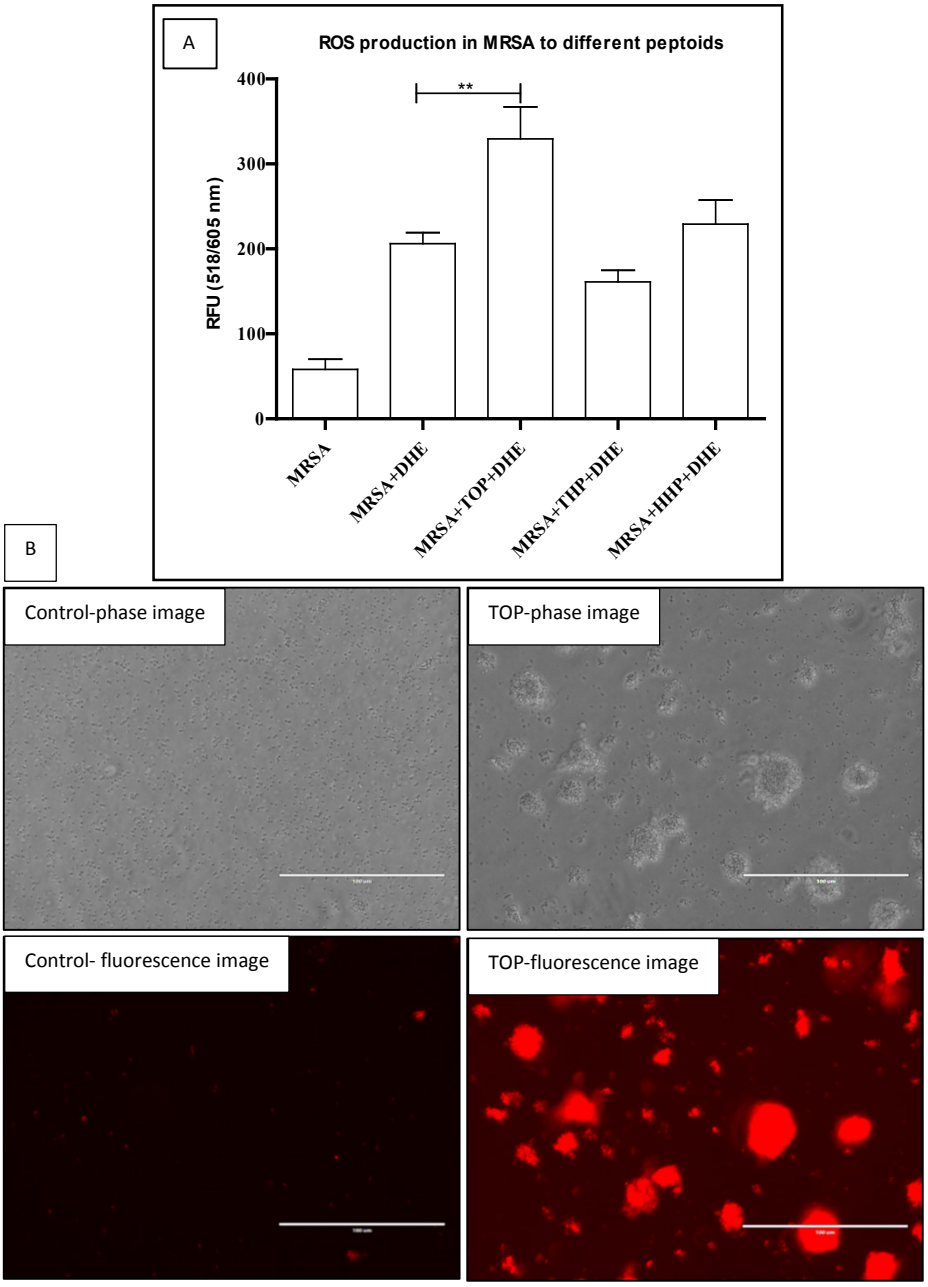

Figure 3.16: TOP induces ROS production in MRSA. (A) The production of ROS in MRSA by TOP measured by the plate reader in 96 well plates. (Panels represent mean values ± SEM for n = 3) (B) Representative epifluorescence microscopy images showing TOP inducing ROS production in MRSA (DHE red fluorescence) (magnification x60).

3.12. TOP induced toxicity in mammalian cells

Freshly isolated human neutrophils and mammalian lung epithelial cells (A549) were exposed to TOP for prolonged periods and neutrophil viability/apoptosis (flow cytometric) and epithelial cell mitochondrial function (MTS assay) assessed. Interestingly and surprisingly, TOP induced apoptosis and secondary necrosis in neutrophils in a caspase-dependent manner. TOP did not induce epithelial cell toxicity.

3.12.1. TOP induced neutrophil apoptosis

Neutrophil apoptosis is the process of programmed cell death with anti-inflammatory sequela. Conversely, primary necrosis results in pro-inflammatory sequela. Apoptosis prevents the release of neutrophil-toxic contents to the surrounding tissue and promotes the resolution of inflammation (Li *et al*., 2009). Resolution of the inflammatory response is a complex process and includes production of host-derived anti-inflammatory mediators and apoptosis of neutrophils. Neutrophil apoptosis and removal of apoptotic neutrophils by macrophages facilitates the resolution of inflammation (Savill *et al*., 1989; Kennedy and DeLeo, 2009; Moret *et al*., 2011).

Given the pivotal role played by neutrophils in orchestrating the inflammatory response, TOP was incubated with neutrophils to delineate any toxicity. Surprisingly TOP induced neutrophil apoptosis and subsequent secondary necrosis. Neutrophils were incubated with TOP (50 μM and 100 μM), Roscovitine (Cyclin-dependent kinase inhibitor that induces neutrophil apoptosis) and control buffer in 96 well plates for 6 and 20 hrs. Neutrophil apoptosis and necrosis was analysed by flow cytometry with Annexin V and propidium iodide (PI) staining respectively (Figure 3.17 and Figure 3.18).

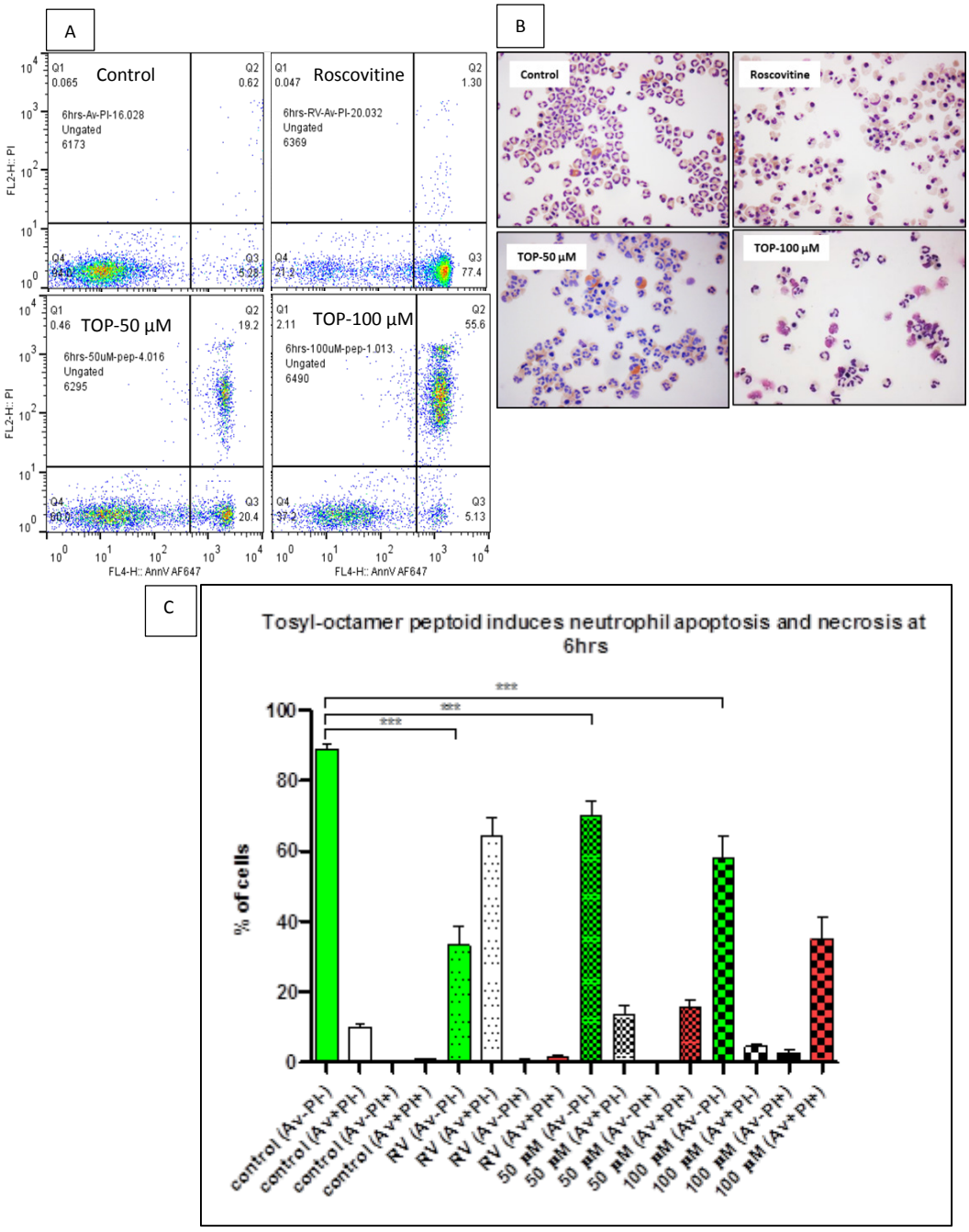

Figure 3.17: Induction of neutrophil apoptosis and necrosis by TOP at 6 hrs. (A) Representative FACS plots show PI and Annexin V labelling of neutrophils. (B) Representative images of neutrophils (magnification x40). (C) Graph shows the percentages of cell labelling. The control shows 90% healthy cells (Annexin V and PI negative) and no PI positive (no necrotic cells). Roscovitine (10 µM) causes apoptosis in neutrophils but not necrosis. Treatment with 50 µM TOP shows around 20% Annexin V and 20% Annexin V and PI positive cells indicating they are undergoing apoptosis and necrosis. This population increases with higher concentration of TOP to 100 µM. (Panels represent mean values ± SEM for n = 3).

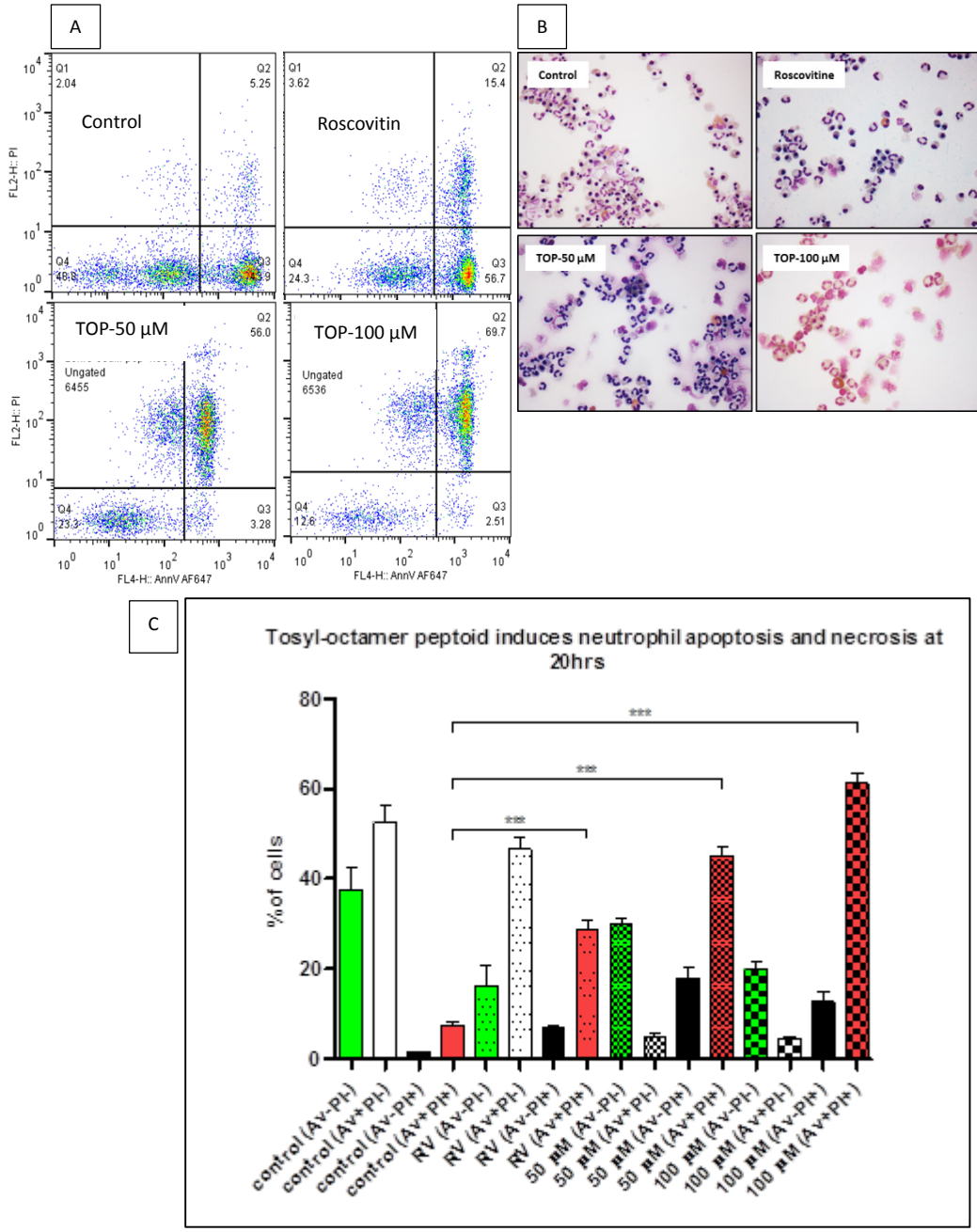

Figure 3.18: Induction of neutrophil apoptosis and secondary necrosis by TOP at 20 hrs. (A) Representative FACS plots show PI and Annexin V labelling of neutrophils. (B) Representative images of neutrophils (magnification x40). (C) The graph shows the percentages of cell labelling. TOP induces neutrophil necrosis at 50 µM and 100 µM concentrations at 20 hrs compared to the control and Roscovitine (10 µM). (Panels represent mean values ± SEM for n = 4).

To further clarify if TOP was inducing apotosis or necrosis as a primary process, neutrophils were incubated with TOP in the presence or absence of QVD-OPh a potent pan-caspase inhibitor that inhibits neutrophil apoptosis. QVD-OPh was

chosen as it has superior aqueous stability, cell permeability, and efficacy than fluoromethylketone (FMK)-based caspase inhibitors and displays no cytotoxic effects alone (Caserta *et al*., 2003). Experiments analogous to Figures 3.17 and 3.18 were conducted and results are described in Figure 3.19, 3.20 and 3.21.

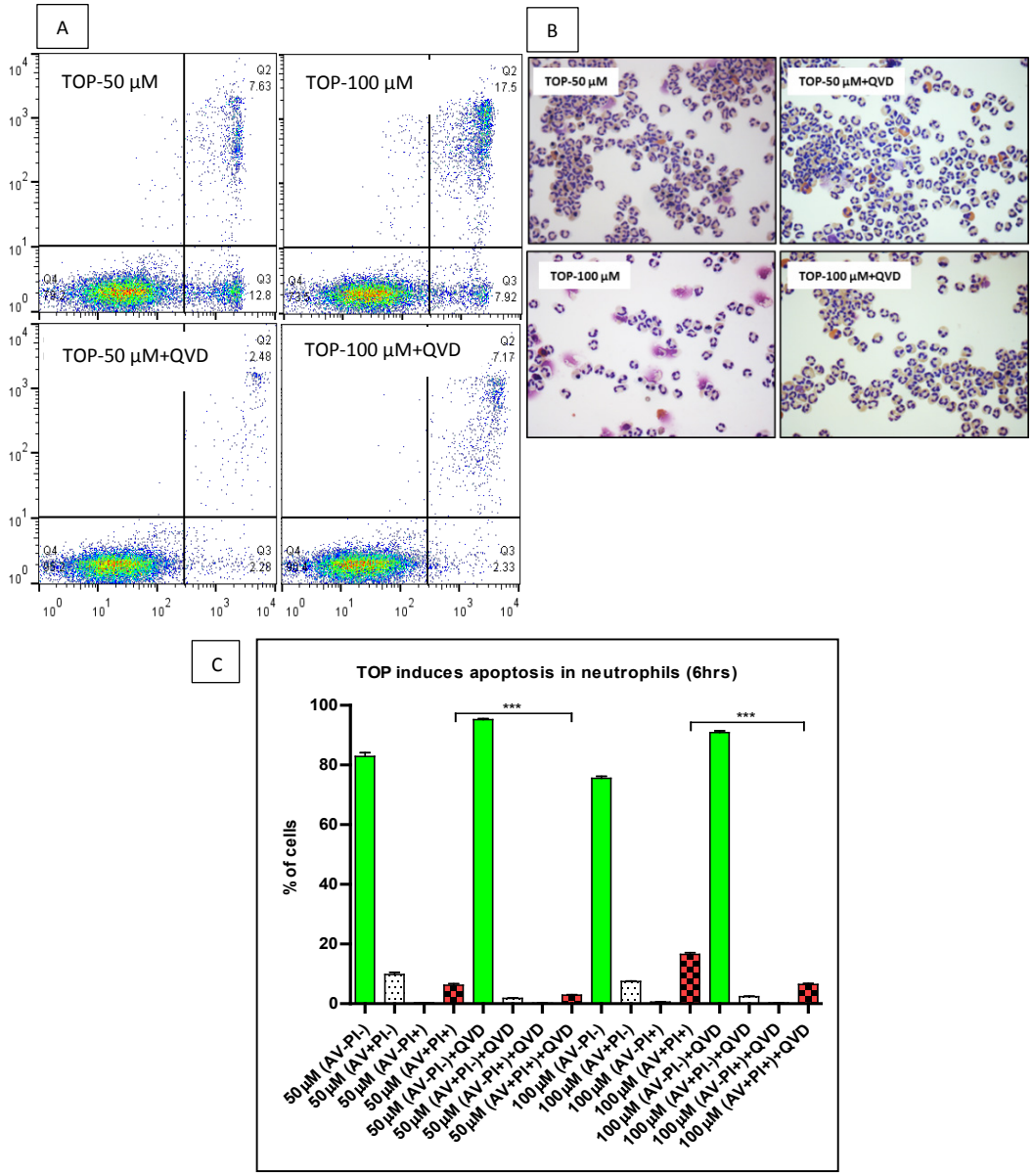

Figure 3.19: QVD blocks secondary necrosis induced by TOP at 6 hrs. (A) Representative FACS plots show PI and Annexin V labelling of neutrophils. (B) Representative images of neutrophils (magnification x40). (C) Graph shows the percentages of cell labelling. Neutrophils have been incubated with QVD and TOP for 6 hrsand labelled with Annexin V and PI and analysed by FACS. (Panels represent mean values ± SEM for n = 4).

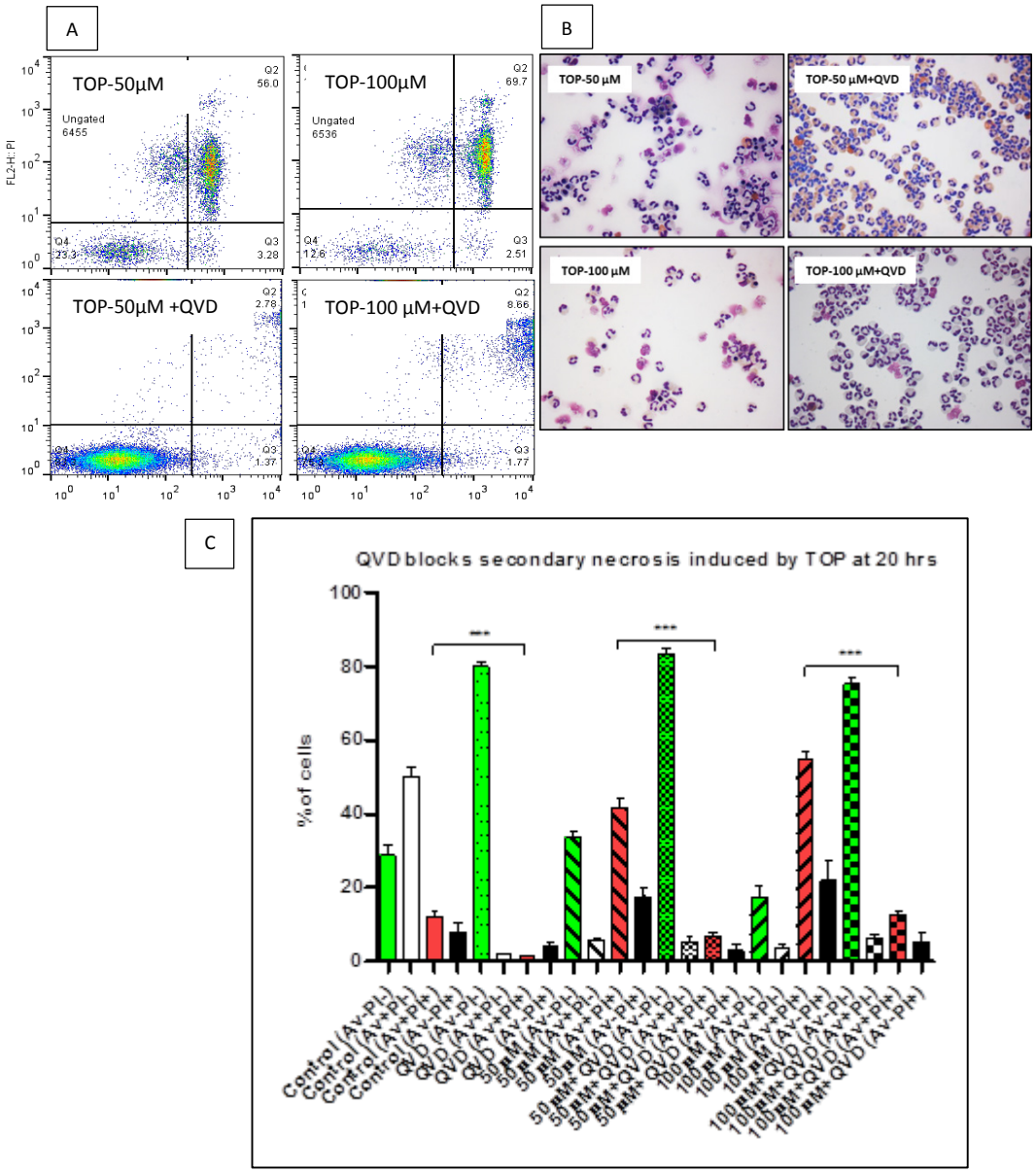

Figure 3.20: QVD blocks secondary necrosis induced by TOP at 20 hrs. (A) Representative FACS plots show PI and Annexin V labelling of neutrophils. (B) Representative images of neutrophils (magnification x40). (C) Graph shows the percentages of cell labelling. Neutrophils were incubated with QVD 10 µM and TOP for 20 hrs and analysed by flow cytometric staining with Annexin V and PI. (Panels represent mean values ± SEM for n = 4).

To further investigate if TOP had a role in specifically inducing secondary necrosis of apoptotic neutrophils, neutrophils were aged for 20 hours before addition of TOP.

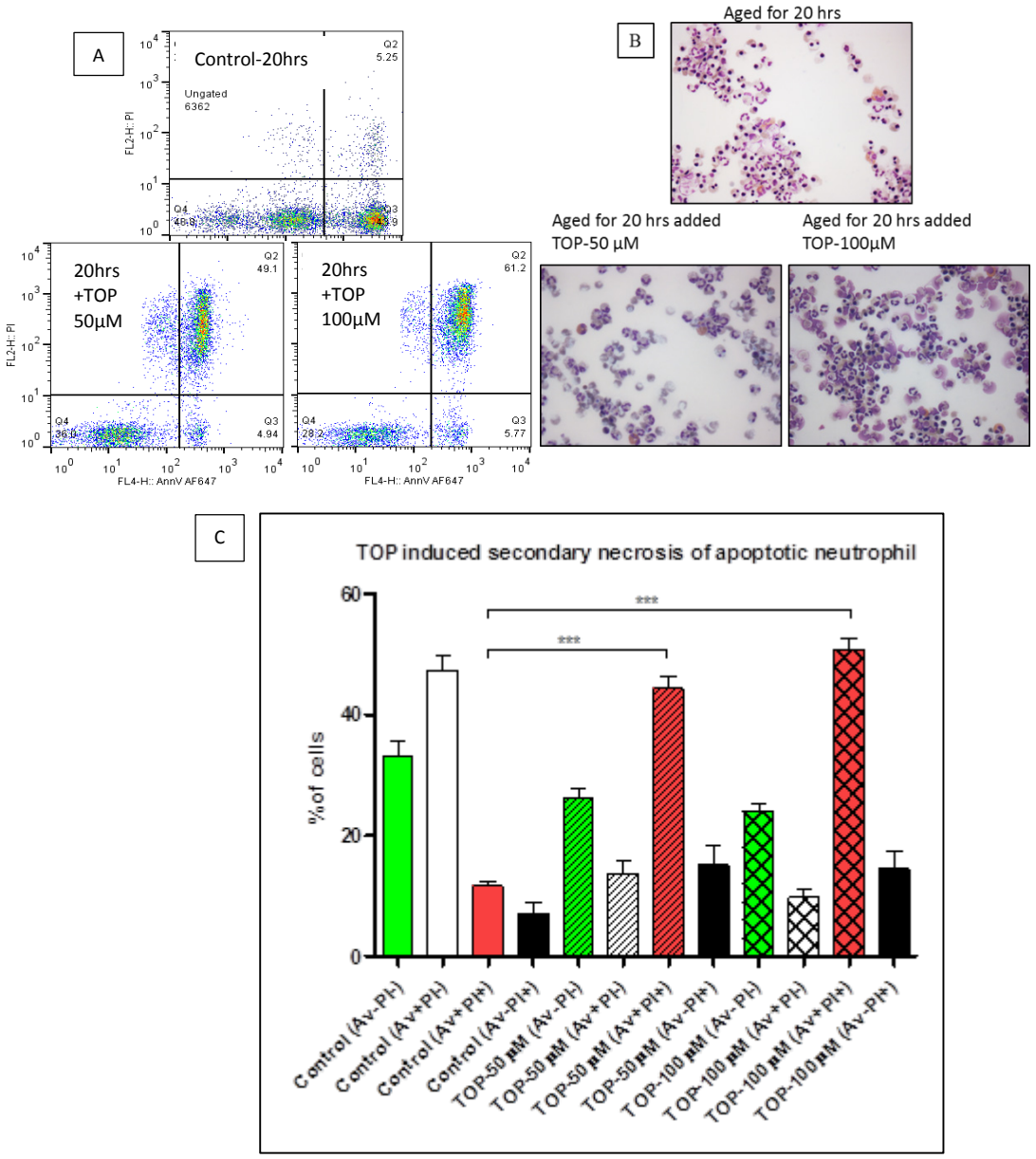

Figure 3.21: TOP induces rapid secondary necrosis of apoptotic neutrophils. (A) Representative FACS plots show PI and Annexin V labelling of neutrophils. (B) Representative images of neutrophils (magnification x40). (C) Graph shows the percentages of cell labelling. Neutrophils were aged for 20 hrs and then pulsed with TOP for 10 minutes before staining with the Annexin V and PI and analysed by FACS. (Panels represent mean values ± SEM for n = 6).

3.12.2. TOP shows no toxicity to A549 cells

MTS assays were carried out to observe TOP cytotoxicity on A549 cells at 3 hrs and 24 hrs incubation (Figures 3.22 and 3.23).

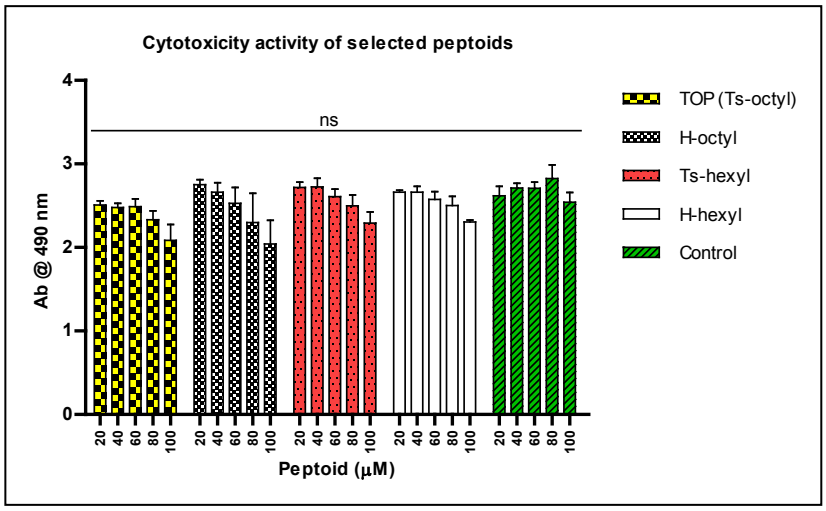

Figure 3.22: TOP has low toxicity on A549 cells. A549 cells were incubated with four different peptoids including TOP at different concentrations for 3 hrs. MTS assay was performed at the end of the assay. Significance was assessed by one-way ANOVA with Bonferroni's multiple comparison tests comparing each treatment with control. (Panels represent mean values ± SEM for n = 3; P=0.1665).

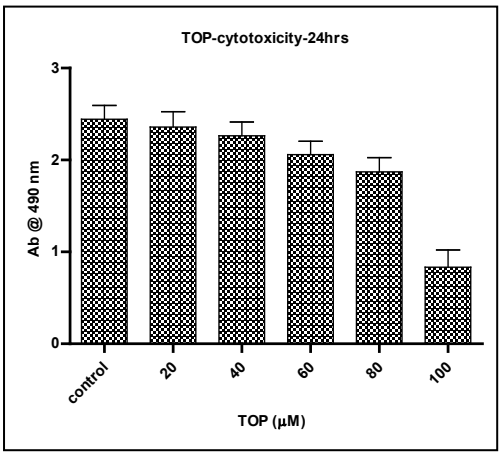

Figure 3.23: TOP toxicity on A549 cells at 24 hrs incubation. A549 cells were incubated with TOP at different concentrations for 24 hrs. MTS assay was performed at the end of the assay. TOP was toxic to A549 cells at 100 µM concentrations at 24 hrs but no significant toxicity lower than 80 µM. (Panels represent mean values ± SEM for n = 3; P=0.0068).

3.13. Discussion

In the discussion summarises the TOP activity on bacterial killing, selectivity over mammalian cells, inflammatory response on neutrophils and evaluate the A549 cell toxicity as shown in the schematic model below.

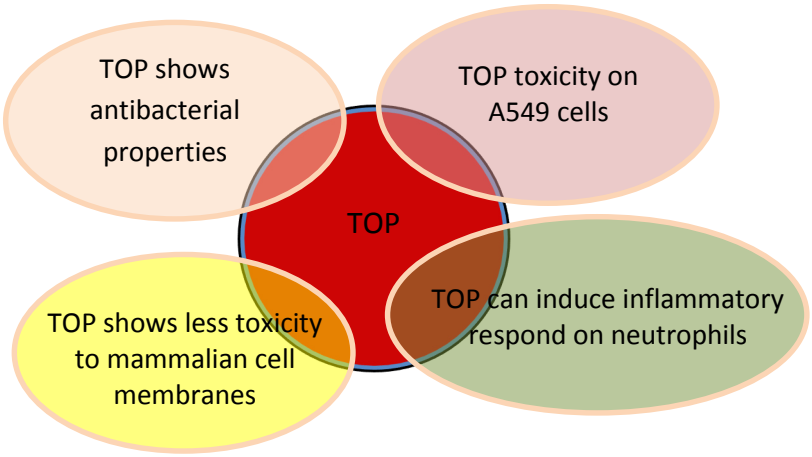

TOP activity on gram positive and gram negative bacteria:

Emergence of multidrug resistant bacteria such as vancomycin-resistant *Enterococci* and methicillin-resistant *Staphylococcus aureus* (MRSA) are major global challenges (Theuretzbacher, 2011; Arias and Murray, 2012; Gould *et al*., 2012; Phoenix *et al*., 2013). Resistance is due to decades of widespread and indiscriminate usage of existing antibiotics Despite this, most novel antibacterial drugs are designed through modifications of existing scaffolds resulting in the high likelihood of resistance emerging in even new drugs (Jabes, 2011; Livermore, 2011; Tomasini *et al*., 2013). Hence there is an urgent need for new antibiotics with novel mechanisms of antimicrobial action. AMPs show high potential to serve in this capacity. However the major obstacle in the further development of lead AMPs is difficulty in the transition of *in-vitro* activity into *in-vivo* efficacy (Hancock and Sahl, 2006). In contrast to AMPs, Peptoids represent a class of peptidomimetic that are not found in nature. Peptoids are highly resistant to proteolysis, providing vast opportunity for biomedical applications such as cell target drug delivery and cell labelling (Park *et al*., 2013).

A library of peptoids have been synthesised based on a group of achiral cationic peptoid polymers with the department of chemistry based on the previous published data (Unciti-Broceta *et al*., 2009; Dhaliwal *et al*., 2011) to study the structure-activity relationships (S.A.R) on bacterial killing. The core structure of the whole peptoid library was 9-mer lysine-like peptoids unit (Figure 1.13) and the peptoid derivatives have been made by; (i) changing the length of the carbon side chain; and (ii) N-terminus modifications (Figure 1.15 and Table 1.3).

This study evaluated the efficacy of TOP on gram negative and gram positive bacterial species including clinically isolated bacteria and multidrug resistance strains such as methicillin resistant *Staphylococcus aureus* (MRSA). However in future work it is important to investigate the effect of TOP on other clinically important bacterial/fungal/virus strains and species including vancomycin resistant enterococci (VRE), *Mycobacterium tuberculosis* and other multidrug-resistant microbes to study the full spectrum of the efficacy of this drug to be used in clinical settings.

To investigate the antibacterial activity of these peptoids, growth inhibition assays have been carried out in MHB for 16 hrs on MRSA, MSSA, PAO1 and *E. coli* at 200 μM peptoid concentrations. The summary results show that TOP has significant growth inhibition on MRSA, MSSA, PAO1 and *E.coli* compared to other peptoids tested (Figure 3.1 and Figure 3.2). The octyl derivatives such as H-octamer and BnCO-octamer peptoids show variable bacterial growth inhibition leaving TOP as the 'lead' antibacterial candidate. This analysis further indicated that the tosyl group and octamer carbon side chain (long carbon chain) are important peptoid structures in order to retain antibacterial activity as a linear 9-mer peptoid. However the presence of tosyl groups with butyl and hexamer carbon chain shows no bacterial killing indicating that the importance of the length of the carbon side chain (octly) for bacterial killing. Therefore TOP was selected as the lead compound to carry out for further analysis.

According to the figure 3.1 and figure 3.2, the results show that some of the peptoids tested are supporting the growth of bacteria instead of killing them. All the bacterial strains tested for the initial screening of the peptoids show increase of bacterial growth compared to control with some of the peptoids tested. As example peptoid Suc-octyl induce the growth in PAO1, MRSA and MSSA, but not in *E.coli*. Peptoid H-hexyl shows similar effect on *E.coli*, MRSA and MSSA, however not in PAO1 strain. This may be due to the probiotic effect of peptoids on bacterial species. Probiotic effects of peptides have been studied by (Janer *et al*., 2004) and (Azuma *et al*., 1984) concluded that casein macropeptide (CMP) can effectively stimulate growth for lactic acid bacteria. However the mechanism of action may be the effect of hydrolysis of these peptoids on the growth-promoting activity of these peptoids or may be an hormonal effect on bacterial growth.

TOP has two major components; (i) lysine-like (octyl) 9-mer unit and (ii) N-substitute-Tosyl (sulphonamide) group. Previous studies have identified that several lysine-peptide hybrids have broad-spectrum activity against clinically important bacteria and fungi (Ryge *et al*., 2008). Recent studies on the lysine-peptoid hybrid LP5 ([N-(1-naphthalenemethyl)glycyl]-[N-4-methylbenzyl)glycyl]-[N-(1naphthalenemethyl)glycyl]-N-(butyl)glycin amide and 5 lysines) revealed that it traverses the cytoplasmic membrane of *S. aureus* without causing lethal damage to the membrane and binding to the chromosomal DNA inducing bacterial killing (Gottschalk *et al*., 2013).

It has been postulated that the cationic and amphiphatic nature of AMPs selectively kill bacteria by penetrating the negatively charged cell membrane leading to membrane disintegration. However, AMPs may also act by other mechanisms without destruction of the cell membrane targeting intracellular enzymatic activities such as cell wall synthesis and RNA, DNA and protein synthesis (Hale and Hancock, 2007; Jenssen *et al*., 2006). The inhibition of RNA, DNA and protein synthesis in bacteria may result from AMPs interacting with DNA repair by collapsing replication forks (Dubois *et al*., 2013; Gunderson and Segall, 2006). Higher concentrations of LP5 also target the cell membrane leading to leakage of

intracellular compounds like ATP, resulting in cell death (Dubois *et al*., 2013; Gottschalk *et al*., 2013).

TOP has N-substitution sulphonamide group. Sulphonamides are one of the most frequently used antibacterial agents in veterinary medicine in Europe (Grave *et al*., 2010; Zessel *et al*., 2013). A considerable number of sulphonamides are well known as antibacterial, anti-cancerous, and also as anti-inflammatory agents (Badr, 2008; Jain *et al*., 2013). Recent studies on sulphonamide have shown their matrix metalloproteinase (MMP) inhibitory activity (Jain *et al*., 2013).

According to the initial screening results with the growth inhibition assay, the presence of the sulphonamide groups on octyl-peptoid shows antibacterial activity. However, Hexyl and Butyl peptoids with the N-sulphonamide group did not show any antimicrobial activity on PAO1 (Tosyl-Butyl and Tosyl-Hexyl) and *E. coli* (Tosyl-Hexyl). But some growth inhibition was observed with MRSA and MSSA with Tosyl-Hexyl, indicating that the sulphonamide group synergises with octyl-9-mer combination to promote the broad range of bactericidal activity on gram positive and negative bacteria. Previous studies on sulfonamide derivatives revealed that the given chain length of the lipophilic moiety and the nature of the hydrophilic group substituted at the amino nitrogen of the sulfonamide molecule had a marked influence on surfactant properties and mutual lipophilic and hydrophilic groups may have surface activity and bacterial effect (Badr, 2008). These studies suggest that the proper combination of different groups to the sulphonamide may have beneficial effects.

Latent or slow-growing bacteria frequently exhibit tolerance to antibiotics that are active against rapidly dividing bacteria. These pathogens persist in the intracellular niche and multiply very slowly providing a residual bacterial niche in the host from which further growth, infection and spread may occur (Zeiler *et al*., 1985). Both the intracellular niche and the slower replication of these pathogens allow them to be relatively protected from conventional antimicrobial therapeutics (Yanmin *et al*., 2010). Therefore the activity of TOP against non-multiplying cultures of MRSA and

PAO1 using well characterized techniques is important (Bahl *et al*., 1997). Under these conditions, TOP displayed dose-dependent antibacterial activity (Figure 3.3).

The results of PBS killing assay data show that the TOP kills non-dividing gram-positive MRSA within 3 hrs at 100 μM concentration and gram-negative bacteria, PAO1 with in 1hr at 50 μM concentration. These results indicate that the microbicidal mechanism of TOP may not be through interfering with metabolic pathways such as DNA, RNA, protein or cell wall syntheses but rather through primary membrane damage (Coates *et al*., 2002; Ooi *et al*., 2010).

The growth inhibition assays were carried out to investigate the bactericidal effect of TOP on dividing bacteria in MHB. The data revealed that killing of gram negative and positive bacteria was observed except in *B.cepacia* at 100 μM TOP concentrations. The PBS killing assay and growth inhibition assays suggests that the TOP may have multiple mechanisms of bacterial killing (Coates *et al*., 2002; Ooi *et al*., 2010). However the exact killing mechanisms remain to be elucidated. Since TOP has the two potent characters 9-mer-octyl lysine peptoid group and the sulphanilamide group, the killing may involve complex mechanisms. However cationic properties on 9-mer-octyl lysine group may also involve binding to the negatively charged bacterial surface (Dubois *et al*., 2013) and penetration into the bacteria. The sulphanilamide group may block the production of folic acid synthesis in the bacteria and proceed to death (Lascelles and Woods, 1952). The ability of the TOP to kill bacteria in non-dividing cultures suggests a mechanism that does not solely involve the synthetic machinery of the bacteria as well. Many AMPs possess hydrophobic elements that traditionally have been thought to mediate membrane insertion and pore formation (Brogden, 2005). The absence of such moieties in our compound implies that alternative mechanisms may play a role in membrane disruption in bacterial cells upon exposure to positively charged molecules and the probable mechanism may be involved with the sulphanilamide group of the TOP.

Investigate the mechanisms of bacterial killing by TOP:

The hydrophilic nature of the TOP may not describe the AMPs mechanisms of bacterial killing. Current understanding of structure-function relationships and mechanisms of AMPs and peptoid-mediated bacterial killing postulates variable mechanisms from cell wall disruption and membrane leakage to direct chromosomal damage (Coates *et al*., 2002; Ooi *et al*., 2010). Since TOP has the sulphanilamide group, the killing may involve blocking the production of folic acid synthesis in the bacteria and proceed to death (Lascelles and Woods, 1952). However to evaluate these mechanisms the TEM and ROS detection strategies were utilised. TEM (Figure 3.15) visualised the ultra-structural damage of MRSA and PAO1 by TOP. These images clearly show bacterial membrane disruption leading to bacterial killing.

Haney and Hancock, (2013) observed similar results with AMPs but the disruption to bacterial membrane may or may not be the primary mechanism of killing. Therefore the production of ROS has been studied during the killing process. However the ROS production also may not be the primary factor for killing but involvement of the high ROS production with TOP compared with the other peptoids are very interesting results for further investigation (Figure 3.16). It is clear that high ROS production with the TOP plays a key role to kill the bacteria and the ROS involved DNA and protein damage. Vilchèze *et al*., (2013) observed ROS production in *M. tuberculosis* to vitamin C lead to DNA and protein damage. However the exact mechanism of ROS production in TOP treated bacterial cells are to be investigated but the production of ROS and membrane damage lead to bacterial killing.

TOP shows high selectivity on bacteria over mammalian cells:

The selective toxicity of antibiotics means that they must be highly effective against the microbe but have minimal or no toxicity to humans. In practice, this is expressed by a drug's therapeutic index (TI) or selective ration (SR). These studies demonstrate that the TOP shows higher toxicity on bacterial membrane over mammalian cell membrane. The MIC and MBC values were used to determine the bacteriostatic or bactericidal activity of the TOP. The table 3.2, summaries the MIC and MBC values for the TOP. MIC shows the bacteriostatic values and MBC shows the bactericidal values. All seven bacterial strains show MIC values below 80 μM and MBC below 100 μM. These data indicates that the lower concentrations of TOP confer antiseptic properties while higher concentrations show bactericidal activity. However MIC values of TOP for different bacterial strains are higher than the previously studied antimicrobial peptides (Chongsiriwatana *et al*., 2008). Balancing high antimicrobial activity with low toxicity to the host is fundamental for clinical application and this has been quantified using TI or SR (the ratio of the dose causing 10% haemolysis to the MIC). Hence the TI was calculated using haemolysis assay data (Figure 3.7) and MIC values (Table 3.2) resulting higher TI value for TOP as 100 compared with the peptoids described in Chongsiriwatana *et al*., (2008) was around 20 (Table 3.3). This indicates that the TOP has more tendencies to kill bacteria rather than mammalian cells.

The table 3.3 summarises the previous publications of MICs of peptoids, AMPs and conventional antibiotics on *P. aeruginosa*. The data show that the TOP shows higher MIC value compared to most of the peptoids and AMPs. Kanamycin (100 μM) shows higher MIC compared with the TOP but much lower compared with Ciprofloxacin (0.4 μM) and Tobramycin (1.6 μM). However according to the summary table 3.3 the SR of all the peptoids are lower than the TOP indicating that the TOP has higher selectivity on bacterial killing over mammalian cell membrane toxicity.

Table 3.3: Peptoids, AMPs, and conventional antibiotics and their antimicrobial activities against planktonic PA14 (Chongsiriwatana *et al*., 2008; Kapoor *et al*., 2011).

Peptoid, AMP, or antimicrobial	MIC for *P. aeruginosa* (PA 14) (μM)	Selectivity ratio (SR)
TOP	80 (PAO1 strain)	100
1	12.5	6
1-11mer	12.5–25	>3.9
1-Pro_9	25–50	20
1-achiral	25	Not available
1-$C13_{4mer}$	12.5–25	Not available
1_{4mer}	>100	Not available
1-Nssb	>100	Not available
LL-37	25–50	Not available
Pexiganan	12.5–25	24
Ciprofloxacin	0.4	Not available
Tobramycin	1.6	Not available
Kanamycin	>100	Not available

Bacteria and A549 cells co-culture assay shows TOP selective killing bacteria:

The TOP TI value postulated that it can kill bacteria while protecting the mammalian cells. To study this outcome *in-vitro*, co-culture assays were designed to study the extra cellular bacterial killing ability of TOP and quantified the bacterial counts (cfu/ml) and A549 cell death (sytox-orange). The TOP treated cultures showed less bacterial counts (Figure 3.9) compared to non-treated cultures. Further analysis with sytox-orange revealed that the TOP treated A549 cell cultures were protected (Figure 3.10) from invasion of extracellular bacteria and their toxins. The figure 3.10 shows the A549 dead cell counts on treated and non-treated cells; less dead cells indicates that the TOP shows selectivity over mammalian cells as postulated with the TI values previously.

Bacterial pathogens persist in the intracellular niche and multiply very slowly providing residual bacterial counts in the host from which further growth, infection and spread (Eltahawy, 1983; Zeiler *et al*., 1985; Almeida *et al*., 1996; Bouchard *et al*., 2013). Hence it is very important to treat the intracellular bacteria to have complete recovery from the infection. However most antibiotics do not reach the intracellular niche to kill the bacteria (Qazi *et al*., 2004; Yanmin *et al*., 2010; Bouchard *et al*., 2013). To determine the TOP mammalian cell membrane permeability and intracellular localisation, a confocal microscopy study was carried out with TOP-TAMRA and TAMRA alone (5, 10 and 50 μM) [Figure 3.11(a) and (b)]. The results revealed that the TOP-TAMRA were internalised within 1, 5 and 10 minutes intervals at 50 μM concentrations. Therefore the activity of the TOP has been evaluated by intracellular killing assays (Figure 3.12 and 3.13).

These confocal data [Figure 3.11 (a)] also demonstrated that lysine like peptoids enters cells rapidly via endosomal uptake (Peretto *et al*., 2003; Unciti-Broceta *et al*., 2009). The bioluminescence and gfp-fluorescence were measured after internalisation of RN6390; *S. aureus* expressing a *gfp-luxABCDE* reporter operon under the control of a growth-dependent promoter to track bacterial replication within mammalian cells in 96-well micro-plate format described by (Qazi *et al*., 2004). The results suggest that the TOP internalised into A549 cells and has potent activity against internalised RN6390. This also revealed that the TOP continues its bacterial killing ability within mammalian intracellular environments *ex-vivo*. This further confirms that the TOP internalised into the A549 cells and acts irrespective of cellular conditions like pH interference and salt concentration when using novel host defence peptoids.

The potent intracellular microbicidal activity of TOP led to evaluate the microbicidal potential of cells pre-loaded with TOP, as a model of prophylaxis and augmentation of cellular antimicrobial activity. The previous experiments described above have proven that the TOP can kill extracellular and intracellular bacteria without toxicity to A549 cells. Subsequent assays have been designed to understand the prophylactic clearance of bacteria *in-vitro*. Prophylaxis treatment of antibiotics has been

recommended for high risk patients such as immune compromised patient to prevent infection (Capitano *et al*., 2001). The results show that TOP was retained within the A549 cells and the internalised TOP can reduce the intracellular bacterial growth in a dose dependent manner (Figure 3.14). Since the lung epithelial surfaces are constantly exposed to bacteria and are often a site for persistent bacterial survival, the pre-treatment of TOP could prevent epithelial cell death and apoptosis in response to bacterial infection and also contribute to pathological damage to the host and within the lung leading to compromised barrier function and consequent acute lung injury (van Schilfgaarde *et al*., 1999; Martin, 2008).

TOP induces inflammatory response on neutrophils:

Neutrophils play an important role as antimicrobial innate effector cells recruited to sites of acute inflammation and constitute the first line of cellular defence in bacterial infection (Haslett, 1999). The appropriate regulation of neutrophils function, death and clearance is critical to innate immunity and dysregulation is implicated in disease pathogenesis (Li *et al*., 2009). Therefore it is important to understand the regulation of neutrophils activity by TOP. Neutrophils were incubated with TOP at 50 μM and 100 μM concentrations for 6 hrs and 20 hrs. The data indicated that the TOP can induce secondary necrosis at 6 hrs and 20 hrs incubation. A longer incubation TOP induces primary necrosis in the neutrophils (Figure 3.17 and Figure 3.18). Primary and secondary necrosis by the TOP can be blocked by QVD, the caspase inhibitor (Figure 3.19 and Figure 3.20). This indicates that TOP influenced apoptosis and secondary necrosis at lower concentrations (50 μM) but at higher concentrations (100 μM) it induced primary necrosis and this may be pro-inflammatory. However, AMPs like LL-37 induce rapid secondary necrosis in neutrophils and promote the resolution of inflammation (Barlow *et al*., 2006; Li *et al*., 2009). The low concentration (50 μM) of TOP promotes the resolution of inflammation however higher concentrations may pro-inflammatory. Therefore modulation of the TOP is very important to optimise the bacterial killing while promoting the resolution of inflammation in lung infection. However more experiments have to be done to investigate the consequence of these secondary necrotic neutrophils on macrophages

and their inflammatory responses. (Li *et al*., 2009) showed that the LL-37-induced secondary necrosis did not inhibit neutrophil ingestion by monocyte-derived macrophages and was not pro-inflammatory.

TOP shows cytotoxicity activity on A549 lung epithelial cells:

Further studies have been carried out to investigate the TOP-cytotoxicity activity on A549 cells (Figure 3.22 and 3.23). Four different peptoids were tested including TOP at different concentrations and no significant toxicity was observed among all peptoids. This suggests that the TOP shows selectivity between bacterial and mammalian cells as observed in previous haemolysis data.

In conclusion, TOP displayed potent antimicrobial activity compared to 13 other tested peptoids. It exhibited antibacterial activity against non-dividing and multiplying gram negative and gram positive bacteria. A high SR supports further *in-vivo* testing of TOP. Extracellular and intracellular bacterial killing and prophylactic properties of the TOP are important characteristics which support its further development. TOP induces ROS production in bacteria and membrane damage whilst remaining nontoxic to A549 lung epithelial cells. At low concentrations TOP induces secondary necrosis of apoptotic neutrophils similar to other antimicrobial peptides.

Chapter 4:
PBP2A protein

Chapter 4: PBP2A protein

4.1. Abstract

This chapter details the cloning, over-expression and purification of PBP2A protein. This purified protein has been used to develop aptamer and peptide probes to detect MRSA. The gene transcribing this protein is *mecA* in MRSA and it has been well documented that the methicillin resistance in MRSA is due to the presence of this gene. The *mecA* gene has been amplified from genomic DNA of MRSA strains and cloned into pET21d(+) vector using restriction enzymes and DNA ligase, respectively. The cloned products were sequenced and analysed using restriction enzyme digestion to confirm the insert and its right orientation before transformation into the over expression *E. coli* strain BL21. Under the optimum culture conditions and the presence of IPTG the protein was over-expressed and purified using Ni-NTA columns. The protein purity was analysed by running a protein gel and quantified using BCA protein assay. Finally the purified protein was confirmed using Latex Agglutination test. The results confirmed that the purified protein demonstrates the same functional properties to its native protein present in MRSA but not in MSSA. The purified PBP2A protein coated Ni beads were used to develop aptamer and peptide probes.

4.2. Introduction

Methicillin resistance in *S. aureus* is due to the presence of *mecA* gene, which transcribes the PBP2A protein (78 kDa). PBP2A catalyses the formation of peptide crosslinks (transpeptidation) between glycan chains of the bacterial cell wall in the presence of β-lactam antibiotics (Pinho *et al*., 2001). Therefore PBP2A is a potential bacterial protein for the development of molecular probes.

This chapter details *mecA* gene cloning, PBP2A protein over-expression and purification in order to develop specific aptamer and peptide molecular probes against PBP2A protein.

4.3. Bioinformatics data mining

The whole genome of an MRSA strain has been sequenced (Holden *et al*., 2004). The bioinformatics data for *mecA* gene was obtained from Comprehensive Microbial Resource (http://cmr.jcvi.org/tigr-scripts/CMR/CmrHomePage.cgi) and data was obtained as mentioned in the materials and methods section (2.2.1). The gene sequence and the protein sequence were obtained as mentioned and the *mecA* gene consists of 2007 base pairs (bp) and the transcribed PBP2A protein is 668 amino acids (aa) with molecular weight of 78 kDa.

4.4. *mecA* gene specific primer designing

As described in the Materials and Methods section, the primers were designed to remove N-terminal transmembrane region of the PBP2A protein. This removes the insoluble part of the protein up to 23aa. The 24aa to 668aa of the protein has been over-expressed with His tag at the C-terminus. The primers used in this study are shown in Table 4.1, incorporating NcoI and XhoI restriction sites for cloning.

Table 4.1: Oligonucleotide primers used for cloning of *mecA* gene in this study

Name	Sequence 5'-3'
Forward primer-	ATAATA**CCATGG**CTTCAAAAGATAAAGAAATTAATAATAC
Reverse primer-	ATAATA**CTCGAG**TTCATCTATATCGTATTTTTTATTACC

The restriction enzyme digestion of *mecA* gene was analysed using NEBcutter V2.0 (http://tools.neb.com/NEBcutter2/) to study the suitability of using NcoI and XhoI enzymes for cloning (Figure 4.1). The searches indicated that the two restriction enzymes are not splicing the *mecA* gene were suitable to use for *mecA* cloning.

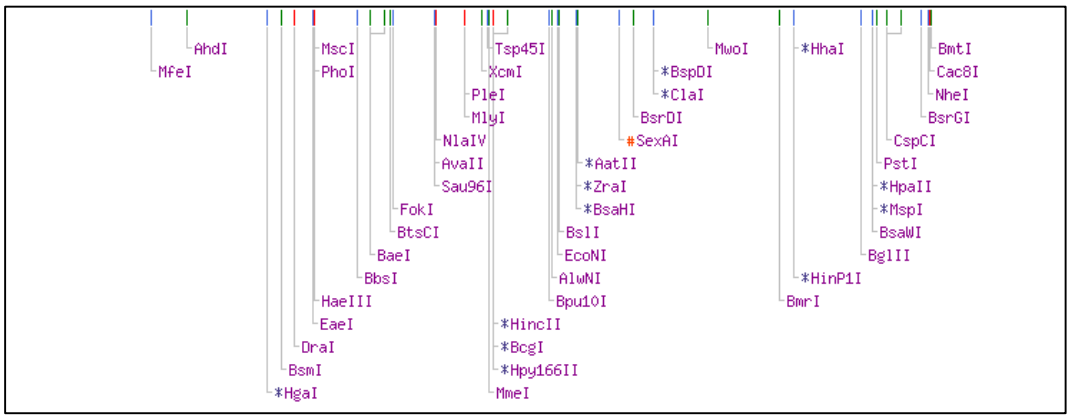

Figure 4.1: The map of the restriction enzyme digestion of *mecA* gene

4.5. PCR amplification of *mecA* gene

The *mecA* gene was PCR amplified using the protocol described in the Materials and Methods section (2.2.3) and the agarose gel confirmed that the presence of the *mecA* gene (2007bp) is only observed in the MRSA strains (Figure 4.2). The amplified products were used for cloning.

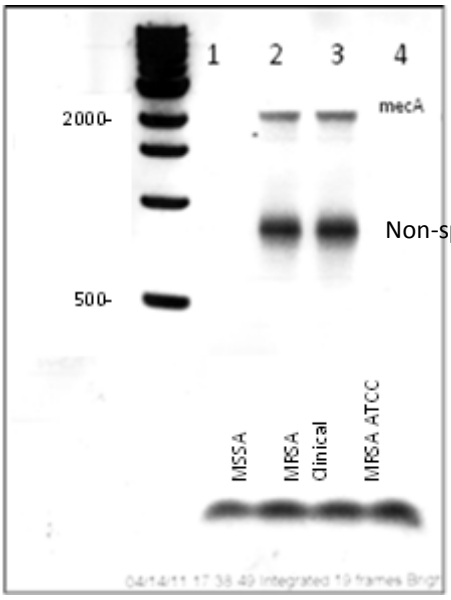

Figure 4.2: Agarose gel electrophoresis images; PCR amplification of *mecA* gene in MRSA. Lane 1-MSSA; Lane 2-MRSA Clinical strain; Lane 3-MRSA ATCC252 strain; Lane 4-negative control.

4.6. Restriction enzyme digestion and ligation

Both the vector pET21d(+) (Figure 4.3) and the insert (*mecA*) were cut with restriction enzymes (NcoI and XhoI) and run on an agarose gel to confirm the purity of the products (Figure 4.4).

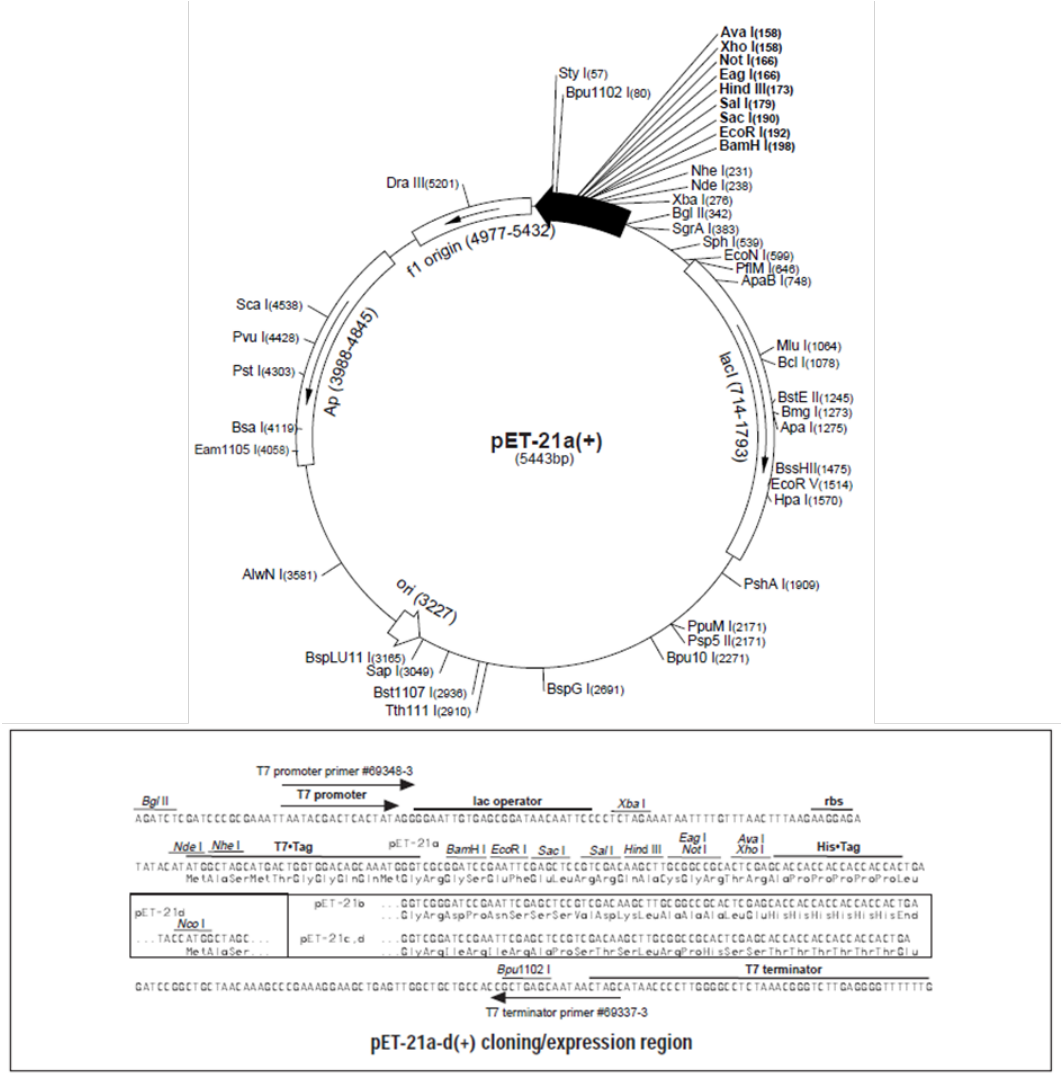

Figure 4.3: The plasmid vector pET-21d(+).The pET21d(+) plasmid vector was used to clone the *mecA* gene into multiple cloning site using NcoI and XhoI restriction enzymes.

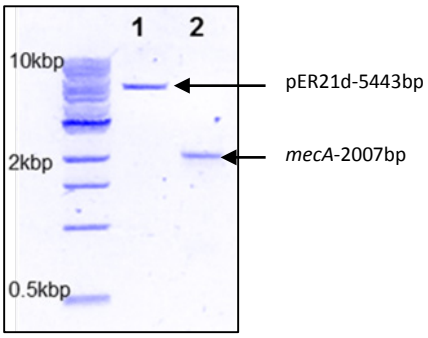

Figure 4.4: Agarose gel electrophoresis image. Showing restriction digested products; Lane 1-Plasmid vector (pET21d+) cut with XhoI and NcoI; Lane 2-Insert (*mecA*) cut with XhoI and NcoI.

4.7. Transformation of cloned plasmid to *E. coli* BL21 cells

Transformation of the ligated products into BL21 cells was carried out as detailed in the Materials and Methods section. Ten colonies were selected after overnight incubation in ampicillin (50 µg/ ml) LB plates and colony PCR was carried out on ten selected colonies using the same primers. PCR amplification demonstrated that the *mecA* gene was correctly cloned into 7 out of 10 colonies of the pET21d(+) vector (Figure 4.5).

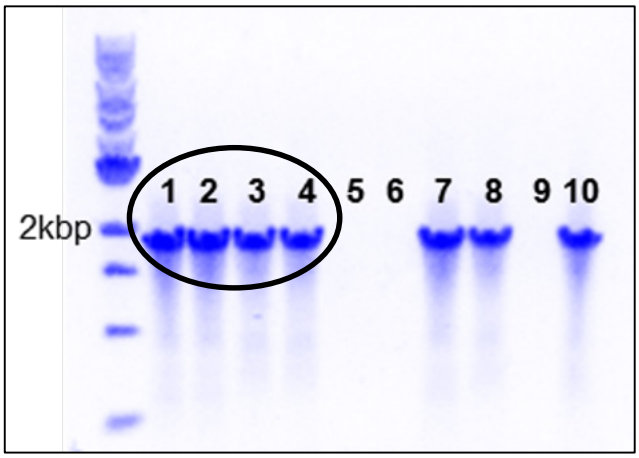

Figure 4.5: Agarose gel electrophoresis image investigating the *mecA* gene amplification in 10 different colonies of BL21. Colony numbers 5, 6 and 9 were negative for PCR amplification for *mecA* gene. Therefore colonies 1-4 (circled) were selected for further analysis.

4.8. Sequencing of cloned plasmids

Four *mecA* positive colonies were selected from the colony PCR results for further studies. Plasmids of these colonies were extracted as mentioned in the protocol using Qiagen kits. The plasmids were sequenced using T7 sequencing primers to determine the presence of the correct sequence of the *mecA* gene in the vector pET21d(+). The Sanger sequencing results were analysed using ClustalW software. Data showed that the *mecA* gene sequence was present in all four colonies (1 to 4) and these were hence ready for over-expression of the protein PBP2A (Figure 4.6).

```
JCK138-34-A>      TCAGGATCGTAAAATAAAAAAAGTATCTAAAAATAAAAAACGAGTAGATGCTCAATATAA 298
PBP2A>            TCAGGATCGTAAAATAAAAAAAGTATCTAAAAATAAAAAACGAGTAGATGCTCAATATAA 299
                  ************************************************************

JCK138-34-A>      AATTAAAACAAACTACGGTAACATTGATCGCAACGTTCAATTTAATTTTGTTAAAGAAGA 358
PBP2A>            AATTAAAACAAACTACGGTAACATTGATCGCAACGTTCAATTTAATTTTGTTAAAGAAGA 359
                  ************************************************************

JCK138-34-A>      TGGTATGTGGAAGTTAGATTGGGATCATAGCGTCATTATTCCAGGAATGCAGAAAGACCA 418
PBP2A>            TGGTATGTGGAAGTTAGATTGGGATCATAGCGTCATTATTCCAGGAATGCAGAAAGACCA 419
                  ************************************************************

JCK138-34-A>      AAGCATACATATTGAAAATTTAAAATCAGAACGTGGTAAAATTTTAGACCGAAACAATGT 478
PBP2A>            AAGCATACATATTGAAAATTTAAAATCAGAACGTGGTAAAATTTTAGACCGAAACAATGT 479
                  ************************************************************

JCK138-34-A>      GGAATTGGCCAATACAGGAACAGCATATGAGATAGGCATCGTTCCAAAGAATGTATCTAA 538
PBP2A>            GGAATTGGCCAATACAGGAACAGCATATGAGATAGGCATCGTTCCAAAGAATGTATCTAA 539
                  ************************************************************

JCK138-34-A>      AAAAGATTATAAAGCAATCGCTAAAGAACTAAGTATTTCTGAAGACTATATCAAACAACA 598
PBP2A>            AAAAGATTATAAAGCAATCGCTAAAGAACTAAGTATTTCTGAAGACTATATCAAACAACA 599
                  ************************************************************

JCK138-34-A>      AATGGATCAAAATTGGGTACAAGATGATACCTTCGTTCCACTTAAAACCGTTAAAAAAAT 658
PBP2A>            AATGGATCAAAATTGGGTACAAGATGATACCTTCGTTCCACTTAAAACCGTTAAAAAAAT 659
                  ************************************************************
```

Figure 4.6: ClustalW data showing the alignment of sequenced data (JCK138-34-A) with the *mecA* gene sequence.

4.9. Over-expression and purification of PBP2A protein

Over-expression and purification of PBP2A protein was carried out according to the Materials and methods section (2.2.3.10.). Purified proteins were visualised by running a SDS-polyacrylamide protein gel and staining with coomassie brilliant blue (Figure 4.7).

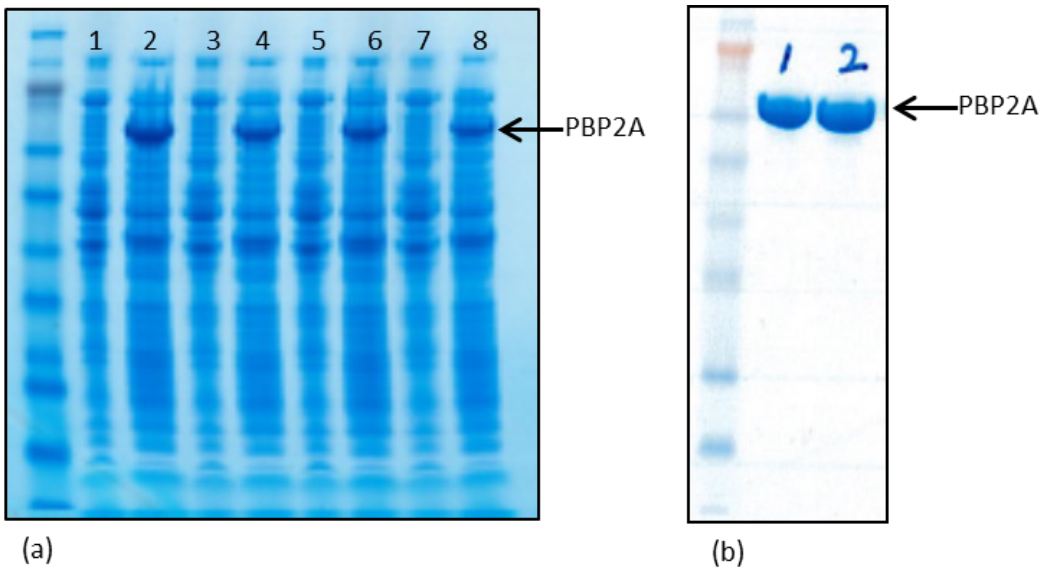

Figure 4.7: SDS-polyacrylamide protein gel showing the over expressed PBP2A protein and purified protein (a) Lane 1, 3, 5 and 7 are the four colonies before over-expression and 2, 4, 6 and 8 are after PBP2A over-expression with IPTG (1 to 4 colonies were selected-Figure 6). (b) Lane 1 (sample-34) and 2 (sample-35) represent the purified PBP2A protein (Two colonies were selected).

4.10. Quantification of the protein PBP2A

The BCA assay was performed to quantify the over-expressed protein as detailed in the Materials and Methods section. Two samples were chosen numbered 34 and 35 corresponding to the colony numbers on the plates (Table 4.2).

Table 4.2: Quantification of purified PBP2A protein in sample 34 and 35

Sample	Absorbance (100 µl)			Average (Y)	X=(Y-0.118)/0.001	µg/ ml	mg/ ml
	1	2	3				
34	0.242	0.251	0.242	0.245	127	1270	1.27
35	0.257	0.258	0.269	0.261	143	1433	1.43

The above data shows that the PBP2A protein is purified (Figure 4.7) and concentrations are above 1 mg/ ml of 10 ml (Table 4.2).

4.11. Penicillin binding protein (PBP2A) Latex Agglutination test

To confirm the activity of the over-expressed PBP2A protein, Latex Agglutination test was carried out. Therefore as mentioned in the Material and Methods section (2.2.3.15.) PBP2A antibody binding assay was carried out. The PBP2A latex agglutination test (Oxoid, Hampshire, United Kingdom) is a 20-min phenotypic test that detects PBP2A in isolated colonies (Doern *et al*., 1994). This assay showing the over-expressed PBP2A protein is responding to the active proteins in the MRSA not MSSA (Figure 4.8).

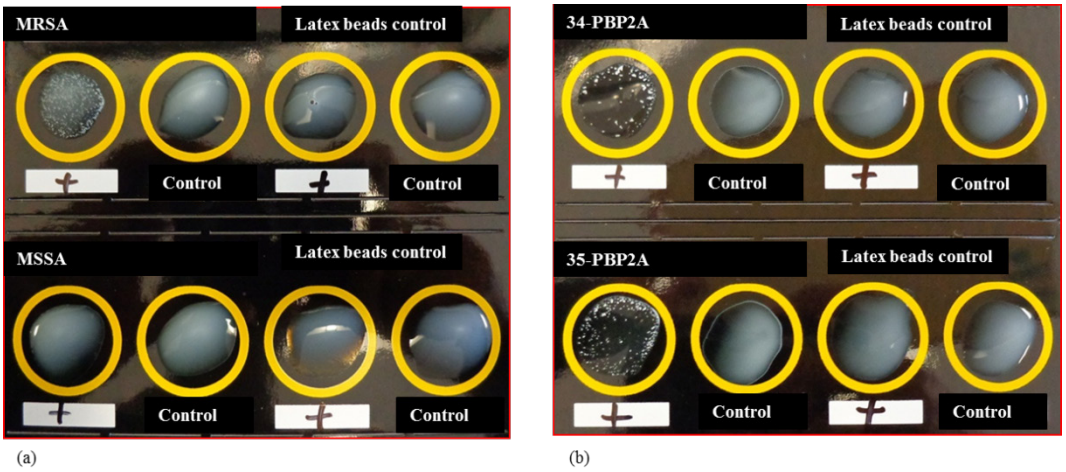

(a) (b)

Figure 4.8: Latex beads agglutination assay for purified PBP2A protein (a) MRSA and MSSA bacterial strains showing the positive and negative results respectively for the latex beads agglutination test. (b) Two samples of PBP2A over-expressed protein (34 and 35) respond to the test as MRSA. This indicates that the over-expressed PBP2A protein is showing the same functional properties to its native protein present in MRSA but not in MSSA.

4.12. Discussion

MRSA has developed clinical resistance to β-lactam antibiotics by acquisition of the *mecA* gene (Enright *et al*., 2002) which encodes PBP2A and provides transpeptidase activity to allow cell wall synthesis at β-lactam concentrations that inhibit the β-lactam-sensitive strains (Lim and Strynadka, 2002; Otero *et al*., 2013). *S. aureus* normally produces four PBPs, (Georgopapadakou *et al*., 1986) which are susceptible to inhibition by β-lactam antibiotics. The irreversible acylation of the active site of the PBPs by the β-lactam antibiotics causes the death of the bacteria due to the non-functional PBPs. However, PBP2A is resistant to all commercially available β-lactams (Otero *et al*., 2013) and MRSA has become resistant to almost all commercially available antibiotics. Thus the detection of the PBP2A protein is an important goal of clinical microbiology. The aim of this chapter work has been to produce PBP2A to enable efforts to develop molecular diagnostics in the following chapters. Importantly PBP2A is located on the outer surface of the bacterial cell wall (Ohwada *et al*., 1999; Roth *et al*., 2006). The truncated PBP2A protein has been selected for over-expression from the *mecA* gene coding elements of the membrane spanning segment which is lack in the over-expressed PBP2A protein (Wu *et al*., 1992).

A 242 bp fragment of *mecA* gene was amplified by PCR from *S. aureus*, expressed, purified and used to stimulate humoral immune response in a murine model. This investigation revealed that PBP2A as a potential to develop vaccine against MRSA infection (Haghighat *et al*., 2013). In another study, PBP2A and $PBP2A_{LGA}$ (PBP2A from MRSA strain LGA251) were over-expressed to study the MRSA strain-to-strain variation in resistance level (Kim *et al*., 2012). Inactivation of the transglycosylase domain and the activation of the transpeptidase domain were studied using over-expressed PBP2A protein by (Pinho *et al*., 2001). Hence similar cloning methods were adopted from previous publication in my research work.

Holden *et al*., (2004) sequenced the 2.8 Mbp genomes of two disease causing *S. aureus* strains isolated from hospital-acquired MRSA (MRSA252). The sequence data has been obtained using online bioinformatics data base called 'Comprehensive Microbial Resource' (http://cmr.jcvi.org/tigr-scripts/CMR/CmrHomePage.cgi). Using the *mecA* gene sequence, *mecA* specific primers were designed to PCR amplify the *mecA* gene. The results of the PCR amplification showed that the *mecA* gene was only present in MRSA. This indicated that my chosen *mecA* specific primers were and could be used to identify MRSA strains in the clinical samples.

The PBP2A latex agglutination test (Oxoid, Hampshire, United Kingdom) is a 20-min phenotypic test that detects PBP2A in isolated colonies (Doern *et al*., 1994). The PBP2A assay is faster and less complicated than PCR for *mecA* and has been shown to be more sensitive than other phenotypic methods, such as the use of oxacillin screen agar (van Griethuysen *et al*., 1999). The positive results with the purified PBP2A protein indicates that the purified protein function as same as native PBP2A protein in MRSA and the activity of the protein is remain the same. Finally it can be confirmed that the cloning, over-expression and purification of the biologically active PBP2A protein was possible and will be used in Chapter 5 and 6 to develop molecular probes.

The purified soluble PBP2A protein has been used to develop PBP2A specific aptamer and peptide molecular probes to detect MRSA. The Ni-NTA beads were coated with His-tagged PBP2A protein. SELEX and the bio-panning assays were carried out on those beads to develop PBP2A specific probes.

Chapter 5:
Aptamer bio-imaging probe development

Chapter 5: Aptamer bio-imaging probe development

5.1. Abstract

This chapter investigates the development of aptamer bio-imaging probes to detect bacterial infection. Two different aptamer libraries have been used in this study and characterised the best library and the optimum selection buffer conditions for SELEX protocol. Then the PCR conditions for the aptamer amplification have been optimised for the number of PCR cycles to have high yields of DNA and low non-specific PCR amplifications. The preparation of ssDNA from the dsDNA PCR products were optimised using biotin labelled primers and streptavidin sepharose beads. SELEX protocols have been carried out on whole MRSA bacterial cells and PBP2A coated Ni beads to generate MRSA and PBP2A specific aptamer bio-imaging probes. Fifteen rounds of SELEX were carried out against PBP2A coated Ni beads and five rounds of parallel SELEX carried out on five different bacterial strains and A549 cells before Ion Torrent sequencing. The sequenced data have been analysed and overlapping sequences between bacteria eliminated to generate unique sequences for PBP2A and MRSA. Remarkably these two probes are 50% similar in DNA sequence. The PBP2A specific probe shows high specificity towards the PBP2A protein over other tested proteins such as FBS, BSA and trypsin in Ni beads assay. It also binds to MRSA but shows non-specific binding to other bacterial strains in similar manner. MRSA probe shows higher binding capacity towards MRSA bacteria over the rest of the bacteria tested. Aptamers show no cellular toxicity at 50 μM concentration on 3T3 cells and show potential *in-vivo* applications. MRSA and PBP2A specific aptamer probes were not antibacterial according to growth inhibition assay in MHB at the 50 μM level.

5.2. Designing of Aptamer libraries

Aptamers are single stranded DNA or RNA molecules. The length of the molecules are variable, typically <100-mer long. In this study eight DNA aptamer libraries have been tested. They were made up of two main libraries termed G and M with two different primer binding sites. Each G and M library had four sub groups having different lengths of variable regions of 30 and 40 nucleotides (shown as -30N- and -40N-) in the Table 5.1 and Figure 5.1, including G-quadruplex (shown as -GGG-) where guanines are located at fixed positions in the variable regions. The prime objective of having different libraries is to give higher diversity within the aptamer libraries for SELEX protocol. I designed the primer binding sequences for library G and library M primer sequences were taken from previous publication (Sefah *et al*., 2010).

Table 5.1: Eight aptamer libraries used in this study.

Variable region	Library G Primer binding sites 5′ CTACACGACGCTCTTCCGATCT (-NNN-) AGATCGGAAGAGCGGTTCAGCA 3'	Library M Primer binding sites 5′ ATACCAGCTTATTCAATT (-NNN-) AGATAGTAAGTGCAATCT 3'
-(30N)-	G1 (74bp)	M1 (66bp)
-(40N)-	G2 (84bp)	M2 (76bp)
-(NNGGNNNNNNGGNNNNNNG GNNNNNNGGNN)-	G3 (74bp)	M3 (66bp)
-(NNNGGGNNNNGGGNNNNGG GNNNNGGGNNN)-	G4 (74bp)	M4 (66bp)

Primer sequences:

Jck11GA- Forward-AminoMod 5'CTACACGACGCTCTTCCGATCT3'

Jck11GB- Reverse-biotin 5' TGCTGAACCGCTCTTCCGATCT 3'

Jck10MA- Forward-AminoMod 5' ATACCAGCTTATTCAATT 3'

Jck10MB- Reverse-biotin 5' AGATTGCACT TACTATCT 3'

5.3. Agarose gel electrophoresis to visualise the aptamer libraries

An agarose gel was run (4%) to visualise the designed aptamer libraries before (Figure 5.1.) and after PCR amplification. Agarose gel electrophoresis determined the length of the aptamer generated by each PCR round and visualised any non-specific PCR products amplified during PCR. Agarose gel electrophoresis was performed as a quality control for each round of PCR amplification and after purification of ssDNA to monitor any false positive PCR products.

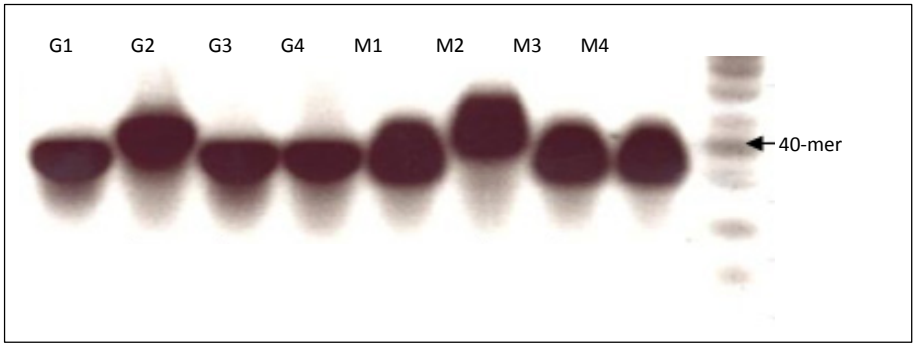

Figure 5.1: Agarose (4% TBE) gel electrophoresis image showing the products of the naïve eight aptamer libraries (1µl/ lane). G2 and M2 contained 40 nucleotides in the variable region whilst the remaining libraries possessed 30 nucleotides.

Before the SELEX protocol, the libraries were PCR amplified using specific primers to determine the optimum PCR conditions for the full amplification of the libraries. Figure 5.2 shows the DNA gel after amplification of these libraries showing products double the size due to the dsDNA. The optimum PCR amplification used the following amplification conditions: hot start 95^{o}C for 2 minutes, denaturation at 95^{o}C for 30 second, annealing at 60^{o}C for 30 second, extension at 72^{o}C for 30 second and final extension at 72^{o}C for 2 minutes.

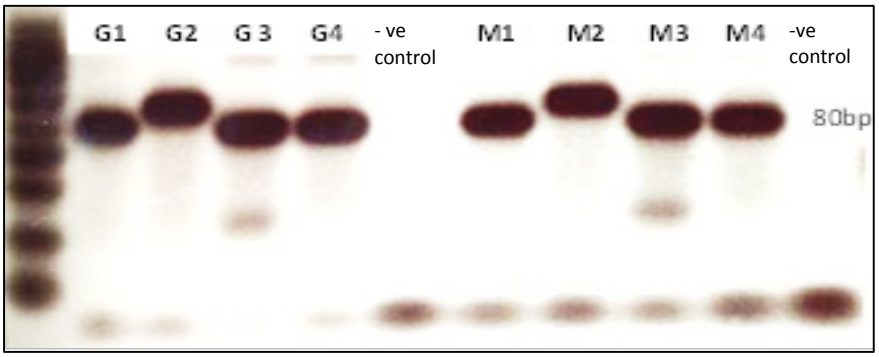

Figure 5.2: Agarose (4% TBE) gel electrophoresis image showing the PCR amplified G and M aptamer libraries (5µl/ lane). The negative control has been run with a template sequence and the remaining contained 0.1 µl of each ssDNA aptamer libraries (100µM).

5.4. Study of different buffers on the efficiency of SELEX protocol

After optimising the PCR conditions to amplify the aptamer libraries, optimisation of selection buffers were studied. Aptamer binding capacity may vary depending on buffer components such as pH, solutes conditions (osmolality) and different buffers have been used for SELEX screening in different studies. Experiments were designed to evaluate how different buffers reacted with the libraries. False positive and false negative results occurred under poor buffer binding conditions. Library G and M were utilised in this experiment and selection was carried out with bacteria (MRSA) and without bacteria (control). Four different buffers were evaluated as mentioned below.

1. PBS (with Ca^{+2} and Mg^{+2})
2. Buffer B (Tris–HCl-25 mM, KCl-50 mM, NaCl-200 mM, EDTA-0.2 mM, Glycerol-5% (v/v), DTT-0.5 mM)
3. IMDM
4. DMEM

All of these alone were not optimal giving false positive results (without 1% BSA: Data are not shown). PBS and Buffer B gave the most promising results. The addition of 1% BSA further reduced the non-specific binding of aptamer to the eppendorf tube and optimised the SELEX procedure. Figure 5.3 shows the combination of experimental conditions carried out to evaluate the suitability of buffers (Buffer 2 and PBS).

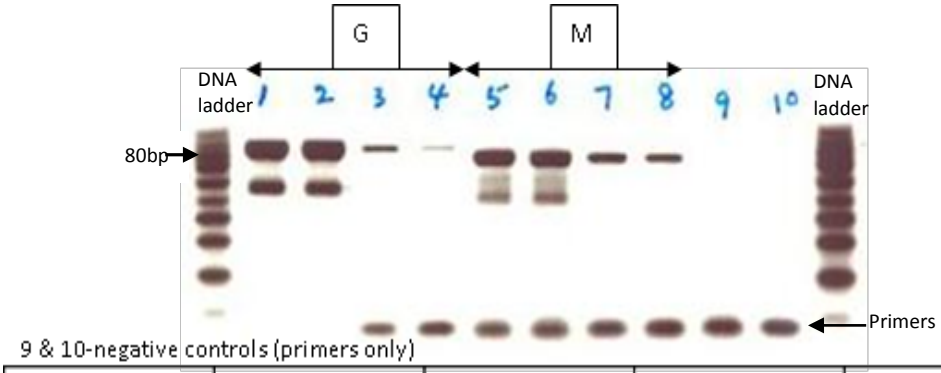

Buffers	G-library+ Bacteria	G-library + No Bacteria	M-library+ Bacteria	M-library + No Bacteria
Buffer 2 (1% BSA)	1	3	5	7
PBS (1% BSA)	2	4	6	8

Figure 5.3: Agarose (4% TBE) gel electrophoresis image showing the PCR amplified G and M aptamer libraries after first round of SELEX. Lane 9 and 10 represent G and M negative controls. Two bands of PCR products show non-specific amplification.

According to the above Figure 5.3, lane 3, 4, 7 and 8 shows PCR products indicating that the aptamer can bind to the walls of eppendorf tubes (used eppendorf low binding tubes) non-specifically (control) and may give false positive bands. However these false positive bands can be reduced by increasing the BSA (1%) in the

selection buffer. The non-specific binding of aptamers to non-target objects can be reduced by increasing BSA concentrations up to 1% in the selection buffers of Buffer 2 and PBS (Figure 5.3). These results indicate that the best binding buffer for bacterial cell SELEX is PBS with 1% BSA. In addition the G library showed lower false positive binding. Therefore the rest of the SELEX studies have been carried out using the G library.

5.5. Determination of the number of PCR cycles that yields enough DNA without nonspecific amplification

Amplifying nonspecific DNA during the PCR amplification is a major problem in SELEX protocol and low PCR cycles also give low yields of DNA for further SELEX rounds. Therefore PCR conditions were optimised to have high yields of DNA and low non-specific DNA during PCR amplification. To determine the number of PCR cycles the library was amplified for three different PCR cycles 10, 15 and 35 (Figure 5.4). The results show that the number of PCR cycles directly proportional to the number of nonspecific PCR products. The results suggest that this can be minimised by keeping the number of PCR cycles to 10 while still generally sufficient PCR products for the further rounds of SELEX.

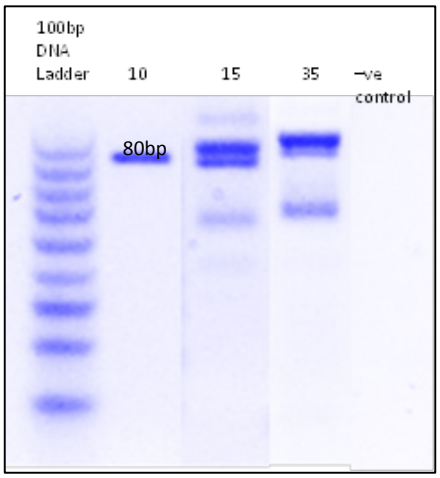

Figure 5.4: Agarose (4% TBE) gel electrophoresis image showing the products of the various PCR cycles (10, 15 and 35) of selected DNA library amplification. Lane 1- DNA ladder; Lane 2- 10 PCR cycles; Lane 3- 15 PCR cycles; Lane 4- 35 PCR cycles. More than one band of PCR products indicates the non-specific amplification.

5.6. Preparation of ssDNA from PCR products

It is an important step to prepare ssDNA from the dsDNA for further SELEX cycles. Selected ssDNA pools were amplified using biotin labelled reverse primer and the forward primer. The PCR products were incubated with streptavidin sepharose beads suspension. This allows dsDNA to bind to sepharose beads forming an interaction between streptavidin and biotin. Then increasing the pH by adding 200 mM NaOH allows the separation of the two strands leaving the biotin labelled ssDNA strand behind. The supernatant of the non-biotin labelled (forward primer amplified strands) ssDNA were collected by centrifugation at 13,000rpm for 1 minute and diluted into 1 ml of PBS-T, containing 10 µl of 200 mM monobasic phosphate buffer to adjust the pH to 7.5. Finally, the material was heated to 95°C for 10 minutes then immediately placed at 4°C until the next round of SELEX. The purified ssDNA samples were run on an agarose gel to confirm the efficiency of amplification and purity (Figure 5.5).

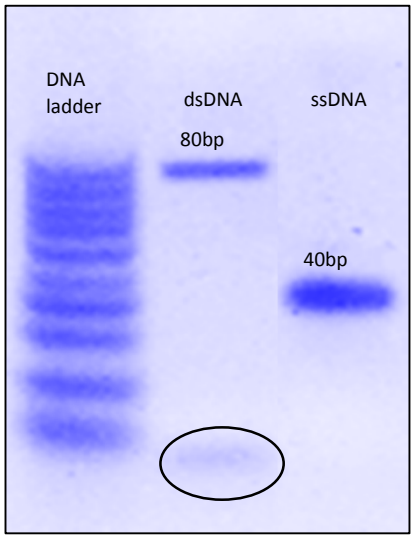

Figure 5.5: Agarose (4% TBE) gel electrophoresis image showing the PCR products before and after ssDNA preparation. Each lane contains 5µl of DNA samples. In the gel circle shows the excess primers after PCR amplification and preparation ssDNA removes any primers left behind.

5.7. Experimental design of the SELEX procedure

After optimising PCR conditions including 10 PCR cycles, PBS as SELEX buffer and ssDNA preparation all these optimum conditions were utilised to perform SELEX on MRSA and PBP2A purified protein. The main objective of these experiments was to develop MRSA specific aptamer probe. To achieve these goals two approaches were developed.

A) Whole bacterial cell SELEX-against MRSA

B) Purified protein SELEX-against MRSA specific cell division protein PBP2A (see chapter 4)

The whole bacterial cell SELEX was successfully carried out in previous publications using counter selection against other bacteria to reduce the nonspecific binding. However MRSA specific aptamer probes have not yet been discovered according to the recent publications (Cao *et al*., 2009). Therefore a novel approaches where no counter selection was involved during the SELEX procedure was used. This also reduced the number of SELEX cycles minimising errors during PCR amplification and mishandling samples. In my experimental procedure five rounds of SELEX were carried out independently against MRSA (ATCC252), MSSA (ATCC 25923), PAO1-*Pseudomonas*, *Kebsiella pneumonia*, *Escherichia coli* (ATCC 25922) and eukaryotic cells A549. This will generate aptamer against individual bacteria and eukaryotic cells but they were not specific due to lack of counter selection. These ssDNA aptamers were sequenced separately using the Ion Torrent sequencing method. Then the elimination of non-specific aptamers was carried out at sequenced level where the sequenced data was analysed and common sequences shared with the other bacteria were eliminated, resulting in the MRSA specific aptamer molecules.

The second approach was carried out using purified PBP2A protein coated Ni-NTA beads where 15 SELEX rounds were successfully carried out before Ion Torrent sequencing. Since this approach is on purified protein the counter selection step was

not performed against any bacteria involved. Agarose gel was run to quantify and visualise the seven samples of dsDNA before sending for sequencing (Figure 5.6).

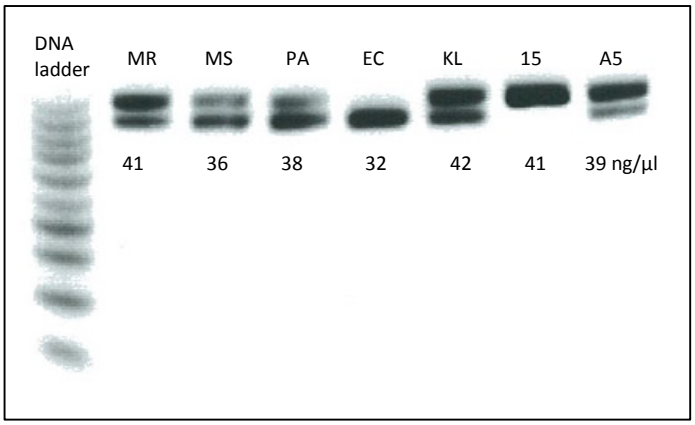

Figure 5.6: Agarose (4% TBE) gel electrophoresis image showing the final PCR products before sending for Ion Torrent sequencing. Two bands of DNA represent the combination of 74bp and 84bp aptamer G-libraries also indicate the concentrations of DNA present in the sample. MR-MRSA; MS-MSSA; PA-PAO1 *Pseudomonas*; EC-*E.coli*; KL- *Kebsiella pneumonia*; 15-PBP2A 15 rounds of SELEX; A5-A549 eukaryotic cells.

5.8. Ion Torrent sequencing and data analysis

Seven DNA samples were sent to The Institute of Genetics and Molecular Medicine, Western General Hospital, Edinburgh, UK for sequencing. The first step in the sequencing was to generate a library of DNA fragments flanked by the Ion Torrent adapters. This was done by adding the adapter sequences during PCR by designing PCR primers with the Ion Torrent adapter sequences at the 5' end. These PCR products were run on a gel to visualise the fragment size for sequencing (Figure 5.7). The barcoded samples were analysed on the Agilent bio analyser, which confirmed all 7 samples showing peaks around 160- 170bp (Figure 5.7).

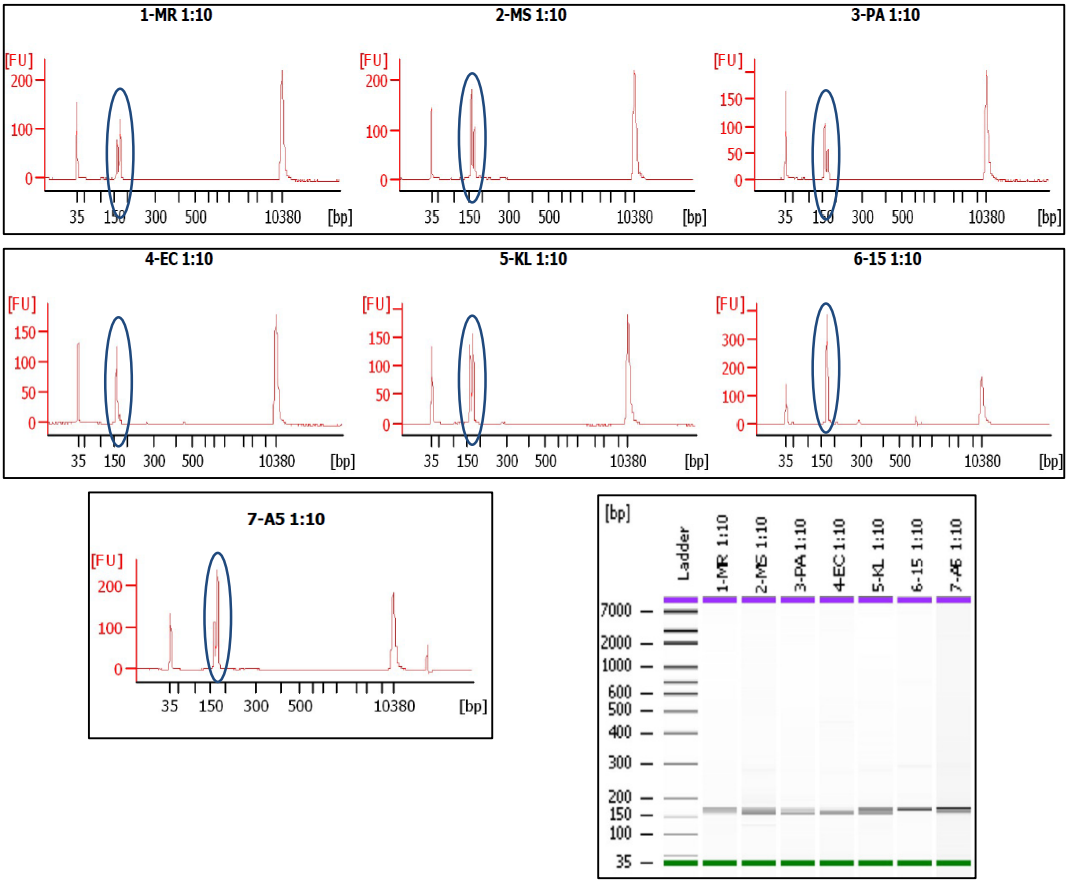

Figure 5.7: Electropherogram Summary from Agilent bio analyser; the graphs show (blue circles) the size of the DNA fragments after adding adapter sequences and the gel electrophoresis showing the dsDNA corresponds to the electropherogram. MR-MRSA; MS-MSSA; PA-PAO1 *Pseudomonas*; EC-*E.coli*; KL- *Kebsiella pneumonia*; 15-PBP2A 15 rounds of SELEX; A5-A549 eukaryotic cells.

Following sequencing the summary results generated the number of bases, reads and means of the read length. Table 5.2 shows the summary of the Ion Torrent sequencing of the aptamer.

Table 5.2: The summary of Ion Torrent sequencing showing the number of bases, reads and mean read lengths. MR-MRSA; MS-MSSA; PA-PAO1 *Pseudomonas*; EC-*E.coli*; KL- *Kebsiella pneumonia*; 15-PBP2A 15 rounds of SELEX; A5-A549 cells.

Barcode Name	Sample	Bases	≥ *Q*20	Reads	Mean Read Length
No barcode	4-EC	4,182,597	2,083,733	97,037	43 bp
IonXpress_020	none	56,559	31,031	1,821	31 bp
IonXpress_025	none	7,397	4,824	237	31 bp
IonXpress_026	1-MR	1,720,012	1,290,338	42,403	40 bp
IonXpress_027	2-MS	1,740,292	1,273,163	40,263	43 bp
IonXpress_028	3-PA	2,167,519	1,652,095	39,815	54 bp
IonXpress_029	4-EC	2,149,502	1,565,200	46,523	46 bp
IonXpress_030	5-KL	2,395,928	1,807,494	52,466	45 bp
IonXpress_031	6-15	2,070,587	1,621,156	33,369	62 bp
IonXpress_032	7-A5	1,489,663	1,113,925	30,674	48 bp

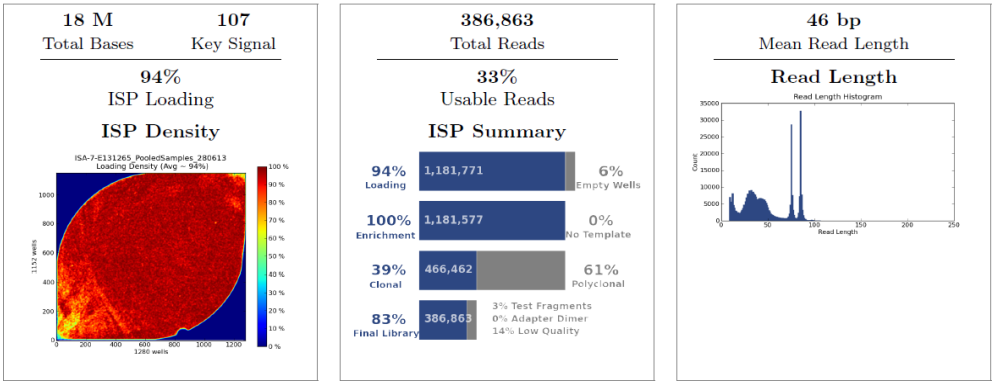

The quality of the DNA was analysed by the Agilent Bioanalyzer, which provided that the size of the DNA, details of contamination and the concentration of the samples. According to the data, all the DNA samples used in this study were around 150bp size and intact DNA was observed on both the gel electrophoresis and electrophotogram, indicating that there is no DNA degradation or contamination (Figure 5.7). After passing through the quality checks of the DNA samples, they were run through Ion Torrent sequencing to obtain the DNA sequences.

The Ion Torrent summary data are shown in the table 5.2 and it shows the statistical data of the sequenced samples. The data show that the number of bases, reads and mean length of the each sample. The expected mean length of the sequenced DNA should be around 150 bp as observed in the Agilent Bioanalyzer because the quality

of the samples were already analysed and checked before running the Ion Torrent sequencing. However, Ion Torrent sequencing data show that the 7 samples are very short lengths (less than 50 bp). This may have been caused by having sequences which were difficult to amplify due to long homo-polymer stretches or high GC content (Table 5.2). The failure of getting full length of the sequence will lose the data required for the analysis and predict the possible aptamer probe.

The summary report (Table 5.2) detailed barcodes aligning with each sample. Sample 6 which corresponds to PBP2A (barcoded with barcode 31) looks much better than the other 6 samples (there are far fewer short reads). The summary report indicated that the number of polyclonal reads was very high (61%), this occurs when the software detects that there are two templates per sphere and not just one. Ideally we would usually expect this number to be around 30%. The controls indicate that there isn't a problem with the sequencing run itself, other than the high polyclonality.

After removing the truncated primers, the data have been analysed to identify more reads by looking for truncated primers which may have been trimmed by the software. The analysis was performed using TextWrangler, (text editor software) and two probable aptamer probes named PBP2A specific and MRSA specific were generated (Figure 5.8).

Sequence alignment between two aptamer probes (randomised region):

Sequences of two aptamer probes are shown below indicating that they share 50% identity.

PBP2A-aptamer-

CGCGGTGTGGAATGGAAAGGCAGAGGGGGTAGACGGAGA

MRSA-aptamer-

GGCGGCGGGGGATGGTGGCGGAATGGTGGTGGTGAGCTGG

PBP2A-aptamer:

5'CTACACGACGCTCTTCCGATCTCGCGGTGTGGAATGGAAAGGCAGAGG GGGTAGACGGAGAAGATCGGAAGAGCGGTTCAGCA

MRSA-aptamer:

5'CTACACGACGCTCTTCCGATCTGGCGGCGGGGGATGGTGGCGGAATGG TGGTGGTGAGCTGGAGATCGGAAGAGCGGTTCAGCA

Underlined sequences are the primer binding sites of the probes.

The figure 5.8 shows the hairpin structures of the aptamer probes. Their minus Gibbs free energy (ΔG) indicates higher stability and higher melting temperatures also indicating that they are very stable aptamer probes at room temperature.

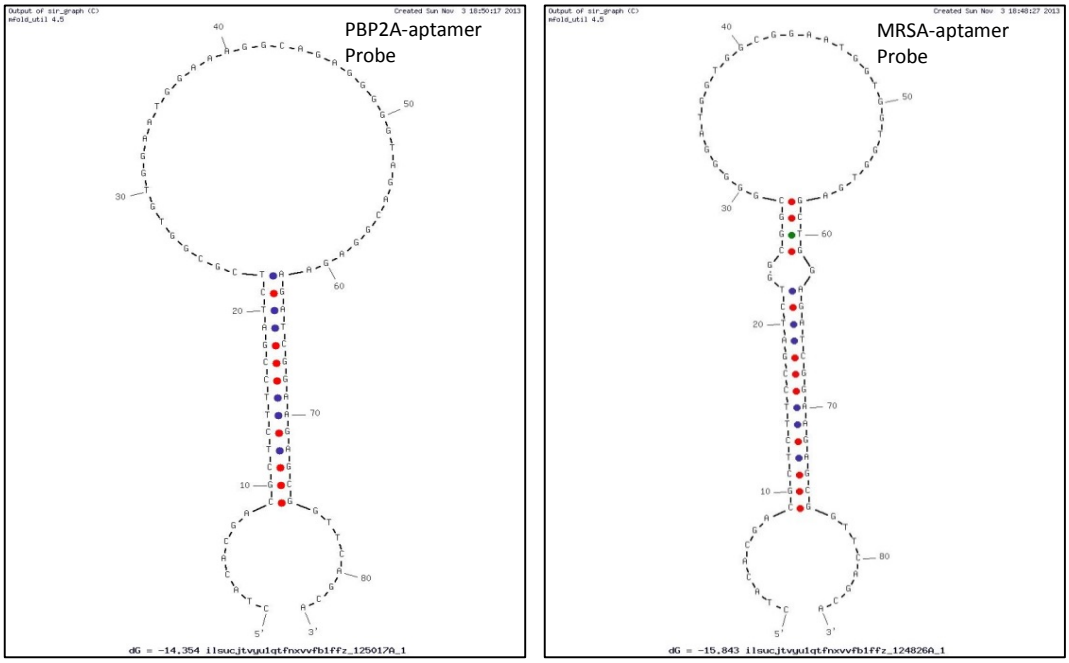

	ΔG (kcal/mole)	Tm (°C)
PBP2A-probe	-14.35	64.4
MRSA-probe	-15.84	60.7

Figure 5.8: The hairpin structures of MRSA and PBP2A aptamer probes. The minus Gibbs free energy (ΔG) indicates that the hairpin structures of aptamer probes are stable and the melting temperatures are well above room temperature.

5.9. Evaluation of PBP2A-aptamer probe binding *in-vitro*; Ni-NTA beads assay

The two lead aptamer probes were re-synthesised with 5' FITC modification form SIGMA-ALDRICH. For the assays, FITC modified PBP2A-aptamer probe was used to evaluate specificity of the aptamer candidate on different proteins including PBP2A protein. This assay was carried out as previously described in the SELEX protocol to develop PBP2A specific aptamer probe. Ni-NTA beads (300 µl) were incubated with 100 µg/ ml of PBP2A, BSA, FBS and trypsin separately and unbound proteins washed away. These protein coated beads were used as target molecules for the PBP2A-aptamer probe and efficacy of binding evaluated by using plate reader, confocal microscopy and confocal laser endomicroscopy.

The different imaging modalities were used to quantify and image the PBP2A-aptamer probe. The plate reader data showed that the PBP2A protein coated beads gives much higher fluorescence reads at 488/520 compared with the other three proteins and naked Ni beads. This suggests that the PBP2A-aptamer probe binds to PBP2A protein at higher efficacy than the BSA, FBS and trypsin (Figure 5.9). Another way of analysing this data is to visualise these beads under the confocal microscope (Figure 5.9). The images clearly indicate that only the PBP2A coated Ni beads are fluorescently labelled with the PBP2A-aptamer probe showing the expected protein specificity of the probe.

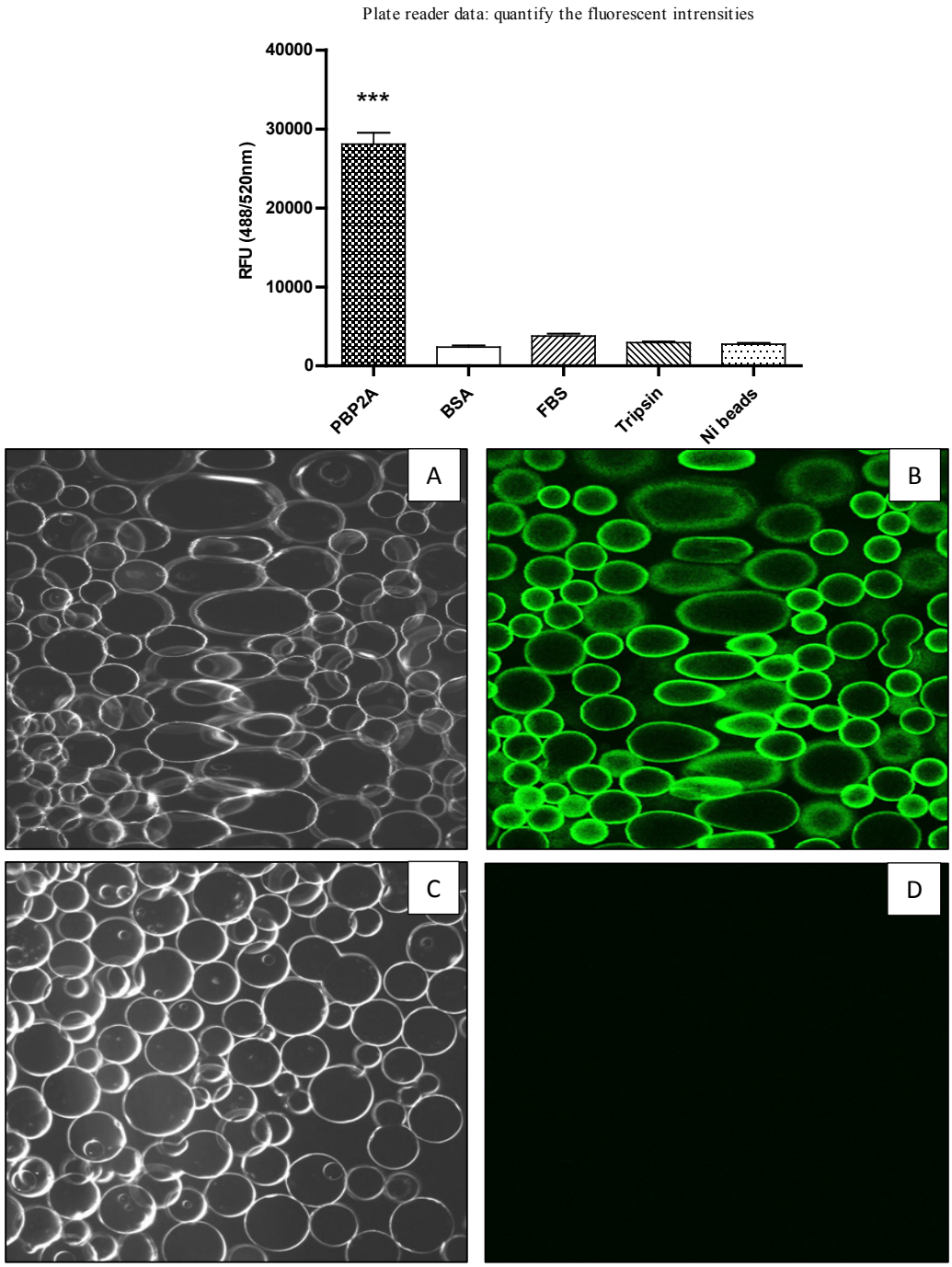

Figure 5.9: Ni-NTA protein binding assay shows that the PBP2A-aptamer is more specific to PBP2A protein compared with the BSA, FBS and Trypsin. A. Transmitted image of PBP2A protein coated beads; B. Fluorescent image of PBP2A coated beads; C. Transmitted image of FBS coated beads; D. Fluorescent image FBS coated beads.

The laser endomicroscopy (Cellvizio) experiments were carried out to prove that the FAM labelled aptamer can be used in parallel with the clinically approved Cellvizio imaging platform. To achieve this Ni beads were visualised using the Cellvizio mini probe and data analysed using proprietary image analysis tools (Cellvizio Viewer) (Figure 5.10).

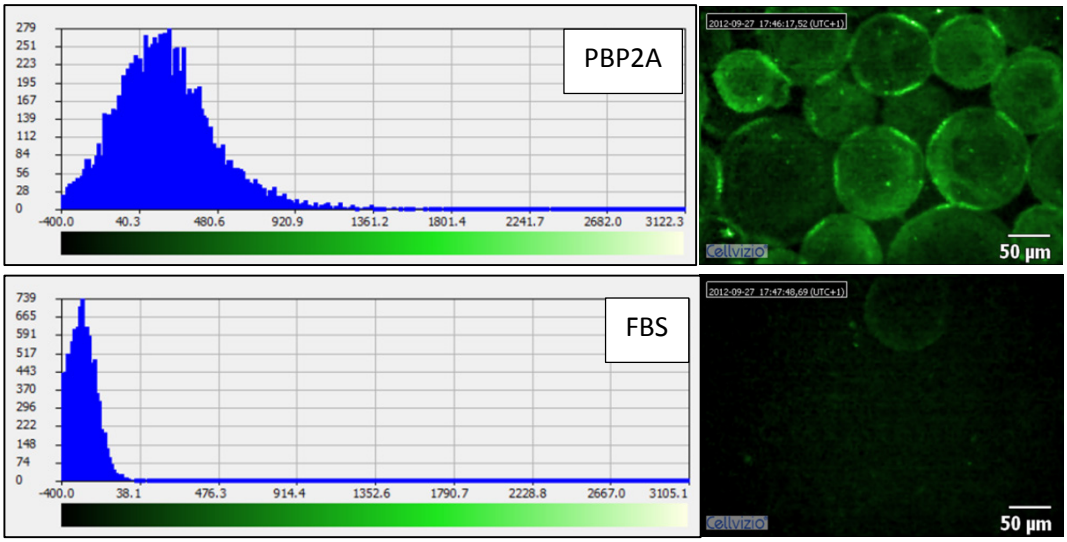

Figure 5.10: Ni-NTA protein binding assay; Cellvizio image analysis. Fluorescent image of the sample and the fluorescent intensity of the image. The reduced fluorescent shift to the right on the histogram indicates that the FBS beads are not labelled with the PBP2A-aptamer probe.

5.10. Evaluation of MRSA-aptamer probe binding *in-vitro* Ni-NTA bead assay

The Ni-NTA beads assay was carried out to evaluate probe binding capacity to other proteins including PBP2A protein (Figure 5.11). The results indicated that the MRSA-aptamer probe also binds to PBP2A protein. This is not unexpected as the two aptamer probes share 50% sequence homology.

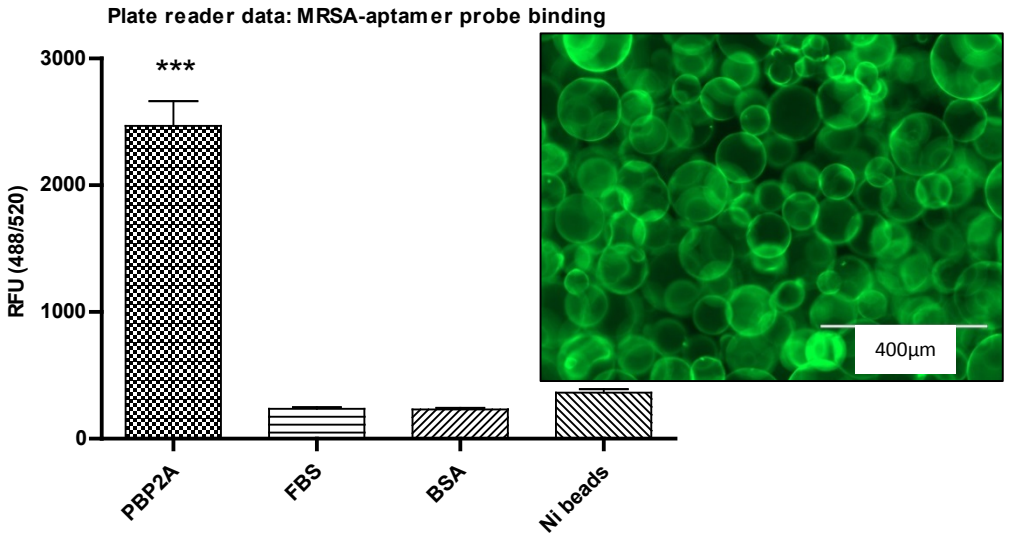

Figure 5.11: Ni-NTA protein binding assay shows that the MRSA-aptamer binds to PBP2A protein at higher rate compared to FBS and BSA. The confocal image shows that the PBP2A coated Ni beads are labelled with MRSA-probe.

5.11. Evaluation of MRSA and PBP2A-aptamer probe binding *in-vitro* bacterial binding assay

The ultimate objective of developing these probes was to detect MRSA specifically over other bacterial species. To assess the specificity of these probes, bacterial binding assays were carried out and bacterial cells were analysed using flow cytometry (Figure 5.12). A panel of bacteria were used at 10^8 cfu/ml bacteria and probes at 100 nM in PBS. Reassuringly the MRSA-probe showed a trend for higher affinity to MRSA compared with the rest of the bacterial panel, yet was not significantly increased compared to some strains. The PBP2A-probe showed no specificity towards MRSA though it shows very high specificity to PBP2A protein in Ni-NTA beads binding assay. This may be the fact that the aptamer has been developed against the whole protein and it may share the similar binding sites with the other bacterial proteins as well.

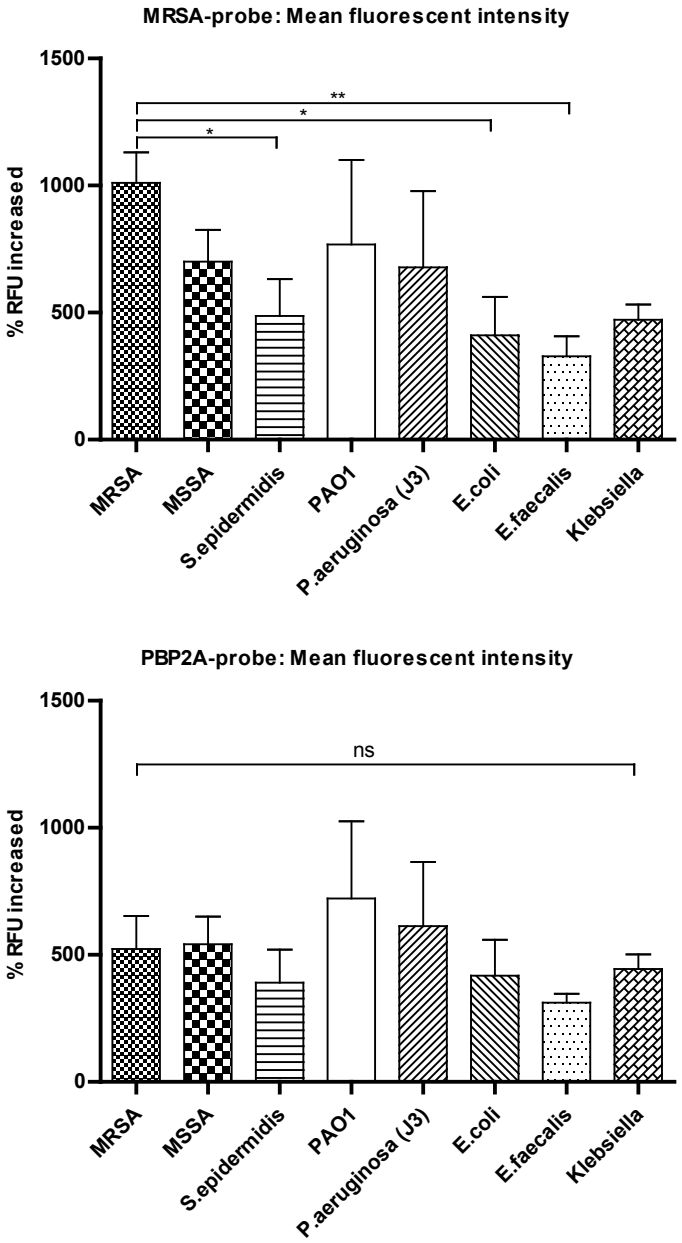

Figure 5.12: Flow cytometry data showing percentage increased in mean fluorescence intensity. Top graph shows the MRSA-probe and the bottom graph shows the PBP2A-probe. MRSA-probe shows higher binding to MRSA bacteria compared to the rest of the bacteria. However PBP2A-probe shows no specificity (Panels represent mean values ± SEM for n = 3).

5.12. Aptamer cytotoxicity studies on 3T3 cells

This assay was carried out to investigate aptamer toxicity on mammalian cell line to study the feasibility of using these probes *in-vivo* in murine models. The 3T3 cells have been used as a standard cell line to study the cellular toxicity of potential drug targets. Mouse 3T3 cells were cultured in 96 well plates overnight and incubated with aptamer and H_2O_2 at 50 µM concentrations separately and the control cells with normal cell culture media. After 24 hours incubation, the ATP activity was quantified. The aptamers demonstrated no celleular toxicity at the concentrations used (Figure 5.13). However more extensive studies are necessary before a conclusion could be made concerning the *in-vivo* safety or toxicity of these aptamer.

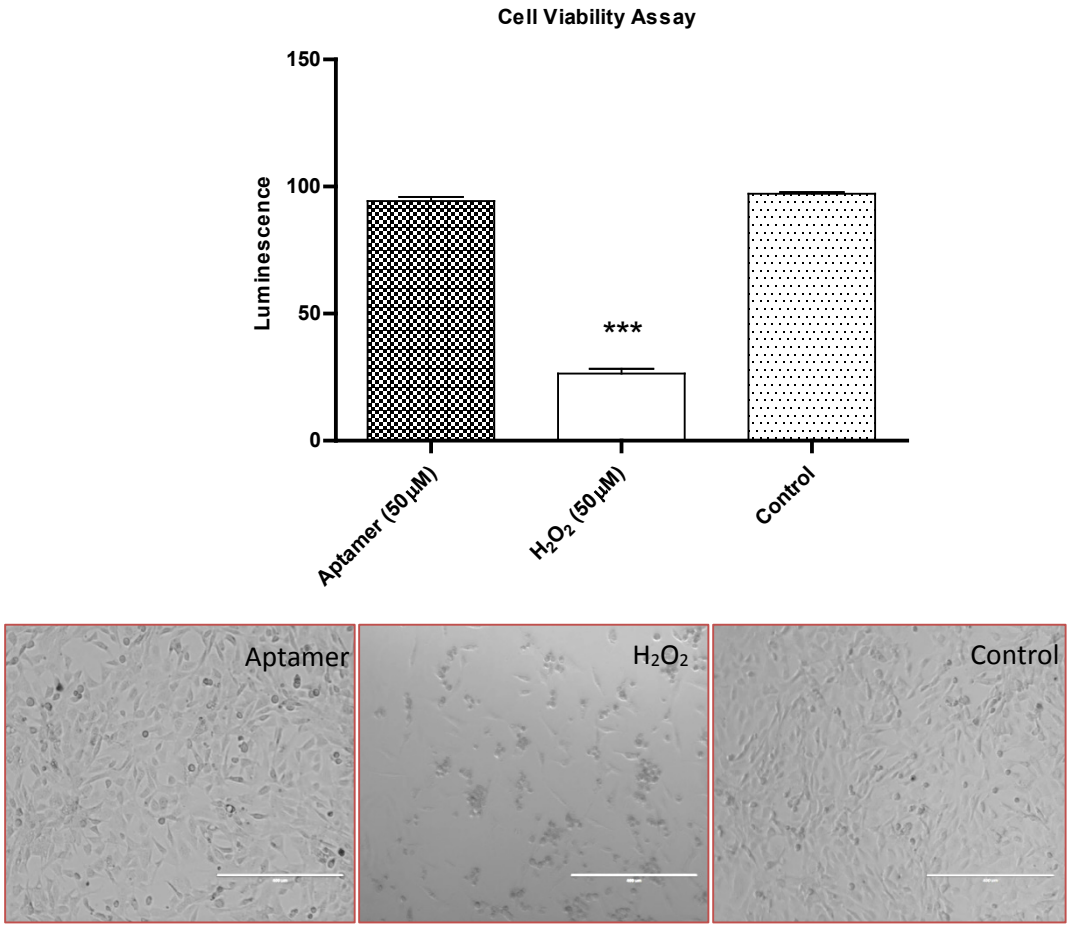

Figure 5.13: Aptamer toxicity: The graph shows the ATP derived luminescence after incubation for 24 hrs. Below are the light microscopy images of healthy and non-viable 3T3 cells (Panels represent mean values ± SEM for n = 3). (Magnification x40)

5.13. Study of aptamer as a therapeutic agent for bacterial infection

Aptamers can be used as a therapeutic agent if they bind to bacterial essential proteins leading to killing of bacteria. The protein PBP2A is an essential cell division protein in MRSA and it is a potential antibacterial drug target. Blocking its function will prevent bacterial cell division. Therefore assays have been conducted to study MRSA growth inhibition by PBP2A-aptamer probe and the MRSA-aptamer probe. The binding of MRSA-aptamer probe to MRSA essential proteins was evaluated by this assay since it has been developed against whole bacterial cells and there is a potential that it may block unknown essential protein's function in MRSA (Figure 5.14).

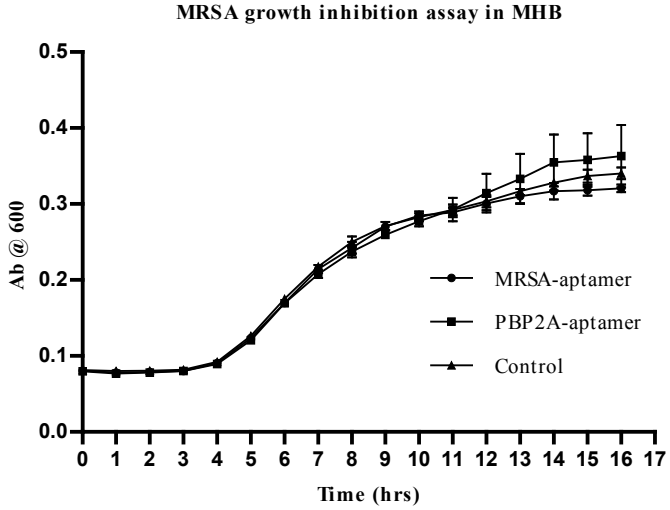

Figure 5.14: MRSA growth inhibition assay in MHB. 1 µM of aptamer has been used for this assay in MHB (100 µl) and 10^6 cfu/ ml bacterial. The growth of bacteria was assessed by measuring the absorbance at 600 nm for 16 hrs. The data shows that there is no effect on MRSA growth from aptamer probes.

5.14. Bio-distribution and bio-availability of aptamer in mouse model

Mice have been used to study the bio-distribution and bio-availability of the aptamers. Naïve aptamer library was amplified using Cy5.5 conjugated primers and aptamer were delivered into mice. Intratracheal (i.t.) delivery shows the aptamers are localised in the lung at 20 minutes. In contrast to i.t delivery, intravenous (i.v.) delivery shows the distribution of aptamer in the mouse body and higher concentrations are present in the kidneys, liver and bladder. This work revealed that the Cy5.5 conjugated aptamer can be used as an optical bio-imaging probe (Figure 5.15).

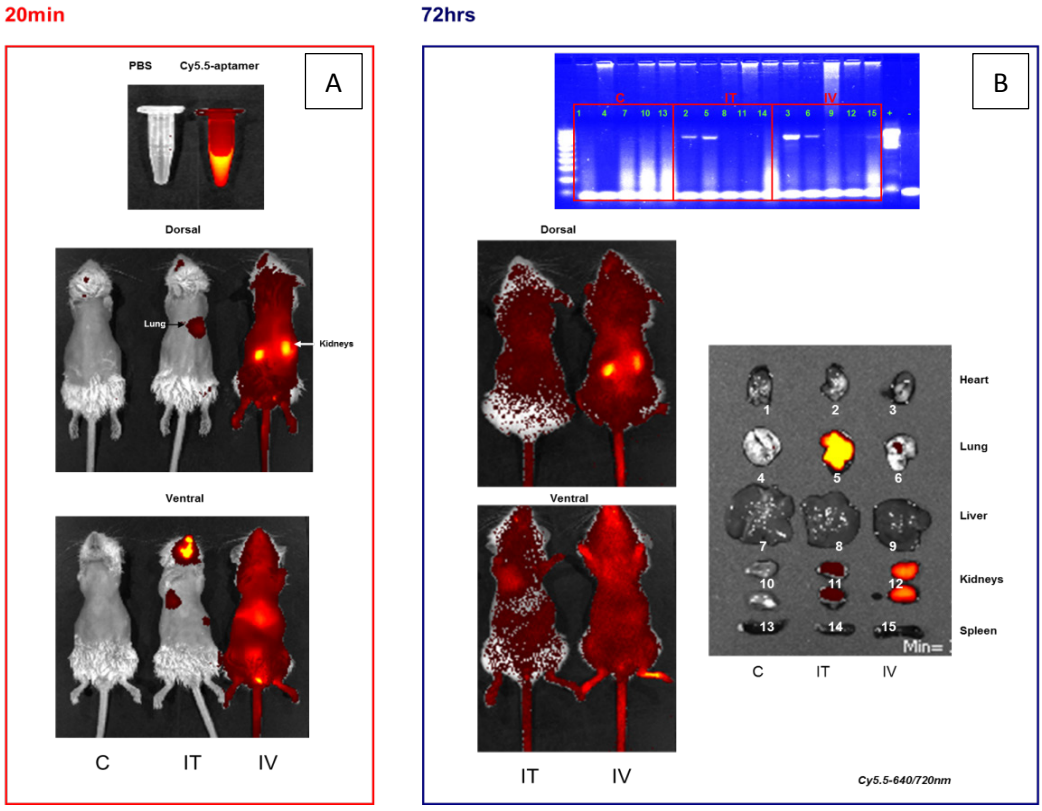

Figure 5.15: Optical images of mice injected with Cy5.5 conjugated aptamer library. 125µg/mice of Cy5.5 conjugated aptamer were injected. The images show the distribution of Cy5.5 conjugated aptamer *in-vivo* mouse model after 20 min (panel A) and 72 hours (panel B). Organs were removed and imaged and then digested and PCR amplification using aptamer specific primers to confirm aptamer distribution. Organs are numbered and numbers ascribed to gel lanes top panel of figure B.

5.15. Discussion

This chapter described efforts to develop two types of aptamer probes to detect MRSA; (1) whole MRSA cell SELEX aptamer probe, and (2) purified PBP2A protein specific aptamer probe. For the first approach five rounds of bacterial cell SELEX were carried out on different gram positive and negative bacteria separately using the aptamer library G. Then ion torrent sequencing was carried out separately and careful analysis of the sequenced results eliminated the common conserved sequences among bacterial species, hopefully predicting the MRSA specific aptamer sequences unique to the MRSA. For the PBP2A specific aptamer probe development, SELEX has been carried out 15 times on purified PBP2A protein (purified the PBP2A protein in the previous chapter) and the conserved sequences were elucidated from the sequenced data. The probes were analysed using *in-vitro* assays to evaluate the binding affinity towards the purified protein and MRSA.

Five prime (5') FITC labelled PBP2A and MRSA specific aptamer probes were evaluated using *in-vitro* assay, PBP2A coated Ni beads assay and bacterial binding assay. The results show that the two probes bound to PBP2A protein at a much higher rate than the FBS, BSA and trypsin. FITC labelled PBP2A aptamer probe binding to the purified PBP2A indicates that the aptamer probe shows higher specificity towards the PBP2A protein compared to the rest of the proteins tested. In a similar manner the MRSA specific probe also shows a trend for higher binding towards the PBP2A. Careful analysis of these probes sequences indicated that they are 50% similar to each other. Bacterial binding assays were performed to evaluate the binding efficacy of these probes towards MRSA (Figure 5.12). However, these probes demonstrated no specificity towards MRSA in bacterial binding assays carried out. This may be due to the non-specific binding of the probes towards the other elements on the rest of the bacteria tested. The *in-silico* counter selection has not been successful, likely due to the far fewer short reads at the ion torrent sequencing (see Table 5.2). Shorter sequences may have lost the important and key potential aptamer sequences to be determined. Likewise there are several factors that

may contribute to the unsuccessful SELEX and the development of aptamer probes (Lakhin *et al*., 2013).

There is another possibility that the PBP2A specific probe may not recognise MRSA due to the low level of PBP2A expression and not sufficient enough protein to bind the aptamer probe. This could be investigate in the future studies by culturing the MRSA at sub-inhibitory oxacillin concentrations to induced PBP2A expression in MRSA and run the binding assay (Rudkin *et al*., 2014). This may increase the higher binding ability to MRSA by the PBP2A specific probe.

Table 5.3 shows that the relative binding pattern of MRSA specific aptamer developed by Turek *et al*., (2013) using fixed bacterial cells. This table summarizes the results obtained with the binding assays on clinical strains of methicillin-resistant *Staphylococcus aureus* (MRSA), *S. aureus* and *E. faecalis* bacteria. Ten clinical strains were tested against the four aptamers developed by them (Table 5.3). DTMRSA1 and DTMRSA3 showed the best specificity and appeared to be the best candidates for MRSA treatment investigation, DTMRSA1 being the best one of the two, while DTMRSA2 and DTMRSA4 bound to all three types of clinical bacteria strains. Consequently, the binding ability of these four aptamers was compared in the context of different clinical MRSA strains, as well as *S. aureus* and *E. faecalis* (Table 5.3). They observed that the selected aptamers bound to all MRSA clinical strains tested except DTMRSA1 with strain MRSA 7. This also indicates that all MRSA clinical strains are not sharing the similar surface properties. MRSA, *S. aureus* and *Enterococcus* are all gram-positive bacteria. Based on their similarities, some common binding can be expected by the commonality of proteins among the strains, whereas others are more specific to each type of bacterium. DTMRSA1 and DTMRSA3 show the best specificity and therefore appear to be the best candidates for MRSA treatment investigation, DTMRSA1 being the best one of the two, while DTMRSA2 and DTMRSA4 bind to all three types of bacteria. But they have not tested with gram negative bacterial strains to study the efficacy of binding of these aptamers.

They also showed that the DTMRSA1-4 collectively represents a powerful tool by which to study the membrane structure of MRSA, as well as develop potential treatment modalities to combat this pathogen.

Table 5.3: Relative binding of the selected aptamers to various clinical cell lines (Turek *et al*., 2013)

Clinical strains	**DTMRSA1**	**DTMRSA2**	**DTMRSA3**	**DTMRSA4**
MRSA 2	+++	++++	+++	++++
MRSA 4	+++	+++	+++	++++
MRSA 6	++++	++++	+++	++++
MRSA 7	-	++++	+++	++++
S. aureus 164	-	++++	+	+++
S. aureus 165	-	++++	+	+++
S. aureus 166	-	++++	+	+++
E. faecalis 43	-	++++	+	+++
E. faecalis 44	-	++++	+	++
E. faecalis 45	-	++++	+	+++

(-) no binding; (+) 0%-25%; (++) 25-50%; (+++) 50%-75%; (++++) 75%-100%

When aptamer technology was first developed almost a quarter of a century ago, a suggestion was immediately put forward that it might be a revolutionary solution to solve many problems associated with diagnostics and the therapy of diseases. However, multiple attempts to use aptamers in practice, although sometimes successful, have been generally much less efficient than had been expected initially (Lakhin *et al*., 2013).

To carry out SELEX protocol in this study, two different libraries (G and M) have been used initially, with primer binding site variation. Library G was chosen for further studies as it demonstrated reduced non-specific amplification of DNA (Figure 5.3) with the buffer conditions. To increase the diversity of the aptamer libraries, different lengths of the variable region were incorporated (30 and 40 bp) (Table 5.1) as previous studies have used variable lengths and no fixed lengths have been recommended (Sefah *et al*., 2009; Shangguan *et al*., 2006). Some of the libraries also

possessed G-quadruplex (shown as -GGG-) regions to increase the stability of the aptamers and increase the diversity. A significant proportion of these oligonucleotides display G-quadruplex structures that enable molecular recognition of their ligands. G-quadruplex structures couple a common scaffold to varying loop motifs that act in target recognition (Tucker *et al*., 2012).

Different buffer conditions were evaluated with the two libraries to establish the optimum conditions for the SELEX protocol, minimising the non-specific binding and amplification of DNA. Modifying and optimising the selection buffer conditions may counter-act or otherwise stabilise the interactions between the target and the unselected aptamer pool. With a negatively charged target, decreasing the pH below a target's isoelectric point (pI) will neutralise the negative charge and encourage the binding of the negatively charged pool (Stovall *et al*., 2004).

The SELEX buffer conditions may also vary with monovalent salt(s) identity; monovalent salt(s) concentration, and divalent salt identity, divalent salt concentration, buffer identity, buffer concentration, and pH. The optimised buffer conditions likely increase the probability of a successful selection and therefore promote higher ratios of successful aptamer selections against a variety of targets. Therefore different buffer conditions were selected and tested on two different aptamer libraries with and without bacteria. The best buffer condition was selected as PBS (Park *et al*., 2012; Sosic *et al*., 2011) with Ca^{+2} and Mg^{+2} to eliminate the non-specific binding and PCR amplification. Throughout the experimental protocol, I used DNA low binding eppendorf tubes to eliminate non-specific binding of DNA onto the wall of tubes. The BSA concentration in the selection buffer (PBS with Ca^{+2} and Mg^{+2}) was increased to 1% to minimise the non-specific binding and increase the stringency of the selection.

The number of PCR cycles were adjusted to 10 to get optimum PCR products but with low non-specific PCR amplification (Sefah *et al*., 2010). PCR amplification was carried out by using biotinylated primers and the PCR products were incubated with streptavidin sepharose beads suspension allowing dsDNA bind to sepharose beads

forming interaction between streptavidin and biotin. The increased pH (200 mM NaOH) allows the separation of the two strands leaving the biotin labelled ssDNA strand behind. The supernatant of the non-biotin labelled (forward primer amplified strands) ssDNA have been collected by centrifugation and diluted into 1 ml of PBS-T, containing 10 µl of 200 mM monobasic phosphate buffer to adjust the pH to 7.5. Finally, the material was heated to 95°C for 10 minutes then immediately placed at 4°C until the next round of SELEX (Murphy *et al*., 2003). This allows the generation ssDNA after PCR amplification and materials for the following SELEX round.

Previous *in-vitro* assays showed that the two probes were binding to the PBP2A protein in a similar manner despite showing non-specific binding to other bacteria in bacterial binding assays. However binding of aptamer probes can block the function of a protein, e.g. pegaptanib sodium (Macugen) an RNA aptamer directed against vascular endothelial growth factor (VEGF)-165, inhibits VEGF-mediated cellular responses (Jellinek *et al*., 1994; Ng *et al*., 2006). Therefore a growth inhibition assay evaluated the effect of the aptamer probe on MRSA killing or the growth inhibition. The results indicated that the binding of low concentrations of aptamer to MRSA showed no bactericidal or bacteriostatic effect.

Laboratory mice have been used to study the bio-distribution and bio-availability of Cy5.5 conjugated aptamer library. The results indicate that the aptamer labelled with Cy5.5 is a very good optical molecular probe use in the mouse model since the distribution of the aptamer can be detected in *in-vivo* mouse model.

In conclusion, the PBP2A specific aptamer molecular probe was able to show high specificity in *in-vitro* Ni-NTA beads assay. However, both PBP2A and MRSA aptamer probes generated were not specific or efficient enough to detect MRSA over other bacteria in bacterial binding assay. This may be due to the several factors described above.

Chapter 6:
Peptide molecular probes development

Chapter 6: Peptide molecular probes development

6.1. Abstract

The phage display technique has been used to develop peptide probes to detect MRSA using peptide library (Ph.D. 12) from New England Biolabs (NEB). This library consists of 10^9 different peptide clones expressed on its phage virus particles. Whole bacterial cells of MRSA and PBP2A protein coated Ni beads were incubated separately with the pool of the phage display library to facilitate binding. The unbound phage was washed followed by elution of specifically bound phage by disrupting the binding interactions between the phage and the target. The eluted phage pools were then amplified *in-vitro* and the process repeated, resulting in stepwise enrichment of the phage pool in favour of the tightest binding sequences towards whole bacterial MRSA and PBP2A purified protein. After 3 rounds of bio-panning and amplification, 120 clones were characterized by DNA sequencing. The resulting DNA sequences were translated into an amino acid sequences using FinchTV software tool and the corresponding 12-mer peptide sequences were analysed using ClustalW online tool. Two different peptide sequences were identified as PBP2A specific peptide GLHTSATNLYLH and MRSA bacterial specific peptide GWTSVSVHIRGG. For further analysis FAM was conjugated to these peptide sequences and binding affinities were evaluated *in-vitro* using bacterial binding selectivity assays. Flow cytometry and confocal microscopy were used to evaluate the peptide binding efficacy to bacteria. Antibacterial activity of these peptides was also studied on MRSA and MSSA. The developed peptides do not show any specificity binding towards the MRSA and show no antibacterial activity.

6.2. Introduction

The microbial cell surfaces consist of unique molecular compositions made of lipids, carbohydrates and proteins. These molecules may alter the mechanism by which peptide molecules might interact with an epitope or receptor, thereby providing unique binding sites for peptide interaction (Yarbrough *et al*., 2011). Phage-displayed peptides have been successfully used to identify *Salmonella typhimurium* (Goldman *et al*., 2006; Olsen *et al*., 2006; Sorokulova *et al*., 2005), *Escherichia coli* using streptavidin conjugated quantum-dots (Edgar *et al*., 2006), use of lytic phage for specific capture and detection of *S. aureus* (Balasubramanian *et al*., 2007) and *Bacillus anthracis* (Sainath Rao *et al*., 2010).

Phage display has been shown to be a powerful tool to study protein-protein or protein ligand interactions (Derda *et al*., 2011). In this study a commercially available random phage-display library was screened against MRSA cells and purified PBP2A protein to identify peptides binding to the bacteria. Elucidating specific peptides that bind to MRSA can be used as molecular probes to detect bacteria and study the antibacterial activity. This study used a 12-mer peptide library against MRSA since most of the previous studies used 12-mer library from New England Biolabs (NEB). Bio-panning experiments have been carried out as described in the material and method section according to the commercial supplier (NEB). The counter selections on MSSA and PAO1 were carried out before bio-panning with PBP2A coated Ni beads and MRSA whole bacterial cells. The counter selection removed any peptides binding to MSSA and PAO1 bacterial strains (Figure 6.1). Then the supernatant contains unbound phage used for the bio-panning experiments on PBP2A and MRSA.

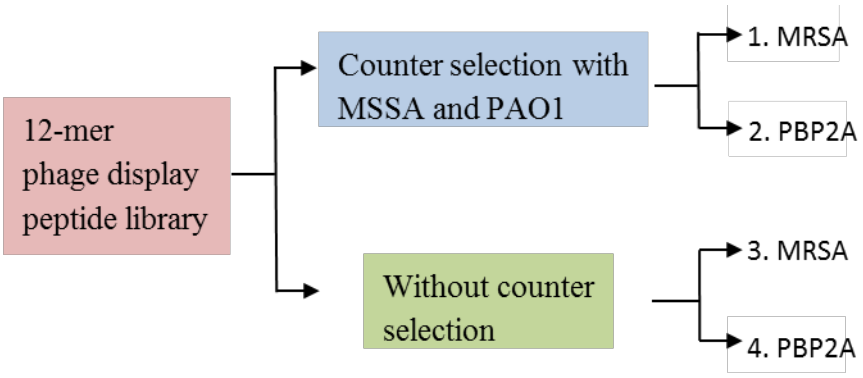

Figure 6.1: This diagram shows the experimental design; four different sets of bio-panning were carried out separately using 12-mer peptide library.

The 12-mer phage-displayed peptide library from NEB was used for bio-panning against MRSA and PBP2A. In this library, five copies of peptides with 12 amino acids were displayed by the phages. The peptides were encoded by random foreign DNA insertion in the phage genome. They were linked with phage coat protein pIII via a short linker sequence, which was Gly-Gly-Gly-Ser. The library contained 1 x 10^{13} plaque forming units per millilitre (PFU/ml) with 1.28 x 10^{9} complexes. The library was stored at -20ºC and thawed on ice before being used to avoid heat shock reactions.

6.3. Selection of Phage-Displayed Peptides Binding to MRSA and PBP2A

In biopanning, phage titer was determined by counting the number of blue plaques formed by individual phage on LB/IPTG/Xgal plate (Figure 6.2). The blue plaque forming units indicate that the affinity-selected phages from the bio-panning were derived from the library with special lac Z gene insertion. At the same time, the titer plate suggested that the phage eluated had no contaminant as no colourless plaques were seen.

After three rounds of bio-panning against MRSA and PBP2A protein, 120 phage infected bacterial clones were randomly selected for sequencing from each group (Figure 6.2). Blue colonies were selected ‘randomly’ but only well isolated and blue

colonies were selected to achieve zero contamination for sequencing. Single stranded phage DNA was prepared for sequencing and a DNA gel was run to confirm the correct size of the plasmid and to determine the purity of the colonies selected (Figure 6.3).

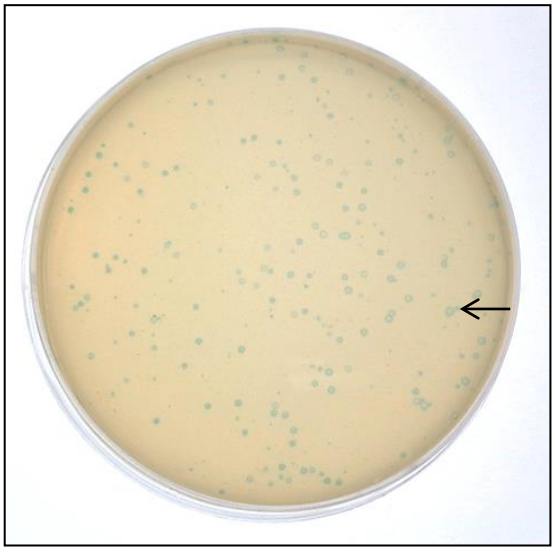

Figure 6.2: Phage titer of eluted phage on IPTG/Xgal Agar plate. The blue colour indicated phage infected bacteria (black arrow). These colonies were selected for sequencing after three rounds of bio-panning against PBP2A and MRSA.

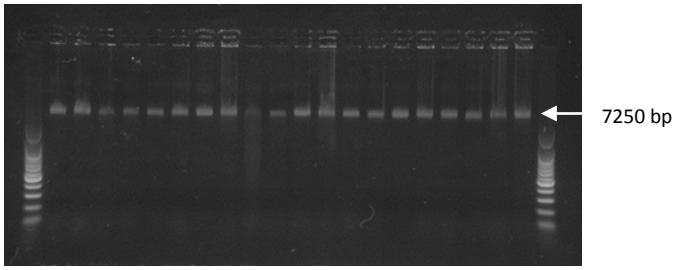

Figure 6.3: Agarose (1% TBE) gel electrophoresis image showing the phage DNA before sending for Sanger sequencing. The size of the viral DNA was correct size. Control DNA, purified single-stranded M13mp18 DNA was run parallel to the purified phage DNA.

According to Table 6.1, the output titer, which was also the phage eluate titer, was ranged in between 10^5-10^7 PFU/ ml over the three rounds of biopanning in both probe screening. The eluted phage from the first round of biopanning had the lowest output titer with 1.3 x 10^5 PFU/ ml while the eluted phage from the third round of biopanning had the highest output titer which is 1.6 x 10^6 PFU/ ml in MRSA probe development. This indicated that the output titer increased from the first round to the third round of biopanning. The similar results were observed in PBP2A probe development where the output titer increased from $3.0x10^{-4}$ PFU/ ml to $1.8x10^{-3}$ PFU/ ml from first round to third round of biopanning.

The yield of selection (Table 6.1) of phages for each round of biopanning was calculated as the percentage of the output titer divided by the input titer. It was maintained in between the percentage of $10^{-3}$and 10^{-5}. This indicated that only certain numbers of the input phage was being selected in the biopanning. The yield of selection was increased from the first round ($1.3x10^{-5}$%) to the third round ($1.6x10^{-4}$ %) of biopanning in MRSA probe development. The yield of selection in PBP2A probe development also increased from the first round ($3.0x10^{-4}$%) to the third round ($1.8x10^{-3}$%) indicating that there was an enrichment of peptide sequences during the screening. In short, the highest yield of selection was observed at the third round of biopanning. A total of hundred and twenty individual phage clones were randomly selected for sequencing.

Table 6.1: Yield of selection for three rounds of biopanning.

Rounds of biopanning	MRSA probe			PBP2A probe		
	Input titer (PFU/ml)	Output titer (PFU/ml)	Yield of Selection (%)	Input titer (PFU/ml)	Output titer (PFU/ml)	Yield of Selection (%)
1	$1x10^{12}$	$1.3x10^5$	$1.3x10^{-5}$	$1x10^{12}$	$3x10^6$	$3.0x10^{-4}$
2	$5x10^{11}$	$4.8x10^5$	$9.6x10^{-5}$	$1.8x10^{12}$	$4x10^6$	$2.2x10^{-4}$
3	$1x10^{12}$	$1.6x10^6$	$1.6x10^{-4}$	$1x10^{12}$	$1.8x10^7$	$1.8x10^{-3}$

6.4. Sequencing results and data analysis after three rounds of enrichment

The Sanger sequencing generated 40 individual results for each four groups of bio-panning (Figure 6.1). The resulting DNA sequences were translated into an amino acid sequences using FinchTV software tool (the DNA sequences are not listed) and the corresponding 12-mer peptide sequences were analysed by ClustalW online tool. The analysis data are shown below in four groups (Figure 6.4, 6.5, 6.6, 6.7. and Table 6.2 and 6.3).

```
CLUSTAL 2.1 multiple sequence alignment


58>             --GWTSVSVHIRGG 12
59>             --GWTSVSVHIRGG 12
57>             --GWTSVSVHIRGG 12
54>             --GWTSVSVHIRGG 12
52>             --GWTSVSVHIRGG 12
50>             --GWTSVSVHIRGG 12
49>             --GWTSVSVHIRGG 12
48>             --GWTSVSVHIRGG 12
46>             --GWTSVSVHIRGG 12
44>             --GWTSVSVHIRGG 12
43>             --GWTSVSVHIRGG 12
47>             --GWTSNSPHLRNN 12
51>             --GWTSNSPHLRNN 12
42>             --GYTSSSWNWPFN 12
60>             --GYTSSSWNWPFN 12
53>             TMNYTSSSQNLS-- 12
56>             TMNYTSSSQNLS-- 12
41>             --SEDTANYFLLAR 12
45>             --SEDTANYFLLAR 12
55>             --SEDTANYFLLAR 12
```

GWTSVSVHIRGG

Figure 6.4: ClustalW analysed data; 1. Clones from 41 to 60; MRSA with counter selection. The highest frequency was observed in the sequence of GWTSVSVHIRGG.

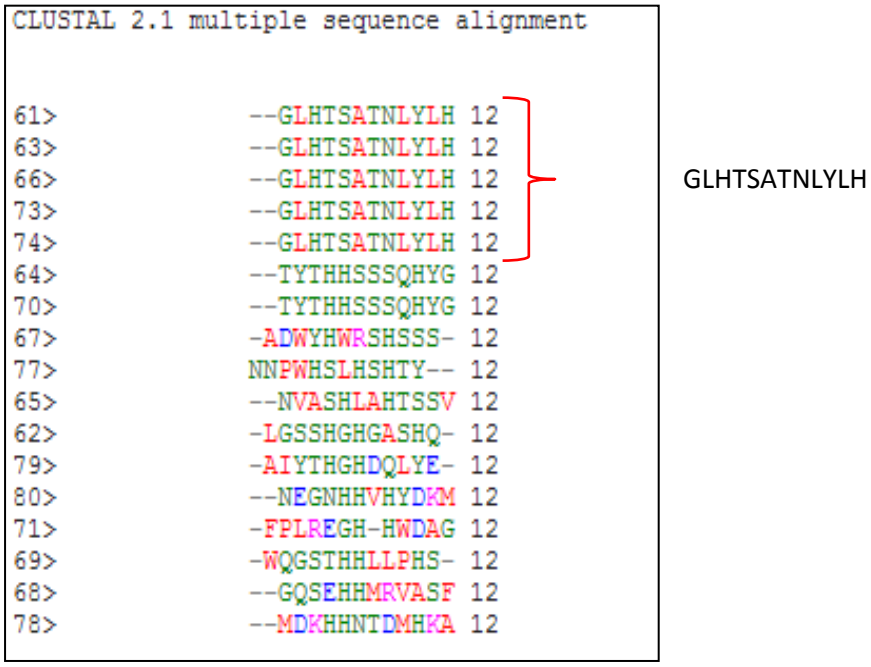

Figure 6.5: ClustalW analysed data; 2. Clones from 61 to 80; PBP2A with counter selection. The highest frequency was observed in the sequence of <u>GLHTSATNLYLH.</u>

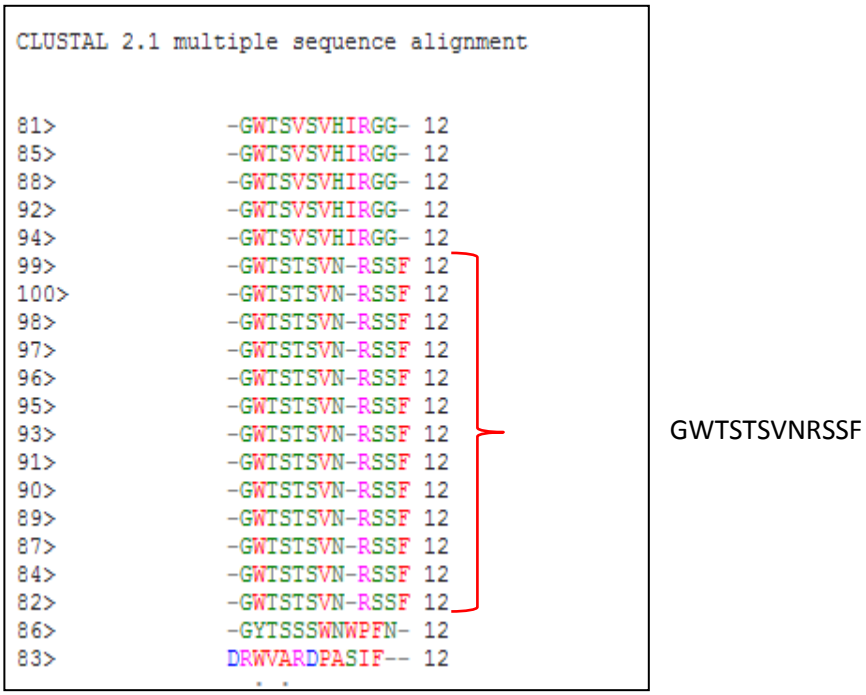

Figure 6.6: ClustalW analysed data; 3. Clones from 81 to 100; MRSA no counter selection. The highest frequency was observed in the sequence of <u>GWTSTSVNRSSF.</u>

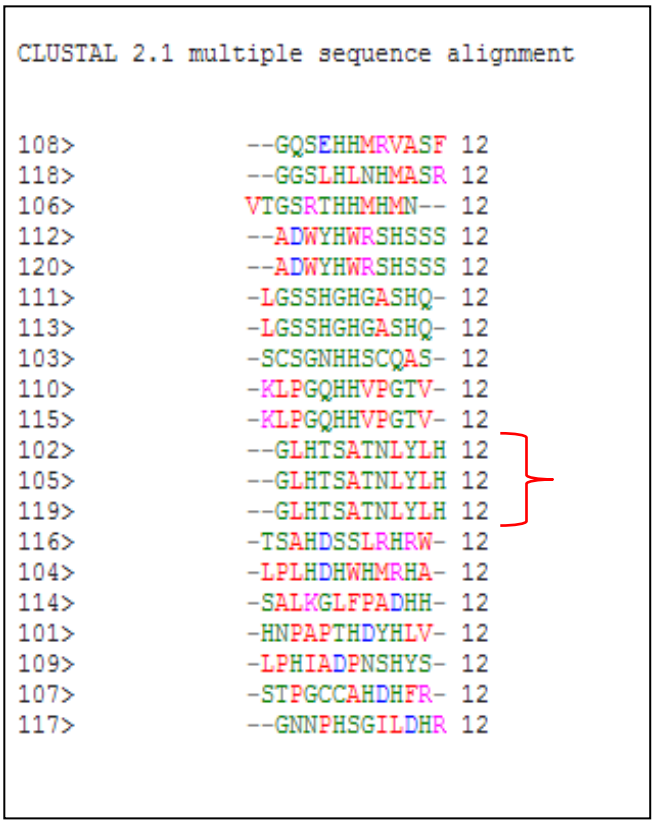

Figure 6.7: ClustalW analysed data; 4. Clones from 101to 120; PBP2A no counter selection. The highest frequency was observed in the sequence of <u>GLHTSATNLYLH.</u>

Table 6.2: The table shows the peptide sequences of four different bio-panning procedures. The high to low frequency peptides have been identified using the ClustalW analysis from the 40 different colonies.

Sequencing sets	Peptide sequences	Frequency
41-60 (MRSA with counter selection)	**GWTSVSVHIRGG**	11/20
	SEDTANYFLLAR	3/20
	GYTSSSWNWPFN	2/20
	TMNYTSSSQNLS	2/20
	GWTSNSPHLRNN	2/20
61-80 (PBP2A with counter selection)	**GLHTSATNLYLH**	5/17
	TYTHHSSSQHYG	2/17
81-100 (MRSA NO counter selection)	GWTSTSVNRSSF	13/20
	GWTSVSVHIRGG	5/20
101-120 (PBP2A NO counter selection)	**GLHTSATNLYLH**	3/20
	LGSSHGHGASHQ	2/20
	KLPGQHHVPGTV	2/20
	ADWYHWRSHSSS	2/20

Table 6.3: The summary table shows the final peptide sequences for MRSA and PBP2A bio-panning experiments with and without counter selection generated similar peptide sequences.

Targets	Peptide sequences	Frequency (%)
PBP2A	**GLHTSATNLYLH**	34-AM1
	GQSEHHMRVASF	6
	TYTHHSSSQHYG	4
	LGSSHGHGASHQ	4
	KLPGQHHVPGTV	4
	ADWYHWRSHSSS	4-AM2
MRSA	**GWTSVSVHIRGG**	38-AM3
	GWTSTSVNRSSF	32
	SEDTANYFLLAR	7
	GYTSSSWNWPFN	5
	TMNYTSSSQNLS	5
	GWTSNSPHLRNN	5-AM4

6.5. Bacterial biding assay

In-vitro bacterial binding assays were carried out to investigate the peptide probe binding efficacy. MRSA and PBP2A probes were derivatived to detect MRSA over other gram positive and negative bacteria. All peptides were FAM labelled. Peptide probes were dissolved in DMSO (1 mM) and the working concentration was 10 µM in PBS. After incubation with the peptide probes, bacterial cells were washed with PBS and binding assessed using flow cytometry and confocal microscopy (Figure 6.8, 6.9, 6.10 and 6.11).

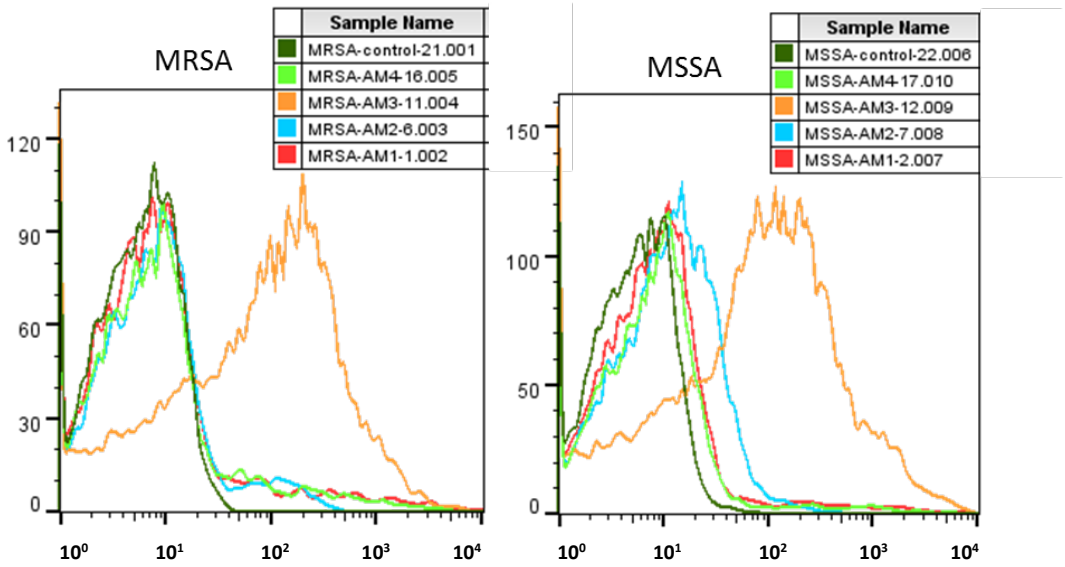

Figure 6.8: Flow cytometry data showing the FAM-AM3 peptide binding to gram positive bacteria. 10 µl of peptides were incubated with 10^8 cfu/ml bacteria at 37ºC for 30 minutes in PBS with 10% FBS. Washed bacteria were analysed using flow cytometry.

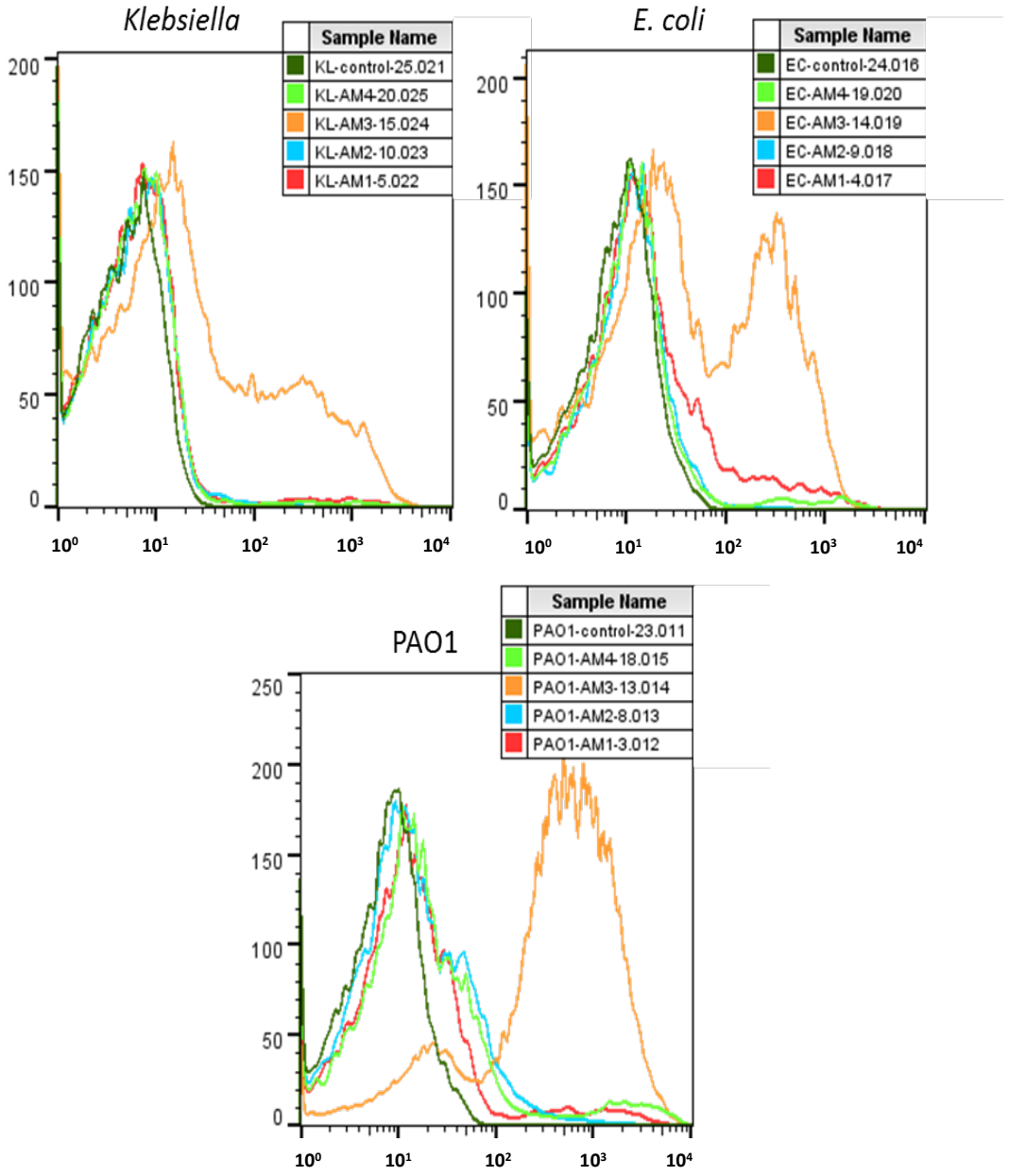

Figure 6.9: Flow cytometry data showing the AM3 peptide binding to gram negative bacteria. 10 µl of peptides were incubated with 10^8 cfu/ ml bacteria at 37ºC for 30 minutes in PBS with 10% FBS. Washed bacteria were analysed using flow cytometry.

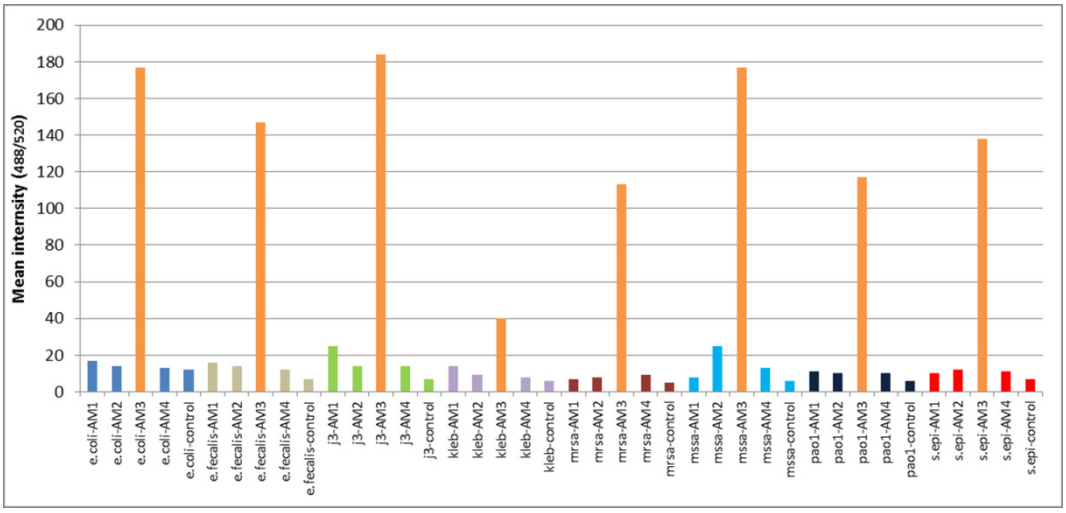

Figure 6.10: The mean fluorescent intensity of the flow cytometry data. AM3 peptide shows high mean fluorescent intensity with all bacteria while the rest of the probes show low intensity.

Live confocal microscopic image analysis was carried out to investigate the binding of AM3 peptide to MRSA (Figure 6.11). The results indicate that the high signal coming from the AM3 peptide was due to the precipitation effect rather binding to the MRSA bacteria.

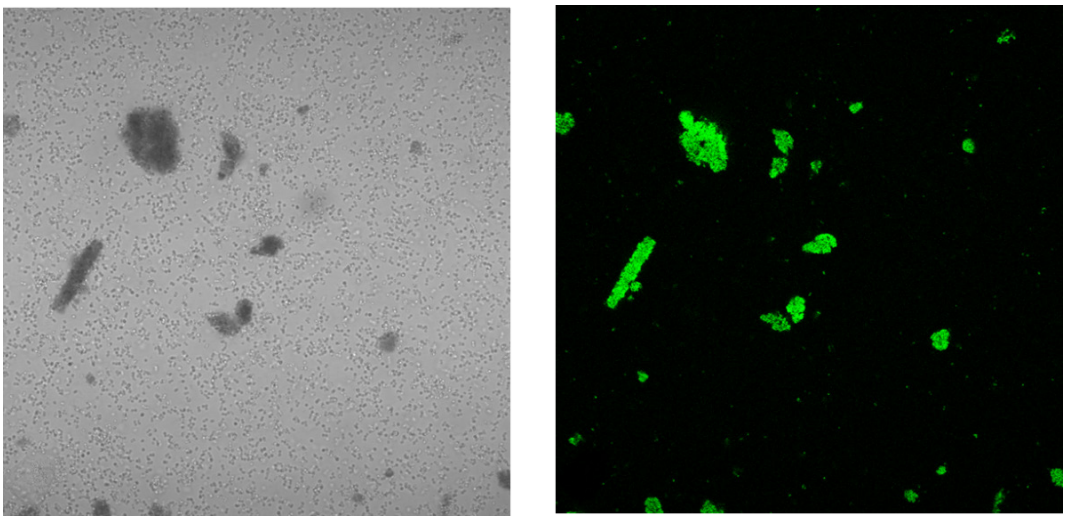

Figure 6.11: Live confocal microscopic images showing the precipitation of the peptide probe AM3 in PBS incubated with MRSA. The precipitation of the probe is the result of false positive signalling given with the flow cytometry analysis. However other AM probes (AM1, AM2 and AM4) do not precipitate in PBS at 10 µM concentrations.

6.6. Discussion

Phage display is a powerful tool for discovering ligands for various targets and the technology has been described since 1985. The technique has been used widely in basic and applied biosciences to study molecular biology mechanisms involving protein-protein (Sidhu *et al*., 2003) or protein to non-protein interactions (Yu *et al*., 2009). A phage display library is a complex mixture of phage clones displaying random foreign peptides or protein domains displayed on the phage surface (Smith and Petrenko, 1997). Filamentous phages with displayed peptides fused to the N-terminus of capsid proteins are typically used; however, several alternative phage display formats aiming to avoid the limitations of the conventional display system are also available. Commercially available phage display libraries based on filamentous phage M13 (Ph.D.^{TM}-7, Ph.D.^{TM}-12, Ph.D.^{TM}C7C; New England Biolabs) or spherical T7 phage (T7Select$^{®}$, Merck) are most commonly used (Bratkovič, 2010). Large phage populations are screened against target molecules or cells called biopanning to yield ligands that exhibit the desired target binding. Phage clones from the library are incubated with the immobilized target molecule or in solution. Nonbinding virions are removed by multiple washing steps and phage bound to the target are recovered by different elution strategies. A typical screening procedure involves several rounds of biopanning, until the phage pool is enriched in specific binding phage (Smith and Petrenko, 1997).

In this study the Ph.D.TM-12 from New England Biolabs was used to derive MRSA and PBP2A specific peptides. A biopanning procedure was carried out in solutions for MRSA and PBP2A coated Ni-beads. Two sets of biopanning experiments were carried out and one set of biopanning was subjected to counter selection against MSSA and *Pseudomonas* (PAO1) to reduce the non-specific binding and the other one carried out without counter selection. Therefore four sets of enriched phage populations were generated for sequencing; 1) MRSA-without counter selection 2) MRSA-with counter selection 3) PBP2A-without counter selection 4) PBP2A-with counter selection. After three rounds of biopanning the enriched phages were amplified and sequenced after DNA isolation. Sanger sequencing has been carried

out at the University of Edinburgh, at the Gene Pool facility. The analysis of data was able to generate two different peptide sequences identifiable to biopanning for MRSA (GWTSVSVHIRGG) and PBP2A (GLHTSATNLYLH). These peptides were synthesised with a FAM conjugate including two control peptides, using solid phase synthesis at the Chemistry department, University of Edinburgh to assess the bacterial binding. The bacterial binding assay data showed that the peptides showed no binding to MRSA at 10 μM concentration.

Binding success during the screening and the enrichment (first and second rounds of screening) was observed by calculating the yield of selections (Table 6.1) and it showed the enrichment of phage clones during the screening. A decrease in titer from the input phages to the output phages indicates the selection of phages. The weak and non-specific binding phages which contribute mostly to the portion of input phages were being washed away during the biopanning. As shown in Figure 6.1, a decrease in selection from the first to the second round of biopanning could be explained by the high portion of non-specific binding phages which were being washed away using the washing buffer with higher concentration of Tween-20 in the second round of biopanning. Upon each round of selection, the eluted phages were amplified prior to the subsequent round of biopanning, and this could increase the titer of specific binding phages that was used in later round of biopanning. The yield of selection that was increased from the second to the third round of biopanning indicates more phages were bound to the target bacteria in the later round of biopanning. Thus, it is assumed that the specific binding phage clones were enriched. As a result, the clones of phage-displayed peptides that were isolated from the third round of biopanning probably had the highest binding affinity and specificity towards the target MRSA and PBP2A. After the third round 120 randomly collected clones were sequenced to determine the peptide sequences. These were well isolated blue colonies to minimise the cross contamination with environmental M13-like phage during panning and amplification.

All peptide probes were N-terminus FAM conjugated probes where C-terminus was free. Since the synthetic peptide did not bind to the target, it is possible that the selected sequence requires additional elements from the adjacent spacer sequence for binding. During biopanning, the N-terminus of the selected peptide sequence was free; the C-terminus was fused to the phage. Furthermore, the C-terminal residue of the selected sequence did not have a free negatively charged carboxylate during panning. Therefore a simple synthetic peptide with a free carboxy terminus will introduce a negatively charged group at a position occupied by a neutral peptide bond during panning, which may completely abolish binding. When designing synthetic peptides corresponding to selected sequences, it is recommended to add the spacer sequence Gly-Gly-Gly-Ser to the C-terminus and aminating the C- terminal carboxylate to block the negative charge (Wu *et al*., 2010). During the chemical conjugation of the peptide to FAM, the C-terminal serine can be replaced with cysteine (if there are no other cysteines present in the sequence). As these recommendations are available in the NEB, the possible sequences can be resynthesized and reassessment of bacterial binding performed.

Chapter 7:
Concluding remarks and future studies

Chapter 7: Concluding remarks, limitations and future studies

The increasing drug resistance among gram-positive bacteria is a significant problem because they are responsible for one third of nosocomial infections. Drug resistance in gram-positive organisms (i.e. *staphylococci*, *pneumococci*, vancomycin resistance in *enterococci*, and *mycobacteria*) has increased in the last 15 years (Johannsson *et al*., 2012; Robert *et al*., 2005). MRSA is one of the most frequently reported nosocomial pathogens in developed countries. MRSA infections are responsible for more deaths (20,000 deaths per year) in the U.S. each year than AIDS (Klein *et al*., 2007). Therefore developing new antibacterial agents to interfere with unexploited bacterial molecular target(s) are important.

Over the last decade there have been few novel antimicrobials reaching the marketplace. Linezolid was the first oxazolidinone antibacterial agent for treatment of gram-positive bacterial infections in 2000 (Manfredi, 2006). Linezolid was approved for the treatment of vancomycin resistant *Enterococcus faecium* infections, and *S. aureus* (Gales *et al*., 2006). Daptomycin is a cyclic lipopeptide antibiotic used in the treatment of certain CA-MRSA and HA-MRSA infections. It is worth noting that daptomycin can not be used for community associated pneumonia as it is inactivated by pulmonary surfactant (Anthony *et al*., 2008). Vancomycin remains the choice for the treatment of systemic infection caused by MRSA because it shows relatively safe profile and secondly it limited anti-MRSA regimens are available (the lack of other approved alternatives). However, the oral absorption of vancomycin is very low, and thus, vancomycin must be administered intravenously to control systemic infections (Scott, 2007). Thus, treatment of MRSA infection with vancomycin can often be complicated, due to its inconvenient route of administration. Several newly discovered strains of MRSA show antibiotic resistance even to vancomycin and teicoplanin (a glycopeptide antibiotic). These new evolutions of the MRSA bacterium have been called vancomycin intermediate-resistant *Staphylococcus aureus* (VISA). For the moment, there are limited and rather expensive therapeutic options for the infections by *S. aureus* in the critically ill (e.g. chemotherapy with linezolid) (Rayner and Munckhof, 2005).

Ceftobiprole (a fifthgeneration cephalosporin) has been approved for use in limited countries. Ceftobiprole shows activity against systemic MRSA infections when given intravenously (Jacqueline *et al*., 2005) for community-associated bacterial pneumonia and acute bacterial skin and skin structure infections including MRSA. The high affinity of ceftaroline for penicillin-binding proteins is responsible for the potent activity observed against clinically relevant pathogens (Biek *et al*., 2010).

Therefore the continuing development of currently available antibiotic arsenals to be effective against drug resistant bacteria should remain important. This also suggests redefining infectious disease therapy, shortening length of therapy, reducing side effects profile, and reducing drug resistance profiles of currently available antibacterial products. However, the ultimate goal of drug development for MRSA infections is to discover novel antibacterial agents which interfere with unexploited bacterial molecular target(s).

Therefore my PhD studies were focused on antibacterial drug development coupled with attempts to develop molecular diagnostics for bacterial infections. During the first part of my work in chapter 3, I investigated the antibacterial properties of peptoid molecules for therapeutic purposes against gram positive and gram negative bacteria. The latter part of my research, in chapters 4, 5 and 6 investigated the development of MRSA specific diagnostic optical molecular probes using aptamer and peptide combinatorial libraries.

(a) Study and characterisation of peptoids as novel antimicrobial agents.

The first hypothesis of my study was to investigate the antimicrobial properties of lysine monomeric peptoids as a novel class of antibiotics. A library of peptoids were synthesised and antibacterial properties were studied on clinically relevant bacterial species. TOP demonstrated significant broad-spectrum bactericidal activity out of 13 different peptoids tested. Therefore further studies were carried out on TOP investigating the mammalian cell toxicity and immunomodulatory properties on TOP in chapter 3.

Therapeutic options for antibiotic-resistant bacterial pathogens remain inadequate and new approaches are urgently required. With the introduction of antibiotics in 1940s and 1950s patients with bacterial infections were handed a 'golden bullet'. But with the over usage of antibiotics throughout the last century and this century, most bacteria have become resistant to antibacterial drugs. No new classes of antibiotics have been produced in the last 37 years (Bax *et al*., 1998). Therefore discovery of new therapeutic approaches are urgently required.

Cationic antimicrobial peptides (CAMPs) are important components of the innate immune systems in all living organisms including bacteria, fungi, plants and animals. These peptides are active against bacteria, fungi, viruses, and pests such as insects. Peptoids have been generated to mimic the biological functions of naturally occurring cationic host defense peptides (Steiner *et al*., 1981). However peptoids have not been used as antibacterials in the clinic. Compared to peptides, peptoids have higher stability under *in-vivo* conditions and have great potential as new classes of antimicrobials. Therefore developing peptoids antimicrobials were focused in the chapter 3 aiming to discover new therapeutics for multidrug resistant bacteria.

Chapter 3 discussed 9-mer lysine-like peptoid library development and their antibacterial properties followed by investigations of mammalian cell toxicity and immunomodulatory properties. A library of 9-mer lysine-like peptoid was made to determine the structure-activity relationship of these peptoids and peptoid derivatives. These peptoids were screened against clinically important gram positive and negative bacterial species to determine the antibacterial properties. The 9-mer lysine-like peptoid library was made based on the well-known cell penetrating HIV Tat protein and the lysine-like cell-penetrating peptoids (Unciti-Broceta *et al*., 2009, Dhaliwal *et al*., 2012). To determine the structure-activity relationship of these peptoids, peptoid derivatives were made by; (i) changing the length of the carbon side chain (Figure 1.14); and (ii) N-terminus modifications (Figure 1.15). The three different side chain lengths were introduced to a 9-mer which consisted of butyl (four-carbon), hexyl (six-carbon) and octyl (eight-carbon) monomers. Further structural changes were made to the N-terminus end of the polymer encompassing

different chemical groups conjugated to the N-terminus end such as H-non modified, BnCO-Phenyl acetamide, Tosyl-Toluene sulfonamide, Suc-Succinic amide, Ac-Acetamide and Fmoc-9-Fluorenemethanol (Figure 1.15 and Table 1.3). A number of different bioassays were developed and carried out to study the structure-activity relationship on these peptoids on bacterial killing and potential mechanisms.

In chapter 3, it was concluded that out of 13 different peptoids derivatives, only one peptoid called Tosyl-octyl-peptoid (TOP) demonstrated significant broad-spectrum bactericidal activity. TOP kills bacteria under non-dividing and dividing conditions. The MIC values of TOP for *S. epidermidis*, *E. coli* and *Klebsiella* were 20 μM, whereas Methicillin-resistant *Staphylococcus aureus* (MRSA) and Methicillin-sensitive *Staphylococcus aureus* (MSSA) were 40 μM. The highest MIC values were observed for *Pseudomonas aeruginosa* (PAO1) at 80 μM. The selectivity ratio (SR) or Therapeutic index (TI) was calculated, by dividing the 10% haemolysis activity (5 mM) by the median of the MIC (50 μM) yielding a TI for TOP as 100. This TI is well above previously reported peptidomimetics TI of around 20. TOP demonstrates selective bacterial killing in co-culture systems and intracellular bacterial killing activity. TOP demonstrates killing of bacteria in the intracellular and extracellular compartments suggesting it could be valuable in both prophylaxis and therapy.

Peptoids have been generated to mimic the biological functions of naturally occurring cationic host defense peptides that confer antimicrobial activity including cationicity and amphipathic secondary structure where residues are segregated into cationic and hydrophobic regions (Chongsiriwatana *et al*., 2008). The biophysical characteristics of cationic host defence peptides have been used to design non-natural peptoids with similar properties, termed ‘ampetoids’ (Chongsiriwatana *et al*., 2008). Recent structure/function investigations of these ampetoids suggested a requirement for net cationic charge and moderate hydrophobicity for effective antimicrobial activity, with high hydrophobicity and strongly amphipathic structures causing hemolytic effects (Chongsiriwatana *et al*., 2008). Balancing high antimicrobial activity with low toxicity to the host is fundamental for clinical application, and may

be quantified using a selectivity ratio (Chongsiriwatana *et al*., 2008). Since TOP yields a TI of 100, TOP displays favourable characteristics.

TOP has two major components; (i) lysine-like (octyl) 9-mer unit and (ii) N-substitute-Tosyl (sulphonamide) group. Previous studies have identified that several lysine-peptide hybrids have broad-spectrum activity against clinically important bacteria and fungi (Ryge *et al*., 2008). Recent studies on the lysine-peptoid hybrid LP5 revealed that it traverses the cytoplasmic membrane of *S. aureus* without causing lethal damage to the membrane and binds to the chromosomal DNA inducing bacterial death (Gottschalk *et al*., 2013). It has been postulated that the cationic and amphiphatic nature of AMPs selectively kill bacteria by penetrating the negatively charged cell membrane leading to membrane disintegration. However, AMPs may also act by other mechanisms without destruction of the cell membrane targeting intracellular enzymatic activities such as cell wall synthesis and RNA, DNA and protein synthesis (Jenssen *et al*., 2006; Hale and Hancock, 2007). The inhibition of RNA, DNA and protein synthesis in bacteria may result from AMPs interacting with DNA repair by collapsing replication forks (Gunderson and Segall, 2006; Dubois *et al*., 2013). At higher concentrations, LP5 also targets the cell membrane leading to leakage of intracellular compounds like ATP, resulting in cell death (Dubois *et al*., 2013; Gottschalk *et al*., 2013).

According to the initial screening results with the growth inhibition assay, the presence of the sulphonamide groups on octyl-peptoid showed antibacterial activity. However, Hexyl and Butyl peptoids with the N-sulphonamide group did not show any antimicrobial activity on PAO1 (Tosyl-Butyl and Tosyl-Hexyl) and *E. coli* (Tosyl-Hexyl). But some growth inhibition was observed with MRSA and MSSA with Tosyl-Hexyl, indicating that the sulphonamide group synergises with the octyl-9-mer combination to promote the broad range of bactericidal activity on Gram positive and negative bacteria. Previous studies on sulfonamide derivatives revealed that the given chain length of the lipophilic moiety and the nature of the hydrophilic group substituted at the amino nitrogen of the sulfonamide molecule had a marked influence on surfactant properties and mutual lipophilic and hydrophilic groups may

have surface activity and an antibacterial effect (Badr, 2008). These studies suggest that the proper combination of different groups to the sulphonamide may have beneficial effects.

TOP shows less mammalian cell membrane toxicity and less cytotoxicity activity on A549 cells at low concentrations, suggesting that the TOP shows selectivity between bacterial and mammalian cells. Unlike other antimicrobial peptoids, TOP shows higher MIC values tested. It also has higher SR showing higher selectivity over mammalian cells. However at low concentrations, TOP induces secondary necrosis of apoptotic neutrophils similar to other antimicrobial peptides. In future studies, modulating molecular structure of the TOP could increase the bacterial killing efficacy and reducing the mammalian cell toxicity.

In conclusion these studies, suggest that the antibacterial activity of TOP may have been due to the length of the eight carbon-side chain and the N-terminus sulphonamide group combination. Neither individual octyl-9-mer group nor the sulphonamide groups are antimicrobial as shown in the results section. Therefore the results suggest that the correct combination of different lysine groups with modification on the carbon length and the capping groups generates the antimicrobial active compound. However further studies are required to elucidate the mechanism of action on bacterial killing.

(b) Strategies to develop aptamer and peptide molecules to detect bacterial infection.

Current microbiological diagnosis is inefficient, with a minimum lag of 48 hours between the isolate reaching the laboratory and accurate organism identification. Delay in administering effective antibiotics results in stepwise increases in mortality resulting from bacterial sepsis and use of empirical broad spectrum antibiotics in patients with severe sepsis will become greater, driving selection of resistant microorganisms and exacerbating the problem. Therefore strategies to improve the diagnosis of serious infection such as MRSA are important to avoid unnecessary

antibiotic exposure. The role for novel diagnostic technologies lies in rapid identification of causative organisms with specificity (O'Brien and Gould, 2013). MRSA is currently detected using multiplexed PCR primers that detect specific genes for *S. aureus* (e.g. *nuc* or *fem*) and *mecA* for detection of methicillin resistance (Turek *et al*., 2013). The eradication of multidrug-resistant bacteria is very difficult and it is essential to look for alternative detection options to identify MRSA infection. According to the second hypothesis of my studies, it was focused on aptamer and peptide molecular probes and developed as novel diagnostic tools to detect MRSA infection. To study this hypothesis MRSA specific extracellular PBP2A protein was purified and two different aptamer probes were developed as PBP2A specific and MRSA specific based on bacterial cell based SELEX procedures.

Chapter 4 discussed *mecA* gene cloning and PBP2A protein over-expression in order to carry out the SELEX and phage biopanning against PBP2A protein. SELEX and phage biopanning were carried out separately against the purified PBP2A protein and whole bacterial cells and the results were discussed in the chapter 5 and 6. Aptamer and peptides are small molecules with potential as tools to enable disease diagnostics and treatment. My main target was to develop MRSA specific molecular probes using highly diverse combinatorial libraries of aptamers and peptides. These molecules y bind with high affinity to targets on the cell surface and are selectively displaced by putative ligands. These are the peptide-based phage display and the oligonucleotide-based aptamer techniques, respectively. Aptamer libraries were designed and ordered from commercial Integrated DNA Technologies (IDT) and the phage display libraries were purchased from NEB. I have screened aptamer libraries and peptide libraries against whole MRSA bacteria and purified PBP2A protein. The PBP2A protein is a unique membrane protein expressed by MRSA. I cloned the *mecA* gene and over-expressed and purified the PBP2A protein before testing its functional properties to its native protein present in MRSA using the Latex Agglutination test. The SELEX procedure was carried out against whole MRSA bacteria and PBP2A coated Ni-NTA beads.

Chapter 5 described the aptamer bio-imaging probe development using purified PBP2A protein and MRSA. Optimizing the selection buffer conditions increases the likelihood of producing a good target aptamer. The selection buffer conditions may vary as widely as the selection targets, and therefore buffer optimization is helpful for effective aptamer selections (Stovall *et al*., 2004). Therefore different selection buffer conditions were adopted during SELEX and optimised to minimise the non-specific binding and optimise the target molecular binding in PBS (with Ca^{+2} and Mg^{+2}) instead of others buffer tested (Cho *et al*., 2006). Previous studies suggested that the buffer conditions may vary between monovalent salt(s) identity, monovalent salt(s) concentration, divalent salt(s) identity, divalent salt concentration, buffer identity, buffer concentration, and pH. The optimized buffer conditions likely increase the probability of a successful selection and therefore promote higher ratios of successful aptamer selections against a variety of targets (Stovall *et al*., 2004). Amplifying nonspecific DNA during the PCR amplification is also a major problem in SELEX protocol. Therefore PCR conditions such as annealing temperature and number of PCR cycles were optimised to have high yields of DNA and low non-specific DNA amplification to 10 PCR cycles (Sefah *et al*., 2010). However many other researchers have used more than 10 PCR cycles in their protocols and found no nonspecific amplifications due to variable primers, buffer conditions and annealing temperatures (Shangguan *et al*., 2006; Tang *et al*., 2007; Sefah *et al*., 2009).

The elimination of the negative DNA strand after PCR amplification is usually conducted by either lambda exonuclease digestion of the negative dephosphorylated strand (Oh *et al*., 2011), asymmetric PCR (Berezovski *et al*., 2008), denaturing polyacrylamide gel electrophoresis (Kim *et al*., 2010), or with streptavidin-coated magnetic beads (Tanaka *et al*., 2009; Sefah *et al*., 2010), which I have adopted in my experiments. However each of these approaches has its own advantages and disadvantages which are more broadly discussed elsewhere (Marimuthu *et al*., 2012; Svobodová *et al*., 2012). In addition, a multitude of sequences present in the amplification step of the SELEX procedure make the pool prone to forming non-fully complementary dimers, which may often lead to the appearance of a product of undesired size, mostly larger (Murphy *et al*., 2003). To prevent this effect, the

number of cycles and annealing temperatures for the PCR amplification of the selected library has to be strictly monitored and adjusted (Waybrant *et al*., 2012). In my experiments it was set to 10 PCR cycles to minimise larger PCR fragments.

The theory of SELEX is very simple and relies on Darwinian evolution at a molecular level. Basically, a vast number (10^{14}–10^{16}) of DNA or RNA oligonucleotides with different sequences are subjected to selection for binding to the target molecules. While non-binding oligonucleotides are discarded by washing steps and counter selection, the bound sequences exhibiting affinity for the target are amplified by PCR. Generally, after 8–15 cycles, the oligonucleotide pool is populated by the best binding aptamer candidates, which are finally separated and identified by sequencing (Vater *et al*., 2003; Szeitner *et al*., 2014). However, I implemented a novel approach where no counter selection has been practiced during the SELEX procedure. This also reduced the number of SELEX cycles minimising errors during PCR amplification and mishandling samples (Sefah *et al*., 2010). As in my experimental procedure five rounds of SELEX have been carried out independently against MRSA (ATCC252), MSSA (ATCC 25923), PAO1-*Pseudomonas*, *Kebsiella pneumonia*, *Escherichia coli* (ATCC 25922) and eukaryotic cells A549. This generated aptamer against individual bacteria and eukaryotic cells but they were not specific due to lack of counter selection. The elimination of non-specific aptamer was carried out at sequence level called *in-silico* SELEX. Sometimes SELEX fails to identify aptamers that bind to their target with high affinity. Thus, post-SELEX optimization of aptamers is required to improve aptamer binding affinity. The *in- silico* maturation is based on a genetic algorithm (Savory *et al*., 2010). In another study, *In-silico* maturation was performed to improve a VEGF-binding DNA aptamer (Nonaka *et al*., 2013).

Implementation of aptamer production is much more complex than its simple, theoretical scheme would suggest, and the success of the procedure mainly relies on seemingly minor experimental details of the selection. Consequently, following the introduction of SELEX, numerous alternative approaches have been explored (Gopinath, 2007) with the general intention of increasing the success rate, but also

ensuring high speed (Park *et al*., 2009; Huang *et al*., 2010), low handled volumes (Hybarger *et al*., 2006), minimal contamination and automation (Mathot *et al*., 2013).

Chemically synthesized selected aptamer sequences can be labelled directly with (i) a fluorophore, such as FITC or cy5 or (ii) biotin. Biotin labelled aptamers are detected with streptavidin-conjugated fluorophore, such as Alexa Fluor 488, phycoerythrin or phycoerythrin-cy5.5 (Sefah *et al*., 2010). In this study two aptamer probes were resynthesized with 5' FITC modification from SIGMA-ALDRICH and binding assays were carried out as mentioned in the Sefah *et al*., (2010). Both aptamer probes show higher specificity towards the purified protein but no specificity towards the MRSA bacteria. However previous publications also show that some of the selected aptamers can also bind to the controls and other related cells (Sefah *et al*., 2010; Szeitner *et al*., 2014). The two aptamer probes may bind non-specifically towards the other surface molecules located on the bacteria. Since the counter selection was not carried out during the SELEX nor *in-silico* maturation, therefore the aptamer probes may bind to other bacteria in a non-specific manner. It can also be expected that some selected aptamers will recognize both target and control cells (Cerchia *et al*., 2005; Chen *et al*., 2008).

Chapter 6 described the development of MRSA specific peptide probes using highly diverse phage derived peptide libraries (Ph.D.). This study used 12-mer PhD peptide library against MRSA since most of the previous studies used 12-mer library from New England Biolabs (NEB) (Trepel *et al*., 2008; Zhang *et al*., 2014). Bio-panning experiments were carried out as described in the material and method section according to the commercial supplier (NEB). The counter selections on MSSA and PAO1 were carried out before bio-panning with PBP2A coated Ni beads and MRSA whole bacterial cells. Peptide molecules were developed against viruses (Long *et al*., 2014), bacteria (Sainath Rao *et al*., 2013), cancer cells (Ploss *et al*., 2014; Sainath Rao *et al*., 2013) and other bio molecules (Jiang *et al*., 2014) using phage display library screening elsewhere.

After 3 rounds of bio-panning and amplification, 120 clones were characterized by DNA sequencing and amino acid sequences were analysed using ClustalW online tool. However the number of biopanning rounds can be varied from 3-5, although the commercial supplier recommends 3 rounds of biopanning (Turnbough, 2003; Dane *et al*., 2006). Two different peptide sequences were identified as PBP2A specific peptide GLHTSATNLYLH and MRSA bacterial specific peptide GWTSVSVHIRGG after ClustalW analysis. For further analysis N-terminus FAM conjugated these peptide sequences were synthesised and binding affinity have been evaluated *in-vitro* with bacterial binding selectivity assays. Similar N-terminus conjugations of peptides were reported on cancer cell detection (Dane *et al*., 2006). Flow cytometry and confocal microscopy were used to evaluate the peptide binding efficacy to bacteria (Williams *et al*., 2003). However both probes showed no specificity towards MRSA and bound to the control bacteria tested. These results suggested addressing limitations in this study in future work.

Scientists recent have focused their research on screening novel AMPs by using combinatorial libraries and computational approaches for antimicrobial drug discovery and design. Phage display serves as a valuable tool for the selection of peptides binding to surface epitopes on whole cells (Kay *et al*., 1998; Wang *et al*., 2009). Some studies used a 12-mer phage-display library to identify peptides binding to the whole cell surface of *E. coli*. This focused to identify a novel peptide that showed binding to *E. coli* cells. The peptide exhibited antimicrobial activity against Gram negative organisms and showed significant bactericidal activity against *E. coli* and *P. aeruginosa* (Sainath Rao *et al*., 2013). Therefore the antibacterial activity of these peptides was also studied on MRSA and MSSA. The results suggested that these peptides did not show any specific binding towards the MRSA and show no antibacterial activity.

In this study the two peptides were synthesised as N-terminus FAM conjugated probes. However during the biopanning procedure the N-terminus of the selected peptide sequence was free and the C-terminus was fused to the phage. Therefore, this structural modification may affect the binding ability of these peptides to targeted

molecules. In previous studies structural modification were done to achieve the binding of the peptide to the target molecules (Turnbough, 2003; Jinghui *et al*., 2014). Further to that when designing synthetic peptides corresponding to selected sequences, it is recommended to add the spacer sequence Gly-Gly-Gly-Ser to the C-terminus and amidating the C- terminal carboxylate to block the negative charge. The chemical conjugation of the peptide to FAM, the C-terminal serine can be replaced with cysteine (if there are no other cysteines present in the sequence) (Chichili *et al*., 2013).

Future perspectives:

In summary, my studies on peptide research have produced some positive outcomes and generated more avenues for further studies on peptoid work in the future. I demonstrated the biological effects of modulating the peptoid libraries and *in-vitro* experiments were optimised for future research. These peptoids can be evaluated *in-vivo* mice models and to have better understanding of peptoid biology and to develop drug candidates for bacterial infection.

In future studies, I would like to suggest that the combination of variable lengths of lysine like peptoids (e.g. 10-mer, 11-mer or 12-mer) and different capping groups may be a very good platform to study the antibacterial peptoid biology. This is not only limited to lysine peptoids, we also can study other peptoids derived from amino-acids combinations. This can change the properties of peptoids such as pH, hydrophobicity and hydrophilicity. This study evaluated the efficacy of TOP on Gram negative and Gram positive bacterial species including clinically isolated bacteria and multidrug resistance strains such as MRSA. However in future work it is important to investigate the effect of TOP on other clinically important bacterial/fungal/virus strains and species including vancomycin resistant enterococci (VRE), Mycobacterium tuberculosis and other multidrug-resistant microbes to study the full spectrum of the efficacy of this drug to be used in clinical settings.

The developed aptamer probes show some degree of specificity to purified PBP2A protein (chapter 4). However these probes are not specific to detect MRSA bacterial species over other bacteria. This could be due to several reasons as discussed previously. The most likely cause of failure, were issues regarding the SELEX procedure itself. There are many opportunities to further develop these probes.

It is important to understand the biology and technical pitfalls during the development of MRSA specific aptamer and peptide probes. Since I have experienced the non-specificity of aptamer and peptide probe development I would rather try to repeat previously published aptamer and peptide molecular development protocol to familiarise with the techniques as example using thrombin as a molecular target (Avino *et al*., 2012).

Success of aptamer probe development is mainly depend on the careful planning, meticulous implementation and tracking of progression of selection (Mencin *et al*., 2014). Therefore in future studies monitoring of enrichment could be done after each SELEX round using labelled aptamer. Since most papers feature only a single aptamer, there is little awareness that the selection process generally results in a large number of sequences. Ideally, all selected oligonucleotides need to be evaluated individually in terms of their target binding properties to designate the most suitable aptamer candidates (Lautner *et al*., 2012).

Bibliography

Abraham, E. P., and E. Chain, 1940, An Enzyme from Bacteria able to Destroy Penicillin: Nature, v. 146, p. 837.

Adler, A., N. Forster, M. Homann, and H. U. Göringer, 2008, Post-SELEX chemical optimization of a trypanosome-specific RNA aptamer: Combinatorial Chemistry & High Throughput Screening, v. 11, p. 16-23.

Afacan, N. J., A. T. Y. Yeung, O. M. Pena, and R. E. W. Hancock, 2012, Therapeutic potential of host defense peptides in antibiotic-resistant infections: Current Pharmaceutical Design, v. 18, p. 807-819.

Al-Ahmad, A., D. Laird, P. Zou, P. Tomakidi, T. Steinberg, and K. Lienkamp, 2013, Nature-Inspired Antimicrobial Polymers – Assessment of Their Potential for Biomedical Applications: PLoS ONE, v. 8, p. 1-9.

Almeida, R. A., K. R. Matthews, E. Cifrian, A. J. Guidry, and S. P. Oliver, 1996, *Staphylococcus aureus* invasion of bovine mammary epithelial cells: Journal Of Dairy Science, v. 79, p. 1021-1026.

Alvarez-Ortega, C., I. Wiegand, J. Olivares, R. E. W. Hancock, and J. L. Martínez, 2011, The intrinsic resistome of Pseudomonas aeruginosa to β-lactams: Virulence, v. 2, p. 144-146.

Aminov, R. I., 2010, A brief history of the antibiotic era: lessons learned and challenges for the future: Frontiers In Microbiology, v. 1, p. 134-134.

Andreu, D., and L. Rivas, 1998, Animal antimicrobial peptides: an overview: Biopolymers, v. 47, p. 415-433.

Andreu, N., A. Zelmer, and S. Wiles, 2011, Noninvasive biophotonic imaging for studies of infectious disease: FEMS Microbiology Reviews, v. 35, p. 360-394.

Anthony, K. B., N. O. Fishman, D. R. Linkin, L. B. Gasink, P. H. Edelstein, and E. Lautenbach, 2008, Clinical and Microbiological Outcomes of Serious Infections with Multidrug-Resistant Gram-Negative Organisms Treated with Tigecycline, University of Chicago Press, p. 567.

Aravind, A., P. Jeyamohan, R. Nair, S. Veeranarayanan, Y. Nagaoka, Y. Yoshida, T. Maekawa, and D. S. Kumar, 2012, AS1411 aptamer tagged PLGA-lecithin-PEG nanoparticles for tumor cell targeting and drug delivery: Biotechnology and Bioengineering, v. 109, p. 2920-2931.

Arias, C. A., and B. E. Murray, 2012, The rise of the *Enterococcus*: beyond vancomycin resistance: Nature Reviews. Microbiology, v. 10, p. 266-278.

Armand, P., K. Kirshenbaum, A. Falicov, R. L. Dunbrack, Jr., K. A. Dill, R. N. Zuckermann, and F. E. Cohen, 1997, Chiral N-substituted glycines can form stable helical conformations: Folding & Design, v. 2, p. 369-375.

Arnt, L., and G. N. Tew, 2002, New poly(phenyleneethynylene)s with cationic, facially amphiphilic structures: Journal of thte American Chemical Society, v. 124, p. 7664-7665.

Auvynet, C., and Y. Rosenstein, 2009, Multifunctional host defense peptides: antimicrobial peptides, the small yet big players in innate and adaptive immunity: The FEBS Journal, v. 276, p. 6497-6508.

Bibliography

Avino, A., C. Fabrega, M. Tintore, and R. Eritja, 2012, Thrombin Binding Aptamer, More than a Simple Aptamer: Chemically Modified Derivatives and Biomedical Applications: Current Pharmaceutical Design, v. 18, p. 2036-2047.

Azuma, N., K. Yamauchi, and T. Mitsuoka, 1984, Bifidus growth-promoting activity of a glycomacropeptide derived from human .KAPPA.-casein: Agricultural and Biological Chemistry, v. 48, p. 2159-2162.

Badr, E. E., 2008, Novel Sulfanilamide as Potent Surfactants and Antibacterial Agents: Journal of Dispersion Science & Technology, v. 29, p. 1143-1149.

Bagalkot, V., O. C. Farokhzad, R. Langer, and S. Jon, 2006, An aptamer-doxorubicin physical conjugate as a novel targeted drug-delivery platform: Angewandte Chemie International Edition, v. 45, p. 8149-8152.

Bahl, D., D. A. Miller, I. Leviton, P. Gialanella, M. J. Wolin, W. Liu, R. Perkins, and M. H. Miller, 1997, In vitro activities of ciprofloxacin and rifampin alone and in combination against growing and nongrowing strains of methicillin-susceptible and methicillin-resistant Staphylococcus aureus: Antimicrobial Agents And Chemotherapy, v. 41, p. 1293-1297.

Balasubramanian, S., I. B. Sorokulova, V. J. Vodyanoy, and A. L. Simonian, 2007, Lytic phage as a specific and selective probe for detection of *Staphylococcus aureus* - A surface plasmon resonance spectroscopic study: Biosensors and Bioelectronics, v. 22, p. 948-955.

Baltz, R. H., 2008, Renaissance in antibacterial discovery from actinomycetes: Current Opinion in Pharmacology, v. 8, p. 557-563.

Barber, M., and M. Rozwadowska-Dowzenko, 1948, Infection by penicillin-resistant staphylococci: Lancet, v. 2, p. 641-644.

Barlow, P. G., Y. X. Li, T. S. Wilkinson, D. M. E. Bowdish, Y. E. Lau, C. Cosseau, C. Haslett, A. J. Simpson, R. E. W. Hancock, and D. J. Davidson, 2006, The human cationic host defense peptide LL-37 mediates contrasting effects on apoptotic pathways in different primary cells of the innate immune system: Journal of Leukocyte Biology, v. 80, p. 509-520.

Batoni, G., G. Maisetta, F. L. Brancatisano, S. Esin, and M. Campa, 2011, Use of antimicrobial peptides against microbial biofilms: advantages and limits: Current Medicinal Chemistry, v. 18, p. 256-279.

Bax, R. P., R. Anderson, J. Crew, P. Fletcher, T. Johnson, E. Kaplan, B. Knaus, K. Kristinsson, M. Malek, and L. Strandberg, 1998, Antibiotic resistance--what can we do?: Nature Medicine, v. 4, p. 545-546.

Bayrac, A. T., K. Sefah, P. Parekh, C. Bayrac, B. Gulbakan, H. A. Oktem, and W. Tan, 2011, In vitro Selection of DNA Aptamers to Glioblastoma Multiforme: ACS Chemical Neuroscience, v. 2, p. 175-181.

Beck, W. D., B. Berger-Bächi, and F. H. Kayser, 1986, Additional DNA in methicillin-resistant *Staphylococcus aureus* and molecular cloning of mec-specific DNA: Journal of Bacteriology, v. 165, p. 373-378.

Becker, R. C., C. Rusconi, and B. Sullenger, 2005, Nucleic acid aptamers in therapeutic anticoagulation - Technology, development and clinical application: Thrombosis and Haemostasis, v. 93, p. 1014-1020.

Bentley, R., 2009, Different roads to discovery; Prontosil (hence sulfa drugs) and penicillin (hence β-lactams): Journal of industrial microbiology & biotechnology.

Bibliography

Benveniste, R., and J. Davies, 1973, Aminoglycoside Antibiotic-Inactivating Enzymes in Actinomycetes Similar to those Present in Clinical Isolates of Antibiotic-Resistant Bacteria: Proceedings of the National Academy of Sciences of the United States of America, p. 2276.

Berezovski, M. V., M. Lechmann, M. U. Musheev, T. W. Mak, and S. N. Krylov, 2008, Aptamer-facilitated biomarker discovery (AptaBiD): Journal of the American Chemical Society, v. 130, p. 9137-9143.

Berezovski, M., M. Musheev, A. Drabovich, and S. N. Krylov, 2006, Non-SELEX selection of aptamers: Journal of the American Chemical Society, v. 128, p. 1410-1411.

Bessalle, R., A. Kapitkovsky, A. Gorea, I. Shalit, and M. Fridkin, 1990, All-D-magainin: chirality, antimicrobial activity and proteolytic resistance: FEBS Letters, v. 274, p. 151-155.

Beutler, J. A., 2009, Natural products as a foundation for drug discovery: Current Protocols In Pharmacology / Editorial Board, S.J. Enna, v. Chapter 9, p. 9.11-9.11.

Biedenbach, D. J., G. J. Moet, and R. N. Jones, 2004, Occurrence and antimicrobial resistance pattern comparisons among bloodstream infection isolates from the SENTRY Antimicrobial Surveillance Program (1997-2002): Diagnostic Microbiology and Infectious Disease, v. 50, p. 59-69.

Biek, D., I. A. Critchley, T. A. Riccobene, and D. A. Thye, 2010, Ceftaroline fosamil: a novel broad-spectrum cephalosporin with expanded anti-Gram-positive activity: Journal of Antimicrobial Chemotherapy, v. 65, p. iv9-iv16.

Bierbaum, G., and H. G. Sahl, 1987, Autolytic system of Staphylococcus simulans 22: influence of cationic peptides on activity of N-acetylmuramoyl-L-alanine amidase: Journal of Bacteriology, v. 169, p. 5452-5458.

Birtalan, E., B. Rudat, D. K. Kolmel, D. Fritz, S. B. L. Vollrath, U. Schepers, and S. Brase, 2011, Investigating Rhodamine B-Labeled Peptoids: Scopes and Limitations of Its Applications: Biopolymers, v. 96, p. 694-701.

Bishop-Hurley, S. L., F. J. Schmidt, A. L. Erwin, and A. L. Smith, 2005, Peptides selected for binding to a virulent strain of Haemophilus influenzae by phage display are bactericidal: Antimicrobial Agents and Chemotherapy, v. 49, p. 2972-2978.

Bishop-Hurley, S. L., P. J. Rea, and C. S. McSweeney, 2010, Phage-displayed peptides selected for binding to Campylobacter jejuni are antimicrobial: Protein Engineering, Design & Selection: PEDS, v. 23, p. 751-757.

Blank, M., T. Weinschenk, M. Priemer, and H. Schluesener, 2001, Systematic evolution of a DNA aptamer binding to rat brain tumor microvessels - Selective targeting of endothelial regulatory protein pigpen: Journal of Biological Chemistry, v. 276, p. 16464-16468.

Bleeker-Rovers, C. P., O. C. Boerman, H. J. J. M. Rennen, F. H. M. Corstens, and W. J. G. Oyen, 2004, Radiolabeled compounds in diagnosis of infectious and inflammatory disease: Current Pharmaceutical Design, v. 10, p. 2935-2950.

Blot, S., K. Vandewoude, and F. Colardyn, 1998, *Staphylococcus aureus* infections: N Engl J Med, v. 339, p. 2025-2026.

Bibliography

Bobard, A., N. Mellouk, and J. Enninga, 2011, Spotting the right location- imaging approaches to resolve the intracellular localization of invasive pathogens: Biochimica et Biophysica Acta (BBA) - General Subjects, v. 1810, p. 297-307.

Boman, H. G., B. Agerberth, and A. Boman, 1993, Mechanisms of action on Escherichia coli of cecropin P1 and PR-39, two antibacterial peptides from pig intestine: Infection and immunity (USA).

Bouchard, D. S., L. Rault, N. Berkova, Y. Le Loir, and S. Even, 2013, Inhibition of Staphylococcus aureus invasion into bovine mammary epithelial cells by contact with live Lactobacillus casei: Applied and Environmental Microbiology, v. 79, p. 877-885.

Bradley, E. K., J. M. Kerr, L. S. Richter, G. M. Figliozzi, D. A. Goff, R. N. Zuckermann, D. C. Spellmeyer, and J. M. Blaney, 1997, NMR structural characterization of oligo-N-substituted glycine lead compounds from a combinatorial library: Molecular Diversity, v. 3, p. 1-15.

Bradshaw, J., 2003, Cationic antimicrobial peptides: issues for potential clinical use: Biodrugs: Clinical Immunotherapeutics, Biopharmaceuticals and Gene Therapy, v. 17, p. 233-240.

Brandenburg, K., J. Andra, P. Garidel, and T. Gutsmann, 2011, Peptide-based treatment of sepsis: Applied Microbiology and Biotechnology, p. 799.

Bratkovič, T., 2010, Progress in phage display: evolution of the technique and its applications: Cellular and molecular life sciences.

Brigati, J., D. D. Williams, I. B. Sorokulova, V. Nanduri, I. H. Chen, C. L. Turnbough, and V. A. Petrenko, 2004, Diagnostic probes for Bacillus anthracis spores selected from a landscape phage library: Clinical Chemistry, v. 50, p. 1899-1906.

Brinsley, K., R. Sinkowitz-Cochran, and D. Cardo, 2005, An assessment of issues surrounding implementation of the Campaign to Prevent Antimicrobial Resistance in Healthcare Settings: American Journal Of Infection Control, v. 33, p. 402-409.

Brogden, K. A., 2005, Antimicrobial peptides: pore formers or metabolic inhibitors in bacteria?: Nature Reviews Microbiology, v. 3, p. 238-250.

Brogden, K. A., M. Ackermann, and K. M. Huttner, 1997, Small, anionic, and charge-neutralizing propeptide fragments of zymogens are antimicrobial: Antimicrobial Agents And Chemotherapy, v. 41, p. 1615-1617.

Brogden, K. A., M. Ackermann, P. B. McCray, Jr., and B. F. Tack, 2003, Antimicrobial peptides in animals and their role in host defences: International Journal of Antimicrobial Agents, v. 22, p. 465-478.

Brötz, H., G. Bierbaum, K. Leopold, P. E. Reynolds, and H. G. Sahl, 1998, The lantibiotic mersacidin inhibits peptidoglycan synthesis by targeting lipid II: Antimicrobial Agents And Chemotherapy, v. 42, p. 154-160.

Brown, N. J., J. Johansson, and A. E. Barron, 2008, Biomimicry of surfactant protein C: Accounts of Chemical Research, v. 41, p. 1409-1417.

Bryskier, A., 2000, Novelties in the field of anti-infective compounds in 1999: Clinical Infectious Diseases: An Official Publication of the Infectious Diseases Society of America, v. 31, p. 1423-1466.

Bibliography

Bucki, R., D. B. Namiot, Z. Namiot, P. B. Savage, and P. A. Janmey, 2008, Salivary mucins inhibit antibacterial activity of the cathelicidin-derived LL-37 peptide but not the cationic steroid CSA-13: The Journal of Antimicrobial Chemotherapy, v. 62, p. 329-335.

Bulet, P., R. Stöcklin, and L. Menin, 2004, Anti-microbial peptides: from invertebrates to vertebrates: Immunological Reviews, v. 198, p. 169-184.

Bush, K., and M. J. Macielag, 2010, New β-lactam antibiotics and β-lactamase inhibitors: Expert Opinion On Therapeutic Patents, v. 20, p. 1277-1293.

Cao, X., S. Li, L. Chen, H. Ding, H. Xu, Y. Huang, J. Li, N. Liu, W. Cao, Y. Zhu, B. Shen, and N. Shao, 2009, Combining use of a panel of ssDNA aptamers in the detection of *Staphylococcus aureus*: Nucleic acids research.

Capitano, B., R. Quintiliani, C. H. Nightingale, and D. P. Nicolau, 2001, Antibacterials for the Prophylaxis and Treatment of Bacterial Endocarditis in Children: Pediatric Drugs, v. 3, p. 703-718.

Caserta, T. M., A. N. Smith, A. D. Gultice, M. A. Reedy, and T. L. Brown, 2003, Q-VD-OPh, a broad spectrum caspase inhibitor with potent antiapoptotic properties: Apoptosis: An International Journal on Programmed Cell Death, v. 8, p. 345-352.

Casteels, P., C. Ampe, F. Jacobs, and P. Tempst, 1993, Functional and chemical characterization of Hymenoptaecin, an antibacterial polypeptide that is infection-inducible in the honeybee (Apis mellifera): The Journal of Biological Chemistry, v. 268, p. 7044-7054.

Cerchia, L., F. Ducongé, C. Pestourie, J. Boulay, Y. Aissouni, K. Gombert, B. Tavitian, V. d. Franciscis, and D. Libri, 2005, Neutralizing Aptamers from Whole-Cell SELEX Inhibit the RET Receptor Tyrosine Kinase: PLoS Biology, v. 3, p. 697-704.

Chambers, H. F., 2003, Solving staphylococcal resistance to beta-lactams: Trends In Microbiology, v. 11, p. 145-148.

Chelliserrykattil, J., and A. D. Ellington, 2004, Evolution of a T7 RNA polymerase variant that transcribes 2'-O-methyl RNA: Nature Biotechnology, v. 22, p. 1155-1160.

Chen, F., J. Zhou, F. L. Luo, A. B. Mohammed, and X. L. Zhang, 2007, Aptamer from whole-bacterium SELEX as new therapeutic reagent against virulent Mycobacterium tuberculosis: Biochemical and Biophysical Research Communications, v. 357, p. 743-748.

Chen, H. W., C. D. Medley, K. Sefah, D. Shangguan, Z. W. Tang, L. Meng, J. E. Smith, and W. H. Tan, 2008, Molecular recognition of small-cell lung cancer cells using aptamers: ChemMedChem, v. 3, p. 991-1001.

Cheng, J. C., C. L. Huang, C. C. Lin, C. C. Chen, Y. C. Chang, S. S. Chang, and C. P. Tseng, 2006, Rapid detection and identification of clinically important bacteria by high-resolution melting analysis after broad-range ribosomal RNA real-time PCR: Clinical Chemistry, v. 52, p. 1997-2004.

Chia, I. L., G. Y. Liu, S. Yongcheng, Y. Fenglin, M. E. Hensler, J. Wen-Yih, V. Nizet, A. H. J. Wang, and E. Oldfield, 2008, A Cholesterol Biosynthesis Inhibitor Blocks *Staphylococcus aureus* Virulence: Science, v. 319, p. 1391-1394.

Chichili, V. P. R., V. Kumar, and J. Sivaraman, 2013, Linkers in the structural biology of protein-protein interactions: Protein Science, v. 22, p. 153-167.

Bibliography

Cho, E. J., J. R. Collett, A. E. Szafranska, and A. D. Ellington, 2006, Optimization of aptamer microarray technology for multiple protein targets: Analytica Chimica Acta, v. 564, p. 82-90.

Chongsiriwatana, N. P., J. A. Patch, A. M. Czyzewski, M. T. Dohm, A. Ivankin, D. Gidalevitz, R. N. Zuckermann, and A. E. Barron, 2008, Peptoids that mimic the structure, function, and mechanism of helical antimicrobial peptides: Proceedings Of The National Academy Of Sciences Of The United States Of America, v. 105, p. 2794-2799.

Christensen, D. J., E. B. Gottlin, R. E. Benson, and P. T. Hamilton, 2001, Phage display for target-based antibacterial drug discovery: Drug Discovery Today, v. 6, p. 721-727.

Chu, T. C., J. W. Marks, L. A. Lavery, S. Faulkner, M. G. Rosenblum, A. D. Ellington, and M. Levy, 2006, Aptamer: toxin conjugates that specifically target prostate tumor cells: Cancer Research, v. 66, p. 5989-5992.

Coates, A., Y. Hu, R. Bax, and C. Page, 2002, The future challenges facing the development of new antimicrobial drugs: Nature Reviews Drug Discovery, p. 895.

Coombes, J. L., and E. A. Robey, 2010, Dynamic imaging of host-pathogen interactions in vivo: Nature Reviews Immunology, v. 10, p. 353-364.

Cosgrove, S. E., and Y. Carmeli, 2003, The impact of antimicrobial resistance on health and economic outcomes: Clinical Infectious Diseases, v. 36, p. 1433-1437.

Costa, S. S., C. Falcão, M. Viveiros, D. Machado, M. Martins, J. Melo-Cristino, L. Amaral, and I. Couto, 2011, Exploring the contribution of efflux on the resistance to fluoroquinolones in clinical isolates of Staphylococcus aureus: BMC Microbiology, v. 11, p. 241-241.

Couto, I., S. W. Wu, A. Tomasz, and H. de Lencastre, 2003, Development of methicillin resistance in clinical isolates of *Staphylococcus sciuri* by transcriptional activation of the *mecA* homologue native to the species: Journal of Bacteriology, v. 185, p. 645-653.

Cox, J. C., P. Rudolph, and A. D. Ellington, 1998, Automated RNA selection: Biotechnology Progress, v. 14, p. 845-850.

Crossley, K. B., and G. Archer, 1997, The staphylococci in human disease / edited by Kent B. Crossley, Gordon L. Archer, New York: Churchill Livingstone, 1997.

Cui, Z.Q., Q. Ren, H.P. Wei, Z. Chen, J.Y. Deng, Z.P. Zhang, and X.-E. Zhang, 2011, Quantum dot-aptamer nanoprobes for recognizing and labeling influenza A virus particles: Nanoscale, v. 3, p. 2454-2457.

Curtis, N. A. C., M. V. Hayes, A. W. Wyke, and J. B. Ward, 1980, A mutant of *Staphylococcus aureus* H lacking penicillin-binding protein 4 and transpeptidase activity in vitro: FEMS Microbiology Letters, v. 9, p. 263.

Dai, T., Y. Y. Huang, and M. R. Hamblin, 2009, Photodynamic therapy for localized infections-State of the art: Photodiagnosis and Photodynamic Therapy, v. 6, p. 170-188.

Dane, K. Y., L. A. Chan, J. J. Rice, and P. S. Daugherty, 2006, Isolation of cell specific peptide ligands using fluorescent bacterial display libraries: Journal of Immunological Methods, v. 309, p. 120-129.

Bibliography

D'Costa, V. M., C. E. King, L. Kalan, M. Morar, W. W. L. Sung, C. Schwarz, D. Froese, G. Zazula, F. Calmels, R. Debruyne, G. B. Golding, H. N. Poinar, and G. D. Wright, 2011, Antibiotic resistance is ancient: Nature, p. 457.

De Brucker, K., B. P. A. Cammue, and K. Thevissen, 2011, Apoptosis-inducing antifungal peptides and proteins: Biochemical Society Transactions, v. 39, p. 1527-1532.

de Jonge, B. L., and A. Tomasz, 1993, Abnormal peptidoglycan produced in a methicillin-resistant strain of *Staphylococcus aureus* grown in the presence of methicillin: functional role for penicillin-binding protein 2A in cell wall synthesis: Antimicrobial Agents And Chemotherapy, v. 37, p. 342-346.

de Oca, E. P. M., 2013, Antimicrobial peptide elicitors: New hope for the post-antibiotic era: Innate Immunity, v. 19, p. 227-241.

Dennison, S. R., J. Wallace, F. Harris, and D. A. Phoenix, 2005, Amphiphilic alpha-helical antimicrobial peptides and their structure/function relationships: Protein And Peptide Letters, v. 12, p. 31-39.

Derda, R., S. K. Y. Tang, S. C. Li, S. Ng, W. Matochko, and M. R. Jafari, 2011, Diversity of Phage-Displayed Libraries of Peptides during Panning and Amplification: Molecules, v. 16, p. 1776-1803.

Deslouches, B., K. Islam, J. K. Craigo, S. M. Paranjape, R. C. Montelaro, and T. A. Mietzner, 2005, Activity of the de novo engineered antimicrobial peptide WLBU2 against Pseudomonas aeruginosa in human serum and whole blood: Implications for systemic applications: Antimicrobial Agents and Chemotherapy, v. 49, p. 3208-3216.

Dhaliwal, K., G. Escher, A. Unciti-Broceta, N. McDonald, A. J. Simpson, C. Haslett, and M. Bradley, 2011, Far red and NIR dye-peptoid conjugates for efficient immune cell labelling and tracking in preclinical models: MedChemComm, v. 2, p. 1050-1053.

Diacon, A. H., A. Pym, M. Grobusch, R. Patientia, R. Rustomjee, L. Page-Shipp, C. Pistorius, R. Krause, M. Bogoshi, G. Churchyard, A. Venter, J. Allen, J. C. Palomino, T. De Marez, R. P. van Heeswijk, N. Lounis, P. Meyvisch, J. Verbeeck, W. Parys, K. de Beule, K. Andries, and D. F. Mc Neeley, 2009, The diarylquinoline TMC207 for multidrug-resistant tuberculosis: New England Journal of Medicine, v. 360, p. 2397-2405.

Diekema, D. J., M. A. Pfaller, F. J. Schmitz, J. Smayevsky, J. Bell, R. N. Jones, and M. Beach, 2001, Survey of Infections Due to *Staphylococcus* Species: Frequency of Occurrence and Antimicrobial Susceptibility of Isolates Collected in the United States, Canada, Latin America, Europe, and the Western Pacific Region for the SENTRY Antimicrobial: Clinical Infectious Diseases, v. 32, p. S114.

Diep, B. A., H. F. Chambers, C. J. Graber, J. D. Szumowski, L. G. Miller, L. L. Han, J. H. Chen, F. Lin, J. Lin, T. H. Phan, H. A. Carleton, L. K. McDougal, F. C. Tenover, D. E. Cohen, K. H. Mayer, G. F. Sensabaugh, and F. Perdreau-Remington, 2008, Emergence of multidrug-resistant, community-associated, methicillin-resistant *Staphylococcus aureus* clone USA300 in men who have sex with men: Annals Of Internal Medicine, v. 148, p. 249-257.

Doern, G. V., R. Vautour, M. Gaudet, and B. Levy, 1994, Clinical impact of rapid in vitro susceptibility testing and bacterial identification: Journal Of Clinical Microbiology, v. 32, p. 1757-1762.

Dohm, M. T., R. Kapoor, and A. E. Barron, 2011, Peptoids: bio-inspired polymers as potential pharmaceuticals: Current Pharmaceutical Design, v. 17, p. 2732-2747.

Dollins, C. M., S. Nair, D. Boczkowski, J. Lee, J. M. Layzer, E. Gilboa, and B. A. Sullenger, 2008, Assembling OX40 aptamers on a molecular scaffold to create a receptor-activating aptamer: Chemistry & Biology, v. 15, p. 675-682.

Draker, K.-A., D. D. Boehr, N. H. Elowe, T. J. Noga, and G. D. Wright, 2003, Functional Annotation of Putative Aminoglycoside Antibiotic Modifying Proteins in Mycobacterium tuberculosis H37Rv: The Journal of Antibiotics, v. 56, p. 135-142.

Dransfield, I., A. M. Buckle, J. S. Savill, A. McDowall, C. Haslett, and N. Hogg, 1994, Neutrophil apoptosis is associated with a reduction in CD16 (Fc gamma RIII) expression: Journal Of Immunology (Baltimore, Md.: 1950), v. 153, p. 1254-1263.

Duan, N., S. Wu, C. Zhu, X. Ma, Z. Wang, Y. Yu, and Y. Jiang, 2012, Dual-color upconversion fluorescence and aptamer-functionalized magnetic nanoparticles-based bioassay for the simultaneous detection of *Salmonella typhimurium* and *Staphylococcus aureus* (Report): Analytica Chimica Acta, p. 1.

Dubois, A. V., P. Midoux, D. Gras, M. S. Tahar, D. Bréa, S. Attucci, M. K. Khelloufi, R. Ramphal, P. Diot, F. Gauthier, and V. Hervé, 2013, Poly-l-Lysine Compacts DNA, Kills Bacteria, and Improves Protease Inhibition in Cystic Fibrosis Sputum: American Journal of Respiratory & Critical Care Medicine, v. 188, p. 703-709.

Dubos, R. J., 1939, Studies on a bactericidal agent extracted from a soil bacillus: II. Protective effect of the bactericidal agent against experimental *pneumococcus* infections in mice: The Journal of Experimental Medicine, v. 70, p. 11-17.

Easton, D. M., A. Nijnik, M. L. Mayer, and R. E. W. Hancock, 2009, Potential of immunomodulatory host defense peptides as novel anti-infectives: Trends in biotechnology.

Edgar, R., M. McKinstry, J. Hwang, A. B. Oppenheim, R. A. Fekete, G. Giulian, C. Merril, K. Nagashima, and S. Adhya, 2006, High-sensitivity bacterial detection using biotin-tagged phage and quantum-dot nanocomplexes.(Applied biological sciences) (Author abstract): Proceedings of the National Academy of Sciences of the United States, p. 4841.

Edman, C. F., P. Mehta, R. Press, C. A. Spargo, G. T. Walker, and M. Nerenberg, 2000, Pathogen analysis and genetic predisposition testing using microelectronic arrays and isothermal amplification: Journal of Investigative Medicine, v. 48, p. 93-101.

Ekdahl, K., 1995, Immunological aspects on pneumococcal infections: with special reference to bacteremic pneumococcal infections and recurrent pneumonia: Theses thesis, Lund.

Ellington, A. D., and J. W. Szostak, 1990, In vitro selection of RNA molecules that bind specific ligands: Nature, p. 818.

Eltahawy, A. T., 1983, The penetration of mammalian cells by antibiotics: The Journal Of Antimicrobial Chemotherapy, v. 11, p. 293-298.

Endimiani, A., K. M. Hujer, A. M. Hujer, E. S. Armstrong, Y. Choudhary, J. B. Aggen, and R. A. Bonomo, 2009, ACHN-490, a Neoglycoside with Potent In

Vitro Activity against Multidrug-Resistant Klebsiella pneumoniae Isolates: Antimicrobial Agents and Chemotherapy, v. 53, p. 4504-4507.

Enright, M. C., D. A. Robinson, G. Randle, E. J. Feil, H. Grundmann, and B. G. Spratt, 2002, The evolutionary history of methicillin-resistant Staphylococcus aureus (MRSA): Proceedings - National Academy of Sciences USA, v. 99, p. 7687-7692.

Epand, R. M., and R. F. Epand, 2011, Bacterial membrane lipids in the action of antimicrobial agents: Journal of Peptide Science, v. 17, p. 298-305.

Fadeel, B., and D. Xue, 2009, The ins and outs of phospholipid asymmetry in the plasma membrane: roles in health and disease: Critical Reviews In Biochemistry And Molecular Biology, v. 44, p. 264-277.

Fadnes, B., O. Rekdal, and L. Uhlin-Hansen, 2009, The anticancer activity of lytic peptides is inhibited by heparin sulphate on the surface of the tumour cells: BMC Cancer, v. 9, p. 183-183.

Fara, M. A., J. J. Diaz-Mochon, and M. Bradley, 2006, Microwave-assisted coupling with DIC/HOBt for the synthesis of difficult peptoids and fluorescently labelled peptides -- a gentle heat goes a long way: Tetrahedron Letters, p. 1011.

Fickert H, Fransson IG, and H. U, 2006, Aptamers to small molecules, in K. S, ed., The aptamer handbook: functional oligonucleotides and their applications: Weinheim, Wiley-VCH verlag GmbH & Co. KGaA, p. 94-115.

Fischbach, M. A., and C. T. Walsh, 2009, Antibiotics for emerging pathogens: Science, p. 1089.

Fitzwater, T., and B. Polisky, 1996, A SELEX primer: Combinatorial chemistry, v. 267, p. 275-301.

Fjell, C. D., J. A. Hiss, R. E. W. Hancock, and G. Schneider, 2012, Designing antimicrobial peptides: form follows function: Nature Reviews Drug Discovery, p. 37.

Fleming, A., 1922, On a Remarkable Bacteriolytic Element Found in Tissues and Secretions: Proceedings of the Royal Society of London. Series B, Containing Papers of a Biological Character, p. 306.

Fowler, S. A., and H. E. Blackwell, 2009, Structure-function relationships in peptoids: Recent advances toward deciphering the structural requirements for biological function: Organic & Biomolecular Chemistry, v. 7, p. 1508-1524.

Fuller, A. A., F. J. Seidl, P. A. Bruno, M. A. Plescia, and K. S. Palla, 2011, Use of the Environmentally Sensitive Fluorophore 4-N,N-Dimethylamino-1,8-naphthalimide to Study Peptoid Helix Structures: Biopolymers, v. 96, p. 627-638.

Futaki, S., T. Suzuki, W. Ohashi, T. Yagami, S. Tanaka, K. Ueda, and Y. Sugiura, 2001, Arginine-rich peptides - An abundant source of membrane-permeable peptides having potential as carriers for intracellular protein delivery: Journal of Biological Chemistry, v. 276, p. 5836-5840.

Gaisford, W. C., and P. E. Reynolds, 1989, Methicillin resistance in *Staphylococcus epidermidis*. Relationship between the additional penicillin-binding protein and an attachment transpeptidase: European Journal of Biochemistry, v. 185, p. 211-218.

Gales, A. C., H. S. Sader, S. S. Andrade, L. Lutz, A. Machado, and A. L. Barth, 2006, Emergence of linezolid-resistant *Staphylococcus aureus* during

treatment of pulmonary infection in a patient with cystic fibrosis: International Journal of Antimicrobial Agents, p. 300.

Ganz, T., 2003, Defensins: antimicrobial peptides of innate immunity: Nature Reviews Immunology, p. 710.

Garcia-Martinez, C., M. Humet, R. Planells-Cases, A. Gomis, M. Caprini, F. Viana, E. De la Pena, F. Sanchez-Baeza, T. Carbonell, C. De Felipe, E. Perez-Paya, C. Belmonte, A. Messeguer, and A. Ferrer-Montiel, 2002, Attenuation of thermal nociception and hyperalgesia by VR1 blockers.(Abstract): Proceedings of the National Academy of Sciences of the United States, p. 2374.

Gennaro, R., and M. Zanetti, 2000, Structural features and biological activities of the cathelicidin-derived antimicrobial peptides: Biopolymers, v. 55, p. 31-49.

Georgopapadakou, N. H., B. A. Dix, and Y. R. Mauriz, 1986, Possible physiological functions of penicillin-binding proteins in *Staphylococcus aureus*: Antimicrobial Agents And Chemotherapy, v. 29, p. 333-336.

Giacometti, A., O. Cirioni, F. Barchiesi, M. S. Del Prete, and G. Scalise, 1999, Antimicrobial activity of polycationic peptides: Peptides, v. 20, p. 1265-1273.

Gibbons, J. A., A. A. Hancock, C. R. Vitt, S. Knepper, S. A. Buckner, M. E. Brune, I. Milicic, J. F. Kerwin, Jr., L. S. Richter, E. W. Taylor, K. L. Spear, R. N. Zuckermann, D. C. Spellmeyer, R. A. Braeckman, and W. H. Moos, 1996, Pharmacologic characterization of CHIR 2279, an N-substituted glycine peptoid with high-affinity binding for alpha 1-adrenoceptors: The Journal Of Pharmacology And Experimental Therapeutics, v. 277, p. 885-899.

Gilboa, E., J. McNamara, and F. Pastor, 2013, Use of Oligonucleotide Aptamer Ligands to Modulate the Function of Immune Receptors: Clinical Cancer Research, v. 19, p. 1054-1062.

Giralt, E., 2014, Small Wonders: Peptides for Disease Control. Edited by Kanniah Rajasekaran, Jeffrey W. Cary, Jesse M. Jaynes and Emilio Montesinos: ChemMedChem, v. 9, p. 233.

Gobbo, M., M. Benincasa, G. Bertoloni, B. Biondi, R. Dosselli, E. Papini, E. Reddi, R. Rocchi, R. Tavano, and R. Gennaro, 2009, Substitution of the Arginine/Leucine Residues in Apidaecin Ib with Peptoid Residues: Effect on Antimicrobial Activity, Cellular Uptake, and Proteolytic Degradation: Journal of Medicinal Chemistry, v. 52, p. 5197-5206.

Goessens, W. H. F., A. K. van der Bij, R. van Boxtel, J. D. D. Pitout, P. van Ulsen, D. C. Melles, and J. Tommassen, 2013, Antibiotic trapping by plasmid-encoded CMY-2 β-lactamase combined with reduced outer membrane permeability as a mechanism of carbapenem resistance in Escherichia coli: Antimicrobial Agents and Chemotherapy, v. 57, p. 3941-3949.

Goffin, C., and J. M. Ghuysen, 1998, Multimodular penicillin-binding proteins: an enigmatic family of orthologs and paralogs: Microbiology and Molecular Biology Reviews: MMBR, v. 62, p. 1079-1093.

Gold, L., B. Polisky, O. Uhlenbeck, and M. Yarus, 1995, Diversity of oligonucleotide functions: Annual Review of Biochemistry, v. 64, p. 763-797.

Bibliography

Goldman, E. R., G. P. Anderson, J. L. Liu, J. B. Delehanty, L. J. Sherwood, L. E. Osborn, L. B. Cummins, and A. Hayhurst, 2006, Facile generation of heat-stable antiviral and antitoxin single domain antibodies from a semisynthetic llama library.(Author abstract): Analytical Chemistry, p. 8245.

Goodson, B., A. Ehrhardt, S. Ng, J. Nuss, K. Johnson, M. Giedlin, R. Yamamoto, W. H. Moos, A. Krebber, M. Ladner, M. B. Giacona, C. Vitt, and J. Winter, 1999, Characterization of novel antimicrobial peptoids: Antimicrobial Agents and Chemotherapy, v. 43, p. 1429-1434.

Gopinath, S. C. B., 2007, Methods developed for SELEX: Analytical and Bioanalytical Chemistry, v. 387, p. 171-182.

Gotoh, Y., Y. Eguchi, T. Watanabe, S. Okamoto, A. Doi, and R. Utsumi, 2010, Two-component signal transduction as potential drug targets in pathogenic bacteria: Current Opinion in Microbiology, p. 232.

Gottschalk, S., D. Ifrah, S. Lerche, C. T. Gottlieb, M. T. Cohn, H. Hiasa, P. R. Hansen, L. Gram, H. Ingmer, and L. E. Thomsen, 2013, The antimicrobial lysine-peptoid hybrid LP5 inhibits DNA replication and induces the SOS response in *Staphylococcus aureus*: BMC Microbiology, v. 13, p. 1-8.

Gould, I. M., M. Z. David, S. Esposito, J. Garau, G. Lina, T. Mazzei, and G. Peters, 2012, New insights into meticillin-resistant *Staphylococcus aureus* (MRSA) pathogenesis, treatment and resistance: International Journal Of Antimicrobial Agents, v. 39, p. 96-104.

Grave, K., J. Torren-Edo, and D. Mackay, 2010, Comparison of the sales of veterinary antibacterial agents between 10 European countries: Journal of Antimicrobial Chemotherapy (JAC), v. 65, p. 2037-2040.

Gregory, P. D., R. A. Lewis, S. P. Curnock, and K. G. Dyke, 1997, Studies of the repressor (BlaI) of beta-lactamase synthesis in *Staphylococcus aureus*: Molecular Microbiology, v. 24, p. 1025-1037.

Grün, C. H., F. Hochstenbach, B. M. Humbel, A. J. Verkleij, J. H. Sietsma, F. M. Klis, J. P. Kamerling, and J. F. G. Vliegenthart, 2005, The structure of cell wall α-glucan from fission yeast: Glycobiology, v. 15, p. 245.

Gualerzi, C. O., 2014, Antibiotics [electronic resource]: targets, mechanisms and resistance / edited by Claudio O. Gualerzi ... [et al.], Weinheim, Germany: Wiley-VCH, c2014.

Guani-Guerra, E., T. Santos-Mendoza, S. O. Lugo-Reyes, and L. M. Teran, 2010, Antimicrobial peptides: General overview and clinical implications in human health and disease (Report): Clinical Immunology, p. 1.

Guilhelmelli, F., N. Vilela, P. Albuquerque, L. D. Derengowski, I. Silva-Pereira, and C. M. Kyaw, 2013, Antibiotic development challenges: the various mechanisms of action of antimicrobial peptides and of bacterial resistance: Frontiers in Microbiology, v. 4.

Gunderson, C. W., and A. M. Segall, 2006, DNA repair, a novel antibacterial target: Holliday junction-trapping peptides induce DNA damage and chromosome segregation defects: Molecular Microbiology, v. 59, p. 1129-1148.

Haghighat, S., S. D. Siadat, Rezayat, A. A. Sepahi, and M. Mahdavi, 2013, Cloning, Expression and Purification of Penicillin Binding Protein2a (PBP2a) from Methicillin Resistant *Staphylococcus aureus* : A Study on Immunoreactivity in Balb/C Mouse: Avicenna Journal of Medical Biotechnology, v. 5, p. 204-211.

Hale, J. D., and R. E. Hancock, 2007, Alternative mechanisms of action of cationic antimicrobial peptides on bacteria: Expert Review of Anti-infective Therapy, v. 5, p. 951-959.

Hamasaki, A., F. Sendo, K. Nakayama, N. Ishida, I. Negishi, and S. Hatakeyama, 1998, Accelerated neutrophil apoptosis in mice lacking A1-a, a subtype of the bcl-2-related A1 gene: The Journal Of Experimental Medicine, v. 188, p. 1985-1992.

Hamula, C. L. A., X. C. Le, and X. F. Li, 2011, DNA Aptamers Binding to Multiple Prevalent M-Types of *Streptococcus pyogenes*: Analytical chemistry, v. 83, p. 3640-3647.

Han, D., G. Z. Zhu, C. C. Wu, Z. Zhu, T. Chen, X. B. Zhang, and W. H. Tan, 2013, Engineering a Cell-Surface Aptamer Circuit for Targeted and Amplified Photodynamic Cancer Therapy: ACS Nano, v. 7, p. 2312-2319.

Hanberger, H., S. Walther, M. Leone, P. S. Barie, J. Rello, J. Lipman, J. C. Marshall, A. Anzueto, Y. Sakr, P. Pickkers, P. Felleiter, M. Engoren, and J.-L. Vincent, 2011, Increased mortality associated with methicillin-resistant *Staphylococcus aureus* (MRSA) infection in the intensive care unit: results from the EPIC II study: International Journal Of Antimicrobial Agents, v. 38, p. 331-335.

Hancock, R. E. W., A. Nijnik, and D. J. Philpott, 2012, Modulating immunity as a therapy for bacterial infections: Nature Reviews. Microbiology, v. 10, p. 243-254.

Hancock, R. E. W., and A. Rozek, 2002, Role of membranes in the activities of antimicrobial cationic peptides: FEMS Microbiology Letters, v. 206, p. 143-149.

Hancock, R. E. W., and G. Diamond, 2000, The role of cationic antimicrobial peptides in innate host defences: Trends in Microbiology, v. 8, p. 402-410.

Hancock, R. E. W., and H.G. Sahl, 2006, Antimicrobial and host-defense peptides as new anti-infective therapeutic strategies: Nature Biotechnology, v. 24, p. 1551-1557.

Haney, E. F., and R. E. W. Hancock, 2013, Peptide design for antimicrobial and immunomodulatory applications: Biopolymers, v. 100, p. 572-583.

Harris, M., H. M. Mora-Montes, N. A. R. Gow, and P. J. Coote, 2009, Loss of mannosylphosphate from Candida albicans cell wall proteins results in enhanced resistance to the inhibitory effect of a cationic antimicrobial peptide via reduced peptide binding to the cell surface: Microbiology (Reading, England), v. 155, p. 1058-1070.

Hartman, B., and A. Tomasz, 1981, Altered penicillin-binding proteins in methicillin-resistant strains of *Staphylococcus aureus*: Antimicrobial Agents And Chemotherapy, v. 19, p. 726-735.

Haslett, C., 1999, Granulocyte apoptosis and its role in the resolution and control of lung inflammation: American Journal of Respiratory and Critical Care Medicine, v. 160, p. S5-S11.

Hazlett, L., and M. Wu, 2011, Defensins in innate immunity: Cell and Tissue Research, v. 343, p. 175-188.

Hilary, B., L. Bernard, and V. Eric, 2005, Tat peptide-mediated cellular delivery: back to basics: Advanced Drug Delivery Reviews, v. 57, p. 559-577.

Hilchie, A. L., K. Wuerth, and R. E. W. Hancock, 2013, Immune modulation by multifaceted cationic host defense (antimicrobial) peptides: Nature Chemical Biology, v. 9, p. 761-768.

Hiramatsu, K., L. Cui, M. Kuroda, and T. Ito, 2001, The emergence and evolution of methicillin-resistant *Staphylococcus aureus*: Trends In Microbiology, v. 9, p. 486-493.

Hoban, D. J., D. J. Biedenbach, A. H. Mutnick, and R. N. Jones, 2003, Pathogen of occurrence and susceptibility patterns associated with pneumonia in hospitalized patients in North America: results of the SENTRY Antimicrobial Surveillance Study (2000): Diagnostic Microbiology and Infectious Disease, v. 45, p. 279-285.

Holden, M. T. G., E. J. Feil, J. A. Lindsay, S. J. Peacock, N. P. J. Day, M. C. Enright, T. J. Foster, C. E. Moore, L. Hurst, R. Atkin, A. Barron, N. Bason, S. D. Bentley, C. Chillingworth, T. Chillingworth, C. Churcher, L. Clark, C. Corton, A. Cronin, J. Doggett, L. Dowd, T. Feltwell, Z. Hance, B. Harris, H. Hauser, S. Holroyd, K. Jagels, K. D. James, N. Lennard, A. Line, R. Mayes, S. Moule, K. Mungall, D. Ormond, M. A. Quail, E. Rabbinowitsch, K. Rutherford, M. Sanders, S. Sharp, M. Simmonds, K. Stevens, S. Whitehead, B. G. Barrell, B. G. Spratt, and J. Parkhill, 2004, Complete genomes of two clinical *Staphylococcus aureus* strains: evidence for the rapid evolution of virulence and drug resistance: Proceedings Of The National Academy Of Sciences Of The United States Of America, v. 101, p. 9786-9791.

Hong, H., S. Goel, Y. Zhang, and W. Cai, 2011, Molecular imaging with nucleic acid aptamers: Current Medicinal Chemistry, v. 18, p. 4195-4205.

Hooper, D. C., and J. S. Wolfson, 1993, Quinolone antimicrobial agents / edited by David C. Hooper and John S. Wolfson, Washington, D.C: American Society for Microbiology.

Houghton, J. L., K. D. Green, W. Chen, and S. Garneau-Tsodikova, 2010, The future of aminoglycosides: the end or renaissance: Chembiochem: A European Journal Of Chemical Biology, v. 11, p. 880-902.

Huang, C. J., H. I. Lin, S. C. Shiesh, and G. B. Lee, 2010, Integrated microfluidic system for rapid screening of CRP aptamers utilizing systematic evolution of ligands by exponential enrichment (SELEX): Biosensors & Bioelectronics, v. 25, p. 1761-1766.

Huang, Y. B., J. F. Huang, and Y. X. Chen, 2010, Alpha-helical cationic antimicrobial peptides: relationships of structure and function: Protein & Cell, v. 1, p. 143-152.

Hubbard, B. K., and C. T. Walsh, 2003, Vancomycin assembly: Nature's way: Angewandte Chemie International Edition, v. 42, p. 730-765.

Hwang, P. M., and H. J. Vogel, 1998, Structure-function relationships of antimicrobial peptides, Biochemistry and Cell Biology, p. 235-246.

Hybarger, G., J. Bynum, R. F. Williams, J. J. Valdes, and J. P. Chambers, 2006, A microfluidic SELEX prototype: Analytical and Bioanalytical Chemistry, v. 384, p. 191-198.

Ilker, M. F., K. Nusslein, G. N. Tew, and E. B. Coughlin, 2004, Tuning the hemolytic and antibacterial activities of amphiphilic polynorbornene derivatives: Journal of the American Chemical Society, v. 126, p. 15870-15875.

Ito, T., K. Hiramatsu, A. Tomasz, H. de Lencastre, V. Perreten, M. T. G. Holden, D. C. Coleman, R. Goering, P. M. Giffard, R. L. Skov, K. Zhang, H. Westh, F. O'Brien, F. C. Tenover, D. C. Oliveira, S. Boyle-Vavra, F. Laurent, A. M. Kearns, B. Kreiswirth, K. S. Ko, H. Grundmann, J. E. Sollid, J. F. John, Jr., R. Daum, B. Soderquist, and G. Buist, 2012, Guidelines for reporting novel mecA gene homologues: Antimicrobial Agents And Chemotherapy, v. 56, p. 4997-4999.

Jabes, D., 2011, The antibiotic R&D pipeline: an update: Current Opinion in Microbiology, p. 564.

Jacqueline, C., D. Navas, E. Batard, A. F. Miegeville, V. Le Mabecque, M. F. Kergueris, D. Bugnon, G. Potel, and J. Caillon, 2005, In vitro and in vivo synergistic activities of linezolid combined with subinhibitory concentrations of imipenem against methicillin-resistant *Staphylococcus aureus*: Antimicrobial Agents and Chemotherapy, v. 49, p. 45-51.

Jain, P., C. Saravanan, and S. K. Singh, 2013, Sulphonamides: Deserving class as MMP inhibitors: European Journal of Medicinal Chemistry, p. 89.

Janer, C., C. Pelaez, and T. Requena, 2004, Caseinomacropeptide and whey protein concentrate enhance Bifidobacterium lactis growth in milk: Food Chemistry, v. 86, p. 263-267.

Janion, C., 2008, Inducible SOS response system of DNA repair and mutagenesis in Escherichia coli: International Journal of Biological Sciences, v. 4, p. 338-344.

Jellinek, D., L. S. Green, C. Bell, and N. Janjić, 1994, Inhibition of receptor binding by high-affinity RNA ligands to vascular endothelial growth factor: Biochemistry, v. 33, p. 10450-10456.

Jenison, R. D., S. C. Gill, A. Pardi, and B. Polisky, 1994, High-Resolution Molecular Discrimination by RNA: Science, p. 1425.

Jenssen, H., P. Hamill, and R. E. W. Hancock, 2006, Peptide antimicrobial agents: Clinical Microbiology Reviews, v. 19, p. 491-511.

Jevons, M. P., A. W. Coe, and M. T. Parker, 1963, Methicillin resistance in staphylococci: Lancet, v. 1, p. 904-907.

Jiang, Z., P. Hu, J. Liu, D. Wang, L. Jin, and C. Hong, 2014, Screening Preoperative Peptide Biomarkers for Predicting Postoperative Myocardial Infarction after Coronary Artery Bypass Grafting: PLoS ONE, v. 9, p. 1-8.

Jinghui, W., M. J. Morton, C. T. Elliott, N. Karoonuthaisiri, L. Segatori, and S. L. Biswal, 2014, Rapid detection of pathogenic bacteria and screening of phage-derived peptides using microcantilevers: Analytical Chemistry, p. 1671.

Johannsson, B., S. J. Johnson, E. J. Ernst, S. E. Beekmann, L. Herwaldt, D. J. Diekema, and P. M. Polgreen, 2012, Antimicrobial therapy for bloodstream infection due to methicillin-susceptible *Staphylococcus aureus* in an era of increasing methicillin resistance: opportunities for antimicrobial stewardship: The Annals Of Pharmacotherapy, v. 46, p. 904-905.

Joshi, R., H. Janagama, H. P. Dwivedi, T. Kumar, L. A. Jaykus, J. Schefers, and S. Sreevatsan, 2009, Selection, characterization, and application of DNA aptamers for the capture and detection of Salmonella enterica serovars: Molecular and Cellular Probes, v. 23, p. 20-28.

Kapoor, R., M. W. Wadman, M. T. Dohm, A. M. Czyzewski, A. M. Spormann, and A. E. Barron, 2011, Antimicrobial peptoids are effective against Pseudomonas aeruginosa biofilms: Antimicrobial Agents And Chemotherapy, v. 55, p. 3054-3057.

Katayama, Y., T. Ito, and K. Hiramatsu, 2000, A new class of genetic element, staphylococcus cassette chromosome mec, encodes methicillin resistance in *Staphylococcus aureus*: Antimicrobial Agents and Chemotherapy, v. 44, p. 1549-1555.

Katz, M. L., L. V. Mueller, M. Polyakov, and S. F. Weinstock, 2006, Where have all the antibiotic patents gone: Nature Biotechnology, v. 24, p. 1529-1531.

Kaur, S., K. Harjai, and S. Chhibber, 2012, Methicillin-resistant *Staphylococcus aureus* phage plaque size enhancement using sublethal concentrations of antibiotics: Applied and Environmental Microbiology, v. 78, p. 8227-8233.

Kavanagh, K., and S. Dowd, 2004, Histatins: antimicrobial peptides with therapeutic potential: The Journal of Pharmacy and Pharmacology, v. 56, p. 285-289.

Kay, B. K., M. Yamabhai, J. Kasanov, and A. Kourakine, 1998, Mapping protein-protein interactions with phage-displayed combinatorial peptide libraries: FASEB Journal, v. 12, p. A1320-A1320.

Keefe, A. D., and S. T. Cload, 2008, SELEX with modified nucleotides: Current Opinion in Chemical Biology, v. 12, p. 448-456.

Keefe, A. D., S. Pai, and A. Ellington, 2010, Aptamers as therapeutics: Nature Reviews. Drug Discovery, v. 9, p. 537-550.

Kennedy, A. D., and F. R. DeLeo, 2009, Neutrophil apoptosis and the resolution of infection: Immunologic Research, v. 43, p. 25-61.

Kim, C., C. Milheiriço, S. Gardete, M. A. Holmes, M. T. G. Holden, H. de Lencastre, and A. Tomasz, 2012, Properties of a novel PBP2A protein homolog from *Staphylococcus aureus* strain LGA251 and its contribution to the β-lactam-resistant phenotype: The Journal Of Biological Chemistry, v. 287, p. 36854-36863.

Kim, S., Y. Kim, P. Kim, J. Ha, K. Kim, M. Sohn, J.S. Yoo, J. Lee, J. Kwon, and K. N. Lee, 2006, Improved sensitivity and physical properties of sol-gel protein chips using large-scale material screening and selection: Analytical Chemistry, p. 7392.

Kim, Y. S., C. J. Hyun, I. A. Kim, and M. B. Gu, 2010, Isolation and characterization of enantioselective DNA aptamers for ibuprofen: Bioorganic & Medicinal Chemistry, v. 18, p. 3467-3473.

Klein, E., D. L. Smith, and R. Laxminarayan, 2007, Hospitalizations and Deaths Caused by Methicillin-Resistant Staphylococcus aureus, United States, 1999-2005: Emerging Infectious Diseases, v. 13, p. 1840-1846.

Klevens, R. M., J. R. Edwards, C. L. Richards, Jr., T. C. Horan, R. P. Gaynes, D. A. Pollock, and D. M. Cardo, 2007, Estimating health care-associated infections and deaths in U.S. Hospitals, 2002: Public Health Reports, p. 160.

Klussmann, S., 2006, The aptamer handbook: functional oligonucleotides and their applications / edited by Sven Klussmann, Weinheim : Wiley-VCH, c2006.

Knappe, D., P. Henklein, R. Hoffmann, and K. Hilpert, 2010, Easy strategy to protect antimicrobial peptides from fast degradation in serum: Antimicrobial Agents And Chemotherapy, v. 54, p. 4003-4005.

Kong, H. Y., and J. Byun, 2013, Nucleic Acid Aptamers: New Methods for Selection, Stabilization and Application in Biomedical Science: Biomolecules and Therapeutics, v. 21, p. 423-434.

Kulkarni, O., D. Eulberg, N. Selve, S. Zoellner, R. Allam, R. D. Pawar, S. Pfeiffer, S. Segerer, S. Klussmann, and H. J. Anders, 2009, Anti-Ccl2 Spiegelmer Permits 75% Dose Reduction of Cyclophosphamide to Control Diffuse Proliferative Lupus Nephritis and Pneumonitis in MRL-Fas(lpr) Mice: Journal of Pharmacology and Experimental Therapeutics, v. 328, p. 371-377.

Kulkarni, O., R. D. Pawar, W. Purschke, D. Eulberg, N. Selve, K. Buchner, V. Ninichuk, S. Segerer, V. Vielhauer, S. Klussmann, and H. J. Anders, 2007, Spiegelmer inhibition of CCL2/MCP-1 ameliorates lupus nephritis in MRL-(Fas)lpr mice: Journal of the American Society of Nephrology, v. 18, p. 2350-2358.

Kurlenda, J., M. Grinholc, and P. Szweda, 2010, Lack of correlation between X region spa polymorphism and virulence of methicillin resistant and methicillin sensitive *Staphylococcus aureus* strains: Acta Biochimica Polonica, v. 57, p. 135-138.

Kuroda, M., T. Ohta, I. Uchiyama, T. Baba, H. Yuzawa, I. Kobayashi, L. Cui, A. Oguchi, K.-i. Aoki, Y. Nagai, J. Lian, T. Ito, M. Kanamori, H. Matsumaru, A. Maruyama, H. Murakami, A. Hosoyama, Y. Mizutani-Ui, N. K. Takahashi, and T. Sawano, 2001, Whole genome sequencing of meticillin-resistant *Staphylococcus aureus*: Lancet, v. 357, p. 1225.

Kwon, Y.-U., and T. Kodadek, 2008, Encoded combinatorial libraries for the construction of cyclic peptoid microarrays: Chemical Communications (Cambridge, England), p. 5704-5706.

Lakhin, A. V., V. Z. Tarantul, and L. V. Gening, 2013, Aptamers: problems, solutions and prospects: Acta Naturae, v. 5, p. 34-43.

Lascelles, J., and D. D. Woods, 1952, The synthesis of folic acid by Bacterium coll and Staphylococcus aureus and its inhibition by sulphonamides: British Journal Of Experimental Pathology, v. 33, p. 288-303.

Lautner, G., Z. Balogh, A. Gyurkovics, R. E. Gyurcsányi, and T. Mészáros, 2012, Homogeneous assay for evaluation of aptamer-protein interaction: The Analyst, v. 137, p. 3929-3931.

Laverty, G., S. P. Gorman, and B. F. Gilmore, 2011, The Potential of Antimicrobial Peptides as Biocides: International Journal of Molecular Sciences, v. 12, p. 6566-6596.

Lee, B. C., T. K. Chu, K. A. Dill, and R. N. Zuckermann, 2008, Biomimetic nanostructures: Creating a high-affinity zinc-binding site in a folded nonbiological polymer: Journal of the American Chemical Society, v. 130, p. 8847-8855.

Lee, B.-C., and R. N. Zuckermann, 2011, Protein side-chain translocation mutagenesis via incorporation of peptoid residues: ACS Chemical Biology, v. 6, p. 1367-1374.

Lee, H. J., B. C. Kim, K. W. Kim, Y. K. Kim, J. Kim, and M. K. Oh, 2009, A sensitive method to detect *Escherichia coli* based on immunomagnetic separation and real-time PCR amplification of aptamers: Biosensors & Bioelectronics, v. 24, p. 3550-3555.

Lee, J., D. G. Udugamasooriya, H. S. Lim, and T. Kodadek, 2010, Potent and selective photo-inactivation of proteins with peptoid-ruthenium conjugates: Nature Chemical Biology, v. 6, p. 258-260.

Leevy, W. M., S. T. Gammon, H. Jiang, J. R. Johnson, D. J. Maxwell, E. N. Jackson, M. Marquez, D. Piwnica-Worms, and B. D. Smith, 2006, Optical imaging of bacterial infection in living mice using a fluorescent near-infrared molecular probe: Journal Of The American Chemical Society, v. 128, p. 16476-16477.

Lehrer, R. I., A. Barton, K. A. Daher, S. S. Harwig, T. Ganz, and M. E. Selsted, 1989, Interaction of human defensins with Escherichia coli. Mechanism of bactericidal activity: The Journal of Clinical Investigation, v. 84, p. 553-561.

Lehrer, R. I., and W. Y. Lu, 2012, alpha-Defensins in human innate immunity: Immunological Reviews, v. 245, p. 84-112.

Levy, S. B., and B. Marshall, 2004, Antibacterial resistance worldwide: causes, challenges and responses: Nature Medicine, v. 10, p. S122-S129.

Li, F., Z. Du, L. Yang, and B. Tang, 2013, Selective and sensitive turn-on detection of adenosine triphosphate and thrombin based on bifunctional fluorescent oligonucleotide probe: Biosensors and Bioelectronics, p. 907.

Li, H. N., P. G. Barlow, J. Bylund, A. Mackellar, A. Bjorstad, J. Conlon, P. S. Hiemstra, C. Haslett, M. Gray, A. J. Simpson, A. G. Rossi, and D. J. Davidson, 2009, Secondary necrosis of apoptotic neutrophils induced by the human cathelicidin LL-37 is not proinflammatory to phagocytosing macrophages: Journal of Leukocyte Biology, v. 86, p. 891-902.

Li, J. W. H., and J. C. Vederas, 2009, Drug discovery and natural products: end of an era or an endless frontier: Science (New York, N.Y.), v. 325, p. 161-165.

Lim, D., and N. C. J. Strynadka, 2002, Structural basis for the beta lactam resistance of PBP2a from methicillin-resistant *Staphylococcus aureus*: Nature Structural Biology, v. 9, p. 870-876.

Lindsay, J. A., and M. T. G. Holden, 2004, *Staphylococcus aureus*: superbug, super genome: Trends in Microbiology, v. 12, p. 378-385.

Ling, M., Y. Liu, Z. Xiangxuan, Z. Lucy, Z. Haizhen, L. Chen, and T. Weihong, 2012, Targeted Delivery of Chemotherapy Agents Using a Liver Cancer-Specific Aptamer: PLoS ONE, v. 7, p. 1-8.

Liu, A., G. Abbineni, and C. Mao, 2009, Nanocomposite films assembled from genetically engineered filamentous viruses and gold nanoparticles: Nanoarchitecture- and humidity-tunable surface plasmon resonance spectra: Aus genetisch konstruierten fadenförmigen Viren und Goldnanopartikeln zusammengesetzte Nanoverbunddünnschichten. Durch Nanoarchitektur und Feuchtigkeit abstimmbare Oberflächenplasmonenresonanzspektren, p. 1001.

Liu, G. Y., A. Essex, J. T. Buchanan, V. Datta, H. M. Hoffman, J. F. Bastian, J. Fierer, and V. Nizet, 2005, *Staphylococcus aureus* golden pigment impairs neutrophil killing and promotes virulence through its antioxidant activity: Journal of Experimental Medicine, v. 202, p. 209-215.

Liu, Z., J. H. Duan, Y. M. Song, J. Ma, F. D. Wang, X. Lu, and X. D. Yang, 2012, Novel HER2 Aptamer Selectively Delivers Cytotoxic Drug to HER2-positive Breast Cancer Cells in Vitro: Journal of Translational Medicine, v. 10.

Livermore, D. M., 2011, Discovery research: the scientific challenge of finding new antibiotics: Journal of Antimicrobial Chemotherapy (JAC), v. 66, p. 1941-1944.

Lock, R. L., and E. J. Harry, 2008, Cell-division inhibitors: new insights for future antibiotics: Nature Reviews Drug Discovery, v. 7, p. 324-338.

Lohner, K., and E. J. Prenner, 1999, Differential scanning calorimetry and X-ray diffraction studies of the specificity of the interaction of antimicrobial peptides with membrane-mimetic systems: Biochimica et Biophysica Acta, v. 1462, p. 141-156.

Lolis, E., and R. Bucala, 2003, Therapeutic approaches to innate immunity: severe sepsis and septic shock: Nature Reviews. Drug Discovery, v. 2, p. 635-645.

Long, S. B., M. B. Long, R. R. White, and B. A. Sullenger, 2008, Crystal structure of an RNA aptamer bound to thrombin: Rna-A Publication Of The Rna Society, v. 14, p. 2504-2512.

Long, Y., L. Yuzi, L. Bo, W. Fei, D. Min, V. A. Petrenko, Q. Hua-Ji, and L. Aihua, 2014, Specific ligands for classical swine fever virus screened from landscape phage display library: Antiviral Research, v. 109, p. 68-71.

Lopez-Garcia, B., J. F. Marcos, C. Abad, and E. Perez-Paya, 2004, Stabilisation of mixed peptide/lipid complexes in selective antifungal hexapeptides: Biochimica et Biophysica Acta, v. 1660, p. 131-137.

Lorenz, C., and R. Schroeder, 2006, Aptamers to antibiotics, in K. S, ed., The aptamer handbook: functional oligonucleoitdes and their applications: Weinheim, Wiley-VCH Verlag GmbH & Co. KGaA, p. 116-130.

Lou, X., J. Qian, Y. Xiao, L. Viel, A. E. Gerdon, E. T. Lagally, P. Atzberger, T. M. Tarasow, A. J. Heeger, and H. T. Soh, 2009, Micromagnetic Selection of Aptamers in Microfluidic Channels: Proceedings of the National Academy of Sciences of the United States of America, p. 2989.

Lowy, F. D., 1998, *Staphylococcus aureus* infections - Reply: New England Journal of Medicine, v. 339, p. 2026-2027.

Luxenhofer, R., C. Fetsch, and A. Grossmann, 2013, Polypeptoids: A perfect match for molecular definition and macromolecular engineering: Journal of Polymer Science Part A: Polymer Chemistry, p. 2731.

Malik, A., and J. K. Batra, 2012, Antimicrobial activity of human eosinophil granule proteins: involvement in host defence against pathogens: Critical Reviews In Microbiology, v. 38, p. 168-181.

Mallorquí-Fernández, G., A. Marrero, S. García-Piquè, R. García-Castellanos, and F. X. Gomis-Rüth, 2004, Staphylococcal methicillin resistance: fine focus on folds and functions: FEMS Microbiology Letters, v. 235, p. 1-8.

Manfredi, R., 2006, Update on the appropriate use of linezolid in clinical practice: Therapeutics and Clinical Risk Management, v. 2, p. 455-464.

Mann, A. P., R. C. Bhavane, A. Somasunderam, B. Liz Montalvo-Ortiz, K. B. Ghaghada, D. Volk, R. Nieves-Alicea, K. S. Suh, M. Ferrari, A. Annapragada, D. G. Gorenstein, and T. Tanaka, 2011, Thioaptamer conjugated liposomes for tumor vasculature targeting, Jefferson Digital Commons, 2011-04-01T07:00:00Z.

Mao, C., A. Liu, and B. Cao, 2009, Virus-Based Chemical and Biological Sensing: Angewandte Chemie.

Marcos López, J. F., and M. Gandía Gómez, 2009, Antimicrobial peptides: To membranes and beyond, Expert Opinion on Drug Discovery Taylor & Francis (Informa Healthcare), 2009-07-15T11:58:42Z, p. 659-671.

Marimuthu, C., T. H. Tang, J. Tominaga, S. C. Tan, and S. C. B. Gopinath, 2012, Single-stranded DNA (ssDNA) production in DNA aptamer generation: The Analyst, v. 137, p. 1307-1315.

Martin, T. R., 2008, Interactions between Mechanical and Biological Processes in Acute Lung Injury: Proceedings of the American Thoracic Society, v. 5, p. 291-296.

Mathot, L., M. Wallin, and T. Sjoblom, 2013, Automated serial extraction of DNA and RNA from biobanked tissue specimens: BMC Biotechnology, v. 13.

Matsuhashi, M., M. D. Song, F. Ishino, M. Wachi, M. Doi, M. Inoue, K. Ubukata, N. Yamashita, and M. Konno, 1986, Molecular cloning of the gene of a penicillin-binding protein supposed to cause high resistance to beta-lactam antibiotics in *Staphylococcus aureus*: Journal of Bacteriology, v. 167, p. 975-980.

Mayers, D., 2009, Antimicrobial drug resistance handbook. Volume 1, Mechanisms of drug resistance edited by Douglas Mayers, Totowa, N.J: Humana ; London : Springer.

McIntyre, J. O., and L. M. Matrisian, 2003, Molecular imaging of proteolytic activity in cancer: Journal of Cellular Biochemistry, v. 90, p. 1087-1097.

McManus, M. C., 1997, Mechanisms of bacterial resistance to antimicrobial agents: American Journal of Health-System Pharmacy, v. 54, p. 1420-1433.

McNamara, J. O., D. Kolonias, F. Pastor, R. S. Mittler, L. Chen, P. H. Giangrande, B. Sullenger, and E. Gilboa, 2008, Multivalent 4-1BB binding aptamers costimulate CD8+ T cells and inhibit tumor growth in mice: The Journal Of Clinical Investigation, v. 118, p. 376-386.

Mencin, N., T. Smuc, M. Vranicar, J. Mavri, M. Hren, K. Galesa, P. Krkoc, H. Ulrich, and B. Solar, 2014, Optimization of SELEX: Comparison of different methods for monitoring the progress of in vitro selection of aptamers: Journal of Pharmaceutical and Biomedical Analysis, v. 91, p. 151-159.

Meng, L., L. Yang, X. X. Zhao, L. Zhang, H. Z. Zhu, C. Liu, and W. H. Tan, 2012, Targeted Delivery of Chemotherapy Agents Using a Liver Cancer-Specific Aptamer: PLOS ONE, v. 7.

Messeguer, J., N. Cortés, N. García-Sanz, G. Navarro-Vendrell, A. Ferrer-Montiel, and A. Messeguer, 2008, Synthesis of a positional scanning library of pentamers of N-alkylglycines assisted by microwave activation and validation via the identification of trypsin inhibitors: Journal Of Combinatorial Chemistry, v. 10, p. 974-980.

Meyer, T., T. Schirrmann, A. Frenzel, S. Miethe, J. Stratmann-Selke, G. F. Gerlach, K. Strutzberg-Minder, S. Dübel, and M. Hust, 2012, Identification of immunogenic proteins and generation of antibodies against Salmonella Typhimurium using phage display: BMC Biotechnology, v. 12, p. 29-29.

Mi, J., Y. Liu, Z. N. Rabbani, Z. Yang, J. H. Urban, B. A. Sullenger, and B. M. Clary, 2010, In vivo selection of tumor-targeting RNA motifs: Nature Chemical Biology, v. 6, p. 22-24.

Millar, B. C., J. R. Xu, and J. E. Moore, 2007, Molecular diagnostics of medically important bacterial infections: Current Issues in Molecular Biology, v. 9, p. 21-39.

Miller, S. M., R. J. Simon, S. Ng, R. N. Zuckermann, J. M. Kerr, and W. H. Moos, 1995, Comparison of the proteolytic susceptibilities of homologous L-amino acid, D-amino acid, and N-substituted glycine peptide and peptoid oligomers: Drug Development Research, v. 35, p. 20-32.

Mishra, B., and G. Wang, 2012, The Importance of Amino Acid Composition in Natural AMPs: An Evolutional, Structural, and Functional Perspective: Frontiers In Immunology, v. 3, p. 221-221.

Mo, R. H., J. L. Zaro, and W.C. Shen, 2012, Comparison of cationic and amphipathic cell penetrating peptides for siRNA delivery and efficacy: Molecular Pharmaceutics, v. 9, p. 299-309.

Moore, D. F., and J. I. Curry, 1998, Detection and identification of Mycobacterium tuberculosis directly from sputum sediments by ligase chain reaction: Journal of Clinical Microbiology, v. 36, p. 1028-1031.

Mora, P., I. Masip, N. Cortes, R. Marquina, R. Merino, J. Merino, T. Carbonell, I. Mingarro, A. Messeguer, and E. Perez-Paya, 2005, Identification from a positional scanning peptoid library of in vivo active compounds that neutralize bacterial endotoxins: Journal of Medicinal Chemistry, v. 48, p. 1265-1268.

Morar, M., and G. D. Wright, 2010, The Genomic Enzymology of Antibiotic Resistance: Annual Review of Genetics, vol 44, v. 44, p. 25-51.

Moret, I., M. J. Lorenzo, B. Sarria, E. Cases, E. Morcillo, M. Perpina, J. M. Molina, and R. Menendez, 2011, Increased lung neutrophil apoptosis and inflammation resolution in nonresponding pneumonia: European Respiratory Journal, v. 38, p. 1158-1164.

Mosing, R. K., S. D. Mendonsa, and M. T. Bowser, 2005, Capillary electrophoresis-SELEX selection of aptamers with affinity for HIV-1 reverse transcriptase: Analytical Chemistry, v. 77, p. 6107-6112.

Murphy, M. B., S. T. Fuller, P. M. Richardson, and S. A. Doyle, 2003, An improved method for the in vitro evolution of aptamers and applications in protein detection and purification: Nucleic Acids Research, v. 31.

Nakamura, A., K. Miyake, S. Misawa, Y. Kuno, T. Horii, S. Hori, S. Kondo, Y. Tabe, and A. Ohsaka, 2012, Association between antimicrobial consumption and clinical isolates of methicillin-resistant *Staphylococcus aureus*: a 14-year study: Journal of Infection and Chemotherapy, p. 90.

Negrea, A., E. Bjur, S. E. Ygberg, M. Elofsson, H. Wolf-Watz, and M. Rhen, 2007, Salicylidene acylhydrazides that affect type III protein secretion in Salmonella enterica serovar Typhimurium: Antimicrobial Agents and Chemotherapy, v. 51, p. 2867-2876.

Ng, E. W. M., D. T. Shima, P. Calias, E. T. Cunningham Jr, D. R. Guyer, and A. P. Adamis, 2006, Pegaptanib, a targeted anti-VEGF aptamer for ocular vascular disease: Nature Reviews Drug Discovery, v. 5, p. 123-132.

Nguyen, L. T., E. F. Haney, and H. J. Vogel, 2011, The expanding scope of antimicrobial peptide structures and their modes of action: Trends in Biotechnology, v. 29, p. 464-472.

Nicolas, P., 2009, Multifunctional host defense peptides: intracellular-targeting antimicrobial peptides: The FEBS Journal, v. 276, p. 6483-6496.

Nicolas, P., and C. El Amri, 2009, The dermaseptin superfamily: A gene-based combinatorial library of antimicrobial peptides: Biochimica et Biophysica Acta, v. 1788, p. 1537-1550.

Nicolas, P., D. Vanhoye, and M. Amiche, 2003, Molecular strategies in biological evolution of antimicrobial peptides: Peptides, v. 24, p. 1669-1680.

Nijnik, A., and R. E. W. Hancock, 2009, Host defence peptides: antimicrobial and immunomodulatory activity and potential applications for tackling antibiotic-resistant infections: Emerging Health Threats, v. 2, p. 1-7.

Nijnik, A., and R. E. W. Hancock, 2009, The roles of cathelicidin LL-37 in immune defences and novel clinical applications: Current Opinion in Hematology, v. 16, p. 41-47.

Nimjee, S. M., C. P. Rusconi, and B. A. Sullenger, 2005, Aptamers: an emerging class of therapeutics: Annual Review of Medicine, v. 56, p. 555-C-3.

Nitsche, A., A. Kurth, A. Dunkhorst, O. Pänke, H. Sielaff, W. Junge, D. Muth, F. Scheller, W. Stöcklein, C. Dahmen, G. Pauli, and A. Kage, 2007, One-step selection of Vaccinia virus-binding DNA aptamers by MonoLEX: BMC Biotechnology, v. 7, p. 48-48.

Njoroge, J., and V. Sperandio, 2009, Jamming bacterial communication: New approaches for the treatment of infectious diseases: EMBO Molecular Medicine, v. 1, p. 201-210.

Nonaka, Y., W. Yoshida, K. Abe, S. Ferri, H. Schulze, T. T. Bachmann, and K. Ikebukuro, 2013, Affinity Improvement of a VEGF Aptamer by in Silico Maturation for a Sensitive VEGF-Detection System: Analytical Chemistry, v. 85, p. 1132-1137.

Novick, R. P., 1990, Molecular biology of the staphylococci, Clinical Microbiology & Infection, v. 11, p. 1027-1034.

O'Brien, D. J., and I. M. Gould, 2013, Maximizing the impact of antimicrobial stewardship: the role of diagnostics, national and international efforts: Current Opinion in Infectious Diseases, v. 26, p. 352-358.

Office, U. S. G. A., 1999, Food safety: the agricultural use of antibiotics and its implications for human health: report to the Honorable Tom Harkin, Ranking Minority Member, Committee on Agriculture, Nutrition, and Forestry, U.S. Senate / United States General Accounting Office, Washington, D.C. (P.O. Box 37050, Washington, D.C. 20013).

Oh, S. S., K. M. Ahmad, M. Cho, S. Kim, Y. Xiao, and H. T. Soh, 2011, Improving aptamer selection efficiency through volume dilution, magnetic concentration, and continuous washing in microfluidic channels: Analytical Chemistry, p. 6883.

Ohwada, A., M. Sekiya, H. Hanaki, K. K. Arai, I. Nagaoka, S. Hori, S. Tominaga, K. Hiramatsu, and Y. Fukuchi, 1999, DNA vaccination by mecA sequence evokes an antibacterial immune response against methicillin-resistant *Staphylococcus aureus*: Journal of Antimicrobial Chemotherapy, v. 44, p. 767-774.

Olsen, E. V., I. B. Sorokulova, V. A. Petrenko, I. H. Chen, J. M. Barbaree, and V. J. Vodyanoy, 2006, Affinity-selected filamentous bacteriophage as a probe for acoustic wave biodetectors of Salmonella typhimurium: Biosensors & Bioelectronics, v. 21, p. 1434-1442.

Olsen, E. V., S. T. Pathirana, A. M. Samoylov, J. M. Barbaree, B. A. Chin, W. C. Neely, and V. Vodyanoy, 2003, Specific and selective biosensor for Salmonella and its detection in the environment: Journal of Microbiological Methods, v. 53, p. 273-285.

Oney, S., R. T. S. Lam, K. M. Bompiani, C. M. Blake, G. Quick, J. D. Heidel, J. Y.-C. Liu, B. C. Mack, M. E. Davis, K. W. Leong, and B. A. Sullenger, 2009, Development of universal antidotes to control aptamer activity: Nature Medicine, v. 15, p. 1224-1228.

Ooi, N., K. Miller, C. Randall, W. Rhys-Williams, W. Love, and I. Chopra, 2010, XF-70 and XF-73, novel antibacterial agents active against slow-growing and non-dividing cultures of Staphylococcus aureus including biofilms: The Journal Of Antimicrobial Chemotherapy, v. 65, p. 72-78.

Otero, L. H., A. Rojas-Altuve, L. I. Llarrull, C. Carrasco-Lopez, M. Kumarasiri, E. Lastochkin, J. Fishovitz, M. Dawley, D. Hesek, and M. Lee, 2013, How allosteric control of *Staphylococcus aureus* penicillin binding protein 2a enables methicillin resistance and physiological function: Proceedings of the National Academy of Sciences, USA, v. 110, p. 16808-16813.

Pantosti, A., and M. Venditti, 2009, What is MRSA?: European Respiratory Journal, v. 34, p. 1190-1196.

Papo, N., and Y. Shai, 2005, Host defense peptides as new weapons in cancer treatment: Cellular and Molecular Life Sciences (CMLS), p. 784.

Papo, N., Z. Oren, U. Pag, H. G. Sahl, and Y. Shai, 2002, The consequence of sequence alteration of an amphipathic alpha-helical antimicrobial peptide and its diastereomers: Journal of Biological Chemistry, v. 277, p. 33913-33921.

Park, B. J., Y. S. Sa, Y. H. Kim, and Y. Kim, 2012, Spectroscopic and Electrochemical Detection of Thrombin/5'-SH or 3'-SH Aptamer Immobilized on (porous) Gold Substrates: Korean Chemical Society, v. 33, p. 100-104.

Park, C. B., H. S. Kim, and S. C. Kim, 1998, Mechanism of action of the antimicrobial peptide buforin II: buforin II kills microorganisms by penetrating the cell membrane and inhibiting cellular functions: Biochemical and Biophysical Research Communications, v. 244, p. 253-257.

Park, C. B., K. S. Yi, K. Matsuzaki, M. S. Kim, and S. C. Kim, 2000, Structure-activity analysis of buforin II, a histone H2A-derived antimicrobial peptide: the proline hinge is responsible for the cell-penetrating ability of buforin II: Proceedings of the National Academy of Sciences Of The United States Of America, v. 97, p. 8245-8250.

Park, M., M. Wetzler, T. S. Jardetzky, and A. E. Barron, 2013, A Readily Applicable Strategy to Convert Peptides to Peptoid-based Therapeutics: PLoS ONE, v. 8, p. 1-7.

Park, M., T. S. Jardetzky, and A. E. Barron, 2011, NMEGylation: A Novel Modification to Enhance the Bioavailability of Therapeutic Peptides: Biopolymers, v. 96, p. 688-693.

Park, S. M., J. Y. Ahn, M. Jo, D. K. Lee, J. T. Lis, H. G. Craighead, and S. Kim, 2009, Selection and elution of aptamers using nanoporous sol-gel arrays with integrated microheaters: Lab on a Chip, v. 9, p. 1206-1212.

Pastor, F., M. M. Soldevilla, H. Villanueva, D. Kolonias, S. Inoges, A. L. de Cerio, R. Kandzia, V. Klimyuk, Y. Gleba, E. Gilboa, and M. Bendandi, 2013, CD28 Aptamers as Powerful Immune Response Modulators: Molecular Therapy-Nucleic Acids, v. 2.

Pasupuleti, M., A. Schmidtchen, and M. Malmsten, 2012, Antimicrobial peptides: key components of the innate immune system: Critical Reviews in Biotechnology, v. 32, p. 143-171.

Patch, J. A., and A. E. Barron, 2003, Helical peptoid mimics of magainin-2 amide: Journal of the American Chemical Society, v. 125, p. 12092-12093.

Patrzykat, A., C. L. Friedrich, L. Zhang, V. Mendoza, and R. E. W. Hancock, 2002, Sublethal Concentrations of Pleurocidin-Derived Antimicrobial Peptides Inhibit Macromolecular Synthesis in Escherichia coli: Antimicrobial Agents and Chemotherapy, v. 46, p. 605-614.

Payne, D. J., M. N. Gwynn, D. J. Holmes, and D. L. Pompliano, 2007, Drugs for bad bugs: confronting the challenges of antibacterial discovery: Nature Reviews Drug Discovery, v. 6, p. 29-40.

Peretto, I., R. M. Sanchez-Martin, X. Wang, J. Ellard, S. Mittoo, and M. Bradley, 2003, Cell penetrable peptoid carrier vehicles: synthesis and evaluation: Chemical Communications (Cambridge, England), p. 2312-2313.

Peschel, A., and H. G. Sahl, 2006, The co-evolution of host cationic antimicrobial peptides and microbial resistance: Nature Reviews. Microbiology, v. 4, p. 529-536.

Peschel, A., and L. V. Collins, 2001, Staphylococcal resistance to antimicrobial peptides of mammalian and bacterial origin: Peptides, v. 22, p. 1651-1659.

Phoenix, D., S. Dennison, and F. Harris, 2013, Antimicrobial peptides [electronic resource] / David A. Phoenix, Sarah R. Dennison, and Frederick Harris, Weinheim : Wiley-VCH, 2013.

Pinho, M. G., M. Kjos, and J. W. Veening, 2013, How to get (a)round: mechanisms controlling growth and division of coccoid bacteria.(Report): Nature Reviews Microbiology, p. 601.

Pinho, M. G., S. R. Filipe, H. d. Lencastre, and A. Tomasz, 2001, Complementation of the essential peptidoglycan transpeptidase function of penicillin-binding protein 2 (PBP2) by the drug resistance protein PBP2A in Staphylococcus aureus: Journal of Bacteriology, p. 6525.

Piotto, S. P., L. Sessa, S. Concilio, and P. Iannelli, 2012, YADAMP: yet another database of antimicrobial peptides: International Journal of Antimicrobial Agents, p. 346.

Ploss, M., S. J. Facey, C. Bruhn, L. Zemel, K. Hofmann, R. W. Stark, B. Albert, and B. Hauer, 2014, Selection of peptides binding to metallic borides by screening M13 phage display libraries: BMC Biotechnology, v. 14, p. 1-22.

Pompilio, A., M. Scocchi, S. Pomponio, F. Guida, A. Di Primio, E. Fiscarelli, R. Gennaro, and G. Di Bonaventura, 2011, Antibacterial and anti-biofilm effects of cathelicidin peptides against pathogens isolated from cystic fibrosis patients: Peptides, v. 32, p. 1807-1814.

Poole, K., 2012, Bacterial stress responses as determinants of antimicrobial resistance: Journal of Antimicrobial Chemotherapy (JAC), v. 67, p. 2069-2089.

Potempa, J., D. Fedak, A. Dubin, A. Mast, and J. Travis, 1991, Proteolytic inactivation of alpha-1-anti-chymotrypsin. Sites of cleavage and generation of chemotactic activity: The Journal of Biological Chemistry, v. 266, p. 21482-21487.

Qazi, S. N. A., S. E. Harrison, T. Self, P. Williams, and P. J. Hill, 2004, Real-time monitoring of intracellular *Staphylococcus aureus* replication: Journal of Bacteriology, p. 1065.

Qi, X. B., C. C. Zhou, P. Li, W. X. Xu, Y. Cao, H. Ling, W. N. Chen, C. M. Li, R. Xu, M. Lamrani, Y. G. Mu, S. S. J. Leong, M. W. Chang, and M. B. Chan-Park, 2010, Novel short antibacterial and antifungal peptides with low cytotoxicity: Efficacy and action mechanisms: Biochemical and Biophysical Research Communications, v. 398, p. 594-600.

Queck, S. Y., B. A. Khan, W. Rong, T.H. L. Bach, D. Kretschmer, C. Liang, B. N. Kreiswirth, A. Peschel, F. R. DeLeo, and M. Otto, 2009, Mobile Genetic Element-Encoded Cytolysin Connects Virulence to Methicillin Resistance in MRSA: PLoS Pathogens, v. 5, p. 1-12.

Rao, S. S., K. V. K. Mohan, Y. Gao, and C. D. Atreya, 2013, Identification and evaluation of a novel peptide binding to the cell surface of Staphylococcus aureus: Microbiological Research, v. 168, p. 106-112.

Rasko, D. A., C. G. Moreira, D. R. Li, N. C. Reading, J. M. Ritchie, M. K. Waldor, N. Williams, R. Taussig, S. Wei, M. Roth, D. T. Hughes, J. F. Huntley, M. W. Fina, J. R. Falck, and V. Sperandio, 2008, Targeting QseC Signaling and Virulence for Antibiotic Development: Science, p. 1078.

Ratledge, C., and S. G. Wilkinson, 1988, Microbial lipids / edited by C. Ratledge and S.G. Wilkinson. Vol.1, London: Academic Press, 1988.

Rayner, C., and W. J. Munckhof, 2005, Antibiotics currently used in the treatment of infections caused by *Staphylococcus aureus*: Internal Medicine Journal, v. 35 Suppl 2, p. S3-S16.

Read, J. A., and R. Duncan, 2011, Biophysical and functional assays for viral membrane fusion peptides: Methods, p. 122.

Reddy, M. M., R. Wilson, J. Wilson, S. Connell, A. Gocke, L. Hynan, D. German, and T. Kodadek, 2011, Identification of Candidate IgG Biomarkers for Alzheimer's Disease via Combinatorial Library Screening: Cell, v. 144, p. 132-142.

Rice, L. B., 2012, Mechanisms of resistance and clinical relevance of resistance to β-lactams, glycopeptides, and fluoroquinolones: Mayo Clinic Proceedings, v. 87, p. 198-208.

Robert, G., R. E. Jonathan, and S. The National Nosocomial Infections Surveillance, 2005, Overview of Nosocomial Infections Caused by Gram-Negative Bacilli, University of Chicago Press, p. 848.

Romer, P. S., S. Berr, E. Avota, S. Y. Na, M. Battaglia, I. ten Berge, H. Einsele, and T. Hunig, 2011, Preculture of PBMCs at high cell density increases sensitivity of T-cell responses, revealing cytokine release by CD28 superagonist TGN1412: Blood, v. 118, p. 6772-6782.

Rosales, A. M., H. K. Murnen, R. N. Zuckermann, and R. A. Segalman, 2010, Control of Crystallization and Melting Behavior in Sequence Specific Polypeptoids: Macromolecules, v. 43, p. 5627-5636.

Rosales, A., H. Murnen, S. Kline, R. Zuckermann, and R. Segalman, 2012, Determination of the persistence length of helical and non-helical polypeptoids in solution: Soft Matter, v. 8, p. 3673-3680.

Ross, T. M., R. N. Zuckermann, C. Reinhard, and W. H. Frey, 2008, Intranasal administration delivers peptoids to the rat central nervous system: Neuroscience Letters, v. 439, p. 30-33.

Roth, D. M., J. P. M. Senna, and D. C. Machado, 2006, Evaluation of the humoral immune response in BALB/c mice immunized with a naked DNA vaccine anti-methicillin-resistant *Staphylococcus aureus*: Genetics and molecular research: GMR.

Ruben, S., A. Perkins, R. Purcell, K. Joung, R. Sia, R. Burghoff, W. A. Haseltine, and C. A. Rosen, 1989, Structural and functional characterization of human immunodeficiency virus tat protein: Journal Of Virology, v. 63, p. 1-8.

Ruckman, J., L. S. Green, J. Beeson, S. Waugh, W. L. Gillette, D. D. Henninger, L. Claesson-Welsh, and N. Janjić, 1998, 2'-Fluoropyrimidine RNA-based aptamers to the 165-amino acid form of vascular endothelial growth factor (VEGF165). Inhibition of receptor binding and VEGF-induced vascular permeability through interactions requiring the exon 7-encoded domain: The Journal of Biological Chemistry, v. 273, p. 20556-20567.

Rudkin, J. K., M. Laabei, A. M. Edwards, H. S. Joo, M. Otto, K. L. Lennon, J. P. O'Gara, N. R. Waterfield, and R. C. Massey, 2014, Oxacillin Alters the Toxin Expression Profile of Community-Associated Methicillin-Resistant *Staphylococcus aureus*: Antimicrobial Agents and Chemotherapy, v. 58, p. 1100-1107.

Ryge, T. S., and P. R. Hansen, 2005, Novel lysine-peptoid hybrids with antibacterial properties: Journal of Peptide Science, v. 11, p. 727-734.

Ryge, T. S., N. Frimodt-Møller, and P. R. Hansen, 2008, Antimicrobial activities of twenty lysine-peptoid hybrids against clinically relevant bacteria and fungi: Chemotherapy, v. 54, p. 152-156.

Safo, M. K., T. P. Ko, F. N. Musayev, Q. Zhao, A. H. J. Wang, and G. L. Archer, 2006, Structure of the MecI repressor from Staphylococcus aureus in complex with the cognate DNA operator of mec: Acta Crystallographica. Section F, Structural Biology and Crystallization Communications, v. 62, p. 320-324.

Sainath Rao, S., K. V. K. Mohan, and C. D. Atreya, 2013, A Peptide Derived from Phage Display Library Exhibits Antibacterial Activity against *E. coli* and *Pseudomonas aeruginosa*: PLoS ONE, v. 8, p. 1-11.

Sainath Rao, S., K. V. K. Mohan, N. Nguyen, B. Abraham, G. Abdouleva, P. Zhang, and C. D. Atreya, 2010, Peptides panned from a phage-displayed random peptide library are useful for the detection of Bacillus anthracis surrogates B. cereus 4342 and B. anthracis Sterne: Biochemical and Biophysical Research Communications, v. 395, p. 93-98.

Sanborn, T. J., C. W. Wu, R. N. Zuckerman, and A. E. Barron, 2002, Extreme stability of helices formed by water-soluble poly-N-substituted glycines (polypeptoids) with alpha-chiral side chains: Biopolymers, v. 63, p. 12-20.

Sandegren, L., and D. I. Andersson, 2009, Bacterial gene amplification: implications for the evolution of antibiotic resistance: Nature Reviews. Microbiology, v. 7, p. 578-588.

Sass, P., and H. Brotz-Oesterhelt, 2013, Bacterial cell division as a target for new antibiotics: Current Opinion in Microbiology, p. 522.

Savill, J. S., A. H. Wyllie, J. E. Henson, M. J. Walport, P. M. Henson, and C. Haslett, 1989, Macrophage phagocytosis of aging neutrophils in inflammation. Programmed cell death in the neutrophil leads to its recognition by macrophages: Journal of Clinical Investigation, v. 83, p. 865-875.

Savory, N., K. Abe, K. Sode, and K. Ikebukuro, 2010, Selection of DNA aptamer against prostate specific antigen using a genetic algorithm and application to sensing: Biosensors and Bioelectronics, p. 1386.

Sayyed, S. G., H. Hägele, O. P. Kulkarni, K. Endlich, S. Segerer, D. Eulberg, S. Klussmann, and H. J. Anders, 2009, Podocytes produce homeostatic chemokine stromal cell-derived factor-1/CXCL12, which contributes to glomerulosclerosis, podocyte loss and albuminuria in a mouse model of type 2 diabetes: Diabetologia, v. 52, p. 2445-2454.

Schaberg, D. R., and M. J. Zervos, 1986, Intergeneric and interspecies gene exchange in gram-positive cocci: Antimicrobial Agents and Chemotherapy, v. 30, p. 817-822.

Schimmel, P., J. Tao, and J. Hill, 1998, Aminoacyl tRNA synthetases as targets for new anti-infectives: FASEB Journal: Official Publication of the Federation of American Societies for Experimental Biology, v. 12, p. 1599-1609.

Schittek, B., R. Hipfel, B. Sauer, J. Bauer, H. Kalbacher, S. Stevanovic, M. Schirle, K. Schroeder, N. Blin, F. Meier, G. Rassner, and C. Garbe, 2001, Dermcidin: a novel human antibiotic peptide secreted by sweat glands: Nature Immunology, v. 2, p. 1133.

Schneider, D. J., J. Feigon, Z. Hostomsky, and L. Gold, 1995, High-affinity ssDNA inhibitors of the reverse transcriptase of type 1 human immunodeficiency virus: Biochemistry, p. 9599.

Schnellmann, C., V. Gerber, A. Rossano, V. Jaquier, Y. Panchaud, M. G. Doherr, A. Thomann, R. Straub, and V. Perreten, 2006, Presence of new mecA and mph(C) variants conferring antibiotic resistance in Staphylococcus spp. isolated from the skin of horses before and after clinic admission: Journal of Clinical Microbiology, v. 44, p. 4444-4454.

Scott, T. M., 2007, Alternatives to Vancomycin for the Treatment of Methicillin-Resistant *Staphylococcus aureus* Infections, University of Chicago Press, p. S184.

Sefah, K., D. Shangguan, X. Xiong, M. B. O'Donoghue, and W. Tan, 2010, Development of DNA aptamers using Cell-SELEX: Nature Protocols, v. 5, p. 1169-1185.

Sefah, K., Z. W. Tang, D. H. Shangguan, H. Chen, D. Lopez-Colon, Y. Li, P. Parekh, J. Martin, L. Meng, J. A. Phillips, Y. M. Kim, and W. H. Tan, 2009, Molecular recognition of acute myeloid leukemia using aptamers: Leukemia, v. 23, p. 235-244.

Selsted, M. E., Y. Q. Tang, W. L. Morris, P. A. McGuire, M. J. Novotny, W. Smith, A. H. Henschen, and J. S. Cullor, 1993, Purification, primary structures, and antibacterial activities of beta-defensins, a new family of antimicrobial peptides from bovine neutrophils: The Journal Of Biological Chemistry, v. 268, p. 6641-6648.

Shai, Y., 2002, Mode of action of membrane active antimicrobial peptides: Biopolymers, v. 66, p. 236-248.

Shangguan, D. H., Z. H. C. Cao, Y. Li, and W. H. Tan, 2007, Aptamers evolved from cultured cancer cells reveal molecular differences of cancer cells in patient samples: Clinical Chemistry, v. 53, p. 1153-1155.

Shangguan, D., Y. Li, Z. Tang, Z. C. Cao, H. W. Chen, P. Mallikaratchy, K. Sefah, C. J. Yang, and W. Tan, 2006, Aptamers Evolved from Live Cells as Effective Molecular Probes for Cancer Study: Proceedings of the National Academy of Sciences of the United States of America, p. 11838.

Shankaramma, S. C., K. Moehle, S. James, J. W. Vrijbloed, D. Obrecht, and J. A. Robinson, 2003, A family of macrocyclic antibiotics with a mixed peptide-peptoid beta-hairpin backbone conformation: Chemical Communications (Cambridge, England), p. 1842-1843.

Shi, H., Z. W. Tang, Y. Kim, H. L. Nie, Y. F. Huang, X. X. He, K. Deng, K. M. Wang, and W. H. Tan, 2010, *In-vivo* Fluorescence Imaging of Tumors using Molecular Aptamers Generated by Cell-SELEX: Chemistry-An Asian Journal, v. 5, p. 2209-2213.

Shorr, A. F., 2007, Epidemiology of staphylococcal resistance: Clinical Infectious Diseases: An Official Publication of The Infectious Diseases Society of America, v. 45 Suppl 3, p. S171-S176.

Sidhu, S. S., W. J. Fairbrother, and K. Deshayes, 2003, Exploring protein-protein interactions with phage display: ChemBioChem, v. 4, p. 14-25.

Sievert, D. M. e. a., 2002, *Staphylococcus aureus* resistant to vancomycin-United States, 2002: MMWR: Morbidity & Mortality Weekly Report, v. 51, p. 565-567.

Siller-Matula, J. M., Y. Merhi, J. F. Tanguay, D. Duerschmied, D. D. Wagner, K. E. McGinness, P. S. Pendergrast, J. K. Chung, X. B. Tian, R. G. Schaub, and B. Jilma, 2012, ARC15105 Is a Potent Antagonist of Von Willebrand Factor Mediated Platelet Activation and Adhesion: Arteriosclerosis, Thrombosis, and Vascular Biology, v. 32, p. 902-U100.

Simon, R. J., R. S. Kania, R. N. Zuckermann, V. D. Huebner, D. A. Jewell, S. Banville, S. Ng, L. Wang, S. Rosenberg, C. K. Marlowe, and a. et, 1992, Peptoids: a modular approach to drug discovery: Proceedings Of The National Academy Of Sciences Of The United States Of America, v. 89, p. 9367-9371.

Smith, G. P., and V. A. Petrenko, 1997, Phage Display: Chemical Reviews, v. 97, p. 391-410.

Song, Y., Z. Zhu, Y. An, W. Zhang, H. Zhang, D. Liu, C. Yu, W. Duan, and C. J. Yang, 2013, Selection of DNA aptamers against epithelial cell adhesion molecule for cancer cell imaging and circulating tumor cell capture: Analytical Chemistry, v. 85, p. 4141-4149.

Sooter, L. J., and A. D. Ellington, 2002, Reflections on a novel therapeutic candidate: Chemistry & Biology, v. 9, p. 857-858.

Sorokulova, I. B., E. V. Olsen, I. H. Chen, B. Fiebor, J. M. Barbaree, V. J. Vodyanoy, B. A. Chin, and V. A. Petrenko, 2005, Landscape phage probes for Salmonella typhimurium: Journal of Microbiological Methods, v. 63, p. 55-72.

Sosic, A., A. Meneghello, E. Cretaio, and B. Gatto, 2011, Human Thrombin Detection through a Sandwich Aptamer Microarray: Interaction Analysis in Solution and in Solid Phase: Sensors, v. 11, p. 9426-9441.

Steiner, H., D. Hultmark, A. Engström, H. Bennich, and H. G. Boman, 2009, Sequence and specificity of two antibacterial proteins involved in insect immunity. Nature 292: 246-248. 1981: Journal of Immunology (Baltimore, Md.: 1950), v. 182, p. 6635-6637.

Steiner, H., D. Hultmark, A. Engström, H. Bennich, and H. G. Boman, 1981, Sequence and specificity of two antibacterial proteins involved in insect immunity: Nature, v. 292, p. 246-248.

Steinstraesser, L., U. Kraneburg, F. Jacobsen, and S. Al-Benna, 2011, Host defense peptides and their antimicrobial-immunomodulatory duality: Immunobiology, v. 216, p. 322-333.

Stotz, H. U., J. G. Thomson, and Y. Wang, 2009, Plant defensins: Defense, development and application, Landes Bioscience, 2009-11.

Stovall, G. M., J. C. Cox, and A. D. Ellington, 2004, Automated optimization of aptamer selection buffer conditions: Journal of the Association for Laboratory Automation, v. 9, p. 117.

Stromstedt, A. A., L. Ringstad, A. Schmidtchen, and M. Malmsten, 2010, Interaction between amphiphilic peptides and phospholipid membranes: Current Opinion in Colloid & Interface Science, v. 15, p. 467-478.

Su, Z., and J. F. Honek, 2007, Emerging bacterial enzyme targets: Current Opinion In Investigational Drugs (London, England: 2000), v. 8, p. 140-149.

Subbalakshmi, C., and N. Sitaram, 1998, Mechanism of antimicrobial action of indolicidin: FEMS Microbiology Letters, v. 160, p. 91-96.

Subramanian, N., V. Raghunathan, J. R. Kanwar, R. K. Kanwar, S. V. Elchuri, V. Khetan, and S. Krishnakumar, 2012, Target-specific delivery of doxorubicin to retinoblastoma using epithelial cell adhesion molecule aptamer: Molecular Vision, v. 18, p. 2783-2795.

Sun, J., and R. N. Zuckermann, 2013, Peptoid polymers: a highly designable bioinspired material: ACS Nano, v. 7, p. 4715-4732.

Suntharalingam, G., M. R. Perry, S. Ward, S. J. Brett, N. Panoskaltsis, and M. D. Brunner, 2006, Cytokine storm in a phase 1 trial of the anti-CD28 monoclonal antibody TGN1412: The New England Journal of Medicine, p. 1018.

Sutcliffe, J. A., 2011, Antibiotics in development targeting protein synthesis: Annals of the New York Academy of Sciences, v. 1241, p. 122-152.

Svobodová, M., A. Pinto, P. Nadal, and C. O' Sullivan, 2012, Comparison of different methods for generation of single-stranded DNA for SELEX processes: Analytical & Bioanalytical Chemistry, v. 404, p. 835-842.

Swaminathan, B., and P. Feng, 1994, Rapid detection of food-borne pathogenic bacteria: Annual Review of Microbiology, v. 48, p. 401-426.

Szeitner, Z., J. András, R. E. Gyurcsányi, and T. Mészáros, 2014, Is less more? Lessons from aptamer selection strategies: Journal Of Pharmaceutical And Biomedical Analysis.

Takakusagi, Y., K. Takakusagi, F. Sugawara, and K. Sakaguchi, 2010, Use of phage display technology for the determination of the targets for small-molecule therapeutics: Expert Opinion on Drug Discovery, v. 5, p. 361-389.

Talbot, L. J., Z. Mi, S. D. Bhattacharya, V. Kim, H. Guo, and P. C. Kuo, 2011, Pharmacokinetic characterization of an RNA aptamer against osteopontin and demonstration of in vivo efficacy in reversing growth of human breast cancer cells: Surgery, p. 224.

Tanaka, Y., T. Honda, K. Matsuura, Y. Kimura, and M. Inui, 2009, In Vitro Selection and Characterization of DNA Aptamers Specific for Phospholamban: Journal of Pharmacology and Experimental Therapeutics, v. 329, p. 57-63.

Tang, Y. Q., J. Yuan, G. Osapay, K. Osapay, D. Tran, C. J. Miller, A. J. Ouellette, and M. E. Selsted, 1999, A cyclic antimicrobial peptide produced in primate leukocytes by the ligation of two truncated alpha-defensins: Science (New York, N.Y.), v. 286, p. 498-502.

Tang, Z. W., P. Parekh, P. Turner, R. W. Moyer, and W. H. Tan, 2009, Generating Aptamers for Recognition of Virus-Infected Cells: Clinical Chemistry, v. 55, p. 813-822.

Tang, Z., D. Shangguan, K. Wang, H. Shi, K. Sefah, P. Mallikratchy, H. W. Chen, Y. Li, and W. Tan, 2007, Selection of aptamers for molecular recognition and characterization of cancer cells: Analytical Chemistry, p. 4900.

Tanida, T., T. Okamoto, E. Ueta, T. Yamamoto, and T. Osaki, 2006, Antimicrobial peptides enhance the candidacidal activity of antifungal drugs by promoting the efflux of ATP from Candida cells: Journal of Antimicrobial Chemotherapy, v. 57, p. 94-103.

Taylor, K., P. E. Barran, and J. R. Dorin, 2008, Review: Structure-activity relationships in beta-defensin peptides: Biopolymers, v. 90, p. 1-7.

Teixeira, V., M. J. Feio, and M. Bastos, 2012, Role of lipids in the interaction of antimicrobial peptides with membranes: Progress in Lipid Research, v. 51, p. 149-177.

Tenover, F. C., 2006, Mechanisms of antimicrobial resistance in bacteria: American Journal of Infection Control, v. 34, p. S3-S10.

Theuretzbacher, U., 2011, Resistance drives antibacterial drug development: Current Opinion in Pharmacology, p. 433.

Theuretzbacher, U., 2012, Accelerating resistance, inadequate antibacterial drug pipelines and international responses: International Journal of Antimicrobial Agents, v. 39, p. 295-299.

Thevissen, K., K. K. A. Ferket, I. E. J. A. François, and B. P. A. Cammue, 2003, Interactions of antifungal plant defensins with fungal membrane components: Peptides, v. 24, p. 1705-1712.

Thomas, A., and R. Brasseur, 2006, Tilted Peptides: The History: Current Protein & Peptide Science, v. 7, p. 523-527.

Thomas, S., S. Karnik, R. S. Barai, V. K. Jayaraman, and S. Idicula-Thomas, 2010, CAMP: a useful resource for research on antimicrobial peptides: Nucleic Acids Research, v. 38, p. D774-D780.

Thornsberry, C., D. F. Sahm, L. J. Kelly, I. A. Critchley, M. E. Jones, A. T. Evangelista, and J. A. Karlowsky, 2002, Regional trends in antimicrobial resistance among clinical isolates of *Streptococcus pneumoniae*, *Haemophilus influenzae*, and *Moraxella catarrhalis* in the United States: results from the TRUST Surveillance Program, 1999-2000: Clinical Infectious Diseases: An Official Publication Of The Infectious Diseases Society Of America, v. 34 Suppl 1, p. S4-S16.

Tomasini, C., I. Juc, D. J. Aitken, F. Fulop, M. L. Huang, M. A. Benson, S. B. Y. Shin, V. J. Torres, and K. Kirshenbaum, 2013, Amphiphilic Cyclic Peptoids That Exhibit Antimicrobial Activity by Disrupting *Staphylococcus aureus* Membranes: European Journal of Organic Chemistry, p. 3560.

Tran, H., S. L. Gael, M. D. Connolly, and R. N. Zuckermann, 2011, Solid-phase submonomer synthesis of peptoid polymers and their self-assembly into highly-ordered nanosheets: Journal Of Visualized Experiments: Jove, p. e3373-e3373.

Trepel, M., R. Pasqualini, and W. Arap, 2008, Screening phage-display Peptide libraries for vascular targeted peptides: Methods in Enzymology, v. 445, p. 83-106.

Tsien, R. Y., 2005, Building and breeding molecules to spy on cells and tumors: FEBS Letters, p. 927.

Tsubakishita, S., K. Kuwahara-Arai, T. Sasaki, and K. Hiramatsu, 2010, Origin and molecular evolution of the determinant of methicillin resistance in staphylococci: Antimicrobial Agents And Chemotherapy, v. 54, p. 4352-4359.

Tucker, W. O., K. T. Shum, and J. A. Tanner, 2012, G-quadruplex DNA aptamers and their ligands: structure, function and application: Current Pharmaceutical Design, v. 18, p. 2014-2026.

Tuerk, C., and L. Gold, 1990, Systematic evolution of ligands by exponential enrichment: RNA ligands to bacteriophage T4 DNA polymerase. (SELEX procedure): Science, p. 505.

Turek, D., V. S. Dimitri, J. Judith, O. Ismail, and T. Weihong, 2013, Molecular recognition of live methicillin-resistant *staphylococcus aureus* cells using DNA aptamers: World Journal of Translational Medicine, v. 2, p. 67-74.

Turnbough, C. L., 2003, Discovery of phage display peptide ligands for species-specific detection of Bacillus spores: Journal of Microbiological Methods, v. 53, p. 263-271.

Ueberberg, S., and S. Schneider, 2010, Phage library-screening: A powerful approach for generation of targeting-agents specific for normal pancreatic islet-cells and islet-cell carcinoma *in vivo*: Regulatory Peptides, v. 160, p.1-8.

Unciti-Broceta, A., F. Diezmann, C. Y. Ou-Yang, M. A. Fara, and M. Bradley, 2009, Synthesis, penetrability and intracellular targeting of fluorescein-tagged peptoids and peptide-peptoid hybrids: Bioorganic & Medicinal Chemistry, p. 959.

Utku, Y., E. Dehan, O. Ouerfelli, F. Piano, R. N. Zuckermann, M. Pagano, and K. Kirshenbaum, 2006, A peptidomimetic siRNA transfection reagent for highly effective gene silencing: Molecular BioSystems, v. 2, p. 312-317.

Utsui, Y., and T. Yokota, 1985, Role of an altered penicillin-binding protein in methicillin- and cephem-resistant *Staphylococcus aureus*: Antimicrobial Agents And Chemotherapy, v. 28, p. 397-403.

Van Epps, H. L., 2006, Rene Dubos: unearthing antibiotics: Journal of Experimental Medicine, v. 203, p. 259-259.

van Griethuysen, A., M. Pouw, N. van Leeuwen, M. Heck, P. Willemse, A. Buiting, and J. Kluytmans, 1999, Rapid slide latex agglutination test for detection of methicillin resistance in *Staphylococcus aureus*: Journal of Clinical Microbiology, v. 37, p. 2789-2792.

van Meer, G., D. R. Voelker, and G. W. Feigenson, 2008, Membrane lipids: where they are and how they behave: Nature Reviews Molecular Cell Biology, v. 9, p. 112-124.

van Oosten, M., T. Schäfer, J. A. C. Gazendam, K. Ohlsen, E. Tsompanidou, M. C. de Goffau, H. J. M. Harmsen, L. M. A. Crane, E. Lim, K. P. Francis, L. Cheung, M. Olive, V. Ntziachristos, J. M. van Dijl, and G. M. van Dam, 2013, Real-time in vivo imaging of invasive- and biomaterial-associated bacterial infections using fluorescently labelled vancomycin: Nature Communications, v. 4, p. 2584-2584.

van Schilfgaarde, M., P. Eijk, A. Regelink, P. van Ulsen, V. Everts, J. Dankert, and L. van Alphen, 1999, Haemophilus influenzae localized in epithelial cell layers is shielded from antibiotics and antibody-mediated bactericidal activity: Microbial Pathogenesis, v. 26, p. 249-262.

Vater, A., F. Jarosch, K. Buchner, and S. Klussmann, 2003, Short bioactive Spiegelmers to migraine-associated calcitonin gene-related peptide rapidly identified by a novel approach: Tailored-SELEX: Nucleic Acids Research, v. 31.

Vater, A., S. Sell, P. Kaczmarek, C. Maasch, K. Buchner, E. Pruszynska-Oszmalek, P. Kolodziejski, W. G. Purschke, K. W. Nowak, M. Z. Strowski, and S. Klussmann, 2013, A Mixed Mirror-image DNA/RNA Aptamer Inhibits Glucagon and Acutely Improves Glucose Tolerance in Models of Type 1 and Type 2 Diabetes: Journal of Biological Chemistry, v. 288, p. 21136-21147.

Vavalle, J. P., C. P. Rusconi, S. Zelenkofske, W. A. Wargin, J. H. Alexander, and R. C. Becker, 2012, A phase 1 ascending dose study of a subcutaneously administered factor IXa inhibitor and its active control agent: Journal Of Thrombosis And Haemostasis: JTH, v. 10, p. 1303-1311.

Vilchèze, C., T. Hartman, B. Weinrick, and W. R. Jacobs, Jr., 2013, Mycobacterium tuberculosis is extraordinarily sensitive to killing by a vitamin C-induced Fenton reaction: Nature Communications, v. 4, p. 1881-1881.

Walsh, C., 2000, Molecular mechanisms that confer antibacterial drug resistance: Nature, v. 406, p. 775.

Wang, C. H., Y. F. Huang, and C. K. Yeh, 2011, Aptamer-Conjugated Nanobubbles for Targeted Ultrasound Molecular Imaging: Langmuir, v. 27, p. 6971-6976.

Wang, C., M. Zhang, G. Yang, D. Zhang, H. Ding, H. Wang, M. Fan, B. Shen, and N. Shao, 2003, Single-stranded DNA aptamers that bind differentiated but not parental cells: subtractive systematic evolution of ligands by exponential enrichment: Journal of Biotechnology, v. 102, p. 15.

Wang, G. S., X. Li, and Z. Wang, 2009, APD2: the updated antimicrobial peptide database and its application in peptide design: Nucleic Acids Research, v. 37, p. D933-D937.

Wang, G., 2013, Database-Guided Discovery of Potent Peptides to Combat HIV-1 or Superbugs: Pharmaceuticals (Basel, Switzerland), v. 6, p. 728-758.

Wang, G., X. Li, and M. Zasloff, 2010, A database view of naturally occurring antimicrobial peptides: nomenclature, classification and amino acid sequence analysis, Advances in Molecular and Cellular Microbiology, p. 1-21.

Wang, Z., and G. S. Wang, 2004, APD: the Antimicrobial Peptide Database: Nucleic Acids Research, v. 32, p. D590-D592.

Waybrant, B., T. R. Pearce, P. Wang, S. Sreevatsan, and E. Kokkoli, 2012, Development and characterization of an aptamer binding ligand of fractalkine using domain targeted SELEX: Chemical Communications (Cambridge, England), v. 48, p. 10043-10045.

Wertheim, H. F. L., D. C. Melles, M. C. Vos, W. van Leeuwen, A. van Belkum, H. A. Verbrugh, and J. L. Nouwen, 2005, The role of nasal carriage in *Staphylococcus aureus* infections: Lancet Infectious Diseases, v. 5, p. 751-762.

White, A. G., N. Fu, W. M. Leevy, J. J. Lee, M. A. Blasco, and B. D. Smith, 2010, Optical Imaging of Bacterial Infection in Living Mice Using Deep-Red Fluorescent Squaraine Rotaxane Probes: Bioconjugate Chemistry, v. 21, p. 1297-1304.

White, R. R., B. A. Sullenger, and C. P. Rusconi, 2000, Developing aptamers into therapeutics: Journal of Clinical Investigation, v. 106, p. 929-934.

Williams, D. D., O. Benedek, and C. L. Turnbough, Jr., 2003, Species-specific peptide ligands for the detection of Bacillus anthracis spore: Applied and Environmental Microbiology, v. 69, p. 6288-6293.

Wilson, L. G., 1987, The early recognition of streptococci as causes of disease: Medical History, v. 31, p. 403-414.

Wisplinghoff, H., T. Bischoff, S. M. Tallent, H. Seifert, R. P. Wenzel, and M. B. Edmond, 2004, Nosocomial bloodstream infections in US hospitals: analysis of 24,179 cases from a prospective nationwide surveillance study: Clinical Infectious Diseases: An Official Publication Of The Infectious Diseases Society Of America, v. 39, p. 309-317.

Witte, W., 1998, Medical consequences of antibiotic use in agriculture: Science (New York, N.Y.), v. 279, p. 996-997.

Wong, W. R., A. G. Oliver, and R. G. Linington, 2012, Development of Antibiotic Activity Profile Screening for the Classification and Discovery of Natural Product Antibiotics.(Report): Chemistry & Biology, p. 1483.

Woolhouse, M. E. J., J. P. Webster, E. Domingo, B. Charlesworth, and B. R. Levin, 2002, Biological and biomedical implications of the co-evolution of pathogens and their hosts: Nature Genetics, v. 32, p. 569-577.

Wright, G. D., 2005, Bacterial resistance to antibiotics: Enzymatic degradation and modification: Advanced Drug Delivery Reviews, v. 57, p. 1451-1470.

Wright, G. D., 2007, The antibiotic resistome: the nexus of chemical and genetic diversity: Nature Reviews Microbiology, v. 5, p. 175-186.

Wright, G. D., 2010, Q&A: Antibiotic resistance: where does it come from and what can we do about it?: BMC Biology, v. 8, p. 123-123.

Wu, C. Y., J. Hoskins, L. C. Blaszczak, D. A. Preston, and P. L. Skatrud, 1992, Construction of a water-soluble form of penicillin-binding protein 2a from a methicillin-resistant *Staphylococcus aureus* isolate: Antimicrobial Agents and Chemotherapy, v. 36, p. 533-539.

Wu, S., C. Piscitelli, H. de Lencastre, and A. Tomasz, 1996, Tracking the evolutionary origin of the methicillin resistance gene: cloning and sequencing of a homologue of mecA from a methicillin susceptible strain of *Staphylococcus sciuri*: Microbial Drug Resistance (Larchmont, N.Y.), v. 2, p. 435-441.

Wu, S., H. de Lencastre, and A. Tomasz, 1998, Genetic organization of the mecA region in the methicillin-susceptible and methicillin-resistant strains of *Staphylococcus sciuri*: Journal of Bacteriology, p. 236.

Wu, X., Q. Yan, Y. Huang, H. Huang, Z. Su, J. Xiao, Y. Zeng, Y. Wang, C. Nie, Y. Yang, and X. Li, 2010, Isolation of a novel basic FGF-binding peptide with potent antiangiogenetic activity: Journal Of Cellular And Molecular Medicine, v. 14, p. 351-356.

Yang, L., T. M. Weiss, R. I. Lehrer, and H. W. Huang, 2000, Crystallization of Antimicrobial Pores in Membranes: Magainin and Protegrin: Biophysical Journal, v. 79, p. 2002-2009.

Yang, X. H., J. Huang, K. M. Wang, W. Li, L. Cui, and X. P. Li, 2011, Angiogenin-Mediated Photosensitizer-Aptamer Conjugate for Photodynamic Therapy: ChemMedChem, v. 6, p. 1778-1780.

Yanmin, H., A. Shamaei-Tousi, L. Yingjun, and A. Coates, 2010, A New Approach for the Discovery of Antibiotics by Targeting Non-Multiplying Bacteria: A Novel Topical Antibiotic for Staphylococcal Infections: PLoS ONE, v. 5, p. 1-10.

Yarbrough, D. K., E. Hagerman, R. Eckert, J. He, H. Choi, N. Cao, K. Le, J. Hedger, F. Qi, M. Anderson, B. Rutherford, B. Wu, S. Tetradis, and W. Shi, 2010, Specific binding and mineralization of calcified surfaces by small peptides: Calcified Tissue International, v. 86, p. 58-66.

Yarbrough, D. K., R. Eckert, H. Jian, E. Hagerman, Q. Fengxia, R. Lux, W. Ben, and M. H. A. Wenyuan Shi, 2011, Rapid Probing of Biological Surfaces with a Sparse- Matrix Peptide Library: PLoS ONE, v. 6, p. 1-10.

Ye, M., J. Hu, M. Y. Peng, J. Liu, H. X. Liu, X. L. Zhao, and W. H. Tan, 2012, Generating Aptamers by Cell-SELEX for Applications in Molecular Medicine: International Journal of Molecular Sciences, v. 13, p. 3341-3353.

Yeagle, P. L., 2012, Introduction to lipid bilayers, in Structure of Biological Membranes, Book News, Inc.

Yeaman, M. R., K. D. Gank, A. S. Bayer, and E. P. Brass, 2002, Synthetic peptides that exert antimicrobial activities in whole blood and blood-derived matrices: Antimicrobial Agents and Chemotherapy, v. 46, p. 3883-3891.

Yigit, M. V., D. Mazumdar, H.K. Kim, J. H. Lee, B. Odintsov, and Y. Lu, 2007, Smart "turn-on" magnetic resonance contrast agents based on aptamer-functionalized superparamagnetic iron oxide nanoparticles: Chembiochem: A European Journal Of Chemical Biology, v. 8, p. 1675-1678.

Yonezawa, A., J. Kuwahara, N. Fujii, and Y. Sugiura, 1992, Binding of tachyplesin I to DNA revealed by footprinting analysis: significant contribution of secondary structure to DNA binding and implication for biological action: Biochemistry, v. 31, p. 2998-3004.

Yu, L. M., S. Yu, E. Y. Y. Mui, J. C. McKelvie, T. P. T. Pham, Y. W. Yap, W. Q. Wong, J. W. Wu, W. Q. Deng, and B. P. Orner, 2009, Phage display screening against a set of targets to establish peptide-based sugar mimetics and molecular docking to predict binding site: Bioorganic & Medicinal Chemistry, v. 17, p. 4825-4832.

Zaffiri, L., J. Gardner, and L. H. Toledo-Pereyra, 2012, History of antibiotics. From salvarsan to cephalosporins: Journal Of Investigative Surgery: The Official Journal Of The Academy Of Surgical Research, v. 25, p. 67-77.

Zasloff, M., 1987, Magainins, a class of antimicrobial peptides from Xenopus skin: isolation, characterization of two active forms, and partial cDNA sequence of a precursor: Proceedings Of The National Academy Of Sciences Of The United States Of America, v. 84, p. 5449-5453.

Zasloff, M., 2002, Antimicrobial peptides of multicellular organisms: Nature, v. 415, p. 389-395.

Zeiler, H. J., K. G. Metzger, P. Schacht, and K. Grohe, 1985, Assessment of the in vitro and in vivo activity of ciprofloxacin measured against current standards of therapy: Drugs under Experimental and Clinical Research, v. 11, p. 343-350.

Zessel, K., S. Mohring, G. Hamscher, M. Kietzmann, and J. Stahl, 2013, Biocompatibility and antibacterial activity of photolytic products of sulfonamides: Chemosphere.

Zeya, H. I., and J. K. Spitznagel, 1966, Cationic proteins of polymorphonuclear leukocyte lysosomes. I. Resolution of antibacterial and enzymatic activities: Journal of Bacteriology, v. 91, p. 750-754.

Zhang, C., X. Ji, Y. Zhang, G. Zhou, X. Ke, H. Wang, P. Tinnefeld, and Z. He, 2013, One-pot synthesized aptamer-functionalized Cd Te: Zn^{2+} quantum dots for tumor-targeted fluorescence imaging in vitro and *in vivo*: Analytical Chemistry, v. 85, p. 5843-5849.

Zhang, M.Z., R.N. Yu, J. Chen, Z.Y. Ma, and Y.D. Zhao, 2012, Targeted quantum dots fluorescence probes functionalized with aptamer and peptide for transferrin receptor on tumor cells: Nanotechnology, v. 23, p. 485104-485104.

Zhang, Y., H. Hong, and W. Cai, 2011, Tumor-targeted drug delivery with aptamers: Current Medicinal Chemistry, v. 18, p. 4185-4194.

Zhang, Z. F., X. Shan, Y. X. Wang, W. Wang, S. Y. Feng, and Y. B. Cui, 2014, Screening and selection of peptides specific for esophageal cancer cells from a phage display peptide library: Journal of Cardiothoracic Surgery, v. 9.

Zhao, H. X., and P. K. J. Kinnunen, 2003, Modulation of the activity of secretory phospholipase A(2) by antimicrobial peptides: Antimicrobial Agents and Chemotherapy, v. 47, p. 965-971.

Zhao, M., 2011, Lantibiotics as probes for phosphatidylethanolamine: Amino Acids, v. 41, p. 1071-1079.

Zhen, B., Y. J. Song, Z. B. Guo, J. Wang, M. L. Zhang, S. Y. Yu, and R. F. Yang, 2002, In vitro selection and affinity function of the aptamers to Bacillus anthracis spores by SELEX: Acta Biochimica et Biophysica Sinica, v. 34, p. 635-642.

Zhou, B., and B. Wang, 2006, Pegaptanib for the treatment of age-related macular degeneration: Experimental Eye Research, p. 615.

Zhu, W. L., K. S. Hahm, and S. Y. Shin, 2007, Cathelicidin-derived Trp/Pro-rich antimicrobial peptides with lysine peptoid residue (Nlys): therapeutic index and plausible mode of action: Journal of Peptide Science, v. 13, p. 529-535.

Zhu, W. L., Y. Park, I.S. Park, Y. S. Park, Y. Kim, K.S. Hahm, and S. Y. Shin, 2006, Improvement of bacterial cell selectivity of melittin by a single Trp mutation with a peptoid residue: Protein And Peptide Letters, v. 13, p. 719-725.

Zuckermann, R. N., 2011, Peptoid origins: Biopolymers, v. 96, p. 545-555.

Zuckermann, R. N., and T. Kodadek, 2009, Peptoids as potential therapeutics: Current Opinion in Molecular Therapeutics, v. 11, p. 299-307.

Zuckermann, R. N., E. J. Martin, D. C. Spellmeyer, G. B. Stauber, K. R. Shoemaker, J. M. Kerr, G. M. Figliozzi, D. A. Goff, M. A. Siani, R. J. Simon, and a. et, 1994, Discovery of nanomolar ligands for 7-transmembrane G-protein-coupled receptors from a diverse N-(substituted) glycine peptoid library: Journal Of Medicinal Chemistry, v. 37, p. 2678-2685.

Zuckermann, R. N., J. M. Kerr, S. B. H. Kent, and W. H. Moos, 1992, Efficient method for the preparation of peptoids [oligo(N-substituted glycines)] by submonomer solid-phase synthesis: Journal of the American Chemical Society, v. 114, p. 10646-10647.

Zuo, P., X. Li, D. C. Dominguez, and B.C. Ye, 2013, A PDMS/paper/glass hybrid microfluidic biochip integrated with aptamer-functionalized graphene oxide nano-biosensors for one-step multiplexed pathogen detection: Lab On A Chip, v. 13, p. 3921-3928.